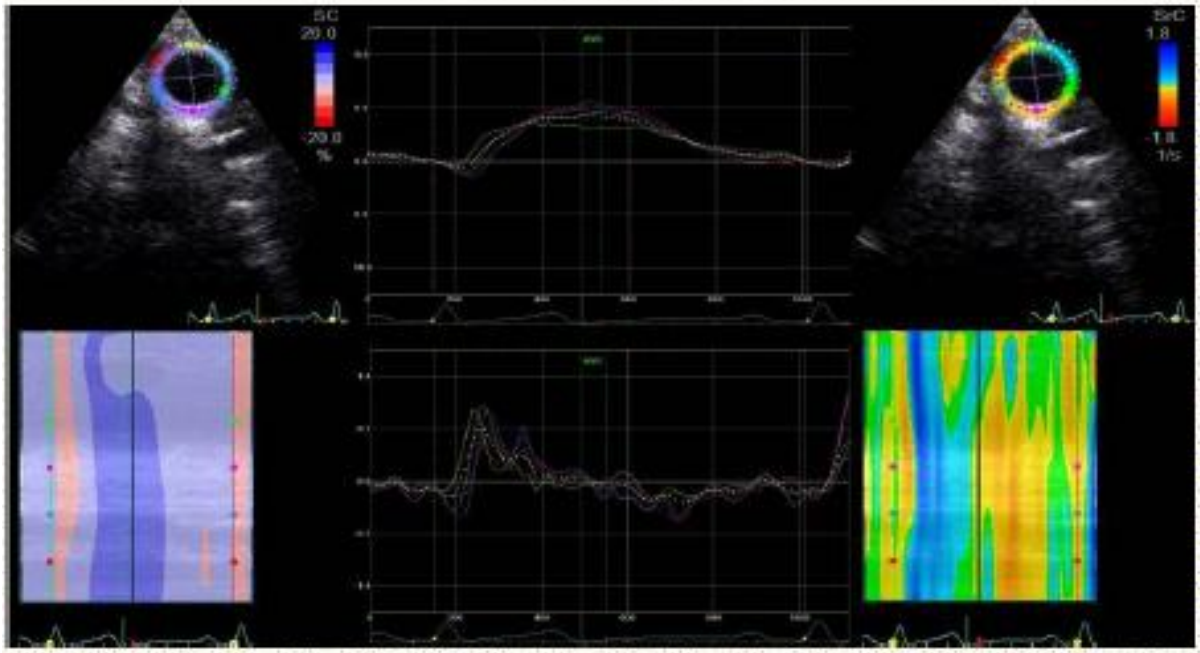

Rogério Paiva Cardoso Teixeira

ULTRASONOGRAPHIC VASCULAR MECHANICS: FEASIBILITY, USEFULNESS AND CLINICAL APPLICATIONS

Tese de doutoramento do Programa de Doutoramento em Ciências da Saúde, ramo de Medicina, orientada pelo Professor Doutor Lino Gonçalves e Professor Doutor Nuno Cardim, e apresentada à Faculdade de Medicina da Universidade de Coimbra

Setembro 2016

UNIVERSIDADE DE COIMBRA

ROGÉRIO PAIVA CARDOSO TEIXEIRA

ULTRASONOGRAPHIC VASCULAR MECHANICS: FEASIBILITY, USEFULNESS AND CLINICAL APPLICATIONS

Coimbra 2016

On the front cover: Representative images of two-dimensional speckle tracking vascular mechanics assessment at the aortic arch level.

Tese de Doutoramento apresentada à Universidade de Coimbra, do Programa de Doutoramento em Ciências da Saúde, para candidatura ao grau de Doutor em Ciências da Saúde – ramo de Medicina, especialidade de Cardiologia. A Tese foi realizada sob a orientação científica do Professor Doutor Lino Gonçalves e do Professor Doutor Nuno Cardim

Aknowledgments

It is my privilege to express my sincere thanks to all that helped me to successfully complete this project.

First of all I would like to convey my heartfelt gratitude to my supervisor **Professor Lino Gonçalves,** who encouraged me to pursue this research from the beginning and didn't allowed me to give up when I moved from Coimbra in 2012. Professor Lino always showed a great deal of interest and enthusiasm to the research. He was always available to discuss and to solve the problems along the years. Moreove, his academic network allowed me to interact with others that gave valuable contributions to the project. Without Professor Lino this project would not had been possible to be done.

I am very thankful to **Professor Nuno Cardim,** for accepting to co-supervise this project and for all the insightful comments and feedbacks.

I am most grateful to the comments, suggestions and reviews of **Professora Alexandra Gonçalves**. Her expertise and skills in the field of clinical science and echocardiography were critical to the success of the project.

I would like to extend my sincerest thanks to **Doctor Rui Baptista** for his help and time spent over the years, regarding data discussion, statistical advise and manuscript critical reviews.

I am thankful to **Professor Telmo Pereira** for his important work on the vascular stiffness assessment in the second task of the project.

I would like to convey my gratitude to **Professor Luís Providência** and **Professora Maria João Ferreira** for the stimulus to pursuit a PhD program.

Special mentions goes to my colleagues and ex-colleagues Doctors: **Rui Martins**, **Graça Castro**, **Nádia Moreira, Miguel Almeida Ribeiro**, **Ana Botelho** and **Nuno Quintal.**

I am grateful to the cardiac fellows that worked with me over the past years in this field of research. In particular I would like to mention **Doctors Luís Leite, Marta Madeira and Paulo Dinis**. I would also like to extend my sincerest thanks to **Doctor Maria João Vieira** for all her work, time and dedication to this research.

I am also very thankful to all the cardiac physiologists that worked with me along the years. In particular I would like to mention **Ricardo Monteiro**, for his work and enthusiasm to this project.

Last but not the least, a special thanks to my family.

I would like to dedicate this thesis to my **parents** for providing me with unfailing support and continuous encouragement throughout my life. It was their love and support that made me who I am today.

There are no proper words to convey my deep gratitude and respect to my wife **Cláudia**, for her love and understanding. Her support and encouragement was in the end what made this thesis possible.

Special love for my four year old daughter **Beatriz**, the pride and joy of my life.

I also would like to express my gratitude to my **parents-in-law** for their continuous help and commitment.

Table of Contents

Abstract

The development of accurate non-invasive methods of early diagnosis of vascular degenerative changes is of considerable clinical interest, given that cardiovascular disease remains the leading cause of death worldwide and large artery damage is a major contributor to cardiovascular disease. Ultrasound delivers dynamic images of the heart and central arteries. Two-dimensional speckle tracking echocardiography (2D-STE) is a semi automated analysis based on frame-by-frame tracking of tiny echo-dense speckles within the myocardium, from which deformation variables such as strain, strain rate, velocity and displacement can be studied. Initial attempts to study cardiac mechanics were focused on the left ventricular chamber, but its usage has been expanded and validated for the right ventricle, as well as the thin-walled atrial chambers. Later, direct vessel-wall tracking has been achievable through 2D-STE. The focus on previous vascular mechanics studies was the circumferential expansion and recoil of the vessel wall, which enabled the assessment of a positive systolic strain plus a positive and negative strain rate. Vascular mechanics assessment with 2D-STE has been validated with sonomicrometry studies and an association with vascular mechanics and the collagen content of vascular wall has also demonstrated, promoting vascular mechanics with 2D-STE as a new imaging surrogate of vascular stiffening.

We used 2D-STE to study aortic mechanics in patients with aortic stenosis (AS), with hypertension, and atrial fibrillation (AF), in order to assess i) the methodology feasibility and reproducibility; ii) to study the variability of vascular mechanics; iii) to assess the association of vascular mechanics and vascular stiffness.

In the first part of our research we studied 45 patients with moderate to severe AS (aortic valve area ≤ 0.85 cm^2/m^2) with 2D-STE at the level of the thoracic ascending aorta. We demonstrated that the left ventricular stroke volume index was the most important variable to explain aortic strain variability. Moreover, the vascular rigidity assessed with the aortic β_1 stiffness index was useful to explain the aortic strain rate variability. As an exploratory results, we have showed that aortic mechanics were associated with mortality.

Subsequently we used 2D-STE to study vascular mechanics at the level of the aortic arch. We enrolled a cohort of 61 apparently healthy participants, and we reported normal values. In this study we have also included a group of 46 hypertensive patients that had lower values of aortic mechanics than the healthy group (strain: 6.3±2.0% vs 11.2±3.2% and strain rate: 1.0±0.3 vs 1.5±0.4 s^{-1}, respectively, both $P<0.01$). We have demonstrated that aortic arch mechanics correlated with the gold standard method used to study vascular stiffness (pulse wave velocity, with the Complior® method) and finally we have also identified that parameters

of vascular mechanics were associated with left ventricular relaxation. After adjustments for age and pulse pressure, aortic arch strain was significantly lower in hypertensive patients, when compared to healthy subjects.

Finally, we studied aortic mechanics at the level of the descending aorta in a cohort of 44 patients with non-valvular AF who needed cardioversion and were referred for transesophageal echocardiography (TEE). We concluded for a positive association of vascular mechanics and the left atrial appendage function. Moreover, as the CHA_2DS_2VASc score increased both the vascular strain (r=-0.38, *P*=0.01) and the vascular strain rate (r=-0.42, *P*<0.01) decreased. Aortic strain remained independently associated with a past history of stroke after adjustment for the CHA_2DS_2VASc score.

The feasibility values for vascular mechanics with 2D-STE ranged from 85% to 95% for the selected patients included in the three studies. Of the total 1176 segments included in the studies, we extracted 2D-STE data for 1075 aortic wall segments. Regarding reproducibility, data was considered adequate, in particular for the assessment of global strain and strain rate.

In conclusion, it was possible to study vascular mechanics with 2D-STE at three different aortic levels. Our worked contributed to promote vascular mechanics as an imaging vascular risk marker. The usefulness of aortic strain and strain rate was established to identify higher risk subgroups of patients with degenerative AS and non-valvular AF. Aortic arch strain remained significantly lower for hypertensive patients, when compared to healthy subjects.

Keywords: Aortic Valve Stenosis; Atrial Fibrillation; Doppler; Ecocardiography; Feasibility; Hypertension; Pulse Wave Velocity; Reproducibility; Speckle-Tracking; Strain; Strain Rate; Vascular Stiffness; Vascular Mechanics; Thoracic Aorta.

Resumo

O desenvolvimento de métodos não-invasivos para o diagnostico de alterações degenerativas vasculares é de considerável interesse clínico, dado que a doença cardiovascular permanece a principal causa de morte em todo o mundo. A ecocardiografia com *speckle-tracking* é um método de análise da imagem ecográfica semi–automatizado, baseado no seguimento de pontos ecodensos da parede do miocárdio ao longo do ciclo cardiaco. A integração informática do movimento dos segmentos miocárdicos, permite a determinação da velocidade, do deslocamento, da deformação (*strain)* e da taxa de deformação *(strain-rate)* dos segmentos miocárdicos. O estudo da mecânica cardiaca por *speckle-tracking* foi inicialmente focado na câmara ventricular esquerda, mas a sua utilização foi alargada e validada para o ventrículo direito, bem como para as câmaras auriculares, que apresentam uma espessura de parede mais reduzida. Recentemente, foi analisada a deformação da parede vascular com a metodologia de *speckle-tracking*. A atenção tem sido centrada na expansão circunferencial e no recuo da parede vascular. Tal conduz a um padrão de deformação vascular característico, com um pico sistólico positivo de deformação (*strain*) circunferencial e um pico positivo da taxa de deformação (*strain rate)* vascular. A avaliação da mecânica vascular com *speckle-tracking* foi validada com estudos de sonomicrometria, e uma associação entre a mecânica vascular e o conteúdo de colágeno da parede vascular foi também demonstrada. Desta forma foi sugerida a utilização da mecânica vascular por *speckle-tracking* como um marcador imagiológico da rigidez vascular.

Com a presente tese tivemos como objetivos a utilização da metodologia de *speckle-tracking* para estudar a mecânica vascular da aorta torácica em doentes com estenose aortica (EA) degenerativa, com hipertensão arterial, e com fibrilhação auricular (FA) não-valvular, a fim de avaliar i) a exequibilidade e reprodutibilidade da metodologia; ii) estudar a variabilidade da mecânica vascular; iii) avaliar a associação da mecânica vasculares à rigidez vascular.

Nos primeiros dois estudos foram incluídos 45 doentes com EA degenerativa moderada a grave (área valvular aórtica ≤ 0,85 cm^2/m^2). Foi analisada a mecânica da aorta torácica ascendente, por ecocardiografia transtoracica e por *speckle-tracking*. Foi demonstrado que o volume ejeção do ventrículo esquerdo indexado foi a variável mais importante para explicar a variabilidade do *strain* da aorta torácica ascendente. Em contraste, a rigidez vascular avaliada com o índice β1 foi útil para explicar a variabilidade do *strain rate* vascular da aorta torácica ascendente. Como um resultado exploratório foi possível associar a mecânica vascular da aorta torácica ascendente ao prognóstico.

Subsequentemente foi utilizada a mesma metodologia de *speckle-tracking* para estudar a mecânica vascular ao nível do arco aórtico. Foi incluída uma coorte de 61 participantes, aparentemente saudáveis, tendo sido apresentados os valores de normalidade para o *strain* e o *strain rate* vascular ao nível da crossa da aorta. Este estudo também incluiu um grupo de 46 doentes com hipertensão arterial, que apresentou valores mais reduzidos da mecânica da aorta do que o grupo saudável (*strain*: 6,3±2,0% vs 11,2±3,2% e *strain rate*: 1,0±0,3 vs 1,5±0,4 s^{-1}, ambos com valor de *P* <0,01). Foi demonstrado que os valores da mecânica vascular do arco aortico se correlacionaram com a velocidade da onda de pulso (avaliada pelo método Complior®). Os parâmetros da mecânica vascular foram também associados à velocidade de relaxamento do miocárdio do ventrículo esquerdo. Após ajuste para idade e pressão de pulso, o *strain* vascular do arco aórtico foi significativamente menor no grupo de doentes hipertensos, quando comparado com o grupo de participantes saudáveis.

Por último, estudamos a mecânica vascular ao nível da aorta torácica descendente, numa coorte de 44 doentes com FA não-valvular, referenciada para cardioversão eléctrica e ecocardiografia transesofágica. Demonstramos uma correlação positiva entre mecânica vascular e a função do apêndice auricular esquerdo. Para além disso, como o aumento da pontuação do *score* CHA2DS2VASc foi observada uma redução do strain vascular (r=-0,38, *P*=0,01) e do strain rate vascular (r = -0,42, *P* <0,01). Após ajuste para o *score* CHA_2DS_2VASc, os valores mais reduzidos de *strain* da aorta torácica descendente permaneceram independentemente associados aos doentes com FA e história prévia de acidente vascular cerebral.

A exequibilidade da mecânica vascular por *speckle tracking* para os doentes selecionados nos referidos estudos variou entre 85 – 95%. Com a referida metodologia, de um total de 1176 segmentos foi possível analisar 1075 segmentos da circumferência da aorta. A reprodutibilidade foi considerada adequada particularmente para o valor global de *strain* e de *strain rate* vascular.

Em conclusão, foi possível analisar com a metodologia ecocardiográfica de *speckle tracking* a mecânica vascular da aorta, em três locais diferentes. O nosso trabalho é um contributo para a promoção da mecânica vascular como uma avaliação imagiológica da doença vascular. *O strain* e o *strain rate* vascular permitiram identificar sub-grupos de doentes com risco superior, quer no contexto da EA degenerativa e da FA não valvular. No que disse respeito à da doença hipertensiva, a mecânica vascular do arco aortico foi significativamente inferior para os doentes hipertensos em comparação com um grupo de indivíduos saudáveis.

Palavras Chave: Aorta torácica, Estenose Valvular Aortica, Fibrilhação Auricular, Hipertensão Arterial; Exequibilidade; Reprodutibilidade; Ecocardiografia; *Doppler; Speckle-Tracking; Strain*; *Strain Rate;* Mecânica Vascular; Rigidez Vascular; Velocidade da Onda de Pulso.

Thesis Outline

This thesis is divided into three parts plus supplements, whose content is summarized below.

Part I is a general introduction to the thesis, giving an overview of the state of the art in the field of left atrial and vascular mechanics and it is based on two reviews.

Left atrial mechanics assessed with two-dimensional speckle tracking echocardiography has been well studied in different clinical scenarios over the past years. Likewise the vascular wall, the atrial wall is a thin structure. Thus the challenges and limitations of the speckle tracking methodology are similar for both structures. In this way, the review entitled *Left Atrial Mechanics: Echocardiographic Assessment and Clinical Implications* was extremely important to subsequently plan and study the aortic wall with two-dimensional speckle tracking echocardiography.

The other review article, *Ultrassonagraphic Vascular Mechanics to Assess Arterial Stiffness* constitutes the genesis of all original research that brought light to this thesis, and*:*

Part II of this thesis contains 4 original articles, published or submitted for publication in international peer-reviewed journals.

Original articles number 1 and 2 are:

-*Circumferential Ascending Aortic Strain and Aortic Stenosis*;

-*Circumferential vascular strain rate to estimate vascular load in aortic stenosis: a speckle tracking echocardiography study.*

These two original papers concern the application of vascular mechanics (strain and strain rate) at the level of the thoracic ascending aorta in patients with moderate to severe aortic stenosis.

The **third original article** comprises the manuscript *Aortic Arch Mechanics Measured with Two-Dimensional Speckle Tracking Echocardiography: Pilot Study.*

The **forth original paper** *Descending Aortic Mechanics and Atrial Fibrillation: a Two-Dimensional Speckle Tracking Transesophageal Echocardiography Study* is presented.

Part III of the thesis provides an integrated discussion summarizing the main results of this thesis and addressing future research in the area.

The **supplements** include original and review articles published in the field of two-dimensional speckle tracking echocardiography.

Purposes

The overall goal of this thesis was to apply the vascular two-dimensional speckle tracking echocardiography methodology to study the aortic circumferential mechanics in three different locations (ascending aorta, aortic arch and descending aorta) in three different clinical scenarios (degenerative aortic stenosis, hypertensive heart disease, and atrial fibrillation).

Aortic stenosis is the most common valvular disease in developed countries and should not be assessed as an isolated disease of the valve itself. Indeed, a loss of arterial elasticity is a common finding in these patients who are relatively old and often have traditional cardiovascular risk factors for atherosclerosis. The purposes of the first part of the thesis were:
i)To study the feasibility and reproducibility of circumferential ascending aorta strain using two-dimensional speckle tracking echocardiography in patients with moderate to severe degenerative aortic stenos;
ii)To analyze the association of circumferential ascending aorta strain with the hemodynamic phenotypes of aortic stenosis patients;
iii)To identify the variables that were independently associated with aortic strain;
iv)To study the feasibility and reproducibility of circumferential ascending aorta strain rate using two-dimensional speckle tracking echocardiography in patients with moderate to severe degenerative aortic stenosis;
v)To analyze the association of aortic mechanics with the left ventricular afterload variables
vi)As an exploratory analysis we analyzed the prognostic significance of aortic mechanics

In the context of hypertensive heart disease, we decided to study vascular mechanics at the level of the aortic arch. Regarding this task, we proposed the following:
i) To study the feasibility and reproducibility of vascular mechanics at the aortic arch, using two-dimensional speckle tracking echocardiography in a normal sample and to estimate its references values;
ii) To compare the aortic arch mechanics between hypertensive patients and healthy subjects;
iii) To access the association between aortic arch mechanics and LV early (e') diastolic velocity.

Regarding atrial fibrillation patients, we decided to study vascular mechanics with two-dimensional speckle tracking echocardiography at the level of the descending thoracic aorta.

We used the transesophageal echocardiogram images, obtained from patients referred for a before a synchronized electrical cardioversion. Regarding this task we planned the following:

i)To study the feasibility and reproducibility of vascular mechanics at the level of the descending thoracic aorta, using two-dimensional speckle tracking echocardiography in a group of atrial fibrillation

ii)To identify the association of vascular mechanics with stroke past history and with the stroke risk score (CHA_2DS_2-VASc score).

ii)To study the association of vascular mechanics with the left atrial appendage performance.

iii) To analyze the association of vascular mechanics and the left atrial appendage function and the presence of a LAA thrombus.

iv)To assess the usefulness of vascular mechanics to predict the response to the cardioversion

Publications List

I Review Article Number 1:

Left Atrial Mechanics: Echocardiographic Assessment and Clinical Implications.

Vieira MJ and Teixeira R, Gonçalves L, Gersh BJ.

J Am Soc Echocardiogr. 2014 May; 27(5): 463-78.

II Review Article Number 2:

Ultrassonagraphic Vascular Mechanics to Assess Arterial Stiffness: A Review.

Teixeira R, Vieira MJ, Gonçalves A, Cardim N, Gonçalves L.

Eur Heart J Cardiovasc Imaging. 2016 Mar; 17(3): 233-46.

III Original Article Number 1:

Circumferential Ascending Aortic Strain and Aortic Stenosis.

Teixeira R, Moreira N, Baptista R, Barbosa A, Martins R, Castro G, Providência L.

Eur Heart J Cardiovasc Imaging. 2013 Jul; 14(7): 631-41.

IV Original Article Number 2:

Circumferential vascular strain rate to estimate vascular load in aortic stenosis: a speckle tracking echocardiography study.

Teixeira R, Monteiro R, Baptista R, Barbosa A, Leite L, Ribeiro M, Martins R, Cardim N, Gonçalves L.

Int J Cardiovasc Imaging. 2015 Apr; 31(4): 681-9.

V Original Article Number 3:

Aortic Arch Mechanics Measured with Two-Dimensional Speckle Tracking Echocardiography.

Teixeira R, Monteiro R, Baptista R, Pereira T, Ribeiro M, Gonçalves A, Cardim N, Gonçalves L

J Hypertension. 2017. Accepted for publication 14th Februrary 2017

VI Original Article Number 4

Descending Aortic Mechanics and Atrial Fibrillation: a Two-Dimensional Speckle Tracking Transesophageal Echocardiography Study.

Teixeira R, Monteiro R, Dinis P, Santos MJ, Botelho A, Quintal N, Cardim N, Gonçalves L.

Int J Cardiovasc Imaging. 2016 Apr; 33(4): 509-519

Supplements

Letter to the editor:

Vascular mechanics and stroke-a critical appraisal: study the arteries but do not forget the flow

Teixeira R, Vieira MJ, Ribeiro M, Cardim N, Gonçalves L.

Am J Hypertens. 2013 Jul; 26(7):946.

Original Article

Aortic valve disease and vascular mechanics: two - dimensional speckle tracking echocardiographic analysis

Leite L and Teixeira R, Oliveira-Santos M, Barbosa A, Martins R, Castro G, Gonçalves L, Pego M.

Echocardiography. 2016 Aug; 33(8): 1121-30.

Original Article

The relationship between tricuspid regurgitation and right atrial mechanics: a speckle tracking echocardiography study

Teixeira R, Monteiro R, Garcia J, Baptista R, Ribeiro M, Cardim N, Gonçalves L.

Int J Cardiovasc Imaging. 2015 Aug; 31(6): 1125-35.

Review Article

Two-dimensional Speckle Tracking Cardiac Mechanics and Constrictive Pericarditis: Systematic Review.

Madeira M and Teixeira R, Costa M, Gonçalves L, Klein A.

Echocardiography 2016 Oct; 33(10): 1589-1599.

Part I: Review Articles

Review Article Number 1

Left Atrial Mechanics: Echocardiographic Assessment and Clinical Implications

J Am Soc Echocardiogr. 2014 May;27(5):463-78.

Maria João Vieira[1*] MD, PHD, Rogério Teixeira[1,2*+] MD, Lino Gonçalves[1,3] MD, PHD, Bernard J. Gersh[4] MB, ChB, DPhil, FRCP

+ Corresponding Author

* Both authors contributed equally to the paper

[1] Faculdade de Medicina Universidade de Coimbra, Coimbra, Portugal

[2] Departamento de Medicina, Serviço de Cardiologia, Hospital Beatriz Ângelo, Loures, Portugal

[3] Serviço de Cardiologia, Centro Hospitalar e Universitário de Coimbra, Coimbra, Portugal

[4] Division of Cardiovascular Disease and Internal Medicine, Mayo Clinic College of Medicine, Rochester,MN, USA

Word Count= 3863 (without references or figures/tables)

Abbreviation List

3D: Three-Dimensional

2D: Two-Dimensional

2D-STE: Two-Dimensional Speckle-Tracking Echocardiography

ACS: Acute Coronary Syndrome

AF: Atrial Fibrillation

DTI: Doppler Tissue Imaging

ε: Strain

ε_{CD}: Strain during the Conduit phase

ε_{CT}: Strain during the Contractile phase

ε_{R}: Strain during the Reservoir phase

HF: Heart Failure

LA: Left Atrial

LV: Left Ventricular

MR: Mitral Regurgitation

MS: Mitral Stenosis

SR: Strain Rate

SR_{CD}: Strain Rate during the Conduit Phase

SR_{CT}: Strain Rate during the Contractile Phase

SR_{R}: Strain Rate during the Reservoir Phase

Abstract

The importance of the left atrium (LA) in cardiovascular performance has long been acknowledged. Quantitative assessment of LA function is laborious, requiring invasive pressure-volume loops and thus precluding its routine clinical use. In recent years, novel post-processing imaging methodologies emerged, providing a complementary approach for the assessment of the LA. Atrial strain (Ɛ) and strain rate (SR) obtained using either tissue Doppler imaging or 2D speckle tracking echocardiography, have proven to be feasible and reproducible techniques to evaluate LA mechanics. It is essential to fully understand its clinical applications, advantages and limitations. Furthermore, the technique's prognostic value and utility in therapeutic decisions also need further elucidation. The aim of this review is to provide a critical appraisal of LA mechanics. We describe the fundamental concepts and methodology of LA Ɛ and SR analysis, the reference values reported with different imaging techniques and the clinical implications.

Keywords: Echocardiography; Left Atrial Mechanics; Strain; Strain Rate; Two-Dimensional Speckle-Tracking Echocardiography

Introduction

The left atrium (LA) has a pivotal role in the sequence of events that modulate left ventricular (LV) filling. That is accomplished by means of four basic functions involving the LA: *phase 1*, reservoir (collection of pulmonary venous flow during left ventricular systole); *phase 2*, conduit (passage of blood to the left ventricle during early diastole); *phase 3*, active contractile pump (15%-30% of left ventricular filling in late diastole) and *phase 4*, suction force (the atrium refills itself in early systole) [1, 2.] LA relaxation, chamber stiffness, and contractility influence the reservoir, conduit and contractile function respectively[3].

Until the middle of the first decade of the 2000s, the echocardiographic study of the LA was performed with two-dimensional (2D) measurements, extrapolation of phasic volumes and with Doppler flow assessment of the mitral valve and the pulmonary veins[4]. These classic parameters improved the understanding of the normal and diseased heart, but they had a number of limitations such as foreshortening, lack of gold standard measurement of LA function, difficulties with the echocardiographic window and with the timing of various atrial events. Moreover, errors were frequent due to a geometric assumption of a biplane volume calculation[5]. Three-dimensional (3D) echocardiography significantly improved LA volume calculation, due to automated border detection and to a 3D dataset at different phases of the cardiac cycle[6, 7]. However the values obtained were heavily influenced by gain settings, resulting in large interobserver and test-retest variability[2], which hampered its daily application.

Since the past decade, echocardiographyc based automated techniques for sophisticated analysis of myocardial displacement have emerged, such as tissue Doppler imaging (TDI) or speckle tracking (ST) [8, 9]. They provide the quantification of regional myocardial function such as displacement, velocity, strain (ε) and strain rate (SR)[2]. Myocardial mechanics have been validated with sonomicrometry [10] and tagged magnetic resonance imaging[11]. These new methodologies were initially used to study the left ventricular (LV) myocardium, and subsequently applied for the LA[12], supporting LA ε and SR as an assessment of the LA active and passive deformation[2].

The aim of this review is to provide a critical appraisal of LA mechanics. We describe the fundamental concepts and the methodology of LA Ɛ and SR, reference values, clinical implications and we discuss its incremental importance.

Left Atrial Mechanics

Left atrial remodeling refers to a time-dependent adaptive regulation of cardiac myocytes in order to maintain homeostasis against external stressors [13]. The type and extent

of remodeling depends on the strength and duration of the exposure to these stressors [14]. A hallmark of LA structural remodeling is dilatation that is often accompanied by a change in LA performance [15, 16]. In healthy individuals, the LA is a highly expandable chamber with relatively low pressures, but in the presence of acute and chronic injury, the LA stretches and stiffens[14, 16, 17].

Myocardial Ɛ and SR represent the magnitude and rate, respectively, of myocardial deformation. Thus, during ventricular systole and late ventricular diastole, atrial Ɛ and SR reflect atrial distensibility (irrespective of the underlying rhythm) and atrial contractility (in the presence of sinus rhythm) respectively [1]. Strain is a fractional change in the length of a myocardial segment. It is unitless and is usually expressed as a percentage. It can have positive or negative values, which reflect lengthening or shortening[2]. Strain rate is the rate of change in Ɛ, and corresponds to the speed at which myocardial deformation occurs, expressed in sec^{-1}.

The LA Ɛ and SR curves display the physiology of atrial function and closely follow LV dynamics during the cardiac cycle (Figure 1) [18]. During the reservoir phase, corresponding to LV isovolumic contraction, ejection and isovolumic relaxation, the LA is stretched as it fills with blood from the pulmonary veins. In this way, longitudinal atrial Ɛ increases, reaching a positive peak at the end of atrial filling. This occurs due to the downward movement of the mitral annulus towards the apex, as the result of LV contraction, just before the opening of the mitral valve. After mitral valve opening, the LA empties quickly and shortens. At this point, the Ɛ decreases, up to a plateau corresponding to the phase of diastasis. Subsequently the atrial wall shortens from a longitudinal perspective, during LA contraction thus allowing for the emptying of blood into both the LV and the pulmonary veins, which reflects a decrease in atrial Ɛ [12, 19, 20]. During the LA conduit and contraction phases, LA Ɛ curve inversely reflects the pattern of LV deformation. Therefore, LA mechanics seems to be influenced not only by LA stiffness but also by LV compliance during ventricular filling and by LV contraction through the descent of the base during LV systole [19].

Assessment

It is possible to assess LA Ɛ and SR, either by ST echocardiography or by TDI modalities. A detailed description of myocardial mechanics, ST and TDI, can be found in a consensus statement from the American Society of Echocardiography and the European Society of Echocardiography (ASE/EAE)[2].

Speckles are acoustic markers equally distributed within the myocardium that are seen in grayscale B-mode images [21]. Two-dimensional speckle tracking echocardiography (2D-STE)

uses standard B-mode images to track blocks of speckles from frame to frame and measure lengthening and shortening relative to the baseline (Lagragian Ɛ) [2]. This provides local myocardial displacement information, from which velocity, Ɛ and SR can be derived[2]. Two-dimensional ST was recently applied to study the myocardial mechanics of a thin wall structure such as the LA [12, 18, 19, 22-25]. For the analysis, apical views are obtained using conventional 2D gray scale echocardiography, during a breath hold, with a stable electrocardiographic (ECG) recording. The frame rate is set between 60 and 80 frames sec^{-1} and recordings are processed using acoustic-tracking software. The LA mechanical indexes are calculated by averaging values observed in all LA segments (global Ɛ) [4, 19] with a 15[22] (six equidistant regions in the apical four-chamber, six in the two-chamber and three in the three-chambers views) or a 12 segment models[18] (six equidistant regions in the four-chamber, and six more in the two-chamber views). Recently a satisfactory agreement has been demonstrated for ST assessment, with different software packages [26].

Doppler imaging uses the phase shift between consecutive echoes for calculation of velocity[2]. With TDI, low-pass wall filter is used to display only low velocity signals originating from moving tissue and exclude high velocity signals originating from blood flow[27]. By integrating the velocity over time, myocardial mechanical indexes can be calculated[2]. In TDI mode, the imaging angle must be adjusted to ensure a parallel alignment of the sampling window with the myocardial segment of interest[27]. This means that not all segments can be analyzed, for example the atrial roof segments. Gain settings, filters, pulse repetition frequency, sector size and depth should also be adjusted to optimize color saturation[2]. The frame rate is adjusted to above 100 sec^{-1} [12, 28]. The longitudinal Ɛ and SR can be measured in the mid portion of the various segments of the LA wall (septum, lateral, posterior, anterior and inferior) using apical two, three and four-chamber views [12, 29].

Left atrial Ɛ and SR

Irrespective of which methodology is used for image acquisition and LA mechanics graphic representation, the software generates a longitudinal Ɛ and SR curve for each atrial segment [19]. The radial deformation cannot be calculated because the LA wall is thin and the spatial resolution is limited[30]. It is possible to quantify LA Ɛ in two different ways, which differ only by the choice of frame from which the software starts the processing. The first uses the P wave onset (Figure 2, panel A) and the second the QRS complex (Figure 2, panel B), as the first reference frame [18, 19, 22]. Regardless of whether the P wave or the QRS complex serves as the first reference frame, the LA SR curve is triphasic (Figure 2, panels C and D).

It worth mentioning that nomenclature becomes confusing, when LA mechanics measurements are labeled according to events of the LV (QRS onset) rather than events of **the** LA (P wave onset), because of resemblance with other Doppler parameters (Table I). According to To *et al*, nomenclature timed to the P wave is preferred to study LA mechanics[5], although in atrial fibrillation (AF) patients that is not applicable. In the present document we will name Ɛ and SR according to the LA cycle phase – $Ɛ_R$ and SR_R (peak during reservoir phase); $Ɛ_{CT}$ and SR_{CT} (peak during the contractile phase) and $Ɛ_{CD}$ and SR_{CD} (peak during the conduit phase).

Normal values of LA Ɛ and SR

The 2D-STE and TDI reference values for LA Ɛ and SR have been published since the last decade (Table II)[4, 18, 22, 31]. Inaba *et al*, [29] and Saraiva *et al*[4] demonstrated that six different parameters ($Ɛ_{CT}/SR_{CT}$, $Ɛ_{CD}/ SR_{CD}$ and $Ɛ_R/SR_R$) may be used to evaluate the contractile, conduit and reservoir components of LA function, respectively. Either with 2D-STE or TDI, It was demonstrated that both the reservoir, the conduit and the contractile LA Ɛ decreased, while SR during the contractile phase increased with aging [4, 29, 32]. Moreover, regional differences in peak velocity, Ɛ and SR were consistently reported, with higher values in the regions adjoining the mitral annulus[22]. The concept of heterogeneous segmental deformation also applies to TDI, especially to the SR profile [12]. Importantly, it has been demonstrated that most LA Ɛ and SR measurements were preload dependent, with the exception of SR during LA contraction phase [33].

Left atrial 3D-ST

The assumption that speckles remain within the 2D imaging plane and can be adequately tracked throughout the cardiac cycle may not always be valid because of the complex 3D motion of the heart chambers. The inability of 2D-STE to measure one of the three components of the local displacement vector is an important limitation, which affects the accuracy of the derived indices of local dynamics [34]. In contrast to 2D-STE, which cannot track motion in and out of the imaging plane, the recently developed 3D-ST can track motion of speckles irrespective of their direction, as long as they remain within the selected scan volume[2] – Figure 3. Moreover, 3D myocardial deformation has theoretical advantage that combines both longitudinal and circumferential Ɛ information[35].

Structural and hemodynamic correlates of LA mechanics

The LA is directly exposed to LV cavity pressure during diastole, thus, in the absence of

LA volume overload, an enlarged LA is a robust marker of increased LV filling pressure, which explains the causal link between LA dilatation and poor outcome[36]. Left atrial structural and functional remodeling has been proposed as a barometer of diastolic burden and a predictor of common cardiovascular outcomes such as new AF, stroke, heart failure (HF), mortality after myocardial infarction, severity of diastolic dysfunction and cardiovascular death [19, 37, 38]. The diastolic corollary of measurement of hemoglobin $A1_{c,}$ used in clinical practice to monitor the diabetic patient, is the LA size, that is considered a marker of average LV diastolic filling pressures. In this way, in the absence of other contributing pathology such as mitral valve disease, if the LA is large, the patient has had a sustained elevation in LV filling pressure, and hence has chronic diastolic dysfunction [39].

It has been demonstrated that LA ε_R correlated significantly with the *Tau* index, with LV end-diastolic pressure (LVEDP) and with mean capillary pulmonary wedge pressure (CPWP). Also, LA ε_R was significantly associated with LV systolic performances variables such as LV ejection fraction (LVEF), and LV systolic indexed volume. To sum up, both diastolic (LVEDP) and systolic (LV systolic volume index) LV related variables were independent predictors of LA ε_R [40]. Moreover, LA ε_R was more accurate to assess LVEDP than LA indexed volume and other Doppler related variables. Recently 3D LA AS was considered to be accurate for LV filling pressures estimation [41]. Besides these hemodynamic associations, LA ε_R has been correlated with the brain natriuretic peptide (BNP) levels [42] – Table III.

The consensus statement of the ASE/EAE suggests that LA mechanics could be assessed in patients with LV diastolic dysfunction, after AF to predict the maintenance of sinus rhythm and after percutaneous atrial septal defect repair[2]. In addition, LA mechanics may be a suitable parameter to identify patients at risk for LA regional failure or arrhythmias or to assess LA characteristics in patients with LA dilatation of undetermined cause[2]. LA size and function provide insights and prognostic markers for a wide range of pathological conditions. New findings are emerging based upon the use of LA mechanics in several clinical scenarios, summarized in Tables IV to VII – Figure 4.

An important publication by Kuppahally *et al* regarding LA remodeling, documented an inverse relationship between the extent of LA fibrosis, detected by delayed enhancement gadolinium cardiac magnetic resonance imaging, and LA ε and SR [43]. In 65 patients with paroxysmal or persistent AF, the authors demonstrated LA ε_R and SR_R inversely predicted the extent of LA fibrosis, independently of other echocardiographic parameters and the rhythm during imaging [43]. Recently, Her *et al* also correlated LA deformation with fibrosis. The authors studied 50 patients referred for mitral valve surgery and concluded that both pre-operative 2D-ST LA ε_R and SR_R were negatively correlated with atrial histology, specifically with the

degree of interstitial fibrosis. The correlation was independent of age, underlying rhythm, presence of rheumatic heart disease and type of predominant MV disease [44]. The results of these two studies support the use of LA Ɛ and SR as non-invasive tools to evaluate the degree of wall fibrosis and as surrogate markers of LA stiffness [8, 43, 44].

Heart Failure

It is well established that in addition to older age, female gender, hypertension, diabetes and coronary artery disease, an increase in LV mass and LA volume, and a decrease in LA contractile reserve, identify patients at higher risk for HF with preserved ejection fraction [45, 46]. In this context LA $Ɛ_R$, seems to be a promising tool, as in a cohort of 64 patients undergoing right heart catheterization, LA $Ɛ_R$ was significantly lower for patients with diastolic HF than for patients with diastolic dysfunction. This was in contrast to LV mass, LA volume, tissue Doppler derived measurements, and to LA $Ɛ_{CT}$. Moreover, HF patients with LV systolic dysfunction had a significantly lower LA Ɛ and SR during the contractile and reservoir phase, when compared to a control group and to diastolic HF patients. The LA stiffness index assessed as the ratio of invasively and non-invasively derived PCWP to LA $Ɛ_R$, was accurate to identify diastolic HF patients, and correlated with pulmonary artery systolic pressure[47] .

Cameli *et al*, demonstrated that LA $Ɛ_R$ provided a better estimation of LV filling pressures than the E/E' ratio in symptomatic patients with LV systolic dysfunction[48].

The LA $Ɛ_R$ could also be useful to estimate exercise capacity either in HF patients with reduced [49] or preserved[50] ejection fraction.

With respect to HF treatment, the response to cardiac resynchronization therapy has been associated with a significant improvement in LA $Ɛ_R$ [24]. Moreover, LA $Ɛ_{CT}$ seemed to be the best predictor of LV reverse remodeling[51].

Regarding prognosis, Helle-Valle *et al* concluded that LA $Ɛ_R$ was an independent and incremental predictor of death or the need for heart transplantation in a cohort of 143 patients with symptomatic systolic dysfunction, in addition to age, LV ejection fraction, and BNP [52].

It is therefore possible that LA mechanics could influence clinical management of HF patients, not only to improve diagnosis but also to estimate functional capacity and prognosis.

Atrial Fibrillation

During AF, LA contractile function is lost while both reservoir and conduit functions are reduced, with demonstrable differences between paroxysmal and persistent AF [43] . It has been showed that both LA $Ɛ_R$ and SR_R were impaired in patients with AF[26,53]. Moreover those indexes

were lower in recurrent AF patients than in those with a first episode of AF [53]. Similar concepts were demonstrated for 3D-ST LA analysis[54,55]. Recently 3D-ST LA mechanics proved to be more accurate than the 2D-ST methodology, to select the paroxysmal AF patients from a control group[34].

Regarding thromboembolic risk assessment, it has been demonstrated that LA ε_R and SR_R decreased proportionately with an increasing $CHADS_2$ score and both parameters were independent predictors of stroke, even when adjusted for age and LA volume[54]. It has also been demonstrated that LA ε_R when associated with LA volume, increase the accuracy of the $CHADS_2$ score to predict mortality and a future hospitalization for cardiac causes in AF patients[56, 57]. Recently it has been proved that in patients with a $CHADS_2$ score ≤ 1, LA ε_R was an independent predictor of stroke, when adjusted for LA size, LVEF and LV mass[58].

Di Salvo *et al* found that LA ε_R and SR_R were independent predictors of maintenance of sinus rhythm 9 months post-cardioversion [59]. A lower LA SR_{CD} and an enlarged LA were independent predictors a shorter duration of sinus rhythm after cardioversion, probably reflecting unfavorable atrial structure remodeling, with reduced LA compliance [60]. After treatment, the SR parameters gradually approach normal values[20, 29, 61]. The LA mechanics were found to be reduced, immediately after cardioversion, followed by short-term (10 days) recovery, reflecting the phenomenon of atrial stunning [62]. In contrast, a TDI based study concluded that up to 6 months after successful cardioversion, the LA myocardial velocity during the contraction phase remained lower than age matched controls, suggesting an underlying myopathy or LA fibrosis [63].

Left atrial ε_R has been considered and independent predictor of LA reverse remodeling after AF catheter ablation, even after adjustment for LA volume and type of AF [64]. Left atrium ε_R and LA volume may provide complementary information on structural changes of the LA, but it is speculated that LA ε_R may be a more sensitive parameter of changes in LA wall structure. Therefore a severely impaired LA ε_R may reflect a more advanced LA remodeling that may not be reversible after catheter ablation[64]. A similar improvement in LA ε_R and SR_R was also found in AF patients submitted to minimally invasive surgical radiofrequency ablation [65]. Moreover, it was demonstrated that patients with higher LA ε_R and SR_R after catheter ablation, may have a greater likelihood to maintain sinus rhythm[66].

In face of this data it is possible that LA mechanics could influence clinical management of AF, either to optimize the selection of AF patients for an invasive rhythm control strategy, either to influence anticoagulation therapy.

Valvular heart disease

Chronic mitral regurgitation (MR) causes increased LV and LA preload. Due to preservation of left ventricular ejection fraction, most MR patients remain asymptomatic for years. LA enlargement plays an important role in the generation of MR symptoms. In patients with various degrees of MR, a gradual reduction in LA ε_R was demonstrated [67]. For the same severity of MR, LA ε_R was significantly lower in those patients with history of paroxysmal AF [68]. Aksakal *et al* confirmed that patients with chronic rheumatic MR had impaired regional longitudinal LA ε during each mechanical phase [69]. The same findings were obtained by Borg *et al* in chronic primary MR patients [70]. The LA ε_R and LA volume, after mitral valve surgery for severe MR, have both been considered independent predictors of post-operative AF [71]. Due to differences between MR patients and controls, it was proposed that LA mechanics could help to select the best time for surgery in asymptomatic severe MR patients[67, 69].

Concerning mitral stenosis (MS), LA mechanics were found to be abnormal in asymptomatic patients with moderate MS when compared with controls, and LA SR_R was able to predict a long-term worse prognosis (combined clinical endpoint) for MS patients, irrespective of LA volume, age and mitral valve area [72].

In aortic stenosis patients it has been demonstrated that the three components of LA mechanics were reduced when compared to controls [73]. Moreover, LA ε during either the reservoir and conduit function, were more impaired than in hypertensive patients, despite a similar extent of LVH and LA dilatation [74]. After aortic valve replacement, LA reverse remodeling was synonymous of a significant increase in LA ε_R [75]. Similar findings were described for aortic regurgitation patients [76].

Acute coronary syndromes

The LA phasic volumes have been related to adverse prognosis during an acute coronary syndrome (ACS)[77]. Recently LA ε_R has been considered a predictor of LA late remodeling after an ACS, irrespective of LA volume, LV filling pressures and culprit vessel lesion[78].

Regarding prognosis, in a cohort of 320 ST-elevation ACS patients, Antoni *et al*, demonstrated that LA ε_R provides incremental value to LA maximal volume, to predict a composite endpoint of death, re-infarction and future admission for HF [79].

Probably with the largest cohort of patients studied (843 patients) to date with 2D-STE, Ersboll *et al* concluded that LA ε_R was not a prognostic marker after an ACS, when adjusted for LV longitudinal systolic function and LA diastolic indexes. An important concept demonstrated

in this study, was the fact that the LA reservoir function was dependent on LA dimensions but also on the LV longitudinal deformation, indicating that LA ε_R was a reflection of LV longitudinal ε and LA dilation and not measure of LA intrinsic functional properties[80].

The hypothesis that LA mechanics reflect ultrastructural changes of the myocardium is of interest, but common to many pathological conditions. The study of LA mechanics has been done in a number of other conditions as is described in detail in table VII.

Future Perspectives

The LA function is considered to be an important clinical variable. Recent studies found a critical correlation between LA fibrosis and echocardiographic derived LA mechanics, supporting the non-invasive assessment of LA compliance, conferring credit to this approach to clinical investigation, and urging specific software for analysis. This optimistic view is in contrast to a more skeptic one regarding the lower spatial resolution of both TDI and 2D-STE to analyze a thin LA wall as compared to the LV. In fact, it is not totally clear in the literature whether the obtained data is picked up from the LA wall or rather a result of the surrounding pressures changes within the LA cavity…

New information over the clinical relevance of LA ε and SR analysis is constantly emerging; the technique is considered to be a promising tool for clinical practice, both for diagnosis and therapeutics decision-making. It is therefore important that further powerful and non-biased studies be reported, to test and strengthen the technique, independently of positive or negative results.

The usefulness of LA mechanics over LA dimensions and conventional Doppler variables, with respect to hemodynamic variables prediction, LA performance status and even clinical endpoints, is still a matter that needs clarification. Moreover LA mechanics seems to be influenced by loading conditions, LV systolic and diastolic function, and therefore its prognostic value over and above LV mechanics remains unclear. Future studies are also warranted to more completely understand the natural history of LA remodeling, the extent of reversibility of LA mechanics with different therapies, and the impact of such changes on outcomes.

Perhaps the lack of standardization from image acquisition, to software application, and data analysis is the main technical limitation to further larger multicenter studies and to LA mechanics clinical daily application.

Conflicts of interests

The authors have no conflicts of interest to declare.

Contributions:

MJ did the literature search and wrote the manuscript. RT conceptualized the review, performed the art-work, and elaborated the manuscript reviewing process. LG and BG reviewed the manuscript.

Table Legends:

Table I: Confusing nomenclature regarding LA mechanics

Table II: LA Ɛ and SR reference values

Table III: Structural and hemodynamic correlates of LA mechanics

Table IV:: LA Ɛ and SR in HF

Table V: LA Ɛ and SR in AF

Table VI: LA Ɛ and SR in VHD and ACS

Table VII: LA Ɛ and SR in cardiomyopathies and other clinical conditions

Figure Legends:

Figure 1: Left atrial phasic functions and their relationship with the cardiac cycle. Mitral inflow, LA volumes, pressure and Ɛ / SR are shown. Left atrial mechanics is represented according to a P-wave timed analysis.

AVO aortic valve opening; D diastasis; EF early filling; ER early reservoir; LA left atrium; LASV LA stroke volume; LR late reservoir; MVC mitral valve closure; MVO mitral valve opening; SR strain rate; $SR_{pos\ peak}$ SR positive peak; $SR_{ear\ neg\ peak}$ SR early negative peak; $SR_{late\ neg\ peak}$ SR late negative peak; Ɛ strain.

Figure 2: 2D-ST LA strain (Ɛ) and strain rate (SR) curves.

Panel A: P-wave timed analysis – LA Ɛ curve, obtained after averaging the 6 segmental curves (dashed curve represents the average atrial longitudinal strain along the cardiac cycle). It is possible to identify a first negative ($Ɛ_{neg}$) peak that corresponds to the LA contraction ($Ɛ_{CT}$) phase that is followed by a positive peak ($Ɛ_{pos}$), which represents the conduit ($Ɛ_{CD}$) phase. The sum of the absolute values of positive and negative Ɛ is considered to be the total LA Ɛ, $Ɛ_{total}$ [4, 22] that reflects the reservoir ($Ɛ_{R}$) phase.

Panel B: QRS-timed analysis – LA Ɛ curve, obtained after averaging the 6 segmental curves. The first peak of the curve is a positive one, $Ɛ_{S}$ (peak atrial Ɛ during ventricular systole), measured at the end of the reservoir phase ($Ɛ_{R}$), just before mitral valve opening. This is followed by a plateau and at second late peak just before the active atrial contractile ($Ɛ_{CT}$) phase begins, at

the onset of the P wave on the ECG, $Ɛ_A$ (peak atrial longitudinal strain in late diastole). The LA $Ɛ_E$ (peak atrial longitudinal strain in early diastole) is defined as the difference between peak $Ɛ_S$ and $Ɛ_A$ and is a surrogate of the conduit phase ($Ɛ_{CD}$)[19, 67]. To represent the contribution of active contraction to the LA filling phase, a new contraction strain index was calculated as (global peak $Ɛ_A$/global peak $Ɛ_S$) x 100 %[67].

Panel C: P-wave timed analysis – LA SR curve obtained after averaging the 6 segmental curves. The curve has a first negative SR peak during LA contraction, in late ventricular diastole ($SR_{late\ neg}$ / SR_{CT} for late negative SR or SR during the contraction phase), which is followed by a positive deflection, corresponding to LA filling (SR_{pos} / SR_R for positive SR or SR during the reservoir phase). Finally the third, negative peak, during early ventricular diastole represents passive emptying of the LA ($SR_{ear\ neg}$ / SR_{CD} for early negative SR or SR during the conduit phase)[4, 19, 67].

Panel D: QRS-wave timed analysis – LA SR curve. It is possible to visualize the same SR pattern as in panel C. Three peaks are identified. A first positive SR peak (SR_S for systolic SR or SR_R), and two negatives SR peaks: SR_e for E wave SR or SR_{CD} and SR_a for A wave SR or SR_{CT}.

AVC, aortic valve closure; AVO, aortic valve opening.

Figure 3: Left atrial 3D-ST assessment. Upper panel: 3D images of the LA generated from a pyramidal 3D data set (left): (A) apical four-chamber view, (B) apical view orthogonal to plane A, and three short-axis planes, including (C1) the basal potion of the left atrium, (C2) the mid left atrium, and (C3) the roof portion of the left atrium and representative measurements of global LA area strain (ASs and ASa) in a healthy subject assessed by 3D STE (right). Lower panel: Representative 16-segment LA area strain curves in a healthy subject (control) (A), a patient with paroxistic AF (B), and a patient with permanent AF (C). Results of calculation of ASs and ASa are presented in each panel.

Reprinted from: *J Am Soc Echocardiogr* 26, Mochizuki A, Yuda S, Oi Y, Kawamukai M, Nishida J, Kouzu H, Muranaka A *el* al, Assessment of left atrial deformation and synchrony by three-dimensional speckle-tracking echocardiography: Comparative studies in healthy subjects and patients with atrial fibrillation 165-174, 2013[34], with permission from Elsevier.

Figure 4: 4-chamber view only, examples of 2D-ST LA strain (Ɛ) and strain rate (SR) in different disease states.

Panel A and B: Hypertension with no diastolic heart failure.

Panel A: 4-chamber LA Ɛ P-wave timed analysis.

Panel B: 4-chamber LA SR P-wave timed analysis.

$Ɛ_R$ was calculated as the sum of the absolute values of $Ɛ_{CT}$ and $Ɛ_{CD.}$

Panel C and D: Symptomatic heart failure with reduced LV ejection fraction.

Panel C: 4-chamber LA Ɛ P-wave timed analysis.

Panel D: 4-chamber LA SR P-wave timed analysis.

Panel E and F: Permanent atrial fibrillation and severe organic mitral regurgitation.

Panel E: 4-chamber LA Ɛ QRS-wave timed analysis.

Panel F: 4-chamber LA SR QRS-wave timed analysis

$Ɛ_R$ Ɛ of the reservoir phase; $Ɛ_{CD}$ Ɛ of the conduit phase; $Ɛ_{CT}$ Ɛ of the contractile phase; $Ɛ_{neg}$ negative Ɛ; $Ɛ_{pos}$ positive Ɛ; $Ɛ_{total}$ total Ɛ; $Ɛ_S$ systolic Ɛ; $Ɛ_e$ early diastolic (E wave) Ɛ; SR_{pos} SR positive; $SR_{late\ neg}$ late negative SR; $SR_{early\ neg}$ early negative peak SR; SR_{CD} SR of the conduit phase; SR_R SR of the reservoir phase; SR_{CT} SR of the contractile phase; SR_S systolic SR; SR_e early diastolic SR (E wave).

Table I: Confusing nomenclature regarding LA mechanics

			Systole	Early Diastole	Late Diastole
			Reservoir	**Conduit**	**Contractile**
Strain (Ɛ)	**TDI (timed to QRS)****	Yu *et al*, [81] 2009	$Ɛ_s$	$Ɛ_e$	$Ɛ_a$
	2D-ST (timed to QRS) **	Kim *et al*, [31]2009	GLS_S	$GLS_E = GLS_S - GLS_A$	GLS_A
	2D-ST (timed to QRS) **	Cameli *et al*, [18, 19, 48] 2009	PALS		PACS
	2D-ST (timed to P) *	Saraiva *et al*,[4] 2010	$Ɛ_{total}$	$Ɛ_{pos}$	$Ɛ_{neg}$
	Proposed nomenclature		**$Ɛ_R$**	**$Ɛ_{CD}$**	**$Ɛ_{CT}$**
Strain rate (SR)	**TDI (timed to P)****	Gulel *et al,* [82] 2009	SR_s	SR_e	SR_a
	TDI (timed to QRS) **	Inaba *et al,* [29] 2005	$SR\text{-}LA_s$	$SR\text{-}LA_e$	$SR\text{-}LA_a$
	2D-ST (timed to QRS) **	Kim *et al*, [31]2009	$GLSR_S$	$GLSR_E$	$GLSR_A$
	2D-ST (timed to P)*	Saraiva et al [4] 2010	SR_{pos}	$SR_{early\ neg}$	$SR_{late\ neg}$
	Proposed nomenclature		**SR_R**	**SR_{CD}**	**SR_{CT}**

Named after events in the LA; ** Named after events in the LV.

Abbreviations: 2D–ST two-dimensional speckle tracking; LA left atrium; TDI tissue Doppler imaging; Ɛ strain; SR strain rate

Proposed nomenclature irrespective of methodology and event timing: $Ɛ_R$ Ɛ of the reservoir phase; $Ɛ_s$ systolic Ɛ; GLS_S global longitudinal Ɛ; PALS peak atrial longitudinal Ɛ during ventricular systole; $Ɛ_{total}$ total Ɛ; $Ɛ_{CD}$ Ɛ of the conduit phase; $Ɛ_e$ early diastolic (E wave) Ɛ; GLS_E global longitudinal Ɛ during early (E wave) diastole; $Ɛ_{pos}$ pos Ɛ; $Ɛ_{CT}$ Ɛ of the contractile phase; $Ɛ_a$ late diastolic Ɛ; GLS_A global longitudinal Ɛ during late (A wave) diastole; PACS peak atrial contraction Ɛ; $Ɛ_{neg}$ negative Ɛ; SR_R SR of the reservoir phase; SR_s systolic SR; $SR\text{-}LA_s$ LA systolic SR; $GLSR_S$ global longitudinal systolic SR; SR_{pos} SR positive; SR_{CD} SR of the conduit phase; SR_e early diastolic (E wave) SR; $SR\text{-}LA_e$ early diastolic LA SR; $GLSR_E$ global longitudinal early diastolic SR; $SR_{early\ neg}$ early negative peak SR; SR_{CT} SR of the contractile phase; SR_a late diastolic (A wave) SR; $SR\text{-}LA_a$ late diastolic LA SR; $GLSR_A$ global longitudinal late diastolic SR; $SR_{late\ neg}$ late negative SR.

Table II: LA Ɛ and SR reference values

			$Ɛ_{CT}$	$Ɛ_{R}$	$Ɛ_{CD}$
Strain (X ±SD)	TDI (timed to P)	Gulel *et al* [82]		Global $^{(2C,4C)}$: BMI<30 Kg/m^2: 38.5± 9.9 % BMI≥30 Kg/m^2: 34.3± 7.8 %	
	2D-ST (timed QRS)	Cameli *et al* [18]		Global$^{(2C,4C)}$: 42.2 ± 6.1 % 4C: 40.1 ± 7.9 % 2C: 44.3 ± 6.0 %	
	2D-ST (timed QRS)	Kim *et al* [31]	Global$^{(2C,4C)}$: 15.3 ± 2.9 % 4C: 13.6 ± 3.4 % 2C: 16.9 ± 4.3 %	Global$^{(2C,4C)}$: 35.7 ± 5.8 % 4C: 33.8 ± 6.3 % 2C: 37.6 ± 7.8 %	Global$^{(2C,4C)}$: 20.4 ± 5.0 % 4C: 20.3 ± 5.1 % 2C: 20.7 ± 6.3 %
	2D-ST (timed P)	*Saraiva et al* [4]	Global $^{(2C,3C, 4C)}$: – 14.6 ± 3.5 %	Global$^{(2C,3C 4C)}$: 37.9 ± 7.6 %	Global$^{(2C,3C, 4C)}$: 23.2 ± 6.7 %
			SR_{CT}	**SR_{R}**	**SR_{CD}**
Strain rate X ±SD)	TDI (timed P)	Gulel *et al* [82]	Global$^{(2C,4C)}$: BMI<30 Kg/m^2: –2.7 ± 0.7 sec^{-1} BMI≥30 Kg/m^2: –2.6 ± 0.6 sec^{-1}	Global$^{(2C,4C)}$: BMI<30 Kg/m^2: 2.4 ± 0.6 sec^{-1} BMI≥30 Kg/m^2 : 2.2 ± 0.5 sec^{-1}	Global$^{(2C,4C)}$: BMI<30 Kg/m^2: –3.1 ± 1.2 sec^{-1} BMI≥30 Kg/m^2 : –2.7 ± 0.9 sec^{-1}
	TDI (timed QRS)	Inaba et al [29]	Global$^{(2C,3C, 4C)}$: – 3.1 ± 1.0 sec^{-1}	Global$^{(2C,3C, 4C)}$: 3.4 ± 1.0 sec^{-1}	Global$^{(2C,3C, 4C)}$: –3.9 ± 1.7 sec^{-1}
	2D-ST (timed QRS)	Kim et al [31]	Global$^{(2C,4C)}$: – 1.95±0.33 sec^{-1} 4C: – 1.71±0.34 sec^{-1} 2C: – 2.19±0.53 sec^{-1}	Global$^{(2C,4C)}$: 1.43±0.24 sec^{-1} 4C: 1.38±0.25 sec^{-1} 2C: 1.48±0.36 sec^{-1}	Global$^{(2C,4C)}$: – 1.65±0.37 sec^{-1} 4C: – 1.69±0.44 sec^{-1} 2C: – 1.61 ± 0.42 sec^{-1}
	2D-ST (timed P)	Saraiva et al [4]	Global$^{(2C,3C, 4C)}$: – 2.3±0.5 sec^{-1}	Global$^{(2C,3C, 4C)}$: 2.0±0.6 sec^{-1}	Global$^{(2C,3C, 4C)}$: – 2.0±0.6 sec^{-1}

Abbreviations: 2C two-chamber; 3C three-chamber; 4C four-chamber; BMI body mass index; 2D–ST two-dimensional speckle tracking; TDI tissue Doppler imaging; Ɛ, strain; SR, strain rate; $Ɛ_R$ reservoir phase Ɛ; $Ɛ_{CD}$ conduit phase Ɛ; $Ɛ_{CT}$ contractile phase Ɛ; SR_R reservoir phase SR; SR_{CD} conduit phase SR; SR_{CT} contractile phase SR.

Table III: Structural and hemodynamic correlates of LA mechanics

Authors	Number	Methodology	Year	Main findings
Saraiva *et al* [4]	64 healthy patients	2D-ST P timed	2010	LA ε_{CD}, ε_{CT}, and ε_{R} correlated with traditional echocardiographic indexes used to evaluate the LA conduit, contractile, and reservoir function respectively.
Wakami *et al* [40]	101 stable sinus rhythm patients undergoing cardiac catheterization	2D-ST QRS timed	2009	LVEDP and LVSVI were independent predictors of LA $\varepsilon_{R.}$ Good correlation between ε_{R} and LVEDP in patients with preserved or reduced LVEF. Most patients with ε_{R} < 30% had elevated LVEDP (≥ 16 mmHg). Most patients with ε_{R} ≥ 45% had normal LVEDP (< 16 mmHg).
Akita *et al* [41]	30 sinus rhythm patients who underwent diagnostic cardiac catheterization	3D-ST	2011	3D-ST LA and ε_{R} correlated significantly with LVEDP.
Kurt *et al* [42]	62 patients who underwent cardiac catheterization	2D-ST QRS timed	2012	LA ε_{R} and ε_{CT} correlated negatively with NT-proBNP. LA ε_{R}, LAV and LVEF were independent predictors of an increase in LVEDP (≥ 16 mmHg). LA ε_{R} ≤ 31.2% predicted LVEDP ≥ 16 mmHg with a sensitivity of 88.2% and a specificity of 92%.
Kuppahally *et al* [43]	65 AF patients (24 paroxysmal 31 persistent)	VVI QRS timed	2010	The extent of LA wall fibrosis assessed by delayed-enhancement MRI was inversely correlated to LA ε_{R} and SR_{R} in AF patients. This relationship was more prominent in patients with persistent compared with paroxysmal AF.
Her *et al* [44]	50 mitral valve surgery patients	2D-ST QRS timed	2012	ε_{R} and SR_{R} correlated significantly with LA interstitial fibrosis (histology) assessed before surgery in patients with mitral valve disease.

Table IV: LA Ɛ and SR in HF

Authors	Number Patients	Methodology	Year	NYHA / LVEF	Main findings
					HF reduced ejection fraction
Cameli *et al* [48]	36 SHF patients	2D-ST QRS timed	2010	NYHA III/IV LVEF 26.1±5 %	$Ɛ_R$ correlated significantly with invasively obtained PCWP (R=-0.81, p<0.01), which was in contrast to the correlation between E/E' and PCWP (R=0.15, p=n.s). $Ɛ_R$ had a higher accuracy to predict an elevated PCWP than LAVI or the E/E' ratio. $Ɛ_R$ < 15.1% had a sensitivity and specificity of 100% and 93.2%, respectively, to predict a PCPW ≥ 18 mmHg.
Donal *et al* [83]	75 CHF patients	TDI QRS timed	2008	NYHA II/III LVEF 30.2±9.6 %	LA $Ɛ_R$ correlated with pVO2 (R = 0.46, p<0,01) and with maximal workload (R=0.41, p<0.01). LA $Ɛ_R$ was an independent predictor of pVO2, in a model adjusted for LAVI and non-invasively obtained LV filling pressures. As other echocardiographic parameters, LA $Ɛ_R$ had a low accuracy (AUC 0.71) to predict a reduced peak VO2 (≤ 14 ml/Kg/m^2).
Helle-Valle *et al* [52]	143 SHF patients	2D-ST	2011	NYHA II-IV LVEF 31±13 %	LA Ɛ was an independent and predictor of a combined endpoint of cardiac death or need for heart transplantation. LA Ɛ when added to age, LVEF and logNT-proBNP increased the quality of the multivariate model to predict the combined endpoint.Mean follow up time: 3 years.
D´Andrea *et al* [49]	314 DCM patients 160 idiopathic 154 ischemic	2D-ST QRS timed TDI QRS timed	2009	NYHA II-IV Idiopathic DCM LVEF 30.1±3.1 % Ischemic DCM LVEF 31.1±3.6 %	LA $Ɛ_R$ was lower for idiopathic than ischemic DCM patients. LA and LAV were independent predictors of peakVO2.
					HF preserved ejection fraction
Kurt *et al* [47]	64 HF patients 25 SHF +20 DHF 19 DD + 27 controls	TDI QRS timed	2009	DHF:62±9 % DD: 63±8 % SHF: 24±9 % Controls: 64±7%	Controls had a higher LA $Ɛ_R$, SR_R, $Ɛ_{CT}$, SR_{CT} than the three groups of patients. SHF had lower LA SR_R, $Ɛ_{CT}$, SR_{CT}, than DD and DHF patients. DHF had lower LA $Ɛ_R$, SR_R than DD patients but similar $Ɛ_{CT}$ and SR_{CT}. LA stiffness (invasive or non-invasive PCWP / $Ɛ_R$) was the most accurate index to distinguish DHF from DD.
Kusunose *et al* [50]	486 patients	2D-ST P timed	2012	56.5%	LA $Ɛ_R$ was the stronger predictor of percent predicted METs, in patients with negative exercise echocardiogram tests.
					Cardiac resynchronization therapy
Yu *et al* [81]	107 HF patients	TDI QRS timed	2007	NYHA III/IV LVEF 26.8±8.0%	LA baseline Ɛ ($Ɛ_R$, $Ɛ_{CD}$ and $Ɛ_{CT}$) improved significantly for the responders (LVESV reduction > 10%) to CRT.
D´Andrea *et al* [24]	90 DCM patients 47 Idiopathic 43 ischemic	2D-ST QRS timed	2007	NYHA III/IV Idiopathic DCM LVEF 30.±4.1 % Ischemic DCM LVEF 31.1±3.2 %	A significant improvement in baseline LA $Ɛ_R$ was obtained only in patients with ischemic DCM who responded (LVESV reduction > 15%) to CRT.
Teixeira *et al* [51]	37 DCM patients 27 Idiopathic 10 ischemic	2D-ST P timed	2012	NYHA III LVEF 23.9±7.1 %	LA $Ɛ_R$ improved significantly with CRT. Baseline LA $Ɛ_{CT}$ was the best predictor of left ventricular reverse remodeling (LVESV reduction > 15%).

s: $Ɛ_R$ strain reservoir phase; $Ɛ_{CD}$ strain conduit phase; $Ɛ_{CT}$ strain contractile phase; SR_R strain rate reservoir phase; SR_{CD} strain rate conduit phase; SR_{CT} strain rate contractile phase; 2D-ST two-dimensional speckle tracking echocardiography; 3D-ST three dimensional speckle tracking; BNP brain natriuretic peptide; CHF chronic heart failu on therapy; DCM dilated cardiomyopathy; DD diastolic dysfunction; DHF diastolic heart failure; HF heart failure; LA left atrium; LAV left atrial volume; LAVI left atrial volume index; LVESV left ventricular end systolic volume; LVEF left ventricular ejection fraction; METs metabolic equivalents; NYHA New York Heart Association; PCWP pulr e; SHF systolic heart failure; TDI tissue Doppler imaging; VVI vector velocity imaging.

Table V: LA Ɛ and SR in AF

Authors	Number	Methodology	Year	Main findings
Inaba *et al* [29]	27 AF patients (8 permanent 19 paroxistic) 50 controls	TDI timed QRS	2005	SR_R, SR_{CD}, SR_{CT} were lower in AF patients than in aged matched controls.
Novo *et al* [53]	50 AF patients 50 controls	2D-ST QRS	2012	LA $Ɛ_R$ was lower in AF patients than in controls and was lower in subjects with recurrent AF than in those with a first episode of AF.
Mochizuki *et al* [34, 54]	40 AF patients[54] (29 paroxistic 11 permanent) 77 controls 47 AF patients[34] (31 paroxistic 16 permanent) 55 controls	3D-ST	2012	3D longitudinal, circumferential and area Ɛ of the reservoir and contractile LA phases were lower for paroxysmal AF patients than for controls, and further reductions were identified for the permanent AF patients. 3D-ST was more accurate than 2D-ST to identify the paroxistic AF patients from a control group.
Cho *et al* [84]	158 CHF patients	Timed QRS	2009	Atrial dyssynchrony (SD of the time to peak $Ɛ_R$ > 39 ms) and LA dimensions were independent predictors for new onset AF in patients with CHF.
				Thromboembolic risk
Shih *et al* [56]	66 permanent AF patients 20 with stroke 46 without stroke	2D-ST timed QRS	2011	Decreased LA $Ɛ_R$ and SR_{CT} were independently associated with stroke in patients with permanent AF.
Saha *et al* [57]	36 AF patients 41 controls	2D-ST timed QRS	2011	LA $Ɛ_R$ was a predictor of a high risk of stroke ($CHADS_2 \geq 2$). LA $Ɛ_R$ and LAVI increased the accuracy of the $CHADS_2$ score to predict a combined endpoint (hospitalization for cardiac causes and/or death).
Azemi *et al* [58]	57 AF patients with stroke/TIA 57 AF controls without stroke/TIA	VVI	2012	Compared to controls, AF patients with a history of stroke / TIA and a low $CHADS_2$ score (≤ 1), had lower LA $Ɛ_R$ and $Ɛ_{CT.}$ LA $Ɛ_{CT}$ was the stronger predictor of stroke / TIA when adjusted to LAVI, LVEF and LV mass.
				Response to cardioversion
Di Salvo *et al* [59]	65 AF patients 40 controls	TDI timed QRS	2005	Baseline (pre CV) LA $Ɛ_R$ and SR_R were independent predictors of sinus rhythm maintenance, 9 months after CV. Baseline $Ɛ_R$ > 22% had a sensitivity of 77% and a specificity of 86% and baseline SR_R > 1.8 s^{-1} had a sensitivity of 92% and a specificity of 79% to predict the maintenance of sinus rhythm, 9 months after CV.
Boyd *et al* [63]	39 AF patients 34 controls	TDI timed QRS	2008	In chronic AF patients, LA myocardial velocity during the LA contraction phase improved up to 6 months after successful CV but remained lower when compared to age matched controls.
Wang *et al* [60]	42 AF patients	TDI timed QRS	2007	Baseline LA SR_{CD} > 2.18 s^{-1} had a sensitivity of 83% and a specificity of 64.3% to predict the maintenance of sinus rhythm 4 weeks after

	27 controls			CV. LA SR_{CD} and LA dimension were independent predictors of CV failure.
Kaya *et al* [62]	22 AF patients	TDI timed QRS	2008	One day after successful CV, LA ε_R ε_{CD} SR_R and SR_{CD} were lower when compared to the baseline values. Ten days after, all values improved significantly. This was similarly to the LAA emptying velocities.
				Response to ablation
Donal *et al* [61]	31 AF patients 15 controls	TDI timed QRS	2010	LA mechanics (ε_R SR_R SR_{CD} SR_{CT}) improved significantly up to 1 year after AF catheter ablation although the values remained lower when compared to a control group.
Tops *et al* [64]	148 AF patients	TDI timed QRS	2011	LA ε_R SR_R ε_{CT} SR_{CT} increased significantly up to 13 months after AF catheter ablation. LA ε_R at baseline was an independent predictor of LA reverse remodeling (LAV reduction ≥ 15%) after catheter ablation.
La Meir *et al* [65]	33 AF patients 20 controls	2D-ST timed QRS	2012	Minimally invasive radiofrequency ablation resulted in significant LA reverse remodeling and improvement in LA ε_R, SR_R, SR_{CD} and SR_{CT} up to 1 year.
Schneider *et al* [66]	118 AF patients (74 paroxistic 44 permanent) 25 controls	TDI timed QRS	2008	LA ε_R SR_R SR_{CT} 24-hours after AF catheter ablation were predictors of sinus rhythm maintenance up to 3 months. Immediately after catheter ablation, a cut-off of 20.5% for ε_R had sensitivity of 99% and a specificity of 78%, to predict the maintenance of sinus rhythm. A baseline cut-off value of 20% for ε_R had a sensitivity of 57% and a specificity of 56% for maintenance of SR after AF catheter ablation.

Abbreviations: ε_R ε reservoir phase; ε_{CD} ε conduit phase; ε_{CT} ε contractile phase; SR_R SR reservoir phase; SR_{CD} SR conduit phase; SR_{CT} SR contractile phase; 2D-ST two-dimensional speckle tracking; 3D-ST three dimensional speckle tracking; AF atrial fibrillation; CHF congestive heart failure; LA left atrium; LAA left atrium appendage; LAV left atrium volume; LAVI left atrium volume index; LV left ventricle; LVEF left ventricular ejection fraction; PAF paroxysmal atrial fibrillation; SD standard deviation; TDI tissue Doppler imaging; TIA transient ischemic accident; VVI vector velocity imaging.

Table VI: LA Ɛ and SR in VHD and ACS

Authors	Number	Methodology	Year	Main findings
				VHD
Mitral valve disease				
Cameli *et al* [67]	126 MR patients (36 mild MR 38 moderate MR 42 severe MR) 52 controls	2D-ST timed QRS	2011	LA $Ɛ_R$ was inversely correlated with MR fraction, LAVI and E/E'. LA $Ɛ_R$ and $Ɛ_{CT}$ were increased in mild MR patients but lower for moderate and further reduced for severe MR patients, when compared to controls.
Cameli *et al* [68]	197 MR patients	2D-ST timed QRS	2012	For each grade of MR, LA $Ɛ_R$ was lower for patients with a history of paroxysmal AF.
Borg et al [70]	27 MR patients 25 controls	TDI timed QRS	2009	LA $Ɛ_R$, SR_R, SR_{CD}, and SR_{CT} were decreased in MR patients.
Candan et al [71]	53 MR patients	2D-ST timed QRS	2013	LA $Ɛ_R$ and LAVI were independent predictors of post-operative AF after surgery for severe MR.
Caso *et al* [72]	53 MS patients 53 controls	TDI timed QRS	2009	LA $Ɛ_R$ and SR_R were lower for moderate MS patients when compared to controls. LA SR_R was an independent predictor of a 3-year combined clinical endpoint (AF, surgery, percutaneous intervention, hospitalization for cardiac cause, thromboembolic events, symptoms) for asymptomatic moderate MS patients, adjusted for age, mitral valve area and LAVI.
Aortic valve disease				
O'Connor *et al* [73]	64 AS patients 20 controls	TDI	2011	All LA Ɛ parameters were reduced in patients with AS, when compared to controls. Poor correlation of LA phasic volumes with LA Ɛ.
Lisi *et al* [75]	43 AS patients 34 controls	2D-ST timed QRS	2012	LA $Ɛ_R$ and $Ɛ_{CT}$ improved up to 3 months after aortic valve replacement. Trans-aortic mean gradient change was an independent predictor of LA $Ɛ_R$. LA $Ɛ_R$ was the strongest predictor LA $Ɛ_R$ was a predictor of post-operative AF.
Mizariene *et al* [76]	34 AR patients (15 moderate AR 19 severe AR 22 controls)	2D-ST	2010	$Ɛ_R$ and SR_R were lower in severe AR patients and were associated with higher LV dimensions and impaired LV diastolic function.
				ACS
Antoni *et al* [79]	320 ST elevation ACS patients	2D-ST	2011	LA $Ɛ_R$ assessed 48 hours after AMI, provided incremental value to LA maximal volume in addition to clinical and echocardiographic parameters, to predict a composite endpoint of death, re-infarction and future admission for HF, up to 27 months of follow up.

Antoni *et al* [78]	407 ST elevation ACS patients	2D-ST	2011	LA $Ɛ_R$ was a predictor of LA late remodeling after AMI, irrespective of LA volume, LV filling pressures and culprit vessel lesion.
Ersbol *et al* [80]	843 AMI patients	2D-ST timed QRS	2013	LA $Ɛ_R$ assessed 48 hours after the AMI, when adjusted for age, LV longitudinal Ɛ and LAVI, was not considered a prognostic predictor of outcome. LV longitudinal Ɛ and LAVI were independent predictors of LA $Ɛ_R$.
Dogan *et al* [85]	90 ST elevation ACS patients 22 controls	2D-ST timed QRS	2013	LA $Ɛ_R$ was lower for AMI patients, when compared to controls. LA $Ɛ_R$ correlated positively with LVEF and negatively with E/E', LA phasic volumes and BNP. LA $Ɛ_R$ > 19.9% had a sensitivity of 55.3% and a specificity of 77.2% to predict a BNP > 100 pg/ml.

Table VII: LA Ɛ and SR in cardiomyopathies and other clinical conditions

Authors	Number	Methodology	Year	Main findings
				Cardiomyopathies
Modesto *et al* [86]	95 AL patients 30 controls 30 DD patients	TDI timed QRS	2005	LA $Ɛ_R$ and SR_R were lower for AL patients with cardiac involvement, when compared to a control group, to a group with LA dilatation and diastolic dysfunction and event to a group with AL but with no cardiac involvement. Contrary to LA ejection fraction, LA $Ɛ_R$ was lower for AL patients with heart failure symptoms.
Telagh *et al* [87]	20 HCM patients 20 controls	TDI timed QRS	2008	LA SR_R SR_{CD} and SR_{CT} were lower in patients with HCM than in controls.
D´Andrea *et al* [88]	40 HT patients 45 elite athletes 25 sedentary controls	2D- ST timed QRS	2008	Contrary to LA diameter, LA $Ɛ_R$ was reduced in patients with hypertension and LVH when compared to athletes. In patients with LVH LA $Ɛ_R$ was a predictor of maximum workload during exercise testing.
				Atrial septal defect
Abd el Rahman *et al* [89]	25 ASD patients (median age 25 y) 30 controls	TDI timed QRS	2005	One week after surgical ASD closure, LA and RA SR_{CT} were significantly diminished when compared to baseline level. This was in contrast to patients submitted to a percutaneous device closure of the ASD.
Di Salvo *et al* [90]	30 ASD patients (mean age 9; 15 device closure 15 surgery closure) 15 controls	TDI timed QRS	2005	6 months after surgical ASD closure, LA and RA $Ɛ_R$ and SR_R where lower when compared to aged matched controls. 6 months after percutaneous device ASD closure LA and RA $Ɛ_R$ and SR_R where similar to aged matched controls.
Boyd *et al* [91]	23 ASO devices patients (mean age 44 years) 30 controls	TDI timed QRS	2008	6 months after percutaneous device closure, LA $Ɛ_R$ SR_{CD} SR_{CT} were significantly reduced when compared to a control group. No difference in LA mechanics between PFO or ASD patients.
				Other Clinical Conditions
D´Ascenzi *et al* [92]	23 soccer athletes 26 controls	2D-ST timed QRS	2011	No significant difference in LA ƐR between soccer players and controls, but LA ƐCT was lower for athletes.
Leong *et al* [93]	100 TEE patients	2D-ST timed QRS TDI	2013	Good correlation between LA $Ɛ_R$ SR_R $Ɛ_{CT}$ SR_{CT} and transesophageal echocardiographic assessed LA appendage emptying velocity and spontaneous echocardiographic contrast. LA mechanics had the highest accuracy to predict LA spontaneous contrast.
Karabay *et al* [94]	153 ischemic stroke patients	2D-ST timed QRS	2013	In ischemic stroke sinus rhythm patients, LA $Ɛ_R$ and $Ɛ_{CT}$ were predictors of LAA thrombus.
Mondillo *et al* [95]	83 HT patients 34 diabetic patients	2D-ST timed QRS	2011	LA $Ɛ_R$ LA $Ɛ_{CD}$ LA $Ɛ_{CT}$ SR_R and SR_{CD} were lower in patients with hypertension or diabetes than in controls, and further reduced in patients with diabetes and hypertension. All patients had a non-dilated LA (LAVI < 28 ml/m^2).

	38 HT + diabetic patients 36 controls			
Motoki *et al* [26]	127 patients	2D-ST VVI	2012	Good agreement for LA mechanics assessed with VVI (Siemens Medical Solutions®) and 2D-ST (GE Medical Systems®) software technologies, especially for the ε_{CT} and SR_{CT}.

Abbreviations: ε_R ε reservoir phase; ε_{CD} ε conduit phase; ε_{CT} ε contractile phase; SR_R SR reservoir phase; SR_{CD} SR conduit phase; SR_{CT} SR contractile phase; 2D-ST two-dimensional speckle tracking; AL amyloidosis; ASD atrial septal defect; ASO atrial septal occluder; HT hypertensive; LA left atrium; LAA left atrium appendage; LAVI left atrium volume index; LVH left ventricular hypertrophy; RA right atrium; TDI tissue Doppler imaging; TEE transesophageal echocardiographic.

Figure 1

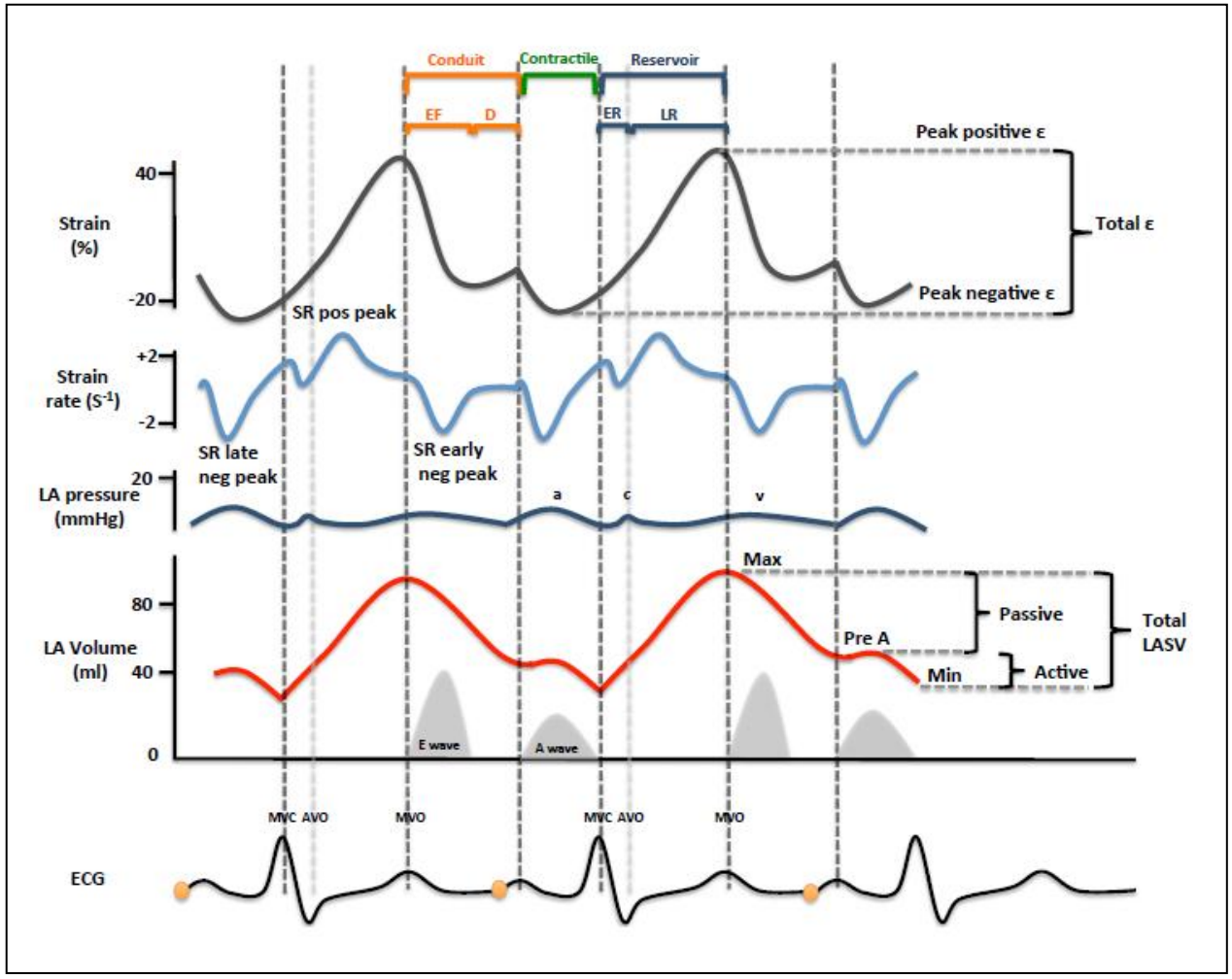
Conduit
Contractile
Reservoir
EF
D
ER
LR
Peak positive ε
Total ε
Peak negative ε
40
Strain (%)
-20
SR pos peak
+2
Strain rate (S-1)
-2
SR late neg peak
SR early neg peak
20
LA pressure (mmHg)
a
c
v
Max
80
LA Volume (ml)
40
Pre A
Passive
Total LASV
Min
Active
0
E wave
A wave
MVC AVO
MVO
MVC AVO
MVO
ECG

Figure 2

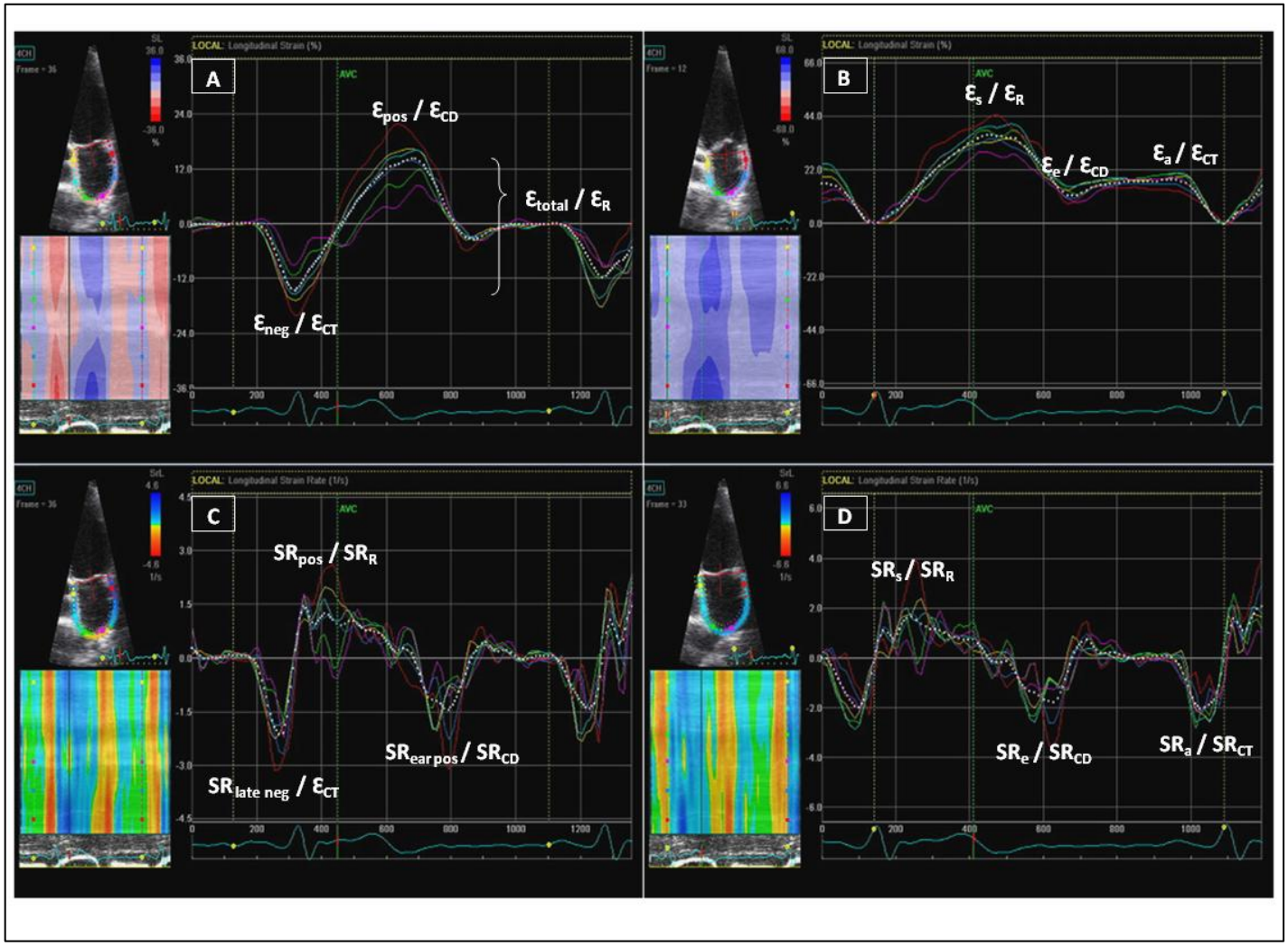
A
ε_{pos} / ε_{CD}
ε_{total} / ε_{R}
ε_{neg} / ε_{CT}
B
ε_{s} / ε_{R}
ε_{e} / ε_{CD}
ε_{a} / ε_{CT}
C
SR_{pos} / SR_{R}
$SR_{ear\ pos}$ / SR_{CD}
$SR_{late\ neg}$ / ε_{CT}
D
SR_{s} / SR_{R}
SR_{e} / SR_{CD}
SR_{a} / SR_{CT}

Figure 3

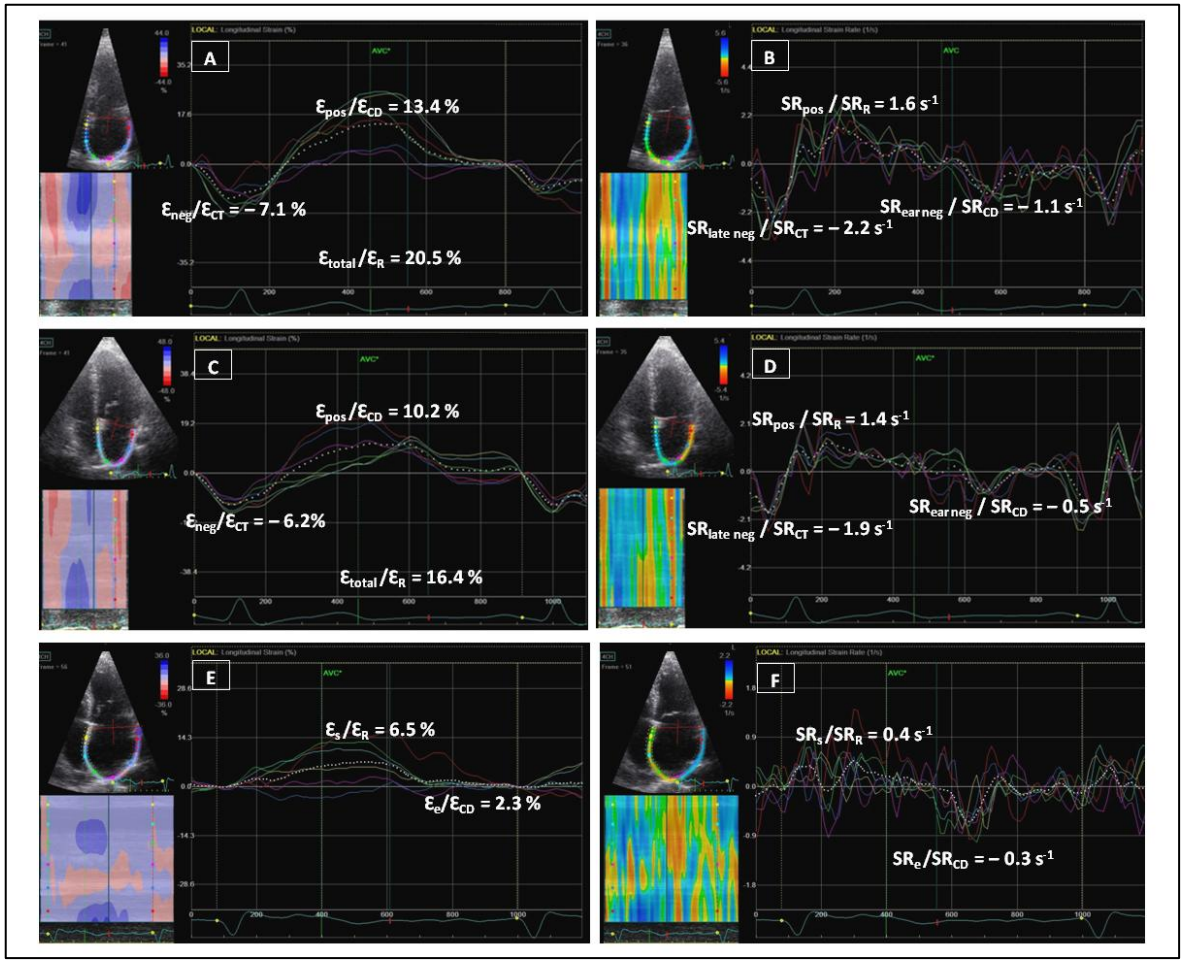
A
$\varepsilon_{pos}/\varepsilon_{CD}$ = 13.4 %
$\varepsilon_{neg}/\varepsilon_{CT}$ = – 7.1 %
$\varepsilon_{total}/\varepsilon_{R}$ = 20.5 %
B
SR_{pos} / SR_{R} = 1.6 s^{-1}
$SR_{ear\,neg}$ / SR_{CD} = – 1.1 s^{-1}
$SR_{late\,neg}$ / SR_{CT} = – 2.2 s^{-1}
C
$\varepsilon_{pos}/\varepsilon_{CD}$ = 10.2 %
$\varepsilon_{neg}/\varepsilon_{CT}$ = – 6.2%
$\varepsilon_{total}/\varepsilon_{R}$ = 16.4 %
D
SR_{pos} / SR_{R} = 1.4 s^{-1}
$SR_{ear\,neg}$ / SR_{CD} = – 0.5 s^{-1}
$SR_{late\,neg}$ / SR_{CT} = – 1.9 s^{-1}
E
$\varepsilon_{s}/\varepsilon_{R}$ = 6.5 %
$\varepsilon_{e}/\varepsilon_{CD}$ = 2.3 %
F
SR_{s}/SR_{R} = 0.4 s^{-1}
SR_{e}/SR_{CD} = – 0.3 s^{-1}

Figure 4

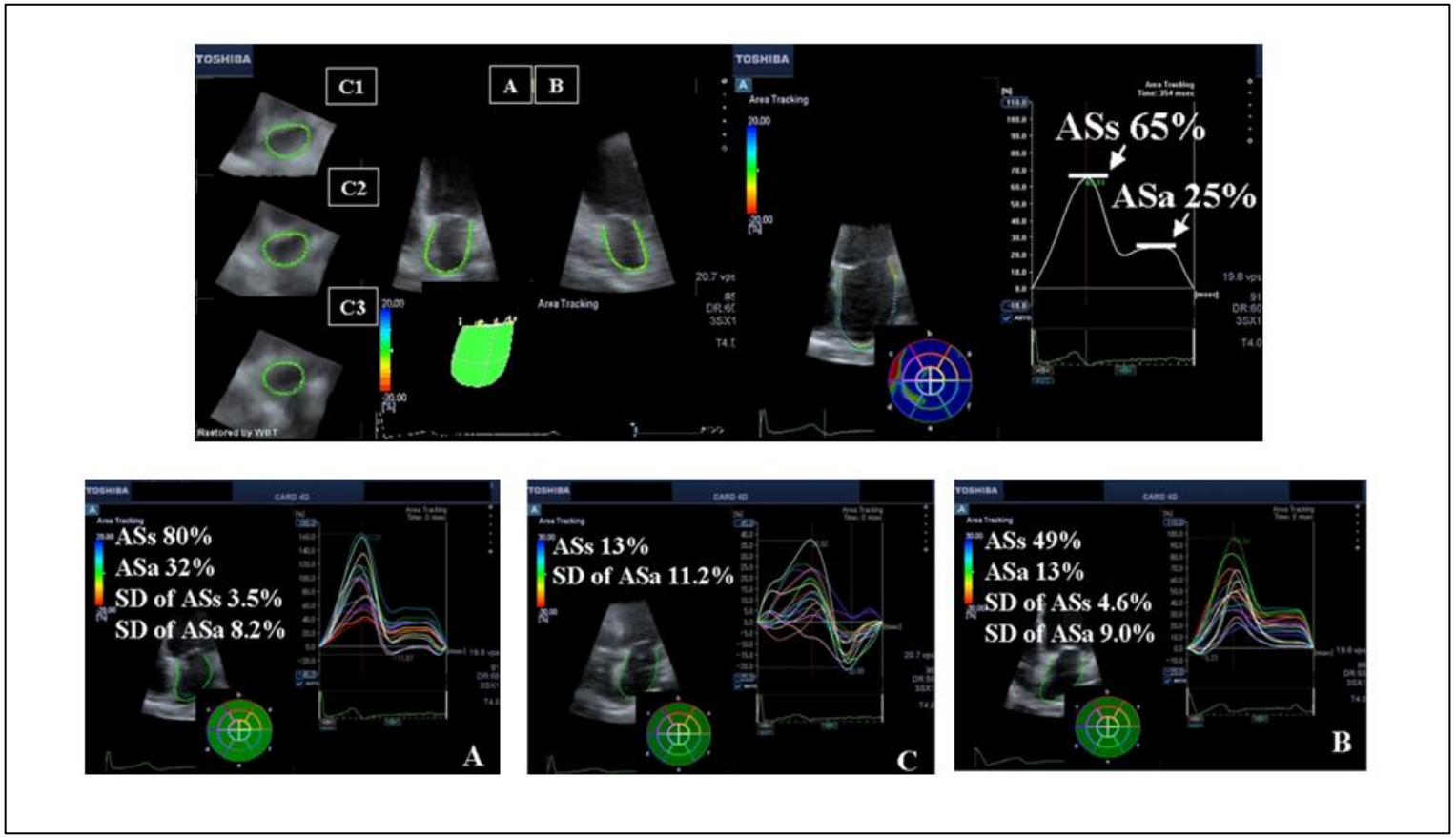
C1
C2
C3
A
B
Area Tracking
ASs 65%
ASa 25%
ASs 80%
ASa 32%
SD of ASs 3.5%
SD of ASa 8.2%
A
ASs 13%
SD of ASa 11.2%
C
ASs 49%
ASa 13%
SD of ASs 4.6%
SD of ASa 9.0%
B

References

1. Hoit BD. Assessing atrial mechanical remodeling and its consequences. *Circulation*. 2005;112:304-306.
2. Mor-Avi V, Lang RM, Badano LP, Belohlavek M, Cardim NM, Derumeaux G, *et al*. Current and evolving echocardiographic techniques for the quantitative evaluation of cardiac mechanics: Ase/eae consensus statement on methodology and indications endorsed by the japanese society of echocardiography. *J Am Soc Echocardiogr*. 2011;24:277-313.
3. Barbier P, Solomon SB, Schiller NB, Glantz SA. Left atrial relaxation and left ventricular systolic function determine left atrial reservoir function. *Circulation*. 1999;100:427-436.
4. Saraiva RM, Demirkol S, Buakhamsri A, Greenberg N, Popovic ZB, Thomas JD, *et al*. Left atrial strain measured by two-dimensional speckle tracking represents a new tool to evaluate left atrial function. *J Am Soc Echocardiogr*. 2010;23:172-180.
5. To AC, Flamm SD, Marwick TH, Klein AL. Clinical utility of multimodality la imaging: Assessment of size, function, and structure. *JACC Cardiovasc Imaging*. 2011;4:788-798.
6. Poutanen T, Jokinen E, Sairanen H, Tikanoja T. Left atrial and left ventricular function in healthy children and young adults assessed by three dimensional echocardiography. *Heart*. 2003;89:544-549.
7. Anwar AM, Geleijnse ML, Soliman OI, Nemes A, ten Cate FJ. Left atrial frank-starling law assessed by real-time, three-dimensional echocardiographic left atrial volume changes. *Heart*. 2007;93:1393-1397.
8. Kim KH. Echocardiographic measurement of left atrial strain as a tool for assessing left atrial function and geometric change. *Korean Circ J*. 2012;42:302-303.
9. Sutherland GR, Di Salvo G, Claus P, D'Hooge J, Bijnens B. Strain and strain rate imaging: A new clinical approach to quantifying regional myocardial function. *J Am Soc Echocardiogr*. 2004;17:788-802.
10. Korinek J, Wang J, Sengupta PP, Miyazaki C, Kjaergaard J, McMahon E, *et al*. Two-dimensional strain--a doppler-independent ultrasound method for quantitation of regional deformation: Validation in vitro and in vivo. *J Am Soc Echocardiogr*. 2005;18:1247-1253.
11. Cho GY, Chan J, Leano R, Strudwick M, Marwick TH. Comparison of two-dimensional speckle and tissue velocity based strain and validation with harmonic phase magnetic resonance imaging. *Am J Cardiol*. 2006;97:1661-1666.
12. Sirbu C, Herbots L, D'hooge J, Claus P, Marciniak A, Langeland T, *et al*. Feasibility of strain and strain rate imaging for the assessment of regional left atrial deformation: A study in normal subjects. *Eur J Echocardiogr*. 2006;7:199-208.
13. Nattel S. Electrophysiologic remodeling. *J Cardiov Electrophys*. 1999;10:1553-1556.
14. Casaclang-Verzosa G, Gersh BJ, Tsang TS. Structural and functional remodeling of the left atrium: Clinical and therapeutic implications for atrial fibrillation. *J Am Coll Cardiol*.51:1-11.
15. Hoit BD, Shao Y, Gabel M, Walsh RA. Left atrial mechanical and biochemical adaptation to pacing induced heart failure. *Cardiovasc Res*. 1995;29:469-474.
16. Hoit BD, Shao Y, Gabel M. Left atrial systolic and diastolic function accompanying chronic rapid pacing-induced atrial failure. *Am J Phys - Heart Circ Phys*. 1998;275:H183-H189.
17. Khan A, Moe GW, Nili N, Rezaei E, Eskandarian M, Butany J, *et al*. The cardiac atria are chambers of active remodeling and dynamic collagen turnover during evolving heart failure. *J Am Coll Cardiol*. 2004;43:68-76.
18. Cameli M, Caputo M, Mondillo S, Ballo P, Palmerini E, Lisi M, *et al*. Feasibility and reference values of left atrial longitudinal strain imaging by two-dimensional speckle tracking. *Cardiovasc Ultrasound*. 2009;7:6 . doi: 10.1186/1476-7120-7-6.
19. Cameli M, Lisi M, Righini FM, Mondillo S. Novel echocardiographic techniques to assess left atrial size, anatomy and function. *Cardiovasc Ultrasound*. 2012;10:4 doi: 10.1186/1476-7120-10-4.
20. Cameli M, Lisi M, Focardi M, Reccia R, Natali BM, Sparla S, *et al*. Left atrial deformation analysis by speckle tracking echocardiography for prediction of cardiovascular outcomes. *Am J Cardiol*. 2012;110:264-269
21. Leitman M, Lysyansky P, Sidenko S, Shir V, Peleg E, Binenbaum M, *et al*. Two-dimensional strain-a novel software for real-time quantitative echocardiographic assessment of myocardial function. *J Am Soc Echocardiogr*. 2004;17:1021-1029.
22. Vianna-Pinton R, Moreno CA, Baxter CM, Lee KS, Tsang TS, Appleton CP. Two-dimensional speckle-tracking echocardiography of the left atrium: Feasibility and regional contraction and relaxation differences in normal subjects. *J Am Soc Echocardiogr*. 2009;22:299-305.

23. Okamatsu K, Takeuchi M, Nakai H, Nishikage T, Salgo IS, Husson S, *et al*. Effects of aging on left atrial function assessed by two-dimensional speckle tracking echocardiography. *J Am Soc Echocardiogr*. 2009;22:70-75.

24. D'Andrea A, Caso P, Romano S, Scarafile R, Riegler L, Salerno G, *et al*. Different effects of cardiac resynchronization therapy on left atrial function in patients with either idiopathic or ischaemic dilated cardiomyopathy: A two-dimensional speckle strain study. *Eur Heart J*. 2007;28:2738-2748.

25. Di Salvo G, Pacileo G, Castaldi B, Gala S, Morelli C, D'Andrea A, *et al*. Two-dimensional strain and atrial function: A study on patients after percutaneous closure of atrial septal defect. *Eur J Echocardiogr*. 2009;10:256-259.

26. Motoki H, Dahiya A, Bhargava M, Wazni OM, Saliba WI, Marwick TH, *et al*. Assessment of left atrial mechanics in patients with atrial fibrillation: Comparison between two-dimensional speckle-based strain and velocity vector imaging. *J Am Soc Echocardiogr*. 2012;25:428-435.

27. McDicken WN, Sutherland GR, Moran CM, Gordon LN. Colour doppler velocity imaging of the myocardium. *Ultrasound Med Biol*. 1992;18:651-654.

28. Liu Y-T, Li R-J, Fang F, Zhang Q, Yan BP-Y, Lam Y-Y, *et al*. Left atrial function assessed by tissue doppler imaging as a new predictor of cardiac events after non-st-elevation acute coronary syndrome. *Echocardiography*. 2012;29:785-792.

29. Inaba Y, Yuda S, Kobayashi N, Hashimoto A, Uno K, Nakata T, *et al*. Strain rate imaging for noninvasive functional quantification of the left atrium: Comparative studies in controls and patients with atrial fibrillation. *J Am Soc Echocardiogr*. 2005;18:729-736.

30. D'hooge J, Heimdal A, Jamal F, Kukulski T, Bijnens B, Rademakers F, *et al.* Regional strain and strain rate measurements by cardiac ultrasound: Principles, implementation and limitations. *Eur J Echocardiogr*. 2000;1:154-170.

31. Kim DG, Lee KJ, Lee S, Jeong S-Y, Lee YS, Choi YJ, *et al*. Feasibility of two-dimensional global longitudinal strain and strain rate imaging for the assessment of left atrial function: A study in subjects with a low probability of cardiovascular disease and normal exercise capacity. *Echocardiography*. 2009;26:1179-1187

32. Boyd AC, Richards DAB, Marwick T, Thomas L. Atrial strain rate is a sensitive measure of alterations in atrial phasic function in healthy ageing. *Heart*. 2011;97:1513-1519.

33. Park CS, Kim Y-K, Song HC, Choi EJ, Ihm S-H, Kim H-Y, *et al*. Effect of preload on left atrial function: Evaluated by tissue doppler and strain imaging. *Eur Heart J Cardiovasc Imaging*. 2012; 13(11):938-47.

34. Mochizuki A, Yuda S, Oi Y, Kawamukai M, Nishida J, Kouzu H, *et al*. Assessment of left atrial deformation and synchrony by three-dimensional speckle-tracking echocardiography: Comparative studies in healthy subjects and patients with atrial fibrillation. *J Am Soc Echocardiogr*. 2013;26:165-174.

35. Luo X, Fang F, Sun J, Xie J, Lee A, Zhang Q, *et al*. Three-dimensional endocardial strain: A novel parameter for assessment of left ventricular systolic function in heart failure. *Eur J Echocardiogr*. 2011;12:ii48.

36. Moller JE, Hillis GS, Oh JK, Seward JB, Reeder GS, Wright RS, *et al*. Left atrial volume: A powerful predictor of survival after acute myocardial infarction. *Circulation*. 2003;107:2207-2212.

37. Tsang TS, Barnes ME, Gersh BJ, Bailey KR, Seward JB. Left atrial volume as a morphophysiologic expression of left ventricular diastolic dysfunction and relation to cardiovascular risk burden. *Am J Cardiol*. 2002;90:1284-1289.

38. Møller JE, Hillis GS, Oh JK, Seward JB, Reeder GS, Wright RS, *et al*. Left atrial volume: A powerful predictor of survival after acute myocardial infarction. *Circulation*. 2003;107:2207-2212.

39. Douglas PS. The left atrium: A biomarker of chronic diastolic dysfunction and cardiovascular disease risk. *J Am Coll Cardiol*. 2003;42:1206-1207.

40. Wakami K, Ohte N, Asada K, Fukuta H, Goto T, Mukai S, *et al*. Correlation between left ventricular end-diastolic pressure and peak left atrial wall strain during left ventricular systole. *J Am Soc Echocardiogr*. 2009;22:847-851.

41. Akita N, Ohte N, Wakami K, Kikuchi S, Ikehara N, Fujita H, *et al*. Left atrial endocardial surface area strain assessed by 3-dimensional speckle tracking imaging is a useful method in assessing left ventricular end-diastolic pressure. *Circulation*. 2011;124:A15077-A15077.

42. Kurt M, Tanboga IH, Aksakal E, Kaya A, Isik T, Ekinci M, *et al*. Relation of left ventricular end-diastolic pressure and n-terminal pro-brain natriuretic peptide level with left atrial deformation parameters. *Eur Heart J Cardiovasc Imaging*. 2012;13:524-530.

43. Kuppahally SS, Akoum N, Burgon NS, Badger TJ, Kholmovski EG, Vijayakumar S, *et al*. Left atrial strain and strain rate in patients with paroxysmal and persistent atrial fibrillation / clinical perspective. *Circulation Cardiovasc Imaging*. 2010;3:231-239.

44. Her A-Y, Choi E-Y, Shim CY, Song BW, Lee S, Ha J-W, *et al*. Prediction of left atrial fibrosis with speckle tracking echocardiography in mitral valve disease: A comparative study with histopathology. *Korean Circ J*. 2012;42:311-318.

45. Gottdiener JS, Kitzman DW, Aurigemma GP, Arnold AM, Manolio TA. Left atrial volume, geometry, and function in systolic and diastolic heart failure of persons > or =65 years of age (the cardiovascular health study). *Am J Cardiol*. 2006;97:83-89.

46. Melenovsky V, Borlaug BA, Rosen B, Hay I, Ferruci L, Morell CH, *et al*. Cardiovascular features of heart failure with preserved ejection fraction versus nonfailing hypertensive left ventricular hypertrophy in the urban baltimore community: The role of atrial remodeling/dysfunction. *J Am Coll Cardiol*. 2007;49:198-207.

47. Kurt M, Wang J, Torre-Amione G, Nagueh SF. Left atrial function in diastolic heart failure. *Circ Cardiovasc Imaging*. 2009;2:10-15.

48. Cameli M, Lisi M, Mondillo S, Padeletti M, Ballo P, Tsioulpas C, *et al*. Left atrial longitudinal strain by speckle tracking echocardiography correlates well with left ventricular filling pressures in patients with heart failure. *Cardiovasc Ultrasound*. 2010;8:14 doi: 10.1186/1476-7120-8-14.

49. D'Andrea A, Caso P, Romano S, Scarafile R, Cuomo S, Salerno G, *et al*. Association between left atrial myocardial function and exercise capacity in patients with either idiopathic or ischemic dilated cardiomyopathy: A two-dimensional speckle strain study. *Int J Cardiol*. 2009;132:354-363.

50. Kusunose K, Motoki H, Popovic ZB, Thomas JD, Klein AL, Marwick TH. Independent association of left atrial function with exercise capacity in patients with preserved ejection fraction. *Heart*. 2012;98:1311-1317.

51. Teixeira R, Moreira N, Soares F, Ribeiro N, Martins R, Elvas L, *et al*. Left atrial total longitudinal strain improves after cardiac resynchronization therapy. *Eur Heart J Cardiovasc Imaging*. 2012;13 (suppl 1):i166.

52. Helle-Valle T, Opdahl A, Broch K, Gude E, Andreassen A, Smiseth OA, *et al*. Left atrial strain by speckle tracking echocardiography in patients with heart failure - an independent and incremental predictor of cardiac death or need of heart transplantation *Circulation*. 2011;124: A8551.

53. Novo G, Zito C, Di Bella G, Fazio G, La Franca ML, Miccichè R, *et al*. Evaluation of atrial function by 2d strain echocardiography in patients with atrial fibrillation. *J Cardiovasc Echography*. 2012;22:118-124.

54. Mochizuki A, Yuda S, Ohi Y, kawamukai M, Nishida J, Kouzu H, *et al*. Assessment of left atrial dysfunction and dyssynchrony by 3 dimensional speckle tracking in patients with atrial fibrilation. *J Am Coll Cardiol*. 2012;59:E1266.

55. Furukawa A, Hoshiba H, Miyasaka C, Sato H, Negai Y, Yamanaka A, *et al*. Assessment of left atrial function in patients with paroxysmal atrial fibrillation by using three-dimensional speckle tracking imaging. *Circulation*. 2011;124:A11870.

56. Shih J-Y, Tsai W-C, Huang Y-Y, Liu Y-W, Lin C-C, Huang Y-S, *et al.* Association of decreased left atrial strain and strain rate with stroke in chronic atrial fibrillation. *J Am Soc Echocardiogr*. 2011;24:513-519.

57. Saha SK, Anderson PL, Caracciolo G, Kiotsekoglou A, Wilansky S, Govind S, *et al*. Global left atrial strain correlates with chads2 risk score in patients with atrial fibrillation. *J Am Soc Echocardiogr*. 2011;24:506-512.

58. Azemi T, Rabdiya VM, Ayirala SR, McCullough LD, Silverman DI. Left atrial strain is reduced in patients with atrial fibrillation, stroke or tia, and low risk chads(2) scores. *J Am Soc Echocardiogr*. 2012;25:1327-1332.

59. Di Salvo G, Caso P, Lo Piccolo R, Fusco A, Martiniello AR, Russo MG, *et al*. Atrial myocardial deformation properties predict maintenance of sinus rhythm after external cardioversion of recent-onset lone atrial fibrillation. *Circulation*. 2005;112:387-395.

60. Wang T, Wang M, Fung JWH, Yip GWK, Zhang Y, Ho PP, *et al*. Atrial strain rate echocardiography can predict success or failure of cardioversion for atrial fibrillation: A combined transthoracic tissue doppler and transoesophageal imaging study. *Int J Cardiol*. 2007;114:202-209.

61. Donal E, Ollivier R, Veillard D, Hamonic S, Pavin D, Daubert JC, *et al*. Left atrial function assessed by trans-thoracic echocardiography in patients treated by ablation for a lone paroxysmal atrial fibrillation. *Eur J Echocardiogr*. 2010;11:845-852.

62. Kaya EB, Tokgozoglu L, Aytemir K, Kocabas U, Tulumen E, Deveci OS, *et al*. Atrial myocardial deformation properties are temporarily reduced after cardioversion for atrial fibrillation and correlate well with left atrial appendage function. *Eur J Echocardiogr*. 2008;9:472-477.

63. Boyd AC, Schiller NB, Ross DL, Thomas L. Segmental atrial contraction in patients restored to sinus rhythm after cardioversion for chronic atrial fibrillation: A colour doppler tissue imaging study. *Eur J Echocardiogr*. 2008;9:12-17.

64. Tops LF, Delgado V, Bertini M, Marsan NA, Den Uijl DW, Trines SA, *et al*. Left atrial strain predicts reverse remodeling after catheter ablation for atrial fibrillation. *J Am Coll Cardiol*. 2011;57:324-331.

65. La Meir M, Gelsomino S, Lucà F, Pison L, Rao CM, Wellens F, *et al*. Improvement of left atrial function and left atrial reverse remodeling after minimally invasive radiofrequency ablation evaluated by two-dimensional speckle tracking echocardiography. *J Thorac Cardiovasc Surg. 2013; 146(1):72-7*. .

66. Schneider C, Malisius R, Krause K, Lampe F, Bahlmann E, Boczor S, *et al*. Strain rate imaging for functional quantification of the left atrium: Atrial deformation predicts the maintenance of sinus rhythm after catheter ablation of atrial fibrillation. *Eur Heart J*. 2008;29:1397-1409.

67. Cameli M, Lisi M, Giacomin E, Caputo M, Navarri R, Malandrino A, *et al*. Chronic mitral regurgitation: Left atrial deformation analysis by two-dimensional speckle tracking echocardiography. *Echocardiography*. 2011;28:327-334.

68. Cameli M, Lisi M, Righini F, Focardi M, Alfieri O, Mondillo S. Left atrial speckle tracking analysis in patients with mitral insufficiency and history of paroxysmal atrial fibrillation. *Int J Cardiovasc Imaging. 2012 28; (7):1663-1670.*

69. Aksakal E, Simsek Z, Sevimli S, Karakelleoglu S, Tanboga IH, Kurt M. Quantitative assessment of the left atrial myocardial deformation in patients with chronic mitral regurgitation by strain and strain rate imaging: An observational study. *Anadolu Kardiyol Derg*. 2012;12:377-383.

70. Borg AN, Pearce KA, Williams SG, Ray SG. Left atrial function and deformation in chronic primary mitral regurgitation. *Eur J Echocardiogr*. 2009;10:833-840.

71. Candan O, Ozdemir N, Aung SM, Dogan C, Karabay CY, Gecmen C, *et al*. Left atrial longitudinal strain parameters predict postoperative persistent atrial fibrillation following mitral valve surgery: A speckle tracking echocardiography study. *Echocardiography. 2013;30(9):*1061-8.

72. Caso P, Ancona R, Di Salvo G, Comenale Pinto S, Macrino M, Palma V, *et al*. Atrial reservoir function by strain rate imaging in asymptomatic mitral stenosis: Prognostic value at 3 year follow-up. *Eur J Echocardiogr*. 2009;10:753-759.

73. O'Connor K, Magne J, Rosca M, Pierard LA, Lancellotti P. Left atrial function and remodelling in aortic stenosis. *Eur J Echocardiogr*. 2011;12:299-305.

74. Calin A, Popescu B, Beladan C, Rosca M, Moise B, Voinea F, *et al*. Assessment of left atrial function in patients with left ventricular hypertrophy: Comparison between aortic stenosis and hypertension. *Eur Heart J*. 2010;31:952.

75. Lisi M, Henein MY, Cameli M, Ballo P, Reccia R, Bennati E, *et al*. Severity of aortic stenosis predicts early post-operative normalization of left atrial size and function detected by myocardial strain. *Int J Cardiol. 2013; 167 (4): 1450–55*.

76. Mizariene V, Bucyte S, Pociute E, Zaliaduonyte-Peksiene D, Baronaite-Dudoniene K, Sileikiene R, *et al.* Left atrial function by speckle tracking echocardiography in aortic regurgitation patients. *Eur J echocardiogr*. 2010;11:ii89.

77. Kuhl JT, Moller JE, Kristensen TS, Kelbaek H, Kofoed KF. Left atrial function and mortality in patients with nstemi an mdct study. *JACC Cardiovasc Imaging*. 2011;4:1080-1087.

78. Antoni ML, Ten Brinke EA, Marsan NA, Atary JZ, Holman ER, van der Wall EE, *et al*. Comprehensive assessment of changes in left atrial volumes and function after st-segment elevation acute myocardial infarction: Role of two-dimensional speckle-tracking strain imaging. *J Am Soc Echocardiogr*. 2011;24:1126-1133.

79. Antoni ML, ten Brinke EA, Atary JZ, Marsan NA, Holman ER, Schalij MJ, *et al*. Left atrial strain is related to adverse events in patients after acute myocardial infarction treated with primary percutaneous coronary intervention. *Heart*. 2011;97:1332-1337.

80. Ersboll M, Andersen MJ, Valeur N, Mogensen UM, Waziri H, Moller JE, *et al*. The prognostic value of left atrial peak reservoir strain in acute myocardial infarction is dependent on left ventricular longitudinal function and left atrial size. *Circ Cardiovasc Imaging*. 2013;6:26-33.

81. Yu C-M, Fang F, Zhang Q, Yip GWK, Li CM, Chan JY-S, *et al*. Improvement of atrial function and atrial reverse remodeling after cardiac resynchronization therapy for heart failure. *J Am Coll Cardiol*. 2007;50:778-785

82. Gulel O, Yuksel S, Soylu K, Kaplan O, Yilmaz O, Kahraman H, *et al*. Evaluation of left atrial functions by color tissue doppler imaging in adults with body mass indexes >or=30 kg/m(2) versus those <30 kg/m (2). *Int J Cardiovasc Imaging*. 2009;25:371-377.

83. Donal E, Raud-Raynier P, De Place C, Gervais R, Rosier A, Roulaud M, *et al*. Resting echocardiographic assessments of left atrial function and filling pressure interest in the understanding of exercise capacity in patients with chronic congestive heart failure. *J Am Soc Echocardiogr*. 2008;21:703-710.

84. Cho G-Y, Jo S-H, Kim M-K, Kim H-S, Park W-J, Choi Y-J, *et al*. Left atrial dyssynchrony assessed by strain imaging in predicting future development of atrial fibrillation in patients with heart failure. *Int J Cardiol*. 2009;134:336-341.

85. Dogan CD, Ozdemir ND, Hatipoglu SD, Bakal RBD, Omaygenc MOD, Dindar BD, *et al*. Relation of left atrial peak systolic strain with left ventricular diastolic dysfunction and brain natriuretic peptide level in patients presenting with st-elevation myocardial infarction. *Cardiovasc Ultrasound*. 2013;11(1):24.

86. Modesto KM, Dispenzieri A, Cauduro SA, Lacy M, Khandheria BK, Pellikka PA, *et al*. Left atrial myopathy in cardiac amyloidosis: Implications of novel echocardiographic techniques. *Eur Heart J*. 2005;26:173-179.

87. Telagh R, Hui W, Abd El Rahman M, Berger F, Lange P, Abdul-Khaliq H. Assessment of regional atrial function in patients with hypertrophic cardiomyopathies using tissue doppler imaging. *Pediatric Cardiology*. 2008;29:301-308.

88. D'Andrea A, De Corato G, Scarafile R, Romano S, Reigler L, Mita C, *et al.* Left atrial myocardial function in either physiological or pathological left ventricular hypertrophy: A two-dimensional speckle strain study. *Br J Sports Med*. 2008;42:696-702.

89. Abd El Rahman MY, Hui W, Timme J, Ewert P, Berger F, Dsebissowa F, *et al*. Analysis of atrial and ventricular performance by tissue doppler imaging in patients with atrial septal defects before and after surgical and catheter closure. *Echocardiography*. 2005;22:579-585.

90. Di Salvo G, Drago M, Pacileo G, Rea A, Carrozza M, Santoro G, *et al*. Atrial function after surgical and percutaneous closure of atrial septal defect: A strain rate imaging study. *J Am Soc Echocardiogr*. 2005;18:930-933.

91. Boyd AC, Cooper M, Thomas L. Segmental atrial function following percutaneous closure of atrial septum using occluder device. *J Am Soc Echocardiogr*. 2009;22:508-516.

92. D'Ascenzi F, Cameli M, Zaca V, Lisi M, Santoro A, Causarano A, *et al*. Supernormal diastolic function and role of left atrial myocardial deformation analysis by 2d speckle tracking echocardiography in elite soccer players. *Echocardiography*. 2011;28:320-326.

93. Leong DP, Penhall A, Perry R, Shirazi M, Altman M, Chong D, *et al*. Speckle-tracking strain of the left atrium: A transoesophageal echocardiographic validation study. *Eur Heart J Cardiovasc Imaging*. 2013;11:11.

94. Karabay CY, Zehir R, Güler A, Oduncu V, Kalayci A, Aung SM, *et al*. Left atrial deformation parameters predict left atrial appendage function and thrombus in patients in sinus rhythm with suspected cardioembolic stroke: A speckle tracking and transesophageal echocardiography study. *Echocardiography*. 2013;30:572-581.

95. Mondillo S, Cameli M, Caputo ML, Lisi M, Palmerini E, Padeletti M, *et al*. Early detection of left atrial strain abnormalities by speckle-tracking in hypertensive and diabetic patients with normal left atrial size. *J Am Soc Echocardiogr*. 2011;24:898-908.

Review Article Number 2

Ultrasonagraphic Vascular Mechanics to Assess Arterial Stiffness: A Review

Eur Heart J Cardiovasc Imaging. 2016 Mar; 17(3): 233-46

Rogério Teixeira[1,2*] MD; Maria João Vieira[3] MD, PhD; Alexandra Gonçalves[4,5] MD, MMSc, PhD; Nuno Cardim[6] MD, PhD, FESC, Lino Gonçalves[1,2] MD, PhD, FESC

*Corresponding Author

[1] Serviço de Cardiologia, Centro Hospitalar e Universitário de Coimbra – Hospital Geral, Coimbra, Portugal

[2] Faculdade de Medicina Universidade de Coimbra, Coimbra, Portugal

[3] Serviço de Cardiologia, Hospital de Santarém, Santarém, Portugal

[4] Cardiovascular Division, Brigham and Women's Hospital, Boston, MA, USA

[5] Faculdade de Medicina da Universidade do Porto, Porto, Portugal

[6] Serviço de Cardiologia, Hospital da Luz, Lisboa, Portugal

Word count: 4764 words (no references or tables)

Abrreviation List

2D-STE: Two-Dimensional Speckle Tracking Echocardiography

β_1: Aortic Stiffness Index

ε: Strain

AS: Aortic Stenosis

AR: Aortic Regurgitation

AVA: Aortic Valve Area

CAD: Coronary Artery Disease

CCA: Commom Carotid Artery

CIMT: Carotid Intima-Media Thickening

LV: Left Ventricular

SR: Strain Rate

TEE: Transesophageal Echocardiography

VVI: Vector Velocity Imaging

Abstract

In recent years, the role of arterial stiffness in development of cardiovascular diseases has been explored more extensively. Local arterial stiffness may be gauged via ultrasound, measuring pulse transit time relative to changing vessel diameters and distending pressures. Recently, direct vessel-wall tracking systems have been devised based on new ultrasonographic methodologies, such as tissue Doppler imaging and speckle-tracking analysis – vascular mechanics. These advances have been evaluated in varying arterial distributions, are proven surrogates of pulse wave velocity, and are ascending in clinical importance. In the course of this review, we describe fundamental concepts and methodologies involved in ultrasound assessment of vascular mechanics. We also present relevant clinical studies and discuss the potential clinical utility of such diagnostic pursuits.

Keywords: Arterial Stiffness; Speckle Tracking, Tissue Dopper Imaging; Vascular Mechanics; Strain; Strain Rate

Introduction

The development of accurate, noninvasive methods for early diagnosis of vascular degenerative changes is of significant clinical interest, given that cardiovascular disease remains the leading cause of death worldwide (1).

Arterial stiffness refers to arterial wall rigidity (2). It increases with age but it is also problematic in a number of systemic diseases. Moreover, changes in arterial stiffness are thought to occur in advance of clinically apparent cardiovascular disease (3). Consequently, appraisal of arterial stiffness in routine clinical practice may detect, predict and eventually prevent cardiovascular diseases (4).

The gold standard for study of arterial stiffness is carotid-femoral pulse wave velocity (PWV), which is usually obtained by tonometry or through mechanotransducers (4). Recently, a combination of echocardiography and pulse-wave Doppler has been optimized for PWV testing, but it has not attained gold-standard status as yet (5).

Ultrasound technology is capable of delivering dynamic images of the heart and central arteries. During the past decade, automated techniques for sophisticated analysis of cardiac mechanics have evolved (6), such as Doppler-based tissue velocity measurements (known as tissue Doppler imaging [TDI]) and speckle tracking (ST), based on displacement measurement (6). Regional and global parameters of myocardial mechanics, including displacement, velocity, strain (ε), and strain rate (SR), are currently quantifiable (7). Early applications of these new methodologies involved the study of cardiac chambers (6), but its usage has been expanded and validated for the study of vascular wall mechanics.

This manuscript is primarily intended to provide a critical review of and TDI and ST, as emergent techniques for assessing vascular wall mechanics. Herein, fundamental concepts and methodologies are detailed. We also summarize key clinical studies, stratified by methods used and by vascular territories examined. Finally, the drawbacks and the growing importance of evaluating arterial stiffness are discussed.

Vascular Stiffening

Arterial stiffening is one of the earliest manifestations of adverse structural and functional changes within vascular walls. Degenerative stiffening of arterial beds (ie, arteriosclerosis) should be differentiated from atherosclerosis (8). Degenerative stiffness implies resistance to vascular deformation and it is greatly influenced by radius, wall thickness, and vessels elastic modulus (E), the latter gauging stress/strain relationship is also known as Young's modulus (2). In other words, vascular stiffening equates with a reduced capacity for arterial expansion and recoil in response to pressure changes (9). In contrast, atherosclerosis represents the occlusive result of endovascular inflammatory disease, lipid oxidation, and plaque formation (8). Arteriosclerosis and atherosclerosis tend to coexist, causing progressive, diffuse, and age-related deterioration in all vascular beds (2).

From a physiopathology perspective, vascular stiffening is essentially a degradative state conferred by a string of biomolecular mishaps, including fragmentation of elastin, increased deposition of collagen, calcification, glycation of both elastin and collagen, and cross-linking of collagen by advanced glycation end-products (10). In consequence, the increased arterial stiffness leads to elevated central arterial blood pressure, resulting in higher central pulse pressure (9) and a subsequent increase in left ventricular (LV) load, which then promotes LV hypertrophy (11). Furthermore, diminished diastolic blood pressure reduces coronary perfusion, predisposing the heart to ischemia (12). Apart from inherent cardiac damage, elevated arterial pulsatility also injures the microcirculation of various organs, especially those with high perfusion requirements, namely kidney and brain, contributing to decline in glomerular filtration rate (11) and in cognitive function (13).

Vascular stiffness is non-uniform disease process that preferentially affects proximal (vs distal) arterial segments (14) which increases with age (15, 16), even in the absence of vascular disease or other risk factors (15). Arteries also stiffen in conditions such as hypertension (17), diabetes (18), and chronic renal disease (19). Some sources have thus suggested that arterial stiffness screening may be appropriate for patients predisposed to hypertension, aiming to prevent or delay the progression of subclinical arterial stiffening and the onset of hypertension (20). An array of medical conditions, such as connective tissue disorders (21), aortic valvular stenosis (22) and regurgitation (23), hypertrophic cardiomyopathy (24), and heart failure with preserved (25, 26) or reduced (27) left ventricular ejection fraction, commonly present vascular stiffening.

Serving as a reliable biomarker, increased arterial stiffness is one of the most important risk factors in cardiovascular mortality(28). Vascular stiffening is an independent

predictor of coronary heart disease and stroke in otherwise healthy subjects and an independent predictor of community-wide mortality (29).

The latest European guidelines for managing arterial hypertension recommend vascular stiffness testing to evaluate target organ damage (3). Considering that aortic stiffness is a function of prevailing blood pressure, effective antihypertensive treatment is expected to encourage pliability. Nevertheless, such medications may differ in their effects on structure and function of arterial walls (2), and calcium channel blockers or angiotensin-converting enzyme inhibitors appear more beneficial than beta-blockers and diuretics in this regard (30).

Classic Vascular Stiffening Assessment

Measurement of PWV is generally viewed as a simple, non-invasive, robust, and reproducible method of assessing arterial stiffness. Carotid-femoral PWV is measured directly, in accordance with the widely accepted propagative model of the arterial system (10). PWV and vascular compliance are inversely related, meaning that a rigid vessel will conduct pulse waves faster than a more distensible and compliant one. The relationship between PWV and arterial distensibility is embodied in the Bramwell and Hill equation as follows: $PWV = \sqrt{(V \times \Delta P/\rho \times \Delta V)}$, where ρ is blood density, V is blood volume, and P is arterial blood pressure. PWV is determined by measuring pulse transit time of pressure waveforms at two points along a vascular segment (figure) (2). Mechanotransducers or high-fidelity applanation tonometers are customary devices for obtaining carotid-femoral PWV measurements (4).

Ultrasound-based methods are also commonly used to assess local mechanical properties of arterial walls (4). In this way, arterial stiffness is directly determined from changes in pressure that dictate volume fluctuations, without need of a circulatory model (4). Derived from pressure and diameter measurements, vascular stiffness may be expressed as distensibility, compliance, Peterson's elastic modulus, or Young's elastic modulus – Table 1. Ultrasound also enables estimation of carotid intima-media thickening (CIMT), a standard marker of atherosclerosis (31). Furthermore, Doppler studies permit calculation of PWV, using the difference between two recording sites in the line of pulse travel and the delay in flow wave between these corresponding points (32).

Echo-tracking systems are based on a radiofrequency tracking of the B-mode image of the vessel (4). The vessel diameter in end diastole and its stroke change in diameter are obtained with a very high spatial and temporal resolution, acheiving highly precise measurements of the vessel distension in real time (33).

It is required the simultaneous measurement of the local blood pressure, usually obtained by applanation tonometry of the vessel (4). In this way the stiffnees index, arterial

compliance and the Young's elastic modulus are determined directly and assumptions regarding models of the circulation are not required (33). The local PWV can be calculated from the time delay between the two adjacent distension waveforms, and some systems also provide the local PWV using online "one-point" measurements (34).

Since the 1970's, many publications have addressed the indices above in terms of its normal reference values, clinical applications, and overall utility (5). However, none has proved superiority, and all present limitations in measurement and interpretation (5). The validity and reproducibility of these methods differ considerably, in consequence, none can be pointed as gold standard for evaluating local arterial stiffness at present time (35).

Vascular Mechanics

In the past decade, a number of semi-automated techniques for sophisticated analysis of cardiac mechanics have emerged from two-dimensional B-mode ultrasound images (6): (a) TDI velocity measurements and (b) ST technology have dominated the field.

The TDI method allows the quantification of regional tissue motion velocity (36). Low-pass wall filters are used to display low-velocity signals originating from moving tissue, thereby excluding high-velocity signals of flowing blood (6). Hence, regional activity is quantified, independently of cardiac rotation, motion, and tethering effect (37). Of note, the imaging angle must be adjusted to ensure parallel alignment of the sampling window with the myocardial segment of interest (38).

Two-dimensional speckle-tracking echocardiography (2D-STE) is another semi-automated technology where tiny echo-dense speckles are tracked frame-by-frame within the myocardium, recording any stretching and retracting relative to baseline (ie, Lagrangian dynamics) (6). Myocardial movement is signaled by displacement of the speckled patterning, thus depicting myocardial deformation (39, 40). Accordingly, angle-independent calculations of motion and deformation variables such as velocity, displacement, ε, and SR are enabled.

Initial attempts to study cardiac mechanics were focused on the left ventricular chamber. Usage was subsequently expanded and validated for the right ventricle (6), as well as the thin-walled atrial chambers (41). Later, direct vessel-wall tracking has been achievable through either 2D-STE or TDI.

Methodology for Vascular Mechanics Evaluation

The analysis of vascular walls is performed with short- and long-axis views of aorta or carotid arteries using conventional 2D gray-scale echocardiography, during breath-holding, along with a stable electrocardiographic (ECG) recording. A frame rate of 60-80 frames sec^{-1} is set, and acoustic-tracking software is applied to process the recordings.

When using 2D-STE to study vascular mechanics, vascular circumference is usually divided into six equally sized regions. Numeric expressions of each regional ST variable represent mean values calculated from all points in respective arterial segments. These six regions contribute segmental determinants, from which a global value may be calculated, defined as the mean of peak values generated by the six aortic wall segments (42).

Various ST software packages are available that differ primarily by tracking and filtering algorithms. Two-Dimensional Speckle-Tracking (GE Medical Systems® Horten, Norway) and Vector Velocity Imaging (VVI; Siemens Medical Solutions®, Mountain View, CA, USA) are the two most commonly used applications, and respective studies have generated comparable values for cardiac mechanics (43, 44). Vascular deformation patterns may be analyzed by longitudinal, radial, and circumferential directions. Nevertheless, circumferential analysis is the one typically performed, including ε and SR determinations. During systole, circumferential vascular ε assumes a positive value, due to vessel-wall expansion. Similarly, vascular SR in systole is identified as the value of the first upward peak, termed early circumferential vascular SR. Upon vessel recoil, circumferential ε returns to a normal value, but SR assumes a negative value (late vascular SR). The ε determinant is expressed as % and SR as sec^{-1} – Figure 1. Validation studies *in vitro* (45) and *in vivo* (46) have demonstrated the potential to analyze both radial and longitudinal mechanics. Radial ε assumes a negative value, based on thinning of the vascular wall during systole, whereas lengthening of arterial wall during systole confers a positive value to the longitudinal ε curve.

From the global circumferential ε value, it is possible to calculate a corrected ε (47) as (circumferential ε) / (pulse pressure); and the β_2 index (42) is then calculated as Ln (systolic blood pressure / diastolic blood pressure) / circumferential ε. Time to peak ε is also considered a promising variable. Segmental time to peak circumferential ε analysis of the six vascular wall regions has served as a means of assessing vascular dyssynchrony (48, 49).

A sampling of anterior (superficial) or posterior (deeper) segments of vessel circumference is generally selected for TDI diagnostics. Gain settings, filters, pulse repetition frequency, sector size, and depth should also be adjusted to optimize color saturation. Motion in the test segment is automatically tracked through the cardiac cycle, from which velocity in

radial direction is determined. Mechanical indices (ie, ε and SR) are then calculated from TDI data by integrating velocity over time (50).

Validation Studies of Vascular Mechanics

The validation of ST technology for determining circumferential, radial, and longitudinal ε values of common carotid artery (CCA) has been attempted experimentally via sonomicrometry. This was accomplished by connecting polyvinyl gel phantoms to a pump capable of simulating carotid flow profiles. Gray-scale ultrasound images of the phantoms were then obtained in long- and short-axis views, using both standard clinical and high-frequency ultrasound systems equipped with linear-array transducers. Sonomicrometry crystals additionally were glued to the phantom surfaces. Ultimately, there was good agreement between systems, confirming the feasibility of carotid ε estimation using ultrasound ST – Figure 2. The investigators further noted that high-frequency ultrasound use increased spatial resolution and thus improved arterial ST diagnostic performance, particularly in circumferential mode (45). Importantly, these results were aligned with those of previous studies examining the feasibility of estimating carotid arterial ε values *in silico* (51, 52) and *in vitro* (53, 54).

The *in vivo* feasibility of ultrasound-based assessment of carotid arterial wall strain by ultrasound ST was similarly proven recently through sonomicrometry use in a sheep model. The results showed acceptable agreement and strong correlation between ST and sonomicrometric ε assessment, especially circumferential and longitudinal testing (46). Critical histological validation of vascular mechanics has been demonstrated by Kim *et al*., who divided a group of 14 female dogs into young (1-2 years) or senescent (8-9 years) animals for VVI of thoracic descending aorta. Subsequent histological analysis revealed significant negative correlation in terms of radial velocity, circumferential ε, and SR of aortic wall collagen content. However, vascular mechanics and aortic wall elastin did not correlate significantly (55).

As summarized in Supplemental Table 1, these validation studies support the clinical use of ultrasonographic vascular mechanics, given the success achieved as a research tool for targeting vascular damage.

Clinical Studies of Speckle-Tracking Circumferential Mechanics at Aortic Level

Clinical investigation of vascular mechanics was first conceived by Oishi *et al.* in 2008 (42), who studied 39 subjects at the level of abdominal aorta, showing feasibility of the ST analysis, with satisfactory inter- and intra-observer variability – Figure 3, Panels A and B. Moreover, significant negative correlation was identified for vascular ε (r=-0.79; *P*<0.01),

vascular SR (r=-0.87; *P*<0.01), and time to peak ε (r=-0.36; *P*<0.01) with respect to age. The ε-derived β_2 index showed a positive association with age (r=0.69; *P*<0.01), as did classic β_1 index. This was the first indication that aortic imaging, using this newly developed technology, could serve as a surrogate marker of the degenerative aging process. Afterwards, an independent association between age and circumferential ε was shown in normal subjects, in contrast with a group of hypertensive patients (56). The latter demonstrated an important non-linear association between age and circumferential ε, as well as β_2 index (57, 58). In a 2013 study, Oishi *et al*. investigated the vascular mechanics of both abdominal aorta and common carotid artery, observing that circumferential ε of abdominal aorta was significantly greater than that of the carotid arteries (58).

A study of thoracic descending aortic mechanics was first reported by Kim *et al*. in 2009. The authors enrolled 137 patients who were referred transesophageal echocardiography (TEE). A majority of the referrals were due to stroke (46.7%) and valvular heart disease (33.6%). The authors found a significant negative correlation between vascular ε and aging identified, but also discovered a negative correlation between ε and aortic intima-media thickness and with heart-femoral and brachial-ankle PWV. This was the first publication supporting the use of vascular ε to estimate global vascular stiffness (59). Subsequently, Petrini *et al*. studied descending aortic mechanics in patients with aortic stenosis (AS) and aortic regurgitation (AR), and shown that patients with AS had lower vascular ε values than those with AR. Vascular stiffness and distensibility were similar, whether an M-mode or a VVI assessment was done. Patients with pure AS displayed both higher vascular stiffness and lower distensibility, relative to those with pure AR. Although reproducibility of vascular ε was excellent, the authors noted an important bias and variability in assessing vascular rotational displacement (60). As well, our group has previously reported a cohort of 45 elderly patients with moderate-to-severe degenerative AS, where stroke-volume index was the most important determinant of circumferential ascending aortic ε (61). Moreover, we identified an independent association between β_1 index and SR of ascending aorta (62), thus concluding that the aortic ε was linked to changes in vascular flow, whereas aortic SR was influenced by local arterial rigidity (62).

The impact of systolic flow on vascular mechanics was again demonstrated by Petrini *et al.* in a study of 140 patients with isolated AS and 52 patients with isolated AR. Here, the authors demonstrated that age, systolic flow, and aortic diameters independently influenced circumferential aortic ε at the level of thoracic descending aorta. It was also demonstrated that patients with AS had lower values of aortic ε, lower aortic distensibility, and higher aortic stiffness (both accessed via VVI methodology) than those with AR. In both groups with valvular

heart disease, VVI-tested stiffness was greater in patients with tricuspid (vs bicuspid) aortic valves (63).

Our research group has recently confirmed the feasibility of measuring aortic arch mechanics. We have established normal reference levels (64) and have shown lower age-matched values of both ε and SR in a group of hypertensive patients, compared with a control group (65). Associations between aortic arch mechanics and PWV, as well as estimated central blood pressure, have also been demonstrated (66). We subsequently proved that hypertensive patients with lower values of aortic arch mechanics, had lower early LV relaxation velocities (e') and higher left atrial volumes (67). ST studies at aortic level are summarized in Supplemental Table 2.

Three-dimensional Aortic Mechanics

The methods previously described, conveying information on aortic wall motion, used one cross-section image for assessment. However, it is now possible to study the change in aortic wall motion in every direction. The first study in this regard used a 3D-volume dataset of abdominal aorta. A computed offline analysis was performed, assessing longitudinal ε, circumferential ε, and temporal wall dyssyncrhony. Custom commercial ST software (Advanced Cardiac Package; Toshiba Medical Systems Corporation®, Otawara, Japan) was engaged, with a finite element analysis to improve spatial resolution. Although the number of subjects was limited, patients with abdominal aortic aneurysms exhibited reduced mean ε values and more pronounced temporal dyssynchrony than a control group – Figure 4 (68).

Another group of investigators have validated 3D abdominal aortic mechanics *in vitro*, using a silicone aneurysm model (perfused by a pulsatile artificial circulatory system), a high-speed laser scan (for radial displacement), and video photogrammetry (for longitudinal and circumferential displacement) (69). An *in vivo* study of five patients with aorto-abdominal aneurysm was also conducted, demonstrating a marked difference between mean and maximum values of longitudinal and circumferential ε within aneurysm wall. These results suggest a strong local heterogeneity of biochemical properties in abdominal aortic aneurysms. It was thus speculated that this novel technology may hold promise in estimating the risk of aortic aneurismal rupture (69).

Tissue Doppler Imaging (TDI) of Ascending Aorta

Considerable research has been done on segmental ascending aortic anterior wall velocity assessment using TDI, usually at a level 3 cm above the aortic valve and in either short-

axis (50) or long-axis parasternal view (70), and it is possible to estimate aortic systolic radial ε from aortic wall velocities using TDI software.

Vitarelli *et al*. have demonstrated that ascending aorta velocities (systolic and diastolic) were significantly lower for hypertensive patients, compared with a group of normal controls. As a marker of vascular stiffening, aortic radial ε correlated significantly with LV mass index and with LV diastolic function (50). In another study, the authors found significantly elevated aortic wall velocities and radial ε in endurance and martial arts athletes, compared with a control group; whereas these values were significantly lower in power athletes. It was hypothesized that aortic velocities in conjunction with LV parameters, as an assessment of ventricular-vascular coupling, may be appropriate to study the cardiac remodelling in various types of athletes (71).

In patients with diabetes, lower ascending aortic velocities have been demonstrated, and a negative association has been shown with metabolic control (72). Lower diastolic velocities have likewise been documented in patients with coronary artery disease (CAD), compared with controls (70), and an independent association between aortic systolic velocity and CAD has been identified (73). In addition, a negative correlation between the severity of CAD and aortic velocities has been reported (74). This methodology has also proven to be useful in studying the aortic elastic properties of patients with hypertension, diastolic dysfunction with elevated filling pressures (75), type 1 diabetes (76), subclinical hypothyroidism (77), and preeclampsia (78). Recently, radial ascending aortic ε value displayed greater sensitivity in detection of vascular stiffening than aortic systolic and diastolic velocities in patients with α1-antitrypsin deficiency (79) and in patients with X-syndrome (80).

Clinical Studies of Circumferential Mechanics at Carotid Arterial Level

In 2010, Bjallmark *et al*. reported outcomes of a 2D-ST study of right CCA circumferential mechanics involving 20 normal subjects. This proved to be a particularly sensitive method for assessing age-dependent elastic properties of CCA, outperforming conventional echo determinations of vascular stiffness (35).

Catalano *et al*. (2011) subsequently studied carotid mechanics in a cohort of 47 patients with no known vascular disease, stratified by cardiovascular risk (low, intermediate, and high) according to an Italian scoring system. Circumferential ε correlated significantly with CIMT (r=-0.52; $P<0.01$), β_1 index (r=-0.54; $P<0.01$) and Ep (r=-0.56; $P<0.01$). Unlike circumferential ε, CIMT, β_1 index, vascular distensibility, and Pearson's elastic modulus,

corrected circumferential ε (for pulse pressure) was the only parameter showing a significant between-group difference (81).

Normal reference values for CCA circumferential ε were recently reported by Yuda *et al.* in 2011. They tested 51 normal subjects (mean age, 29±11 years), with a mean global circumferential ε of 6.7±2.1%. Similar values were reported for segmental analyses, and there were no significant differences between right- and left-sided CCA assessments. Execution was simple and quick, with a mean time for ε analysis of 128±12 seconds per subject, conferring high feasibility and excellent reproducibility ratings (47). It was also shown that diabetic patients had lower values of segmental (far-wall) and global carotid mechanics, compared with controls. This disparity persisted after adjustments for age, gender, race, and blood pressure, underscoring the already known association of diabetes with vascular stiffening. Contrary to the study above, arterial ε was significantly higher in the right (vs left) CCA, with similar differences reported for CIMT. Such discrepancies are possibly explained by differences in blood pressure, shear force, and vascular anatomy (82). The same group later demonstrated the utility of time-interval analysis of the CCA ε curve, whereby slopes of carotid arterial area curve were used to discriminate between patients with hypertension and diabetes, relative to controls (83).

In another study, Saito *et al.* demonstrated greater vascular stiffening in patients with hypertension, compared with an age- and gender-matched control group, based on the β_2 index. Age, heart rate, and the presence of hypertension were independently associated with this index (84).

Yang *et al*. showed the importance of a uniform arterial expansion during systole. In a group of 100 healthy controls, the authors demonstrated an increase in the time to peak plus standard deviation (SD) of both ε and SR of left CCA, across different age groups. They also found a negative correlation of ε (r=-0.48; P<0.01) and SR (r=-0.53; P<0.01) with PWV (assessed via radial tonometry). On the other hand, there was a positive association between SD and PWV, suggesting that asynchronous arterial expansion and arterial stiffening are linked (85).

A pivotal study by Kim *et al.* revealed a correlation between carotid arteriosclerosis and coronary artery atherosclerosis in 104 patients referred for coronary angiography, of whom 49 had CAD. In contrast with CIMT, both carotid circumferential ε and SR values showed significant associations with CAD in a model adjusted for age, gender, hypertension, diabetes, hyperlipidemia, and smoking. This study also disclosed an association between vascular mechanics and severity of CAD (86).

The largest study on vascular mechanics reported to date was the one conducted by Park *et al.* involving 1057 patients, with documented atherosclerosis in 216. The high feasibility

and excellent reliability of circumferential CCA ε was established. Patients with a history of vascular disease had lower values of global ε (3.3±1.3% vs 4.2±1.9%; *P*<0.01). Vascular mechanics and a number of risk factors for vascular disease correlated significantly. When added to CIMT, the utility of vascular ε (vs β_1 index) was proven as an estimate of elevated cardiovascular risk, corresponding with Framingham risk score (87).

Vascular mechanics of CCA were also recently shown to correlate with coronary artery calcium score. In a group of 58 patients referred for cardiac tomography, investigators reported a significant negative correlation between calcium score and circumferential ε (r=-0.4; *P*<0.01), as well as SR (r=-0.39; *P*<0.01). This was in contrast with the classic β_1 stiffness index and carotid distensibility (88).

Assessments of vascular mechanics have been done in a variety of clinical settings, serving as surrogate markers for vascular stiffening in pregnancy-induced hypertension (89), Takayasu arteritis (90), and rheumatoid arthritis (91). CCA circumferential ε and late SR in particular have been used to demonstrate that children with Kawasaki disease develop sclerotic changes during early stages of the disease (92). In addition, assessment of vascular mechanics was performed in patients with Marfan syndrome. These patients displayed times to peak ε and SR values (including standard deviations) that exceeded those of age-matched controls (49). All related studies are summarized in Table 2. An example is showed in Figure 3, Panels C and D.

Another clinical aspect of carotid vascular mechanics has been addressed by Tsai *et al*, showing that ε and SR values were associated with a past history of stroke in older subjects with existing vascular stiffening, after adjustment for age, heart rate, systolic blood pressure, and cholesterol levels (48).

The concept of vascular mechanics as a surrogate of arteriosclerosis and a marker of target organ damage has also been successfully tested in animal studies of aortic abdominal aneurysm (93), intimal hyperplasia (94), and vascular remodeling (95).

Longitudinal Vascular Mechanics

Longitudinal motion of the arterial wall is more difficult to assess in ultrasound imaging, due to low-amplitude signals and inherently lower spatial resolution in azimuthal plane (46). Nevertheless, variations in ultrasound ST approach have shown that longitudinal determinations are feasible (96, 97) and are of the same magnitude as measured radial movement (98).

In both animal experimentation and clinical studies, low longitudinal vascular displacement has shown important associations with high cholesterol levels, atherosclerotic

plaque burden, and CIMT (99). Zahnd *et al.* (2012) observed lower longitudinal carotid (proximal and far-wall) displacement in patients with diabetes, compared with a control population (100). Kawasaky *et al.* also demonstrated that CCA far-wall longitudinal mechanics correlated significantly with CIMT and with distensibility index. In the same study, patients with CAD displayed significantly lower determinants of longitudinal vascular mechanics than a control group. Likewise, TDI vascular mechanics showed a significant negative correlation with Framingham risk scores, resulting in similar predictive accuracies. However, no significant difference was evident in comparing inspiratory and expiratory vascular mechanics (101). In the context of CAD, Svedlund *et al.* studied a group of 441 patients with suspected CAD referred for myocardial perfusion scintigraphy. Those with lower carotid longitudinal displacement suffered more severe myocardial ischemia, leading to worse medium-term outcomes.

It has also been shown an association between periodontal disease and lower longitudinal vascular displacement, independent of cardiovascular risk factors, cross-sectional distensibility, and CIMT. Hence, it seems likely that longitudinal vascular mechanics will emerge as a marker of cardiovascular disease (102). The same group credited with these findings has further demonstrated progressive attenuation of longitudinal vascular displacement along CCA in a group of healthy subjects (103).

Limitations and Future Directions

ST analysis is a new and complementary imaging technology allowing segmental and global assessment of vascular circumference without angle-dependency. In spite of the thinness of the vascular walls this method has been validated by histological and sonomicrometric studies of circumferential vascular mechanics. Nevertheless, the study of vascular mechanics relies heavily upon image quality. Out-of plane motion due to patient and transducer movement and tissue compression must be minimized to limit speckle decorrelation.

As noted in this review, a number of indices may be examined in the course of studying vascular mechanics. In our experience, vascular circumferential ε and SR are the more reliable parameters, being radial and longitudinal motion of arterial walls more difficult to assess. From a mechanistic standpoint, vascular wall systolic expansion and diastolic recoil best fit the concept of circumferential mechanics. Moreover, it is also apparent that circumferential vascular mechanics provide a reliable means of assessing arterial stiffness, surpassing conventional ultrasound-based methods in its performance.

Circumferential vascular mechanics may thus serve as a surrogate of local vascular stiffening, having a significant association with PWV, the gold standard marker of arterial rigidity. Its utility has an imaging vascular risk marker has been demonstrated in a number of disease states and its clinical importance has been globally highlighted. Nevertheless, we must note that the normal variability across the aorta and in the more peripheral arteries has not been fully explored to establish reference ranges. More studies should also be performed with a large number of subjects in relation to age and gender to establish consistent references for vascular mechanics. We have reported in this review adequate values for vascular mechanics feasibility and reproducibility, but we note that most of the studies excluded patients with inadequate image quality or poor tracking. This means that the reported values shouldn't expect to be obtained in unselected subjects. Finally, and in agreement with our experience, we recognize it is still a time consuming methodology.

At the present time, the use of this technology is still investigational, but continued advances in ultrasound technology as well as its use and analysis in large epidemiologic studies, will clarify the part of ultrasonographic assessments of vascular mechanics in clinical diagnosis and prediction of outcomes.

Funding: Dra Alexandra Gonçalves receives funds from Portuguese Foundation for Science and Technology Grant HMSP-ICS/007/2012

Conflicts of interests: The authors have no conflicts of interest to declare.

Table 1: Ultrasound-based classic arterial stiffness assessment

Table 2: Clinical studies of vascular mechanics at carotid arterial level

Supplemental Table 1: Validation studies of vascular mechanics

Supplemental Table 2: Clinical studies of vascular mechanics at aortic level

Figure 1 Panel A: Speckle tracking study of vascular wall starts with short-axis arterial view. Initial studies were done at abdominal aortic level (1), followed by study of descending aorta (2) via trans-esophageal echocardiography, ascending aorta (3), and aortic arch (4). Common carotid artery has also been studied.

Figure 1 Panel B: From short-axis view of vessel, dynamic assessment of vascular circumference is feasible. During systole, vessel wall expands to accommodate blood flow, which represents the role of the large arteries to provide adequate vascular buffering to each ventricular contraction (ventricular-arterial coupling). Opposing movement of the vessel follows (vascular recoil). Speckles represent acoustic back-scatter generated by reflected ultrasound beams. In speckle tracking, blocks of speckles (black dots in vessel wall) are traced frame-to-frame, measuring lengthening and shortening relative to baseline (Lagragian dynamics). Analysis in circumferential (as pictured), longitudinal, or radial direction is also feasible.

Figure 1 Panel C: Schematic of circumferential strain and strain rate curves. Speckle-tracking software generates segmental and global curves. Green curve (upper part) represents strain rate curve, assuming an early positive value during systole due to vessel wall expansion. First upward peak after ventricular systole corresponds with early circumferential ascending aortic strain rate (CAASR), followed by negative component (vascular contraction). Late CAASR corresponds with value of first negative deflection after positive component, usually within systole. Strain rate (deformations/sec) is expressed as sec^{-1}. Global value (average of six segments) is calculated. Blue curve (lower part) represents strain curve, assuming a positive

value during systole due to vessel wall expansion and expressed as percentage. Global value of six vascular wall segments will be used.

Figure 2: *In vitro* vascular strain validation. Comparison of strain curves: radial strain (upper plots), longitudinal strain (mid plots) and circumferential strain (lower plots) obtained from three consecutive pump cycles in polyvinyl alcohol phantoms (3 freeze-thaw cycles) at peak flow of 35 ml/sec. Vascular mechanics assessed by speckle tracking (ST), using clinical ultrasound system (Vivid 7, GE®, Horton Norway,) and by sonomicrometry (SONO). Estimated strain (ST Vivid7) corresponded well with reference (SONO) estimate. Reprinted from Larsson *et al*. (45), with permission from Elsevier.

Figure 3: Panels A and B are examples of the global circumferential strain (panel A) and SR (panel B) assessed at the abdominal aorta. Reprinted from Oishi *et al*. (42), with permission from John Wiley and Sons.
Panels C and D are examples of the global circumferential strain (panel C) and strain rate (panel D) assessed at the right common carotid artery. Reprinted from Podgórski *et al*. (88), with permission from Termedia & Banach Publishing.

Figure 4: 3D circumferential vascular strain. Spatially resolved circumferential strain of abdominal aortic segment in (A) healthy volunteer and (B) patient with abdominal aortic aneurysm during one cardiac cycle. Higher circumferential strain curve in healthy volunteer shows synchronous systolic peak, whereas peak circumferential strain is reduced and shows temporal delay in patient with abdominal aneurysm. Reprinted from Karatolios *et al*. (68), with permission from Elsevier.

Table 1: Ultrasound-based classic arterial stiffness assessment

Parameter	Formula	Description
Arterial compliance	$\Delta D / \Delta P$ (cm/mm Hg) or cm^2 /mm Hg)	• Absolute diameter (or area) change for stated pressure step at fixed vessel length
Pulse wave velocity	Distance / Δt (cm/s)	• Travel speed of pulse along arterial segment
Pearson's Elastic modulus	$\Delta P \times D/\Delta D$ (mm Hg)	• Pressure step required (theoretical) for 100% stretch from resting diameter at fixed vessel length
Young's modulus	$\Delta P \times D / (\Delta D \times h)$ (mm Hg/cm)	• Elastic modulus per unit area; pressure step per cm^2 required (theoretical) for 100% stretch from resting length
Arterial distensibility	$\Delta D/\Delta P \times D$ ($mm\ Hg^{-1}$)	• Relative diameter (or area) change for a pressure increment; inverse of elastic modulus
Stiffness index (β_1)	Ln (Ps/Pd) / [(Ds _ Dd)/Dd] (non-dimensional)	• Ratio of logarithm (systolic/diastolic pressures) to relative change in diameter

Adapted from O'Rourke *et al.* (5)

Table 2: Clinical studies of vascular mechanics at the level of the carotids

Authors	Year	Number	Methodology	Main findings
Bjallmark *et al.*(35)	2010	10 younger (25-28 years) + 10 older (50-59 years) healthy individuals	Right CCA 2D-ST	• Circumferential mechanics were feasible, unlike radial mechanics (18% segments excluded due to high signal-to-noise ratio). Similarly, reproducibility was excellent for circumferential ε and SR, but not for radial mechanics. • Younger patients displayed higher global circumferential ε (8.3±0.8% vs 4.5±1.0%; *P*<0.01), higher global circumferential early SR (1.2±0.2 sec^{-1} vs 0.6±0.1 sec^{-1}; *P*<0.01), and higher global circumferential late SR (-0.43±0.08 sec^{-1} vs -0.26±0.06 sec^{-1}; *P*<0.01), compared with older patients. • Regional circumferential mechanics was also higher in the younger age group. • Among all mechanical and conventional stiffness variables, principal component analysis with regression identified only circumferential systolic strain variables as significant contributors to observed differences between younger and older age groups.
Cho *et al.*(90)	2010	12 patients with Takayasu's arteritis + 12 healthy age- and sex-matched controls	CCA VVI	• Patients with Takayasu's arteritis exhibited lower values of vascular mechanics (velocity, ε, SR and displacement), compared with controls. • Higher standard deviation of vascular mechanics in patients (vs controls) suggested disturbed arterial expansion symmetry.
Yang *et al.*(49)	2010	45 patients with Marfan syndrome + 45 age-matched controls	Right CCA VVI	• CCA size was larger in patients with Marfan syndrome (vs controls), but arterial compliance, CIMT, β_1 index, and distensibility did not differ. • CCA circumferential ε and SR plus radial velocities of both groups were similar, but the time to peak ε and SR plus radial velocities were more delayed. Standard deviations (SDs) of time to peak in three mechanical indices were also higher in the Marfan group. • Marfan syndrome was independently associated with the SD of time to peak ε and SR in a model adjusted for age.
Catalano *et al.*(81)	2011	47 patients with CV risk factors, stratified by risk (low, 16; intermediate, 15; high, 15)	Bilateral CCA 2D-ST	• Circumferential ε and adjusted ε (ε/pulse pressure) showed a significant negative correlation with CIMT (r=-0.52; *p*<0.01; r=-0.60; *P*<0.01), β_1 index (r=-0.54; *P*<0.01; r=-0.61; *P*<0.01), and Ep (r=-0.56; *P*<0.01; r=0.72; *P*<0.01). A positive correlation between circumferential mechanics and vascular distensibility was also noted. • Circumferential adjusted ε (0.11±0.03%/mmHg vs 0.07±0.03%/mmHg vs 0.04±0.01%/mmHg) decreased significantly as CV risk increased. No such differences were noted for circumferential ε (5.5±2.2% vs 2.9±1.2% vs 2.4±0.5%), CIMT, β_1 index, vascular distensibility, and Ep.
Yang *et al.*(82)	2011	20 controls + 20 diabetic patients	Bilateral CCA VVI	• Far-wall (4.3±0.4% vs 5.6±0.3%; *P*<0.01) and global (4.3±0.3% vs 5.5±0.3%; *P*<0.01) circumferential ε values were lower for diabetics, compared with controls. The differences remained significant when adjusted for age, gender, race, smoking, heart rate, and blood pressure (and after appropriate exclusions). • Global and segmental ε values were significantly higher in right (vs left) CCA. • Assessment of carotid mechanics was feasible and modestly reliable. • Speckle-tracking derived ε was more sensitive than luminal-based distension assessment as a measure of vascular stiffness.
Yuda *et al.*(47)	2011	51 controls	Bilateral CCA	• Of 612 carotid wall segments tested, waveforms were adequate for analysis in 94%.

			2D-ST	• Mean global circumferential ε was 6.7±2.1%. Right- and left-sided CCA vascular mechanics did not differ. Age and pulse pressure were independently associated with global circumferential ε. • Corrected ε (ε/pulse pressure) was independently associated with systolic blood pressure, age, and β_1 stiffness index. • Studies of vascular mechanics simply and quick, requiring only 128±12 seconds per subject for ε analysis. The methodology showed high feasibility and excellent reproducibility. Mean absolute difference and coefficient of variation in intra- and inter-observer determinations of mean CAS were 0.7±0.6% (CoV: 8.8%) and 0.5±0.4% (CoV: 5.9%), respectively.
Yang *et al.(85)*	2011	100 healthy volunteers	Left CCA VVI	• Circumferential ε and SR decreased significantly across five age groups: 20-29 years: ε 8.5%; Ts 275±25 ms; SR 0.73 sec^{-1}; Tsr 161±6 ms 30-39 years: ε 7.1%; Ts 293±61 ms; SR 0.63 sec^{-1}; Tsr 157±13 ms 40-49 years: ε 5.1%; Ts 321±73 ms; SR 0.40 sec^{-1}; Tsr 165±21 ms 50-59 years: ε 4.7%; Ts 343±97 ms; SR 0.35 sec^{-1}; Tsr 163±32 ms 60-69 years: ε 3.1%; Ts 361±122 ms; SR 0.26 sec^{-1}; Tsr 159±46 ms • Negative correlations of ε (r=-0.48; *P*<0.01; r=-0.54; *P*<0.01) and SR (r=-0.53; *P*<0.01; r=-0.60; *P*<0.01) with PWV and with AIx were demonstrated. • Positive correlation of the Ts and Tsr with PWV and with AIx were also documented. • Age was independently associated with variability in carotid mechanics, when adjusted for gender, body mass index, and heart rate, similar to PWV and AIx. • Unlike PWV and AIx, a linear association between vascular mechanics (including Ts and Tsr) and age was evident.
Kim *et al.*(86)	2012	104 patients referred for a coronary angiogram (CAD, 49)	Left CCA 2D-ST	• CIMT correlated negatively with circumferential ε (r=-0.19; *P*=0.046) and SR (r=-0.22; *P*=0.022). • Patients with CAD had lower circumferential ε (2.3±0.8% vs 2.8±0.9%; *P*<0.01) and SR (0.3±0.1 sec^{-1} vs 0.5±0.2 sec^{-1}; *P*<0.01) values. • Carotid mechanics were significantly associated with CAD in a model adjusted for age, gender, hypertension, diabetes, hyperlipidemia, and smoking, in contrast with CIMT. • Severity of CAD (ie, number of diseased vessels) and carotid mechanics correlated significantly.
Saito *et al.*(84)	2012	90 healthy subjects + 40 age- and sex-matched hypertensive patients	Right CCA 2D-ST (posterior wall)	• The β_2 index correlated positively with age (r=0.37; *P*<0.01), with classic β_1 index (r=0.31; *P*<0.01), and with brachial-ankle PWV (r=0.26; *P*<0.01). • The β_2 index was significantly higher in hypertensive patients than in controls. • Age, heart rate, and the presence of hypertension correlated significantly with β_2 index. • Inter- and intra-observer variability was superior in assessing β_2 (vs β_1) index.
Park *et al.*(87)	2012	1057 patients; 216 with documented atherosclerosis	Bilateral CCA 2D-ST	• Vascular mechanics showed high feasibility, with excellent inter- and intra-observer reliability. • Circumferential ε values were lower in patients with documented (vs undocumented) without atherosclerosis (3.3±1.3% vs 4.2±1.9%; *P*<0.01). • Circumferential ε decreased stepwise from low- to high-risk Framingham scored risk groups. • As risk factors for atherosclerosis increased (0 to 4), carotid ε decreased accordingly.

				• Addition of vascular ε to CIMT significantly improved the accuracy of detecting patients at high risk of vascular disease (according to Framingham score), unlike the β_1 stiffness index.
Lee *et al.*(91)	2012	120 patients with rheumatoid arthritis + 50 healthy controls	CCA 2D-ST	• Patients with rheumatoid arthritis showed lower values of global circumferential ε and of posterior radial ε, compared with controls. Vascular mechanics were associated as well with hs-CRP, with disease duration, and with disease activity score.
MA *et al.*(89)	2012	24 pregnant women with pre-eclampsia + 34 normotensive pregnant women	Right CCA VVI	• Longitudinal velocity, strain, and strain rate of anterior and posterior walls of CCA were significantly lower in women with pregnancy-induced hypertension, compared with normotensive pregnant women. • Similar results were also found for circumferential velocity, strain, and strain rate of anterior and posterior walls and for interior and exterior lateral walls of CCA
Yang *et al.*(83)	2013	20 controls + 20 patients with hypertension + 21 patients with diabetes	CCA 2D-ST + Time interval analysis of the ε curve + slope analysis of the carotid artery area curve	• Four time intervals of the ε curve were set as follows: i) pre-distension period, ii) peak ε time, iii) distension period, and iv) diastolic time. • Hypertensive and diabetic patients showed greater delays in pre-distension peak and in peak ε time than did controls. The distension period was prolonged and the diastolic time was shortened for both hypertensive and diabetic patients, relative to controls. Adding four time intervals to ε nonsignificantly increased the C-statistic to better distinguish between patients and controls. • The carotid artery area curve allowed estimation of four slopes (S1-S4), relating to arterial distension and contraction periods. S2 and S4 slopes were markedly steeper in the group of patients with hypertension and diabetes, compared with healthy controls. Adding slopes S2 and S4 and the four time intervals to ε achieved the largest improvement in accuracy to differentiate patients from controls.
Tsai *et al.*(48)	2013	89 patients (>60 years) from community health survey program; past history of stroke in 11%	Left CCA 2D-ST	• Carotid circumferential ε and SR were significantly lower in stroke subjects. The association remained significant after adjustments for age, heart rate, systolic blood pressure, and cholesterol levels. This was in contrast to the classic echo-derived stiffness indices (CIMT, β1 index, and distensibility), as well as PWV. • Vascular mechanics did not correlate significantly with PWV or with CIMT.
Oguri *et al.*(92)	2014	75 children with a history of Kawasaki disease (mean age:8±3y) + 50 healthy controls (mean age 8±4 years)	CCA 2D-ST	• Carotid circumferential ε (6.7±4.0% vs 8.6±4.1%; *P*<0.01) and late SR (-0.28±0.26 sec^{-1} vs -0.51±0.31 sec^{-1}; *P*<0.01) were significantly lower for children with a history of Kawasaki disease. No differences were noted in terms of time to peak ε, early SR, CIMT, β_1 index, and Ep. • Values of ε in girls with a history of Kawasaki disease were lower than those of male counterparts. • Both β_1 index and Ep correlated negatively with ε and late SR. • Clinical and laboratory variables such as fever, Gunma score, CRP, and peripheral neutrophil count during acute phase did not influence variability of vascular mechanics.
Podgórski *et al.*(88)	2015	58 patients referred for cardiac tomography	Left CCA 2D-ST+ Multi-slice CT	• Calcium score correlated significantly with circumferential ε (r=-0.4; *P*<0.01) and with SR (r=-0.39; *P*<0.01). No significant correlation was identified between β_1 stiffness index or Ep and calcium score. • Patients with calcium scores >0 had lower circumferential ε (3.2±1.4% vs 4.1±1.5%; *P*<0.01) and SR (0.4±0.2 sec^{-1} vs 0.5±0.2 sec^{-1}; *P*<0.01) values than patients with calcium scores of 0.

2D-ST: two dimensional speckle tracking; Aix: augmentation index; AS: aortic stenosis; AR: aortic regurgitation; CAD: coronary artery disease; CCA: common carotid artery; CIMT carotid intima-media thickness; CV cardiovascular risk; CoV: coefficient of variation; Ep: Peterson's elastic modulus; ICC intraclass correlation coefficient; CHD: congenital heart disease; hs CRP: high sensitivity C-reactive protein. PWV: pulse wave velocity; SR: strain rate; TDI tissue Doppler imaging; TEE: trans-esophageal echocardiogram; Ts: time to peak strain; VHD: valvular heart disease; VVI vector velocity imaging

Supplemental Table 1: Validation studies of vascular mechanics

Authors	Year	Methodology	Main findings
Kim *et al.*(55)	2013	• 14 mongrel dogs, classified as young (1-2 years) or old (8-12 years) • VVI of descending thoracic aorta with TEE • Histological analysis of aorta	• VVI-derived parameters showed wider cross-sectional area of aortic wall and significantly reduced FAC in senescent dogs. • In segmental analysis, instantaneous data of aortic deformation derived from VVI, such as radial velocity circumferential strain (3.82±3.20 vs 2.35±1.85%; *P*=0.01) and strain rate (0.88±0.65 vs 0.55±0.37 sec^{-1}), were significantly reduced in senescent dogs. • Aortic wall tissue quantification revealed significant decrease in elastin content (μg/mg aorta) and significant increase in collagen content (μg/mg aorta) in senescent (vs young) dogs. • Radial velocity (r=-0.38; *P*<0.01), circumferential ε (r=-0.29; *P*<0.01), and SR (r=-0.26; *P*=0.02) correlated significantly with collagen content of corresponding aortic wall segments. However, segmental content of elastin showed no significant correlation with any aortic vascular indices. • After adjusting for age, group, weight, heart rate, systolic blood pressure, diastolic blood pressure, and intima-media thickness, both radial velocity and circumferential ε were independently associated with collagen content of corresponding aortic wall segments. • M-mode-derived β_1 stiffness, distensibility, and Young's pressure-strain (elastic modulus) did not differ between groups.
Larsson *et al.* (45)	*2015*	• In vitro validation study • Four polyvinyl alcohol phantoms simulating carotid artery were constructed and connected to a pump reproducing carotid flow profiles. • Gray-scale ultrasound long- and short-axis images of phantoms were obtained using a standard clinical ultrasound system, Vivid 7 (GE Healthcare, Horten®, Norway) and a high-frequency ultrasound system, Vevo 2100 (FUJIFILM, VisualSonics, Toronto®, Canada) with linear-array transducers (12L / MS250). • Sonomicrometry crystals were glued to the phantom surfaces	• Strain curves estimated by the speckle tracking algorithm cyclically varied over time, showing radial compression (negative ε), circumferential stretching (positive ε), and longitudinal stretching (positive ε) in first half of pump cycle simulating cardiac systole. • Correlation between estimated peak ε in clinical ultrasound images and reference ε determined by sonomicrometry was r=0.91 (*P*<0.01) for radial ε, r=0.73 (*P*<0.01) for longitudinal ε, and r=0.90 (*P*<0.01) for circumferential ε. Acceptable bias and LA were also reported for all. • Similar values were noted for correlation between high-frequency ultrasound images and sonomicrometry: r=0.95 (*P*<0.01) for radial ε, r=0.93 (*P*<0.01) for longitudinal ε, and r= 0.90 (*P*<0.01) for circumferential ε. • A significant larger bias and root mean square error was found for circumferential ε estimation on clinical ultrasound images, compared with high-frequency ultrasound images, but no significant difference in bias was found in radial and longitudinal ε comparison.
Larsson *et al*. (46)	2015	• Animal validation study • Left CCA of 5 sheep was exposed and five sonomicrometry crystals were sutured onto arterial walls	• Excellent correlation between estimated and reference vascular longitudinal (r=0.95; *P*<0.01) and circumferential strain (r=0.87; *P*<0.01). • Low bias with acceptable LA for longitudinal (bias=0.14, LA -0.15 to 0.42) and circumferential strain (bias=-0.02, LA -0.54 to 0.50).

FAC: fractional area change; LA: 95% limits of agreement; VVI: vector velocity imaging; TEE: transesophageal echocardiogram

Supplemental Table 2: Clinical studies of vascular mechanics at the level of the aorta

Authors	Year	Number	Methodology	Main findings
Oishi *et al.*(42)	2008	39 normal subjects (age, 15-85 years)	Abdominal Aorta 2D-ST	• First publication in the field of clinical vascular mechanics. • Significant correlation of vascular ε (r=-0.79; *P*<0.01), vascular SR (r=-0.87; *P*<0.01), time to peak ε (r=-0.36; *P*<0.01), and β_2 (r=0.69, *P*<0.01) with age. • Higher vascular ε and SR values in younger subjects (<30 years) than elderly (>60 years) and middle-aged (30-60 years) subjects.
Kim *et al*.(59)	2009	137 patients referred for TEE (stroke, 46.7%; VHD, 33.6%; HD, 11.7%)	Descending thoracic aorta VVI	• Mean global circumferential strain for 137 patients was 5.4±3.0%. • Significant negative correlation of vascular ε with heart-femoral (r=-0.67; *P*<0.01) and brachial-ankle (r=-0.75; *P*<0.01) PWV, aortic IMT (r=-0.67; *P*<0.01) and with aging (r=-0.54; *P*<0.01). • Excellent (N=15) intra- (0.95) and inter-observer (0.94) concordance for vascular ε.
Petrini *et al*.(60)	2010	85 patients(AS, 54; AR, 29)	Descending thoracic aorta VVI	• Aortic ε values lower in patients with AS vs AR (3.7±1.9% vs 7.6±4.5%; *P*<0.01). • Similar values of aortic ε at proximal and distal segments of descending aorta (5.3±3.8% vs 5.0±3.5%; *P*=0.58). • Strong correlations (r=0.84) between calculated aortic stiffness, based on VVI and via M-mode; although VVI-determined stiffness was higher (*P*<0.01). • Strong correlations between calculated aortic distensibility (r=0.84), based on VVI and via M-mode; although VVI determined distensibility was lower (*P*<0.01). • Patients with pure AS (vs pure AR) had lower distensibility and higher vascular stiffness values. • Age, valvular disorder (AS vs AR), and diastolic blood pressure were independently associated with vascular ε. • Excellent inter- and intra-observer reproducibility (bias, ICC, CoV) recorded for vascular ε, but not for aortic rotational displacement.
Oishi *et al.*(57)	2011	54 controls + 104 patients with CV risk factors, but no established vascular disease	Abdominal aorta 2D-ST	• Significant negative correlation between β_2 index and age (r=-0.54; *P*<0.01), stronger than that between β_1 index and age (r=-0.44; *P*<0.01). • No differences in β_1 and β_2 indices by gender. • Significant increase in vascular stiffness after age 50 years, equivalent to non-linear association.
Oishi *et al.* (56)	2013	112 patients with CV risk factors + 56 healthy individuals	Abdominal aorta 2D-ST	• Vascular circumferential ε (3.7±2.4% vs 3.1±1.7%; *P*=0.94) was similar for patients and controls, but aortic stiffness (β_2 index) was significantly higher in hypertensive patients (22.7±16.0 vs 29.5±18.7; *P*=0.02). In patients, β_2 index correlated with age, SBP, DBP, LV e', E/e', systolic LV strain rate (all directions), LA reservoir and conduit phase mechanics, and with (E/e') / LA systolic strain ratio. • After adjusting for covariates, only LV early longitudinal strain rate and E/e'/LA reservoir phase strain ratio were independently associated with β_2 index variation. • Age was the sole independent predictor of aortic stiffness in controls.
Oishi *et al.*(58)	2013	29 controls + 68 patients with CV risk factors , but no	CCA + Abdominal aorta 2D-ST	• Aortic circumferential ε was higher than the carotid circumferential ε in patients <50 years (7.9±3.3 vs 3.7±1.9; *P*<0.01) and in patients ≥50 years (3.5±2.1 vs 2.6±1.0; *P*<0.01). Aortic (vs carotid) β_2 index was also higher in both age groups.

		established vascular disease		• Both aortic and carotid ε decreased significantly with age (non-linear association), particularly in subjects <50 years. • Both aortic and carotid stiffness (β_2 index) increased non-linearly with age, with a significant increase in subjects >50 years old. • Correlation between vascular mechanics and age was significantly greater than correlations between vascular dimensions and age.
Teixeira *et al.*(61)	2013	45 patients with moderate-to-severe AS	Ascending thoracic aorta 2D-ST	• Mean aortic circumferential ε was 6.3±3.0%, and was significantly lower for the low-flow group of AS patients (3.8±0.9 for low flow vs 8.1±2.7% for normal flow; *P*<0.01). • Circumferential ε cut point of 5.0% displayed 90% sensitivity and 92% specificity for low-flow AS. Aortic circumferential ε was more accurate in predicting low-flow states (stroke-volume index ≤35 ml/m^2) than valvulo-arterial impedance, systolic function, and systemic vascular resistance. • After adjustment for covariates such as body surface area, aortic diameter, and vascular resistance, only the stroke-volume index and the valvulo-arterial impedance sustained significant associations with circumferential ε.
Karatolios *et al.(68)*	2014	6 controls + 2 patients with abdominal aortic aneurysms	3D aortic mechanics	• Longitudinal and circumferential 3D ε values were lower for patients with aortic aneurysms. These patients showed increased spatial heterogeneity and more pronounced temporal dyssynchrony.
Petrini *et al.*(63)	2014	140 isolated AS (BAV, 89; TAV, 51) + 52 isolated AR (BAV, 24; TAV, 28)	Descending thoracic aorta VVI	• Patients with pure AS (vs pure AR) registered lower aortic circumferential ε (3.4% [2.3-4.9%] vs 8.6% [6.3-13%]; *P*<0.01), lower aortic VVI distensibility, and higher aortic VVI-assessed stiffness, all confirmed through age-matched control subject analysis. • In both AS and AR groups, VVI-assessed stiffness was greater in patients with TAV vs BAV • Age, stroke volume, and aortic descending diameter were independently associated with Ln (ε) in patients with either AS or AR. The nature of aortic valve (TAV or BAV) was also independently associated with Ln (ε), but only in patients with AR.
Teixeira *et al.*(62)	2015	45 patients with moderate to severe AS	Ascending thoracic aorta 2D-ST	• Stiffness index (β −0.41; *P*<0.01) was independently associated with circumferential aortic SR in a model adjusted for age, BSA, indexed AVA and E/e'. • Aortic SR was higher in AS patients with normal SAC + normal TVR (n = 22) than: i) AS patients with low SAC + normal TVR and ii) AS patients with low SAC + elevated TVR (*P* < 0.01). • Patients with a baseline SR ≤0.66 s^{-1} had a worse long-term outcome (survival 52.4 vs 83.3 %, Log Rank *P* = 0.04).

2D-ST: two dimensional speckle tracking; AS: aortic stenosis; AR: aortic regurgitation; AVA: aortic valve area; BAV: bicuspid aortic valve; BSA: body surface area; CoV: coefficient of variation; CHD: congenital heart disease; ICC intraclass correlation coefficient; PWV: pulse wave velocity; SAC: systemic arterial compliance; TAV: tricuspid aortic valve; TVR: total vascular resistance; TEE: trans-esophageal echocardiogram; VHD: valvular heart disease; VVI velocity vector imaging;

Figure 1

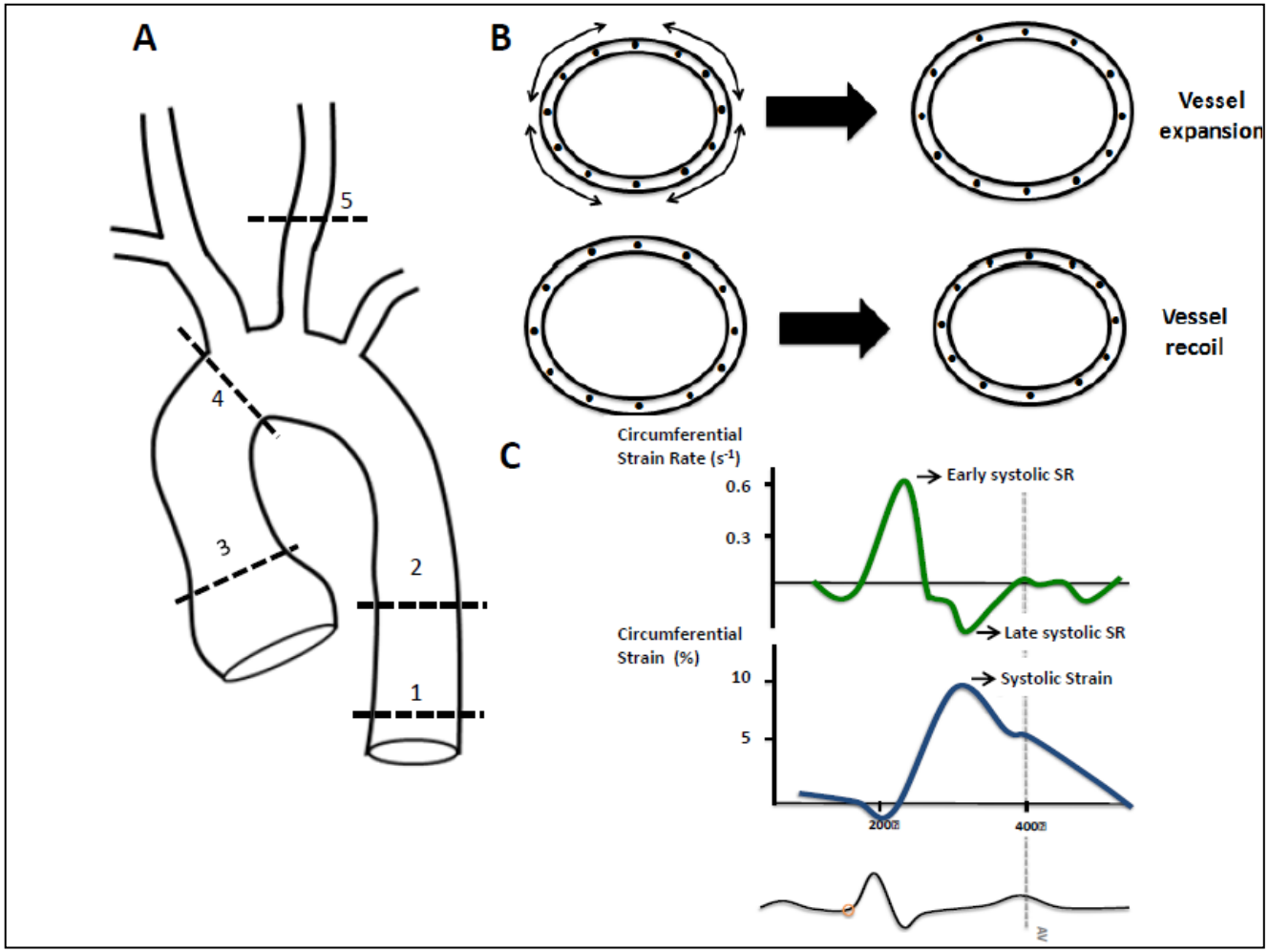
A
5
4
3
2
1
B
Vessel expansion
Vessel recoil
C
Circumferential Strain Rate (s^{-1})
0.6
0.3
Early systolic SR
Late systolic SR
Circumferential Strain (%)
10
5
Systolic Strain
200
400
AV

Figure 2

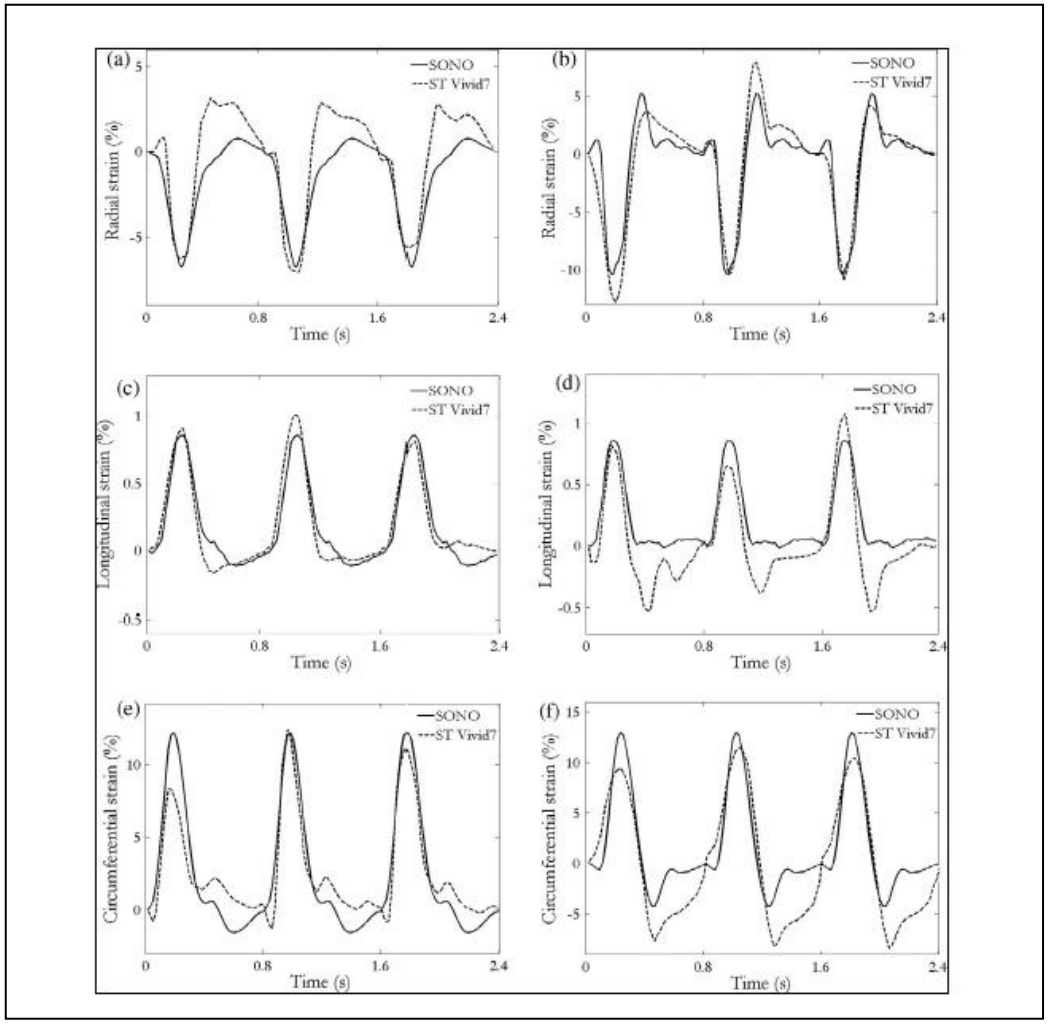
(a)
(b)
(c)
(d)
(e)
(f)
SONO
ST Vivid7
Radial strain (%)
Longitudinal strain (%)
Circumferential strain (%)
Time (s)

Figure 3

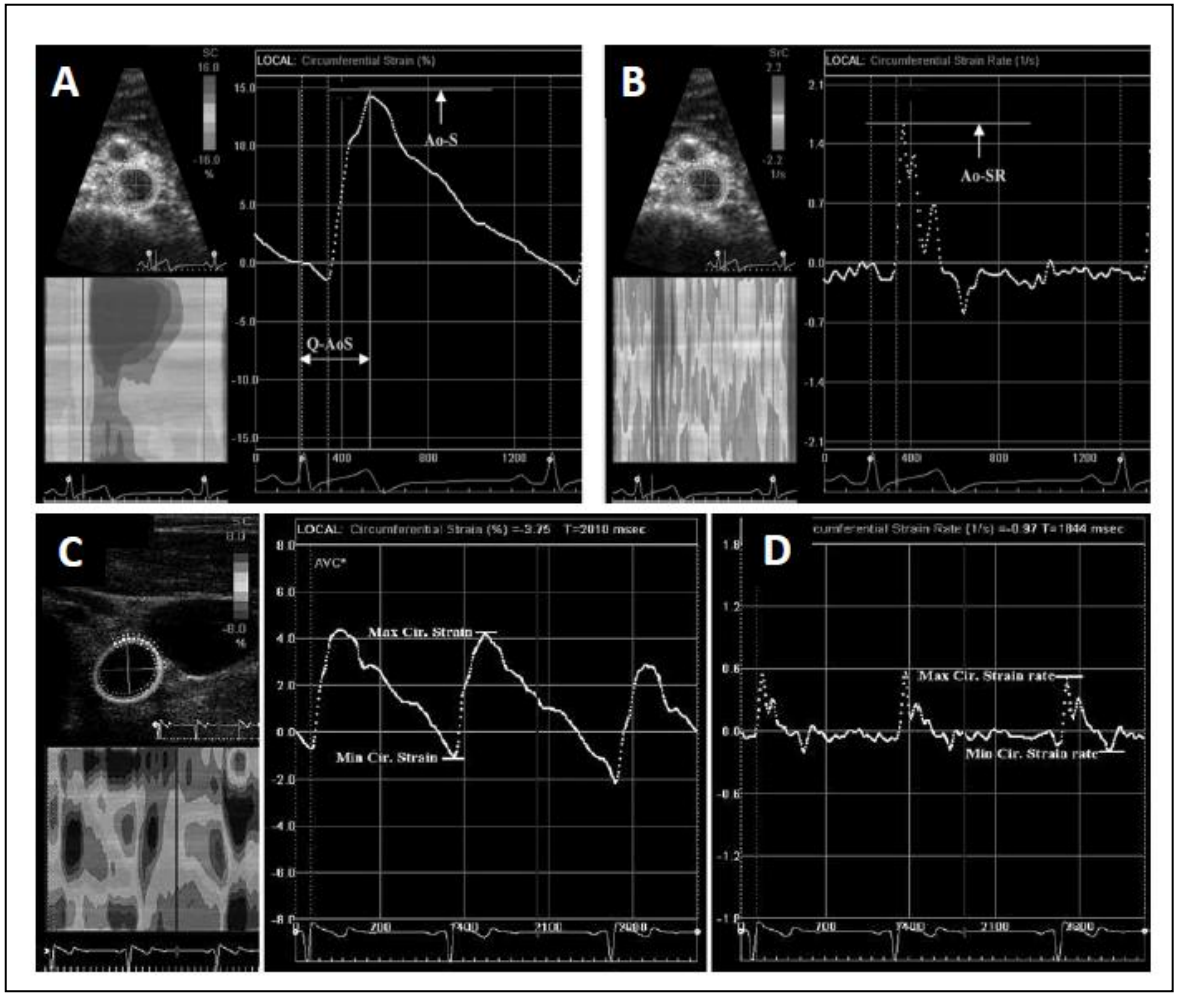
A
LOCAL: Circumferential Strain (%)
Ao-S
Q-AoS
B
LOCAL: Circumferential Strain Rate (1/s)
Ao-SR
C
LOCAL: Circumferential Strain (%) =-9.75 T=2010 msec
AVC*
Max Cir. Strain
Min Cir. Strain
D
Max Cir. Strain rate
Min Cir. Strain rate

Figure 4

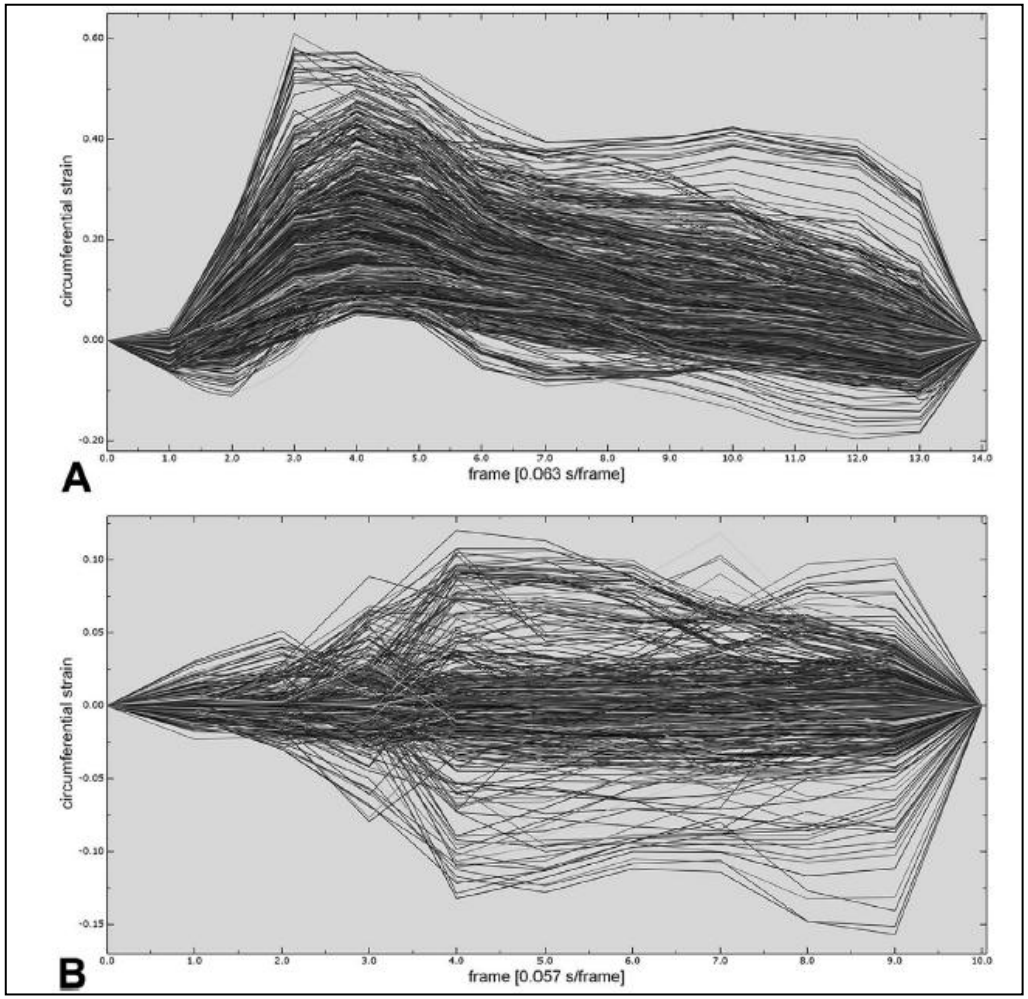
circumferential strain
0.60
0.40
0.20
0.00
-0.20
0.0 1.0 2.0 3.0 4.0 5.0 6.0 7.0 8.0 9.0 10.0 11.0 12.0 13.0 14.0
frame [0.063 s/frame]
A
circumferential strain
0.10
0.05
0.00
-0.05
-0.10
-0.15
0.0 1.0 2.0 3.0 4.0 5.0 6.0 7.0 8.0 9.0 10.0
frame [0.057 s/frame]
B

References

1. Mozaffarian D, Benjamin EJ, Go AS, Arnett DK, Blaha MJ, Cushman M, et al. Heart disease and stroke statistics--2015 update: a report from the American Heart Association. Circulation. 2015 Jan 27;131(4):e29-322.
2. Cavalcante JL, Lima JA, Redheuil A, Al-Mallah MH. Aortic stiffness: current understanding and future directions. J Am Coll Cardiol. 2011 Apr 5;57(14):1511-22.
3. Mancia G, Fagard R, Narkiewicz K, Redon J, Zanchetti A, Bohm M, et al. 2013 ESH/ESC guidelines for the management of arterial hypertension: the Task Force for the Management of Arterial Hypertension of the European Society of Hypertension (ESH) and of the European Society of Cardiology (ESC). Eur Heart J. 2013 Jul;34(28):2159-219.
4. Laurent S, Cockcroft J, Van Bortel L, Boutouyrie P, Giannattasio C, Hayoz D, et al. Expert consensus document on arterial stiffness: methodological issues and clinical applications. Eur Heart J. 2006 Nov;27(21):2588-605.
5. O'Rourke MF, Staessen JA, Vlachopoulos C, Duprez D, Plante GE. Clinical applications of arterial stiffness; definitions and reference values. Am J Hypertens. 2002 May;15(5):426-44.
6. Mor-Avi V, Lang RM, Badano LP, Belohlavek M, Cardim NM, Derumeaux G, et al. Current and evolving echocardiographic techniques for the quantitative evaluation of cardiac mechanics: ASE/EAE consensus statement on methodology and indications endorsed by the Japanese Society of Echocardiography. J Am Soc Echocardiogr. 2011;24(3):277-313.
7. Voigt JU, Pedrizzetti G, Lysyansky P, Marwick TH, Houle H, Baumann R, et al. Definitions for a common standard for 2D speckle tracking echocardiography: consensus document of the EACVI/ASE/Industry Task Force to standardize deformation imaging. Eur Heart J Cardiovasc Imaging. 2015 Jan;16(1):1-11.
8. Izzo JL, Jr. Arterial stiffness and the systolic hypertension syndrome. Curr Opin Cardiol. 2004 Jul;19(4):341-52.
9. Cecelja M, Chowienczyk P. Role of arterial stiffness in cardiovascular disease. JRSM Cardiovasc Dis. 2012;1(4).
10. Laurent S, Boutouyrie P, Lacolley P. Structural and genetic bases of arterial stiffness. Hypertension. 2005 Jun;45(6):1050-5.
11. Wang KL, Cheng HM, Chuang SY, Spurgeon HA, Ting CT, Lakatta EG, et al. Central or peripheral systolic or pulse pressure: which best relates to target organs and future mortality? J Hypertens. 2009 Mar;27(3):461-7.
12. Namasivayam M, Adji A, O'Rourke MF. Influence of aortic pressure wave components determined noninvasively on myocardial oxygen demand in men and women. Hypertension. 2011 Feb;57(2):193-200.
13. Mitchell GF. Effects of central arterial aging on the structure and function of the peripheral vasculature: implications for end-organ damage. J Appl Physiol (1985). 2008 Nov;105(5):1652-60.
14. van der Heijden-Spek JJ, Staessen JA, Fagard RH, Hoeks AP, Boudier HA, van Bortel LM. Effect of age on brachial artery wall properties differs from the aorta and is gender dependent: a population study. Hypertension. 2000 Feb;35(2):637-42.
15. Mitchell GF, Parise H, Benjamin EJ, Larson MG, Keyes MJ, Vita JA, et al. Changes in arterial stiffness and wave reflection with advancing age in healthy men and women: the Framingham Heart Study. Hypertension. 2004 Jun;43(6):1239-45.
16. Kelly R, Hayward C, Avolio A, O'Rourke M. Noninvasive determination of age-related changes in the human arterial pulse. Circulation. 1989 Dec;80(6):1652-9.
17. Laurent S, Boutouyrie P, Asmar R, Gautier I, Laloux B, Guize L, et al. Aortic stiffness is an independent predictor of all-cause and cardiovascular mortality in hypertensive patients. Hypertension. 2001 May;37(5):1236-41.
18. Cruickshank K, Riste L, Anderson SG, Wright JS, Dunn G, Gosling RG. Aortic pulse-wave velocity and its relationship to mortality in diabetes and glucose intolerance: an integrated index of vascular function? Circulation. 2002 Oct 15;106(16):2085-90.
19. Safar ME, London GM, Plante GE. Arterial stiffness and kidney function. Hypertension. 2004 Feb;43(2):163-8.
20. Najjar SS, Scuteri A, Shetty V, Wright JG, Muller DC, Fleg JL, et al. Pulse wave velocity is an independent predictor of the longitudinal increase in systolic blood pressure and of incident hypertension in the Baltimore Longitudinal Study of Aging. J Am Coll Cardiol. 2008 Apr 8;51(14):1377-83.

21. Harada K, Yasuoka K, Shimada Y. Usefulness of tissue doppler imaging for assessing aortic wall stiffness in children with the Marfan syndrome. Am J Cardiol. 2004 Apr 15;93(8):1072-5.

22. Weisz SH, Magne J, Dulgheru R, Caso P, Pierard LA, Lancellotti P. Carotid artery and aortic stiffness evaluation in aortic stenosis. J Am Soc Echocardiogr. 2014 Apr;27(4):385-92.

23. Wilson RA, McDonald RW, Bristow JD, Cheitlin M, Nauman D, Massie B, et al. Correlates of aortic distensibility in chronic aortic regurgitation and relation to progression to surgery. J Am Coll Cardiol. 1992 Mar 15;19(4):733-8.

24. Boonyasirinant T, Rajiah P, Setser RM, Lieber ML, Lever HM, Desai MY, et al. Aortic stiffness is increased in hypertrophic cardiomyopathy with myocardial fibrosis: novel insights in vascular function from magnetic resonance imaging. J Am Coll Cardiol. 2009 Jul 14;54(3):255-62.

25. Chen CH, Nakayama M, Nevo E, Fetics BJ, Maughan WL, Kass DA. Coupled systolic-ventricular and vascular stiffening with age: implications for pressure regulation and cardiac reserve in the elderly. J Am Coll Cardiol. 1998 Nov;32(5):1221-7.

26. Redfield MM, Jacobsen SJ, Borlaug BA, Rodeheffer RJ, Kass DA. Age- and gender-related ventricular-vascular stiffening: a community-based study. Circulation. 2005 Oct 11;112(15):2254-62.

27. Demir S, Akpinar O, Akkus O, Nas K, Unal I, Molnar F, et al. The prognostic value of arterial stiffness in systolic heart failure. Cardiol J. 2013;20(6):665-71.

28. Vlachopoulos C, Aznaouridis K, Stefanadis C. Prediction of cardiovascular events and all-cause mortality with arterial stiffness: a systematic review and meta-analysis. J Am Coll Cardiol. 2010 Mar 30;55(13):1318-27.

29. Mattace-Raso FU, van der Cammen TJ, Hofman A, van Popele NM, Bos ML, Schalekamp MA, et al. Arterial stiffness and risk of coronary heart disease and stroke: the Rotterdam Study. Circulation. 2006 Feb 7;113(5):657-63.

30. Williams B, Lacy PS, Thom SM, Cruickshank K, Stanton A, Collier D, et al. Differential impact of blood pressure-lowering drugs on central aortic pressure and clinical outcomes: principal results of the Conduit Artery Function Evaluation (CAFE) study. Circulation. 2006 Mar 7;113(9):1213-25.

31. Bots ML, Witteman JC, Grobbee DE. Carotid intima-media wall thickness in elderly women with and without atherosclerosis of the abdominal aorta. Atherosclerosis. 1993 Aug;102(1):99-105.

32. Hermeling E, Reesink KD, Reneman RS, Hoeks AP. Measurement of local pulse wave velocity: effects of signal processing on precision. Ultrasound Med Biol. 2007 May;33(5):774-81.

33. Antonini-Canterin F, Carerj S, Di Bello V, Di Salvo G, La Carrubba S, Vriz O, et al. Arterial stiffness and ventricular stiffness: a couple of diseases or a coupling disease? A review from the cardiologist's point of view. Eur J Echocardiogr. 2009 Jan;10(1):36-43.

34. Harada A, Okada T, Niki K, Chang D, Sugawara M. On-line noninvasive one-point measurements of pulse wave velocity. Heart Vessels. 2002 Dec;17(2):61-8.

35. Bjallmark A, Lind B, Peolsson M, Shahgaldi K, Brodin LA, Nowak J. Ultrasonographic strain imaging is superior to conventional non-invasive measures of vascular stiffness in the detection of age-dependent differences in the mechanical properties of the common carotid artery. Eur J Echocardiogr. 2010 Aug;11(7):630-6.

36. Zhang Q, Yip GW-K, Yu C-M. Approaching regional left atrial function by tissue Doppler velocity and strain imaging. Europace. 2008 November 1, 2008;10(suppl 3):iii62-iii9.

37. Inaba Y, Yuda S, Kobayashi N, Hashimoto A, Uno K, Nakata T, et al. Strain Rate Imaging for Noninvasive Functional Quantification of the Left Atrium: Comparative Studies in Controls and Patients With Atrial Fibrillation. J Am Soc Echocardiogr. 2005;18(7):729-36.

38. McDicken WN, Sutherland GR, Moran CM, Gordon LN. Colour Doppler velocity imaging of the myocardium. Ultrasound Med Biol. 1992;18(6-7):651-4.

39. Cameli M, Lisi M, Righini FM, Mondillo S. Novel echocardiographic techniques to assess left atrial size, anatomy and function. Cardiovasc Ultrasound. 2012;10:4.

40. Mondillo S, Galderisi M, Mele D, Cameli M, Lomoriello VS, Zacà V, et al. Speckle-Tracking Echocardiography. Journal of Ultrasound in Medicine. 2011;30(1):71-83.

41. Vieira MJ, Teixeira R, Goncalves L, Gersh BJ. Left atrial mechanics: echocardiographic assessment and clinical implications. J Am Soc Echocardiogr. 2014 May;27(5):463-78.

42. Oishi Y, Mizuguchi Y, Miyoshi H, Iuchi A, Nagase N, Oki T. A novel approach to assess aortic stiffness related to changes in aging using a two-dimensional strain imaging. Echocardiography. 2008 Oct;25(9):941-5.

43. Bansal M, Cho GY, Chan J, Leano R, Haluska BA, Marwick TH. Feasibility and accuracy of different techniques of two-dimensional speckle based strain and validation with harmonic phase magnetic resonance imaging. J Am Soc Echocardiogr. 2008 Dec;21(12):1318-25.

44. Motoki H, Dahiya A, Bhargava M, Wazni OM, Saliba WI, Marwick TH, et al. Assessment of left atrial mechanics in patients with atrial fibrillation: comparison between two-dimensional speckle-based strain and velocity vector imaging. J Am Soc Echocardiogr. 2012 Apr;25(4):428-35.

45. Larsson M, Heyde B, Kremer F, Brodin LA, D'Hooge J. Ultrasound speckle tracking for radial, longitudinal and circumferential strain estimation of the carotid artery--an in vitro validation via sonomicrometry using clinical and high-frequency ultrasound. Ultrasonics. 2015 Feb;56:399-408.

46. Larsson M, Verbrugghe P, Smoljkic M, Verhoeven J, Heyde B, Famaey N, et al. Strain assessment in the carotid artery wall using ultrasound speckle tracking: validation in a sheep model. Phys Med Biol. 2015 Feb 7;60(3):1107-23.

47. Yuda S, Kaneko R, Muranaka A, Hashimoto A, Tsuchihashi K, Miura T, et al. Quantitative measurement of circumferential carotid arterial strain by two-dimensional speckle tracking imaging in healthy subjects. Echocardiography. 2011 Sep;28(8):899-906.

48. Tsai WC, Sun YT, Liu YW, Ho CS, Chen JY, Wang MC, et al. Usefulness of vascular wall deformation for assessment of carotid arterial stiffness and association with previous stroke in elderly. Am J Hypertens. 2013 Jun;26(6):770-7.

49. Yang WI, Shim CY, Cho IJ, Chang HJ, Choi D, Jang Y, et al. Dyssynchronous systolic expansion of carotid artery in patients with marfan syndrome. J Am Soc Echocardiogr. 2010 Dec;23(12):1310-6.

50. Vitarelli A, Giordano M, Germano G, Pergolini M, Cicconetti P, Tomei F, et al. Assessment of ascending aorta wall stiffness in hypertensive patients by tissue Doppler imaging and strain Doppler echocardiography. Heart. 2010 Sep;96(18):1469-74.

51. Larsson M, Kremer F, Claus P, Kuznetsova T, Brodin LA, D'Hooge J. Ultrasound-based radial and longitudinal strain estimation of the carotid artery: a feasibility study. IEEE Trans Ultrason Ferroelectr Freq Control. 2011 Oct;58(10):2244-51.

52. Lopata RG, Nillesen MM, Hansen HH, Gerrits IH, Thijssen JM, de Korte CL. Performance evaluation of methods for two-dimensional displacement and strain estimation using ultrasound radio frequency data. Ultrasound Med Biol. 2009 May;35(5):796-812.

53. Hansen HH, Lopata RG, de Korte CL. Noninvasive carotid strain imaging using angular compounding at large beam steered angles: validation in vessel phantoms. IEEE Trans Med Imaging. 2009 Jun;28(6):872-80.

54. Ribbers H, Lopata RG, Holewijn S, Pasterkamp G, Blankensteijn JD, de Korte CL. Noninvasive two-dimensional strain imaging of arteries: validation in phantoms and preliminary experience in carotid arteries in vivo. Ultrasound Med Biol. 2007 Apr;33(4):530-40.

55. Kim SA, Lee KH, Won HY, Park S, Chung JH, Jang Y, et al. Quantitative assessment of aortic elasticity with aging using velocity-vector imaging and its histologic correlation. Arterioscler Thromb Vasc Biol. 2013 Jun;33(6):1306-12.

56. Oishi Y, Miyoshi H, Iuchi A, Nagase N, Ara N, Oki T. Negative impact of cardiovascular risk factors on left atrial and left ventricular function related to aortic stiffness--new application of 2-dimensional speckle-tracking echocardiography. Circ J. 2013;77(6):1490-8.

57. Oishi Y, Miyoshi H, Mizuguchi Y, Iuchi A, Nagase N, Oki T. Aortic stiffness is strikingly increased with age >/= 50 years in clinically normal individuals and preclinical patients with cardiovascular risk factors: assessment by the new technique of 2D strain echocardiography. J Cardiol. 2011 May;57(3):354-9.

58. Oishi Y, Miyoshi H, Iuchi A, Nagase N, Ara N, Oki T. Vascular aging of common carotid artery and abdominal aorta in clinically normal individuals and preclinical patients with cardiovascular risk factors: diagnostic value of two-dimensional speckle-tracking echocardiography. Heart Vessels. 2013 Mar;28(2):222-8.

59. Kim KH, Park JC, Yoon HJ, Yoon NS, Hong YJ, Park HW, et al. Usefulness of aortic strain analysis by velocity vector imaging as a new echocardiographic measure of arterial stiffness. J Am Soc Echocardiogr. 2009 Dec;22(12):1382-8.

60. Petrini J, Yousry M, Rickenlund A, Liska J, Hamsten A, Eriksson P, et al. The feasibility of velocity vector imaging by transesophageal echocardiography for assessment of elastic properties of the descending aorta in aortic valve disease. J Am Soc Echocardiogr. 2010 Sep;23(9):985-92.

61. Teixeira R, Moreira N, Baptista R, Barbosa A, Martins R, Castro G, et al. Circumferential ascending aortic strain and aortic stenosis. Eur Heart J Cardiovasc Imaging. 2013 Jul;14(7):631-41.

62. Teixeira R, Monteiro R, Baptista R, Barbosa A, Leite L, Ribeiro M, et al. Circumferential vascular strain rate to estimate vascular load in aortic stenosis: a speckle tracking echocardiography study. Int J Cardiovasc Imaging. 2015 Apr;31(4):681-9.

63. Petrini J, Jenner J, Rickenlund A, Eriksson P, Franco-Cereceda A, Caidahl K, et al. Elastic properties of the descending aorta in patients with a bicuspid or tricuspid aortic valve and aortic valvular disease. J Am Soc Echocardiogr. 2014 Apr;27(4):393-404.

64. Teixeira R, Monteiro R, Garcia J, Silva A, Graca M, Baptista R, et al. Feasibility of aortic arch mechanics; a study in normal subjects. Eur Heart J Cardiovasc Imaging. 2014;15(Suppl 2):ii9-ii12.

65. Teixeira R, Monteiro R, Garcia J, Silva A, Graca M, Baptista R, et al. Aortic arch mechanics in hypertensive patients versus controls, a two dimensional speckle-tracking study. Eur Heart J Cardiovasc Imaging. 2014;15(Suppl 2):ii235-ii64

66. Teixeira R, Pereira T, Monteiro R, Baptista R, Graça M, Ribeiro MA, et al. Aortic arch mechanics and vascular stiffness - a pilot study. Rev Port Cardiol. 2015;34:17.

67. Teixeira R, Monteiro R, Garcia J, Silva AX, Graça M, Ribeiro MA, et al. Aortic arch mechanics and left ventricular diastolic function: a two dimensional echocardiographic study Rev Port Cardiol. 2015;34:55.

68. Karatolios K, Wittek A, Nwe TH, Bihari P, Shelke A, Josef D, et al. Method for aortic wall strain measurement with three-dimensional ultrasound speckle tracking and fitted finite element analysis. Ann Thorac Surg. 2013 Nov;96(5):1664-71.

69. Bihari P, Shelke A, Nwe TH, Mularczyk M, Nelson K, Schmandra T, et al. Strain measurement of abdominal aortic aneurysm with real-time 3D ultrasound speckle tracking. Eur J Vasc Endovasc Surg. 2013 Apr;45(4):315-23.

70. Gungor B, Yilmaz H, Ekmekci A, Ozcan KS, Tijani M, Osmonov D, et al. Aortic stiffness is increased in patients with premature coronary artery disease: a tissue Doppler imaging study. J Cardiol. 2014 Mar;63(3):223-9.

71. Vitarelli A, Capotosto L, Placanica G, Caranci F, Pergolini M, Zardo F, et al. Comprehensive assessment of biventricular function and aortic stiffness in athletes with different forms of training by three-dimensional echocardiography and strain imaging. Eur Heart J Cardiovasc Imaging. 2013;14(10):10-20.

72. Mahfouz Badran H, Elnoamany M. Impact of type 2 diabetes mellitus on aortic elastic properties in normotensive diabetes: Doppler tissue imaging study. J Am Soc Echocardiogr. 2006 Dec;19(12):1471-81.

73. Eryol NK, Topsakal R, Cicek Y, Abaci A, Oguzhan A, Basar E, et al. Color Doppler tissue imaging in assessing the elastic properties of the aorta and in predicting coronary artery disease. Jpn Heart J. 2002 May;43(3):219-30.

74. Lu Q, Liu H. Correlation of ascending aorta elasticity and the severity of coronary artery stenosis in hypertensive patients with coronary heart disease assessed by M-mode and tissue Doppler echocardiography. Cell Biochem Biophys. 2015 Mar;71(2):785-8.

75. Suh SY, Kim EJ, Choi CU, Na JO, Kim SH, Kim HJ, et al. Aortic upper wall tissue Doppler image velocity: relation to aortic elasticity and left ventricular diastolic function. Echocardiography. 2009 Oct;26(9):1069-74.

76. Karamitsos TD, Karvounis HI, Didangellos TP, Papadopoulos CE, Dalamanga EG, Karamitsos DT, et al. Usefulness of colour tissue Doppler imaging in assessing aortic elastic properties in Type 1 diabetic patients. Diabet Med. 2006 Nov;23(11):1201-6.

77. Yurtdas M, Gen R, Ozcan T, Aydin MK. Assessment of the elasticity properties of the ascending aorta in patients with subclinical hypothyroidism by tissue Doppler imaging. Arq Bras Endocrinol Metabol. 2013 Mar;57(2):132-8.

78. Orabona R, Sciatti E, Vizzardi E, Bonadei I, Valcamonico A, Metra M, et al. Elastic properties of ascending aorta in patients with a previous pregnancy complicated by early or late preeclampsia. Ultrasound Obstet Gynecol. 2015:DOI: 10.1002/uog.14838.

79. Vizzardi E, Corda L, Pezzali N, Roca E, Pini L, D'Aloia A, et al. Elastic properties of the ascending aorta in patients with alpha1-antitrypsin deficiency (Z homozygotes). Heart. 2012 Sep;98(18):1354-8.

80. Vizzardi E, Trichaki E, Bonadei I, Sciatti E, Salghetti F, Raddino R, et al. Elastic aortic properties in patients with X syndrome. Heart Lung Circ. 2014 Feb;23(2):114-8.

81. Catalano M, Lamberti-Castronuovo A, Catalano A, Filocamo D, Zimbalatti C. Two-dimensional speckle-tracking strain imaging in the assessment of mechanical properties of carotid arteries: feasibility

and comparison with conventional markers of subclinical atherosclerosis. Eur J Echocardiogr. 2011 Jul;12(7):528-35.

82. Yang EY, Dokainish H, Virani SS, Misra A, Pritchett AM, Lakkis N, et al. Segmental analysis of carotid arterial strain using speckle-tracking. J Am Soc Echocardiogr. 2011 Nov;24(11):1276-84 e5.

83. Yang EY, Brunner G, Dokainish H, Hartley CJ, Taffet G, Lakkis N, et al. Application of speckle-tracking in the evaluation of carotid artery function in subjects with hypertension and diabetes. J Am Soc Echocardiogr. 2013 Aug;26(8):901-9 e1.

84. Saito M, Okayama H, Inoue K, Yoshii T, Hiasa G, Sumimoto T, et al. Carotid arterial circumferential strain by two-dimensional speckle tracking: a novel parameter of arterial elasticity. Hypertens Res. 2012 Sep;35(9):897-902.

85. Yang WI, Shim CY, Bang WD, Oh CM, Chang HJ, Chung N, et al. Asynchronous arterial systolic expansion as a marker of vascular aging: assessment of the carotid artery with velocity vector imaging. J Hypertens. 2011 Dec;29(12):2404-12.

86. Kim SA, Park SM, Kim MN, Kim YH, Cho DH, Ahn CM, et al. The relationship between mechanical properties of carotid artery and coronary artery disease. Eur Heart J Cardiovasc Imaging. 2012 Jul;13(7):568-73.

87. Park HE, Cho GY, Kim HK, Kim YJ, Sohn DW. Validation of circumferential carotid artery strain as a screening tool for subclinical atherosclerosis. J Atheroscler Thromb. 2012;19(4):349-56.

88. Podgorski M, Grzelak P, Szymczyk K, Szymczyk E, Drozdz J, Stefanczyk L. Peripheral vascular stiffness, assessed with two-dimensional speckle tracking versus the degree of coronary artery calcification, evaluated by tomographic coronary artery calcification index. Arch Med Sci. 2015 Mar 16;11(1):122-9.

89. Ma XJ, Duan YY, Yuan LJ, Cao TS, Wang Y, Yang HG, et al. Quantitative assessment of maternal common carotid artery mechanics using velocity vector imaging in pre-eclampsia. Eur J Obstet Gynecol Reprod Biol. 2012 Jan;160(1):30-4.

90. Cho IJ, Shim CY, Yang WI, Kim SA, Chang HJ, Jang Y, et al. Assessment of mechanical properties of common carotid artery in Takayasu's arteritis using velocity vector imaging. Circ J. 2010 Jul;74(7):1465-70.

91. Lee JH, Cho KI, Kim SM. Carotid arterial stiffness in patients with rheumatoid arthritis assessed by speckle tracking strain imaging: its association with carotid atherosclerosis. Clin Exp Rheumatol. 2012 Sep-Oct;30(5):720-8.

92. Oguri M, Nakamura T, Tamanuki K, Akita C, Kitaoka C, Saikawa Y, et al. Subclinical arterial stiffness in young children after Kawasaki disease. Cardiol Young. 2014 Feb;24(1):87-94.

93. Favreau JT, Nguyen BT, Gao I, Yu P, Tao M, Schneiderman J, et al. Murine ultrasound imaging for circumferential strain analyses in the angiotensin II abdominal aortic aneurysm model. J Vasc Surg. 2012 Aug;56(2):462-9.

94. Favreau JT, Liu C, Yu P, Tao M, Mauro C, Gaudette GR, et al. Acute reductions in mechanical wall strain precede the formation of intimal hyperplasia in a murine model of arterial occlusive disease. J Vasc Surg. 2014 Nov;60(5):1340-7.

95. Tao M, Mauro CR, Yu P, Favreau JT, Nguyen B, Gaudette GR, et al. A simplified murine intimal hyperplasia model founded on a focal carotid stenosis. Am J Pathol. 2013 Jan;182(1):277-87.

96. Golemati S, Sassano A, Lever MJ, Bharath AA, Dhanjil S, Nicolaides AN. Carotid artery wall motion estimated from B-mode ultrasound using region tracking and block matching. Ultrasound Med Biol. 2003 Mar;29(3):387-99.

97. Persson M, Ahlgren AR, Jansson T, Eriksson A, Persson HW, Lindstrom K. A new non-invasive ultrasonic method for simultaneous measurements of longitudinal and radial arterial wall movements: first in vivo trial. Clin Physiol Funct Imaging. 2003 Sep;23(5):247-51.

98. Cinthio M, Ahlgren AR, Bergkvist J, Jansson T, Persson HW, Lindstrom K. Longitudinal movements and resulting shear strain of the arterial wall. Am J Physiol Heart Circ Physiol. 2006 Jul;291(1):H394-402.

99. Svedlund S, Gan LM. Longitudinal common carotid artery wall motion is associated with plaque burden in man and mouse. Atherosclerosis. 2011 Jul;217(1):120-4.

100. Zahnd G, Boussel L, Marion A, Durand M, Moulin P, Serusclat A, et al. Measurement of two-dimensional movement parameters of the carotid artery wall for early detection of arteriosclerosis: a preliminary clinical study. Ultrasound Med Biol. 2011 Sep;37(9):1421-9.

101. Kawasaki T, Fukuda S, Shimada K, Maeda K, Yoshida K, Sunada H, et al. Direct measurement of wall stiffness for carotid arteries by ultrasound strain imaging. J Am Soc Echocardiogr. 2009 Dec;22(12):1389-95.

102. Zahnd G, Vray D, Serusclat A, Alibay D, Bartold M, Brown A, et al. Longitudinal displacement of the carotid wall and cardiovascular risk factors: associations with aging, adiposity, blood pressure and periodontal disease independent of cross-sectional distensibility and intima-media thickness. Ultrasound Med Biol. 2012 Oct;38(10):1705-15.

103. Zahnd G, Balocco S, Serusclat A, Moulin P, Orkisz M, Vray D. Progressive attenuation of the longitudinal kinetics in the common carotid artery: preliminary in vivo assessment. Ultrasound Med Biol. 2015 Jan;41(1):339-45.

Part II: Original Articles

Original Article Number 1

Circumferential Ascending Aortic Strain and Aortic Stenosis

Eur Heart J Cardiovasc Imaging. 2013 Jul;14(7):631-41.

Rogério Teixeira[1,2]* MD, Nádia Moreira[1] MD, Rui Baptista[1] MD, António Barbosa[1] BSc, Rui Martins[1] MD, Graça Castro[1] MD, Luís Providência[1,2], MD PHD.

*Corresponding Author

[1] Serviço de Cardiologia, Centro Hospitalar e Universitario de Coimbra, Coimbra, Portugal

[2] Faculdade de Medicina Universidade de Coimbra, Coimbra, Portugal

Word Count= 3713 (without references or figures/tables)

Abbreviation List

2D-STE: Two-Dimensional Speckle Tracking Echocardiography

β_1: Aortic Stiffness Index

β_2: Aortic Stiffness index (calculated with 2D-STE)

ε: Strain

AA: Aortic Area

AS: Aortic Stenosis

AVA: Aortic Valve Area

BSA: Body Surface Area

CAAS: Circumferential Ascending Aortic Strain

CO: Cardiac Output

ELI: Energy Loss Index

LV: Left Ventricle

LVEF: Left Ventricular Ejection Fraction

LVOT: Left Ventricular Outflow Tract

MAP: Mean Arterial Pressure

PP: Pulse Pressure

ROI: Region of Interest

SAC: Systemic Arterial Compliance

SR: Strain Rate

SVI: Stroke Volume Index

SVR: Systemic Vascular Resistance

Z_{VA}: Valvulo arterial impedance

Abstract

Introduction: Two-dimensional speckle tracking echocardiography (2D-STE) for the measurement of circumferential ascending thoracic aortic strain (CAAS) in the context of aortic stenosis (AS) is not elucidated. **Purpose**: This study assesses ascending aortic mechanics using 2D-STE in AS patients. **Population and methods**: Forty-five consecutive patients with an aortic valvular area (AVA) ≤ 0.85 cm^2/m^2 were included. Regarding aortic mechanics, global peak CAAS was the parameter used, and an average of six segments of arterial wall deformation was calculated. Corrected CAAS was calculated as global CAAS/pulse pressure. Aortic stiffness (β2) index was assessed according to ln(Ps / Pd) / CAAS. The sample was stratified according to stroke volume index (SVI) as: Group A (low flow, SVI ≤ 35 ml/m^2; n=26) and Group B (normal flow, SVI > 35 ml/m^2; n = 19). **Results**: Mean age was 77±10 years, 53.3% were male, mean indexed AVA was 0.43±0.15 cm2/m2 and mean CAAS was 6.3 ± 3.0%. The CAAS was predicted by SVI (β 0.31, *P*<0.01) and by valvulo-arterial impedance (Z_{VA}) (β 0.59, *P* <0.01). Corrected CAAS was correlated with aortic stiffness index (r=-0.39, *P* <0.01), and was predicted by SVI, Z_{VA} and aortic compliance (β 0.15, *P* <0.01). The β2 index was significantly higher for the low-flow patients (16.1±4.8 vs 9.8±5.3, *P*<0.01), and was predicted by SVI (β -0.58, *P*<0.01) and pulse pressure (β 0.17, *P* <0.01). Global CAAS was more accurate to predict low flow than Z_{VA}, systolic function and systemic vascular resistance. **Conclusions:** In patients with moderate to severe AS, SVI and LV afterload related variables were the most important determinants of 2S-STE global CAAS.

Keywords: Two-Dimensional Spekle Tracking Echocardiography; Circunferential Ascending Aortic Strain; Aortic Stenosis;Low Flow

Introduction

Two-dimensional strain echocardiography (2D-STE) has been developed to allow a rapid, accurate, angle-independent determination of regional myocardial deformation, not only in the longitudinal but also in the radial and circumferential directions without angle dependency (1). Previous authors have demonstrated that circumferential deformation of the descending thoracic aorta, (2) the abdominal aorta (3, 4), or the carotid arteries(5) can be measured using 2D-STE, allowing a simple and accurate determination of the aortic stiffness.

Aortic stenosis (AS) is the most common valvular disease in developed countries, and should not be assessed as an isolated disease of the valve (6). Indeed, a loss of arterial elasticity is a common finding in these patients who are relatively old and often present traditional cardiovascular risk factors for atherosclerosis (7). Previous studies have reported that AS is associated with ascending aortic rigidity, as assessed by aortic stiffness (8), distensibility (9), or elasticity (10). The reduced systemic arterial compliance additionally contributes to the increased systolic load caused by the outflow tract obstruction (6). The double load may have a complementary detrimental effect on left ventricular function (11) and in patient survival (12).

The purpose of the current study was to assess the feasibility and usefulness of circumferential ascending aorta strain (CAAS) using 2D-STE in patients with moderate to severe degenerative AS and to identify its predictors. Moreover, the 2D-STE ascending aortic strain was used as a new echocardiographic measure of aortic stiffness (β_2).

Methodology

Study population

The study population consisted of 53 consecutive patients referred for echocardiography in a single laboratory, between January and February 2012, with a calculated aortic valve area (AVA) ≤ 0.85 cm^2/m^2. Eight patients were eliminated due to poor quality images. The final population consisted of 45 patients with a diagnosis of moderate to severe AS. The sample was initially divided in two groups stratified by left ventricular stroke volume index (SVI). Group A included 19 patients (SVI ≤ 35 ml/m^2) and Group B 26 patients (SVI > 35 ml/m^2). Informed consent was obtained from all patients.

Clinical data

Clinical data included age, weight, height, documented diagnosis of diabetes (patients on antidiabetic medications/insulin, or not medicated but with fasting blood glycemia > 126 mg/dl or HbA1C >6.5%), hypertension (patients on antihypertensive medications or with

known but untreated hypertension, with blood pressure >140/90 mmHg), hypercholesterolemia (patients on cholesterol-lowering medications, or in the absence of such medication, documentation of plasma low-density lipoprotein cholesterol >160 mg/dl), and smoking habits. History of acute myocardial infarction, stroke, and congestive heart failure were documented. Clinical and functional status was assessed according to the New York Heart Association and Canadian Cardiovascular Society classifications.

Systemic arterial hemodynamics

Systemic arterial pressure was measured with the use of an arm cuff sphygmomanometer (right brachial artery) at the same time as the Doppler measurement of stroke volume measured in the left ventricular outflow tract (LVOT). The ratio of SVI to brachial pulse pressure (PP) was used as an indirect measure of total systemic arterial compliance: SAC= SVI/PP (13). The systemic vascular resistance (SVR) was estimated by the formula: SVR =80xMAP/CO, where MAP is the mean arterial pressure defined as diastolic pressure plus one third of brachial pulse pressure and CO is the cardiac output (14).

Echocardiography

Echocardiography was performed using a Vivid 7 (GE Healthcare®, Norway) and a 1.7/3.4 MHz tissue harmonic transducer. Machine settings were manually adjusted to optimize 2D aortic wall tracings and the gray-scale definition for 2D-STE techniques. Care was taken to obtain short-axis views of the ascending aorta after the sino-tubular junction, usually 2 to 3 cm above the aortic valve. Two dimensional image acquisition was performed at a frame rate of > 50 frame per second (mean value for the study population of 71.1±5.3). All images were acquired at end-expiratory apnea. Loops of 3 cardiac cycles were stored digitally and analyzed offline using a customized software package (EchoPAC, GE Healthcare®, Norway).

Two-dimensional and Doppler echocardiographic variables

Aortic valve stenosis severity

The Doppler echocardiographic indices of AS severity included the mean transvalvular pressure gradient obtained with the use of the modified Bernoulli equation, the AVA obtained with the use of the standard continuity equation, and the dimensionless velocity index calculated as the ratio of LVOT velocity-time integral to aortic jet velocity-time integral. AVA was indexed to BSA. The energy loss index (ELI) was determined with the following formula: ELI: (AVAxAA / AA-AVA) / BSA, where AA is the aortic cross-sectional area, and BSA is the body

surface area (15).

Left ventricular geometry, systolic function and filling pressures

Left ventricular (LV) dimensions were acquired in the parasternal long-axis view. LV internal dimension, posterior wall and septal thickness were measured at end-diastole and at end-systole. LV mass was calculated with the corrected formula of the American Society of Echocardiography and indexed for BSA. Indexed LV end-diastolic and end-systolic volumes were calculated using the Simpson method (16).

The LVEF was assessed in all patients using the Simpson (16) and the Dumesnil methods (17), as well as visual estimation. The LV cardiac index was calculated as the product of heart rate and indexed stroke volume for body surface area. Stroke volume was obtained by LV outflow Doppler method as the product between outflow tract area and LV output time–velocity integral (18).

By using pulsed-wave tissue Doppler, peak velocities during systole and early diastole (e') were obtained at the level of the septal and lateral mitral annulus that were measured separately and then averaged. The E/e' ratio, an estimate of LV filling pressures, was then calculated (19).

Global LV afterload

As a measure of global LV afterload, the valvuloarterial impedance (Zva) was calculated with the formula: Zva= SAP+MG / SVI, where SAP is the systolic arterial pressure and MG is the mean transvalvular pressure gradient. Hence, Z_{VA} represents the valvular and arterial factors that oppose ventricular ejection by absorption of the mechanical energy by the left ventricle (13).

Elastic properties of the aorta

Aortic distensibility (D) and stiffness index (β_1) were calculated as: $D=2(A_s - A_d)/[A_d (P_s - P_d)]$, in $cm^2 dyne^{-1} 10^{-6}$, $\beta_1=\ln(P_s / P_d) / (A_s - A_d)/A_d$ (20), where P_s is systolic arterial pressure and P_d is diastolic arterial pressure, . A_s A_d are M-mode guided systolic and diastolic ascending aortic diameters, 2 to 3 cm above the aortic valve; A_d was obtained at the peak of the R wave at the simultaneously recorded electrocardiogram, while A_s was measured at the maximal anterior motion of the aortic wall.

Aortic stiffness (β_2) index was also assessed with 2D-STE peak systolic circumferential strain according to the equation previously used by Oishi *et al.* (3) as $\beta_2=\ln (P_s / P_d)$ / global CAAS.

Speckle tracking two-dimensional strain echocardiography

The 2D-STE technique was used to calculate regional and global ascending aortic wall deformation. For the analysis, a line was manually drawn along the inner side of the aortic wall in the short axis, with high frame rate pictures of the ascending aorta. The software then automatically generated additional lines near the outer side of the vessel wall. Considering the small thickness of the vascular wall in comparison with the cardiac walls, the width of the ROI was reduced to the minimum allowed by the software, as been previously suggested (21). The first systolic frame was usually chosen as the frame of interest to include maximal wall aortic expansion for strain calculation.

Before processing, a cine loop preview feature visually confirmed that the internal line followed the aortic inner side throughout the cardiac cycle. If tracking of the aortic wall was unsatisfactory, then manual adjustments or changing software parameters (eg, region-of-interest size or smoothing functions) were performed.

According to previous authors (2, 5) we divided the aortic wall into 6 equidistant regions: Segment 1, anterior-right (from 10 to 12 o'clock, yellow); Segment 2, anterior-left (from 12 to 2 o'clock, light blue); Segment 3, left (from 2 to 4 o'clock, green); Segment 4, posterior left (from 4 to 6 o'clock, purple); Segment 5, posterior right (from 6 to 8 o'clock, dark blue); and Segment 6, right (from 8 to 10 o'clock, red). All regions were similar in size. In each region, numeric values for each 2D-ST variable represented the mean values calculating from all points in the segment. These were color-coded and shown as a function of time throughout the cardiac cycle. Quantitative curves representing all regions could be expressed for each 2D-ST variable (Fig 1.1 and 1.2).

The tracking process and conversion to Lagrangian strains were performed offline using a dedicated software (EchoPAQ, GE Healthcare). The analysis was performed for CAAS. The peak value was usually identified in the proximity (late peak) of the aortic valvular closure. A global CAAS was then calculated as a mean of the peak value of the six segments. A corrected CAAS was calculated as global CAAS / pulse pressure, according to Yuda *et al* (5).

Statistical analysis

A post hoc achieved power analysis was performed using G-Power version 3.1.3. With the data collected, the sample had a power of 99% to identify differences between low and normal-flow patients regarding global CAAS (calculated d-effect size of 2.1).

The Kolmogorov-Smirnov test was used to confirm that all continuous variables were normally distributed. Continuous data are presented as mean and standard deviation, and the

groups were compared using Student's *t* test. Test of homogeneity of variances was performed for each individual variable with the Levene statistic. Categorical variables are reported as frequencies and percentages, and the χ^2 or Fisher exact tests were used when appropriate.

The method of Bland and Altman (22) was utilized for assessment of systematic bias between measurement of LVEF by the Dumesnil and/or Simpson methods, and also to asses the bias regarding SVI measured by LVOT velocity-time and the Simpson method. Inter and intra-observer reproducibility for the measurement of the global CAAS was assessed on recorded images from 15 randomly selected patients also with the Bland and Altman method.

A receiver-operating characteristic (ROC) curve analysis was used to compute the discriminatory power of CAAS, LVEF, ZVa and SVR to predict low flow. Pairwise comparisons among the areas under the ROC curves were performed with the Delong method (23).

The Pearson correlation was used to analyze the association between global CAAS, corrected CAAS and a number of continuous variables. A linear regression analysis was performed afterward to identify independent predictors of global CAAS and corrected CAAS. Variables that were significant on the bivariate analysis (P<0.01) were included in the model.

A two-tailed *P* value less than .05 was considered statistically significant. Data analyses and calculations were performed using the statistical package from SPSS 15® and MedCalc version 12.1.4®.

Results

Mean age of the population was 77±10 years, with a gender balance. Mean indexed AVA was 0.43±0.15 cm^2/m^2.

Low-flow versus normal-flow aortic stenosis

Baseline demographic data were relatively balanced between groups. Groups were also homogenous for cardiovascular risk factors, and previous cardiovascular history although low-flow aortic stenosis patients were more often associated with a current admission for decompensated heart failure (47.4 vs 11.5%, P<0.01), a higher heart rate during the exam (79.2±13.6 vs 66.2±10.8 beats/min, p<0.01), and a higher SVR. Both groups had a similar blood pressure profile and arterial compliance (Table 1).

Z_{VA} was significantly higher for the low-flow group (5.6.±1.4 vs 4.2±1.0 mmHg/ml m^2 , P<0.01), and ascending aorta diameters were significantly smaller. Low flow was associated with a narrower aortic valve area (0.38±0.13 vs 0.47±0.16 cm^2/m^2, P=0.05), and with a lower LV ejection fraction, whether assessed by Simpson or by the Dumesnil method. Stiffness index β_1 was similar for both groups, but aortic distensibility was higher for the normal-flow patients

(7.8±4.6 vs 13.0±11.0 $cm^2dyne^{-1}10^{-6}$, *P*=0.04). On the contrary, the stiffness index β_2 was significantly higher for the low-flow patients (Table 2). With the method of Bland Altman, the bias for the LVEF calculation with the Simpson and Dumesnil methods was 0.8%, and the 95% limits of agreement were -6.2 to 7.8% (Fig. 2.1). Regarding the SVI estimate, the bias for the LVOT VTI and the Simpson method was 0.5 ml/m^2, and the 95% limits of agreement were -5.4 to 6.3 ml/m^2 (Fig 2.2).

Global circumferential ascending aortic strain

Of the total 270 segments, 246 (91%) had adequate waveforms for measurements of CAAS. Intra-observer variability of global CAAS was 0.02% and the 95% limits of agreement were -0.50 to 0.54% (Fig. 2.3). Inter-observer variability of global CAAS was -0.15% and the 95% limits of agreement were -0.98% to 0.69% (Fig. 2.4).

Mean global CAAS was 6.3±3.0%, and was significantly lower for the low-flow groups (3.8±0.9 vs 8.1±2.7%, *P*<0.01). With the exception of segments 1 and 6, the difference remained highly significant between groups in the segmental CAAS analysis.

A cutoff value for global CAAS of 5.0% had 90% sensitivity and 92% specificity for low-flow AS patients (Figure 3.1). Global CAAS had a higher diagnostic accuracy for low-flow than LVEF (*P*=0.02), Z_{VA} (*P*=0.01) and SVR (*P*<0.01) (Figure 3.2).

In the univariate analysis, global CAAS was significantly associated with BSA, maximal and minimal ascending aortic diameters, and with SVR (r=-0.47, *P*<0.01). A similar strong negative correlation was identified with Z_{VA} (r=-0.54, *P*<0.01). With respect to LV systolic function variables, global CAAS was significantly correlated with SVI (r=0.92, *P*<0.01; Fig. 4.1), and with LVEF. No association was identified between global CAAS and stiffness index, aortic distensibility, means aortic valve gradient, ELI and LV mass (Table 3). With a multiple linear regression analysis, after adjustment for covariates such as BSA, aortic diameter, SVR, Z_{VA}, and AVA, only SVI and Z_{VA} remained significant predictors of global CAAS. The model explained 84% of the global CAAS variability (Table 4.1).

Global corrected circumferential ascending aortic strain

Regarding the corrected CAAS, using the univariate analysis, we note that it correlated significantly negatively with the stiffness index β_1 (r=-0.39, *P*<0.01; Fig. 4.2). A similar strong association was identified for the same variables than global CAAS with the exception of LVEF (Table 3). With respect to the multiple regression analysis, we identified three independent predictors of corrected global CAAS: SAC, Z_{VA}, and SVI. The model explained 88% of corrected

global CAAS variability (Table 4.2).

Two-dimensional speckle tracking stiffness index – β_2

Aortic β_2 index was correlated with age (r=0.33, *P*<0.03), BSA, pulse pressure, SAC (r=0.63, p<0.01), and SVR. There was also an association with the classic stiffness index β_1, but not with aortic distensibility. Regarding AS severity, a negative correlation was identified for indexed AVA (r=-0.47, *P*<0.01) and for SVI (r=0.65, *P*<0.01), and a strong positive association was noted for Z_{VA}. No significant association was identified with respect to gender, symptoms, LVEF, LV filling pressures, and LV mass indexed. In multivariate linear regression analysis, β_2 was significantly negatively correlated with SVI and positively with PP (Table 5).

Discussion

The results of our study demonstrated the following findings: (1) global 2D-STE CAAS has a high feasibility and excellent reproducibility, and could be easily assessed in patients with moderate to severe AS; (2) global CAAS was more accurate to predict low flow than LVEF, Z_{VA} and SVR; (3) global CAAS was independently associated with SVI and Z_{VA}; (4) the corrected global CAAS correlated (univariate analysis) with the classic aortic β_1 stiffness index and was independently predicted by SVI, Z_{VA}, and SAC; (5) A higher 2D-STE defined stiffness index – β_2 was significantly associated with a higher pulse pressure, and a lower SVI.

A previous study analyzed the aortic strain in the ascending aorta in a cohort of hypertensive patients, and concluded that patients had a lower strain than controls (24). Contrary to our study, the authors used strain Doppler echocardiography and based the analysis in radial parameters. The 2D-STE assessment has a significant advantage over tissue Doppler, as the technique is angle independent and is not influenced by tethering or translational motion. It also allows the measurement of the deformation in all the segments of the vessel and not only in one, as was performed by Vitarelli *et al* (24). Moreover, the authors used aortic wall velocities and radial aortic (vessel thinning) wall deformation, with a region of interest of 2 to 4 mm. According to Bijnens *et al.* (25), this analysis was significantly influenced by the right ventricular outflow tract profile, and therefore, was not an adequate measurement of aortic deformation.

The focus of our study was the positive movement of the strain curve during systole, which is the circumferential expansion of the vessel wall. This also means that not only wall properties but also flow could theoretically influence vessel wall deformation. Previous studies have ignored systolic or LV stroke flow as a predictor of vessel circumferential strain (4, 5). In

this paper, we demonstrated that vessel wall properties and systolic flow influenced global ascending thoracic aortic deformation. Circumferential ascending aortic strain is an innovative measurement of the vessel wall mechanical properties not dependent on blood pressure, and performed over the entire circumference of the short axis section. According to our data it had a high accuracy to predict low flow, which lead us to assume that this deformation index could be a surrogate marker for LV afterload.

The most frequent hypothesis explaining the aortic valve degenerative process in the elderly is atherosclerosis, which also involves other components of the vascular system including the thoracic ascending aorta (26). In patients with AS, a combination of factors (aging, hypertension, diabetes) related to the atherosclerotic disease expression leads to an accelerated stiffening process of the vascular tree (7). In fact, degenerative AS is associated with a reduced SAC (13), and with increased aortic stiffness (8). Due to the double load (vascular and valvular) that exists in AS patients, the index of valvulo-arterial global afterload that represents the cost in mmHg for each systemic milliliter of blood indexed for body surface area pumped by the left ventricle during systole is commonly used (27). According to our regression model CAAS especially if corrected for pulse pressure was influenced by aortic compliance and Z_{VA}, which highlight the future usefulness of this index to determine LV afterload.

Degenerative stiffness of the arterial beds is referred as arteriosclerosis and should be differentiated from atherosclerosis, which is defined as the occlusive result of endovascular inflammatory disease, lipid oxidation, and plaque formation (28). Both tend to coexist and are referring to a progressive, diffuse, and age-related process that occurs in all beds (29). Previous studies have demonstrated that peak circumferential vascular strain was significantly associated with age and with the elastic properties of the vessel, such as the stiffness index and the aortic distensibility (2, 30). In this way, aortic circumferential deformation seemed to be a good marker of aortic arteriosclerosis. Contrary to some data, but in agreement with others, we did not found a correlation between global CAAS and arterial stiffness (4, 5). In an effort to explain this finding in our study, we start by noticing that the average age of our patients was 76.8 ±10.3 years, with a mean stiffness index of 11.2±8.0%. This means that our population was significantly older, with a more advance degenerative aortic vessel disease than previously reported. In agreement with the work from Yuda, we note that there was a correlation between corrected (for pulse pressure) CAAS and β_1 stiffness index(5). Moreover, in the multivariate model, corrected global CAAS was less dependent on SVI and was significantly associated with SAC and Z_{VA}. Therefore, the corrected CAAS is more likely to be a

more accurate index of aortic deformation (5). In a recent publication Bjallmark *et al* (31) noted that there was a possible heterogeneity of the vessel degenerative process that could be further accentuated by atherosclerotic plaques and plaque calcification. We believe our data corroborates that concept as we found variations in ascending aortic 2D-STE deformation within the six vessel segments.

A recent study validated the use of abdominal aortic peak circumferential strain, according to the formula previously reported, as a useful method in the assessment of aortic stiffness (3). We believe our data also support its use in clinical assessment of aortic stiffness, as one of its predictors was, in fact, pulse pressure. Due to increased rigidity, one of the earliest markers of aortic degenerative disease is the widening of the pulse pressure, due to early return of reflected wave from the periphery to the aorta (32). According to Rosca *et al*. the increase in aortic stiffness in the context of AS was associated with an unfavorable LV remodeling process, namely, increased LV filling pressure and increased brain natriuretic peptides (8). According to our analysis, the aortic β_2 index was also significantly associated with aortic flow, as a more rigid aorta was associated with a lower SVI.

Clinical Implications

Due to the high feasibility and reproducibility of 2D-ST global CAAS, we suggest its use in the assessment of patient with aortic stenosis, as it correlated significantly with LV afterload variables and SVI.

Limitations

Although powered enough to study the influence of SVI in CAAS in the context of moderate to severe AS, it was a small sample (48 patients) single center study. Brachial blood pressure was used instead of central blood pressure. Brachial pressure usually overestimates central pressure, although recent data showed a clinically acceptable agreement between non-invasive brachial pressures and directly measured central aortic pressure in patients with aortic stenosis (33). Although there was echocardiographic consistency with respect to stroke volume measurements, an invasive hemodynamic study was not performed to confirm the value. The design of the study and the heterogeneity of the study population made it impossible to analyze the prognostic significance of 2D-STE global CAAS. Besides circumferential vascular deformation radial components of the arterial strain have also been evaluated mostly using tissue Doppler strain imaging (34). In our study, it was impossible to measure the radial strain of the ascending aorta due to the noisy profile of the strain curve.

Conclusions

The 2D-STE of the thoracic ascending aorta was performed simply with a high feasibility and excellent reproducibility. In patients with moderate to severe aortic stenosis, SVI and LV afterload related variables were the most important determinants of CAAS.

Acknowledgments

The authors thank Mr Nélson Ribeiro BSc, and Mrs Ana Paula Oliveira BSc, for their help in the initial echocardiographic evaluation of the patients, Mrs Sónia Cancela for her logistic support, and Prof Bárbara Oliveiros for statistical advice.

Conflict of interest: The authors have no conflicts of interest.

Funding: none

Legends

Table 1: Baseline information, risk factors and systemic arterial hemodynamics.

Table 2: Aortic stenosis severity, LV geometry and systolic function and aortic elastic properties.

Table 3: Circumferential ascending aortic strain

Table 4: Correlations with global CAAS and corrected global CAAS.

Table 4.1: Linear regression model to predict global CAAS.

Table 4.2: Linear regression model to predict corrected global CAAS.

Table 5: Correlations of the ascending aortic β_2.

Figure 1.1 Global CAAS in a patient with normal-flow aortic stenosis.

Global and regional CAAS (in %) in a patient with a normal-flow AS, obtained from a short axis view of the aorta, 2 to 3 cm above the aortic valve. (A) Region of interest encompassing the thoracic ascending aorta short axis view. (B) Color M-mode of CAAS of all regions throughout the cardiac cycle. (C) The curves are color coded by the defined aortic segment as depicted in the figure. Global CAAS value is represented by white dotted curve. During systole circumferential strain assumes a positive value due to vessel wall expansion. (D) Pulsed Doppler LVOT velocity profile. This patient had a global peak CAAS of 13.4% and a SVI of 58.5 ml/m^2.

Figure 1.2 Global CAAS in a patient with low-flow aortic stenosis.

Global and regional CAAS (in %) in a patient with low-flow AS, obtained from a short axis view of the aorta, 2 to 3 cm above the aortic valve. (A) Region of interest encompassing the thoracic ascending aorta short axis view. (B) Color M-mode of CAAS of all regions throughout the cardiac cycle. (C) The curves are color coded by the defined aortic segment as depicted in the figure. Global CAAS value is represented by white dotted curve. (D) Pulsed Doppler LVOT velocity profile. This patient had a global CAAS of 2.9% and a SVI of 26.2 ml/m^2.

Figure 2.1 Bland-Altman plot of LVEF using the methods of Simpson and Dumesnil.

Figure 2.2 Bland-Altman plot of SVI using the LVOT VTI and the SVI Simpson methods.

Figure 2.3 Bland-Altman plot of the intra-observer variability of global CAAS (%) measurement.

Figure 2.4 Bland-Altman plot of the inter-observer variability of global CAAS (%) measurement.

Figure 3.1 Accuracy assessments for low flow.

Figure 3.2 Receiver operating characteristic (ROC) curve comparisons

Figure 4.1 Correlation between global CAAS and SVI.

Figure 4.2 Correlation between corrected global CAAS and β_1.

Table 1: Baseline information, risk factors and systemic arterial hemodynamics

	Total Population	SVI ≤35 ml/m^2	SVI > 35 ml/m^2	*P*
Age (years)	77±10	80±8	74±11	0.07
Male gender (%)	24/45 (53.3)	7/19 (36.8)	17/26 (65.4)	0.06
Cardiovascular risk factors, concomitant diseases and symptoms				
Diabetes (%)	14/45 (31.1)	5/19 (26.3)	9/26 (34.6)	0.55
Dyslipidemia (%)	37/45 (82.2)	17/19 (89.5)	20/26 (76.9)	0.28
Hypertension (%)	35/45 (77.8)	15/19 (77.8)	20/26 (76.9)	0.87
Previous MI (%)	4/45 (8.9)	2/19 (10.5)	2/26 (7.7)	0.74
Previous stroke (%)	5/45 (11.1)	3/19 (15.8)	2/26 (7.7)	0.39
Current CHF admission (%)	12/45 (26.7)	9/19 (47.4)	3/26 (11.5)	<0.01
Asymptomatic (%)	7/45 (15.6)	1/19 (5.3)	6/26 (23.1)	0.10
NYHA class	1.4±0.5	2.5±0.8	2.0±0.8	0.05
CCS class	1.3±0.7	1.5±0.8	1.1±0.4	0.04
Systemic arterial hemodynamics				
Systolic arterial pressure, mmHg	133.6±29.1	125.2±29.0	140.8±27.8	0.07
Diastolic arterial pressure, mmHg	69.1±13.5	68.3±12.2	70.4±14.7	0.61
Pulse pressure, mmHg	66.7±24.8	56.9±22.9	70.4±25.0	0.07
Heart rate, bpm	67.4±13.5	79.2±13.6	66.2±10.8	0.01
Systemic arterial compliance, ml mmHg^{-1} m^{-2}	0.7±0.3	0.6±0.2	0.8±0.4	0.14
Systemic vascular resistance, mmHg min L^{-1}	1669.0±540.6	1877.6±572.2	1516.4±467.7	0.03

CHF – congestive heart failure; CCS – Canadian Cardiovascular Society; MI – myocardial infarction; NYHA – New York Heart Association; SVI – stroke volume index

Table 2: Aortic stenosis severity, LV geometry and systolic function and aortic elastic properties

	Total Population	SVI ≤35 ml/m^2	SVI > 35 ml/m^2	*P*
Valvulo-arterial impedance, mmHg / ml m^2	4.8±1.3	5.6±1.4	4.2±1.0	<0.01
Maximal ascending aortic diameter, cm	3.4±0.5	3.1±0.4	3.5±0.5	<0.01
Minimal ascending aortic diameter, cm	3.1±0.4	2.9±0.4	3.3±0.5	0.02
Aortic stenosis severity				
Aortic valve area, cm^2 / m^2	0.43±0.15	0.38±0.13	0.47±0.16	0.05
Energy loss index, cm^2/m^2	0.47±0.18	0.41±0.18	0.50±0.18	0.10
Peak aortic gradient, mmHg	67.5±33.5	64.7±39.2	69.6±29.3	0.63
Mean aortic gradient, mmHg	41.5±21.5	38.1±26.5	43.9±17.0	0.37
Dimensionless velocity index	0.22±0.08	0.21±0.07	0.22±0.08	0.74
Left Ventricular study				
LVOT diameter, mm	2.2±0.3	2.1±0.3	2.2±0.2	0.02
LV mass indexed, g/m^2	129.4±41.6	129.7±48.5	129.1±36.7	0.97
Relative wall thickness	0.44±0.10	0.47±0.11	0.42±0.85	0.13
LV end diastolic volume index, ml/m^2	65.2±20.6	61.7±28.0	67.8±12.8	0.33
LV end systolic volume index, ml/m^2	27.6±20.0	33.0±27.6	23.6±10.7	0.20
LV ejection fraction by Simpson, %	60.6±14.1	52.7±16.0	66.4±9.2	<0.01
LV ejection fraction by Dumesnil, %	60.0±13.9	51.8±15.4	65.6±9.3	<0.01
E/e’	20.4±10.5	26.1±10.8	18.2±9.7	0.07
Aortic elastic properties				
Aortic distensibility (D), (cm^{2}dyne^{-1}10^{-6})	10.8±9.1	7.8±4.6	13.0±11.0	0.04
Stiffness index (β_1)	11.2±8.0	11.3±7.8	11.0±8.2	0.91
Stiffness index (β_2)	12.4±5.9	16.1±4.8	9.8±5.3	<0.01

LV – left ventricular; LVOT – left ventricular outflow tract

Table 3: Circumferential Ascending Aortic Strain

	Total Population	SVI ≤35 ml/m^2	SVI > 35 ml/m^2	*P*
Global CAAS, %	6.3±3.0	3.8±0.9	8.1±2.7	<0.01
Segment 1 CAAS, %	3.5±4.2	2.4±2.7	4.8±4.5	0.07
Segment 2 CAAS, %	6.0±5.6	3.1±2.5	7.1±5.9	0.01
Segment 3 CAAS, %	8.5±5.8	4.3±2.2	9.3±6.2	<0.01
Segment 4 CAAS, %	9.8±4.5	5.0±2.6	11.9±3.9	<0.01
Segment 5 CAAS, %	8.6±5.1	5.2±3.7	10.8±5.9	<0.01
Segment 6 CAAS, %	4.9±4.0	3.7±2.7	5.2±4.7	0.27

CAAS – circumferential ascending aortic strain

Table 4: Correlations with global CAAS and corrected global CAAS

	Global CAAS		Corrected global CAAS	
Variables	**r**	***P***	**r**	***P***
Age, years	-0.26	0.08	-0.21	0.18
BSA, m^2	0.31	0.04	0.48	<0.01
Systemic arterial hemodynamics and aortic elastic properties				
Systolic arterial pressure, mmHg	0.22	0.14	-0.38	0.01
Diastolic arterial pressure, mmHg	0.21	0.16	0.14	0.37
Heart rate, bpm	-0.16	0.29	0.07	0.64
Systemic arterial compliance, ml $mmHg^{-1}$ m^{-2}	0.28	0.06	0.85	<0.01
Maximal ascending aortic diameter, cm	0.41	<0.01	0.41	<0.01
Minimal ascending aortic diameter, cm	0.34	0.02	0.36	0.02
Systemic vascular resistance, mmHg min L^{-1}	-0.47	<0.01	-0.61	<0.01
Aortic distensibility (D), ($cm^2 dyne^{-1} 10^{-6}$)	-0.10	0.50	-0.20	0.19
Stiffness index (β_1)	-0.13	0.39	-0.39	<0.01
Aortic stenosis severity and global LV afterload				
Valvulo-arterial impedance, mmHg / ml m^2	-0.54	<0.01	-0.66	<0.01
Aortic valve area, cm^2 / m^2	0.41	<0.01	0.44	<0.02
Mean aortic gradient, mmHg	0.14	0.24	0.04	0.79
Energy loss index, cm^2/m^2	0.35	0.02	0.32	0.04
LV geometry and systolic function				
SVI, ml/m^2	0.92	<0.01	0.61	<0.01
LV ejection fraction by Simpson, %	0.39	<0.03	0.22	0.16
LV mass indexed, g/m^2	0.15	0.32	0.24	0.12

BSA – body surface area

Table 4.1: Linear Regression Model to predict global CAAS

Variables	Beta	T value	*P*
BSA, m^2	0.37	0.36	0.72
Maximal ascending aortic diameter, cm	-0.07	-0.14	0.89
Systemic vascular resistance, mmHg min L^{-1}	-0.01	-1.86	0.07
Valvulo-arterial impedance, mmHg / ml m^2	0.59	2.00	0.05
Aortic valve area, cm^2 / m^2	1.63	1.00	0.33
SVI, ml/m^2	0.31	11.9	<0.01

B_0= - 7.22 (p=0.05); F 39.9 (<0.01); Adjusted R^2=0.84;

Table 4.2: Linear Regression Model to predict corrected global CAAS

Variables	Beta	T value	*P*
BSA, m^2	0.008	0.33	0.75
Maximal ascending aortic diameter, cm	0.01	0.95	0.35
Systemic vascular resistance, mmHg min L^{-1}	0.00	-1.90	0.07
Systemic arterial compliance, ml $mmHg^{-1}$ m^{-2}	0.15	9.37	<0.01
Valvulo-arterial impedance, mmHg / ml m^2	0.003	2.34	0.02
Aortic valve area, cm^2 / m^2	0.04	1.09	0.28
SVI, ml/m^2	0.003	5.38	0.01
Stiffness index (β_1)	0.00	-0.4	0.69

B_0= - 0.21 (p<0.01); F 33.9 (<0.01); Adjusted R^2=0.88;

Table 5 – Correlations of the ascending aortic β_2

	Univariate analysis		Linear regression	
Variables	**r**	***P***	**β**	***P***
Age, years	0.33	0.03	0.05	0.41
BSA, m^2	-0.36	0.02	1.77	0.59
Gender	0.22	0.15	-	-
NYHA class	0.15	0.35	-	-
Diabetes	-0.04	0.82	-	-
Systemic arterial hemodynamics				
Pulse pressure, mmHg	0.40	<0.01	0.17	<0.01
Systemic arterial compliance, ml $mmHg^{-1}m^{-2}$	-0.63	<0.01	0.61	0.85
Systemic vascular resistance, mmHg min L^{-1}	0.57	<0.01	-001	0.58
Aortic distensibility (D), ($cm^2dyne^{-1}10^{-6}$)	0.20	0.21	-	-
Stiffness index (β_1)	0.38	<0.01	-	-
Aortic stenosis severity and global LV afterload				
Valvulo-arterial impedance, mmHg / ml m^2	0.67	<0.01	-0.66	0.50
Aortic valve area, cm^2 / m^2	-0.47	<0.01	-5.48	0.23
Mean aortic gradient, mmHg	0.03	0.84	-	-
LV geometry, systolic function and LV filling pressures				
SVI, ml/m^2	-0.65	<0.01	-0.58	<0.01
LV ejection fraction by Simpson, %	-0.24	0.11	-	-
LV mass indexed, g/m^2	-0.21	0.16	-	-
E/e’	0.24	0.21	-	-

B_0= 23.5 (p=0.04); F 13.8 (<0.01); Adjusted R^2=0.70;

Figure 1.1

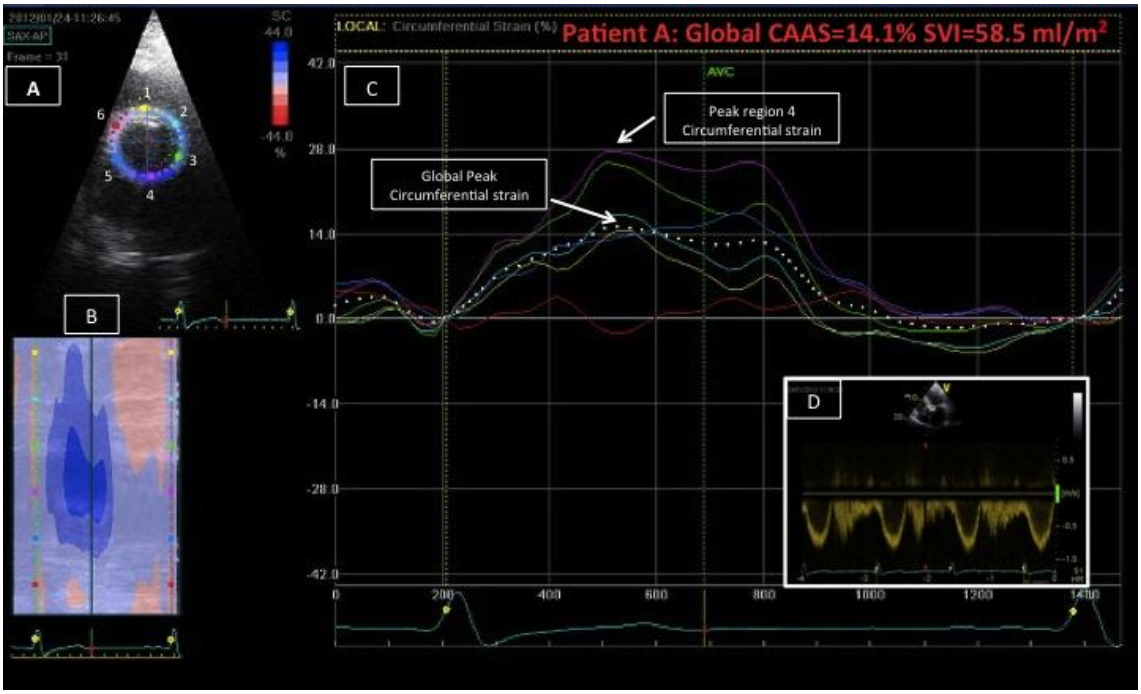
A
B
C
D
LOCAL: Circumferential Strain (%)
Patient A: Global CAAS=14.1% SVI=58.5 ml/m²
AVC
Peak region 4
Circumferential strain
Global Peak
Circumferential strain
42.0
28.0
14.0
0.0
-14.0
-28.0
-42.0
0
200
400
600
800
1000
1200
1400

Figure 1.2

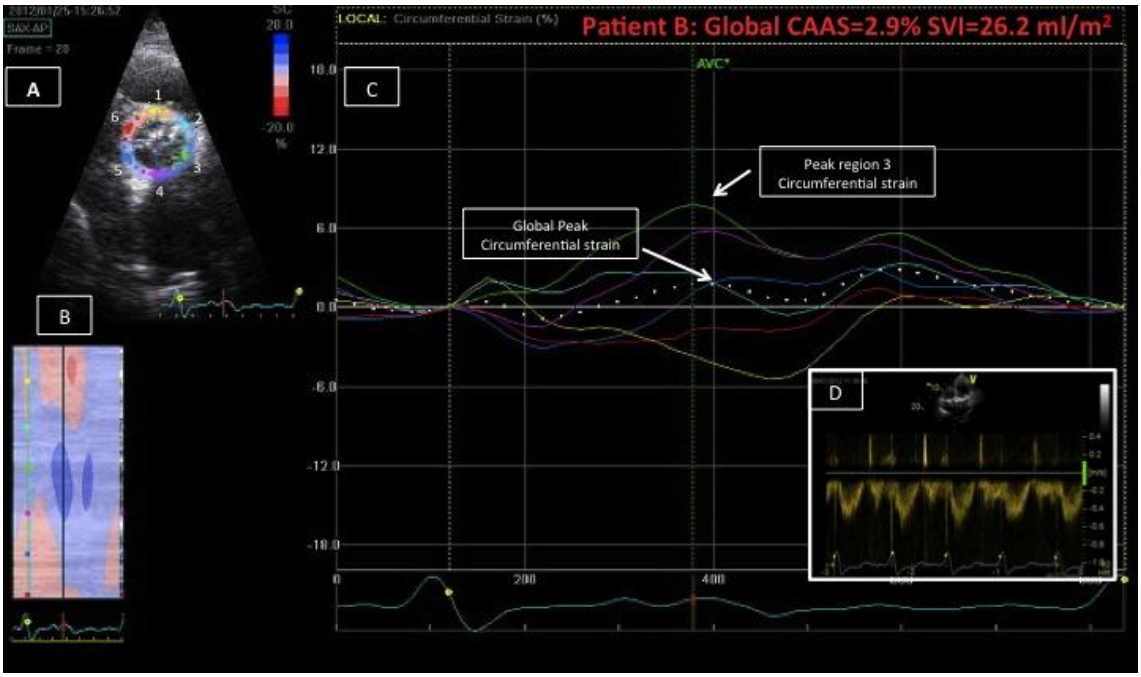
Patient B: Global CAAS=2.9% SVI=26.2 ml/m²
LOCAL: Circumferential Strain (%)
A
B
C
D
AVC*
Peak region 3
Circumferential strain
Global Peak
Circumferential strain
18.0
12.0
6.0
0.0
-6.0
-12.0
-18.0
0
200
400

Figure 2

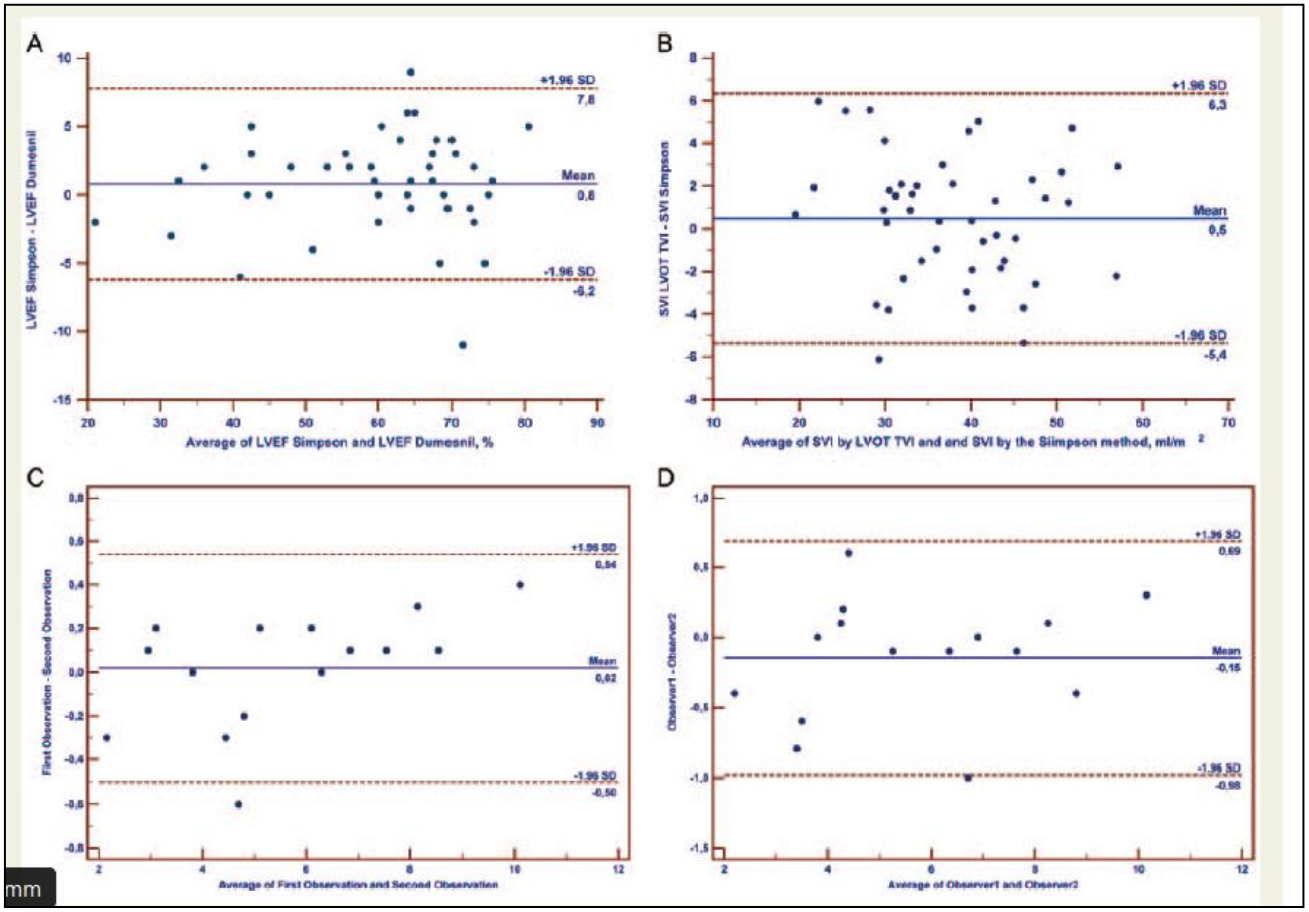
A
LVEF Simpson - LVEF Dumesnil
+1.96 SD
7,8
Mean
0,8
-1.96 SD
-6,2
Average of LVEF Simpson and LVEF Dumesnil, %
B
SVI LVOT TVI - SVI Simpson
+1.96 SD
6,3
Mean
0,5
-1.96 SD
-5,4
Average of SVI by LVOT TVI and and SVI by the Simpson method, ml/m 2
C
First Observation - Second Observation
+1.96 SD
0,54
Mean
0,02
-1.96 SD
-0,50
Average of First Observation and Second Observation
D
Observer1 - Observer2
+1.96 SD
0,69
Mean
-0,15
-1.96 SD
-0,98
Average of Observer1 and Observer2
mm

Figure 3.1

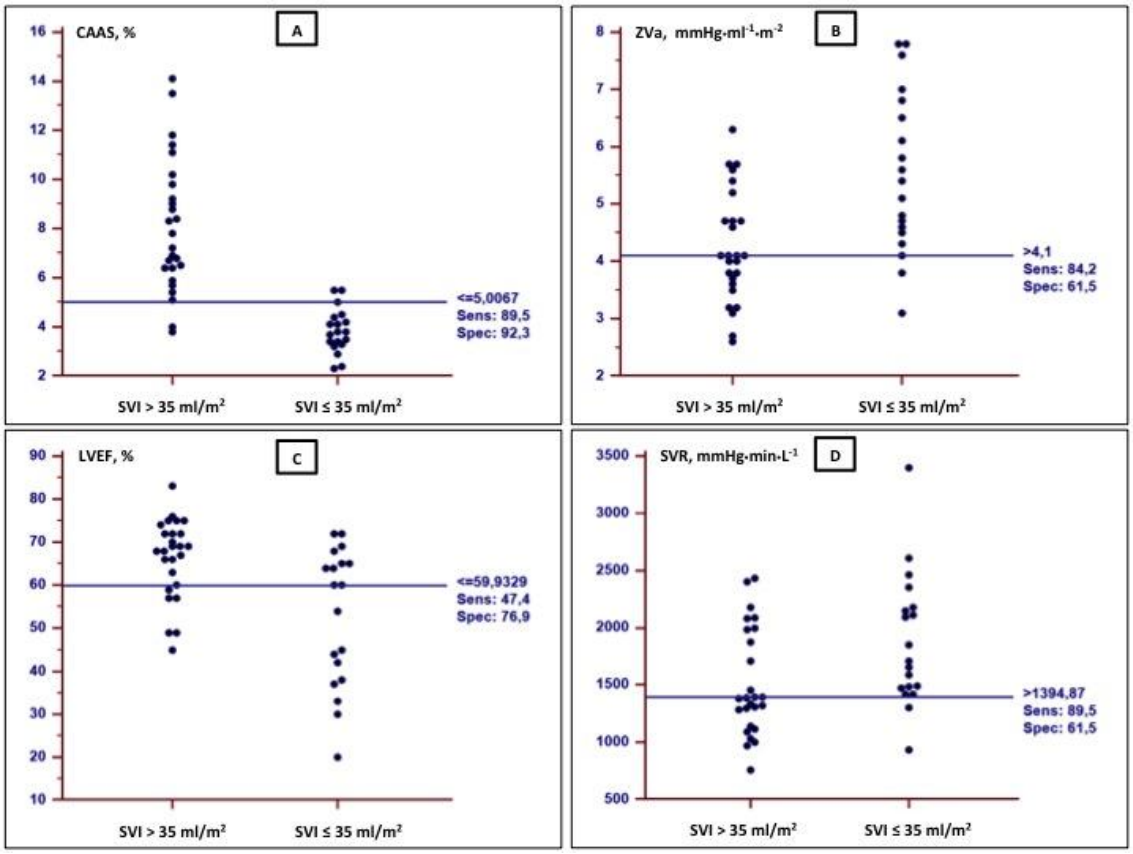

Figure 3.2

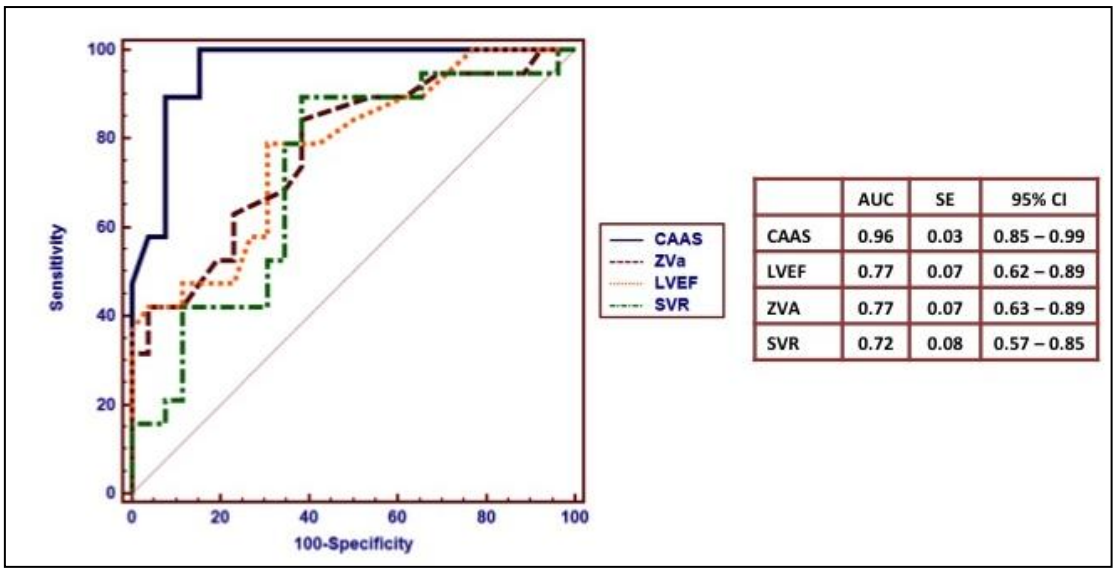

	AUC	SE	95% CI
CAAS	0.96	0.03	0.85 – 0.99
LVEF	0.77	0.07	0.62 – 0.89
ZVA	0.77	0.07	0.63 – 0.89
SVR	0.72	0.08	0.57 – 0.85

Figure 4.1

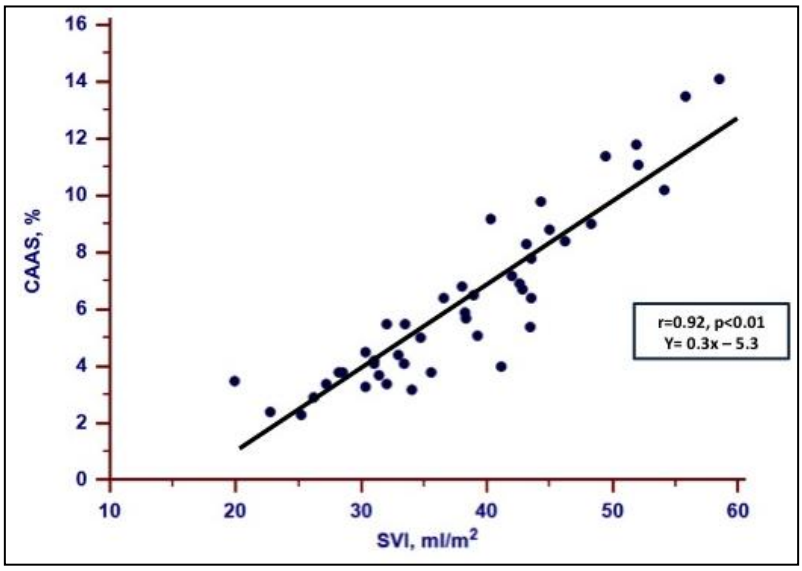
16
14
12
10
8
6
4
2
0
CAAS, %
10
20
30
40
50
60
SVI, ml/m2
r=0.92, p<0.01
Y= 0.3x – 5.3

Figure 4.2

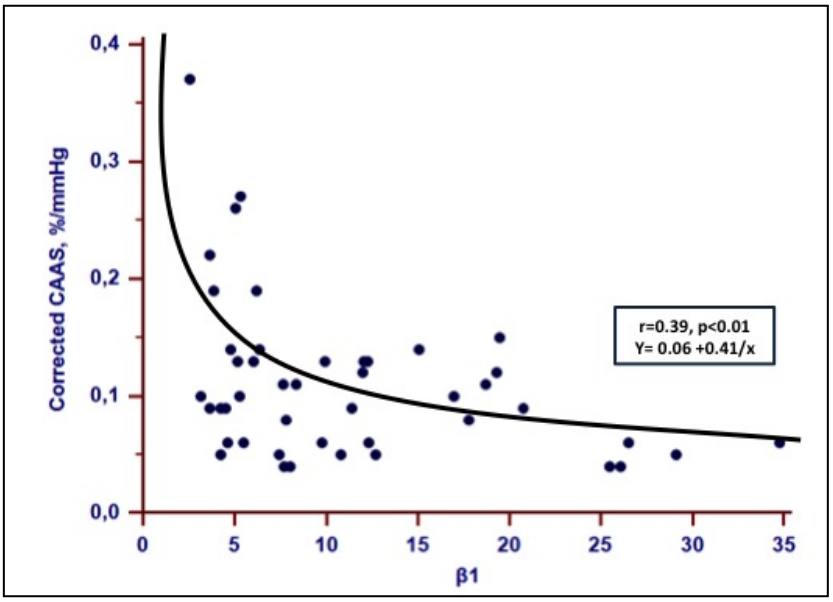
0,4
0,3
0,2
0,1
0,0
Corrected CAAS, %/mmHg
r=0.39, p<0.01
Y= 0.06 +0.41/x
0
5
10
15
20
25
30
35
β1

References

1. Leitman M, Lysyansky P, Sidenko S, Shir V, Peleg E, Binenbaum M, et al. Two-dimensional strain-a novel software for real-time quantitative echocardiographic assessment of myocardial function. J Am Soc Echocardiogr. 2004;17(10):1021-9.
2. Kim KH, Park JC, Yoon HJ, Yoon NS, Hong YJ, Park HW, et al. Usefulness of aortic strain analysis by velocity vector imaging as a new echocardiographic measure of arterial stiffness. J Am Soc Echocardiogr. 2009;22(12):1382-8.
3. Oishi Y, Mizuguchi Y, Miyoshi H, Iuchi A, Nagase N, Oki T. A novel approach to assess aortic stiffness related to changes in aging using a two-dimensional strain imaging. Echocardiography. 2008;25(9):941-5.
4. Oishi Y, Miyoshi H, Mizuguchi Y, Iuchi A, Nagase N, Oki T. Aortic stiffness is strikingly increased with age >/= 50 years in clinically normal individuals and preclinical patients with cardiovascular risk factors: assessment by the new technique of 2D strain echocardiography. J Cardiol. 2011;57(3):354-9.
5. Yuda S, Kaneko R, Muranaka A, Hashimoto A, Tsuchihashi K, Miura T, et al. Quantitative measurement of circumferential carotid arterial strain by two-dimensional speckle tracking imaging in healthy subjects. Echocardiography. 2011;28(8):899-906.
6. Pibarot P, Dumesnil JG. Assessment of aortic stenosis severity: check the valve but don't forget the arteries! Heart. 2007;93(7):780-2.
7. Allison MA, Cheung P, Criqui MH, Langer RD, Wright CM. Mitral and aortic annular calcification are highly associated with systemic calcified atherosclerosis. Circulation. 2006;113(6):861-6.
8. Rosca M, Magne J, Calin A, Popescu BA, Pierard LA, Lancellotti P. Impact of aortic stiffness on left ventricular function and B-type natriuretic peptide release in severe aortic stenosis. Eur J Echocardiogr. 2011;12(11):850-6.
9. Nemes A, Forster T, Csanady M. Patients with aortic valve stenosis and Type 2 diabetes have similar coronary flow reserve and aortic distensibility compared with non-diabetic patients with aortic valve stenosis. Diabetes Res Clin Pract. 2007;77(1):159-60.
10. Nemes A, Forster T, Csanady M. Decreased aortic distensibility and coronary flow velocity reserve in patients with significant aortic valve stenosis with normal epicardial coronary arteries. J Heart Valve Dis. 2004;13(4):567-73.
11. Briand M, Dumesnil JG, Kadem L, Tongue AG, Rieu R, Garcia D, et al. Reduced systemic arterial compliance impacts significantly on left ventricular afterload and function in aortic stenosis: implications for diagnosis and treatment. J Am Coll Cardiol. 2005;46(2):291-8.
12. Hachicha Z, Dumesnil JG, Pibarot P. Usefulness of the valvuloarterial impedance to predict adverse outcome in asymptomatic aortic stenosis. J Am Coll Cardiol. 2009;54(11): 1003-11.
13. Briand M, Dumesnil JG, Kadem L, Tongue AG, Rieu R, Garcia D, et al. Reduced systemic arterial compliance impacts significantly on left ventricular afterload and function in aortic stenosis: implications for diagnosis and treatment. J Am Coll Cardiol. 2005;46(2):291-8.
14. Kadem L, Dumesnil JG, Rieu R, Durand LG, Garcia D, Pibarot P. Impact of systemic hypertension on the assessment of aortic stenosis. Heart. 2005;91(3):354-61.
15. Garcia D, Pibarot P, Dumesnil JG, Sakr F, Durand LG. Assessment of aortic valve stenosis severity: A new index based on the energy loss concept. Circulation. 2000;101(7):765-71.
16. Lang RM, Bierig M, Devereux RB, Flachskampf FA, Foster E, Pellikka PA, et al. Recommendations for chamber quantification: a report from the American Society of Echocardiography's Guidelines and Standards Committee and the Chamber Quantification Writing Group, developed in conjunction with the European Association of Echocardiography, a branch of the European Society of Cardiology. J Am Soc Echocardiogr. 2005;18(12):1440-63.
17. Dumesnil JG, Dion D, Yvorchuk K, Davies RA, Chan K. A new, simple and accurate method for determining ejection fraction by Doppler echocardiography. Can J Cardiol. 1995;11(11):1007-14.
18. Dubin J, Wallerson DC, Cody RJ, Devereux RB. Comparative accuracy of Doppler echocardiographic methods for clinical stroke volume determination. American heart journal. [Comparative Study]. 1990 Jul;120(1):116-23.
19. Ommen SR, Nishimura RA, Appleton CP, Miller FA, Oh JK, Redfield MM, et al. Clinical utility of Doppler echocardiography and tissue Doppler imaging in the estimation of left ventricular filling pressures: A comparative simultaneous Doppler-catheterization study. Circulation. 2000;102(15):1788-94.
20. Stefanadis C, Stratos C, Boudoulas H, Kourouklis C, Toutouzas P. Distensibility of the ascending aorta: comparison of invasive and non-invasive techniques in healthy men and in men with coronary artery disease. Eur Heart J. 1990;11(11):990-6.
21. Catalano M, Lamberti-Castronuovo A, Catalano A, Filocamo D, Zimbalatti C. Two-dimensional speckle-tracking strain imaging in the assessment of mechanical properties of carotid arteries: feasibility and comparison with conventional markers of subclinical atherosclerosis. Eur J Echocardiogr. 2011;12(7):528-35.
22. Bland JM, Altman DG. Statistical methods for assessing agreement between two methods of clinical measurement. Lancet. 1986;1(8476):307-10.
23. DeLong ER, DeLong DM, Clarke-Pearson DL. Comparing the areas under two or more correlated receiver operating characteristic curves: a nonparametric approach. Biometrics. 1988;44(3):837-45.

24. Vitarelli A, Giordano M, Germano G, Pergolini M, Cicconetti P, Tomei F, et al. Assessment of ascending aorta wall stiffness in hypertensive patients by tissue Doppler imaging and strain Doppler echocardiography. Heart. 2010;96(18):1469-74.

25. Bijnens B, Rudenick P, Evangelista A. Assessing aortic strain and stiffness: don't forget the physics and engineering. Heart. 2011;97(4):339.

26. Rajamannan NM, Gersh B, Bonow RO. Calcific aortic stenosis: from bench to the bedside--emerging clinical and cellular concepts. Heart. 2003;89(7):801-5.

27. Pibarot P, Dumesnil JG. New concepts in valvular hemodynamics: implications for diagnosis and treatment of aortic stenosis. Can J Cardiol. 2007;23 Suppl B:40B-7B.

28. Cavalcante JL, Lima JA, Redheuil A, Al-Mallah MH. Aortic stiffness: current understanding and future directions. J Am Coll Cardiol. 2011;57(14):1511-22.

29. Izzo JL, Jr. Arterial stiffness and the systolic hypertension syndrome. Curr Opin Cardiol. 2004;19(4):341-52.

30. Vitarelli A, Conde Y, Cimino E, D'Orazio S, Stellato S, Battaglia D, et al. Assessment of ascending aorta distensibility after successful coarctation repair by strain Doppler echocardiography. J Am Soc Echocardiogr. 2008;21(6):729-36.

31. Bjallmark A, Lind B, Peolsson M, Shahgaldi K, Brodin LA, Nowak J. Ultrasonographic strain imaging is superior to conventional non-invasive measures of vascular stiffness in the detection of age-dependent differences in the mechanical properties of the common carotid artery. Eur J Echocardiogr. 2010;11(7):630-6.

32. Mackenzie IS, Wilkinson IB, Cockcroft JR. Assessment of arterial stiffness in clinical practice. QJM 2002;95(2):67-74.

33. Rajani R, Chowienczyk P, Redwood S, Guilcher A, Chambers JB. The noninvasive estimation of central aortic blood pressure in patients with aortic stenosis. J Hypertens. 2008;26(12):2381-8.

34. Kawasaki T, Fukuda S, Shimada K, Maeda K, Yoshida K, Sunada H, et al. Direct measurement of wall stiffness for carotid arteries by ultrasound strain imaging. J Am Soc Echocardiogr. 2009;22(12):1389-95.

Original Article Number 2

Circumferential Vascular Strain Rate To Estimate Vascular Load In Aortic Stenosis: A Speckle Tracking Echocardiography Study

Int J Cardiovasc Imaging. 2015Aug;31(6):1125-35.

Rogério Teixeira[1,2,3]* MD, Ricardo Monteiro[1] BSc, Rui Baptista[2,3] MD, António Barbosa[3] BSc, Luís Leite[3], MD, Miguel Ribeiro[1] MD, Rui Martins[3] MD, Nuno Cardim[4] MD PHD, Lino Gonçalves[2,3], MD PHD.

*Corresponding Author

[1] Departamento de Medicina, Serviço de Cardiologia, Hospital Beatriz Ângelo, Loures, Portugal

[2] Faculdade de Medicina Universidade de Coimbra, Coimbra, Portugal

[3] Serviço de Cardiologia, Centro Hospitalar e Universitário de Coimbra, Coimbra, Portugal

[4] Serviço de Cardiologia, Hospital da Luz, Lisboa, Portugal

Word Count= 3713 (without references or figures/tables)

Abbreviation List

2D-STE: Two-Dimensional Speckle Tracking Echocardiography

β_1: Aortic Stiffness Index

ε: Strain

AA: Aortic Area

AS: Aortic Stenosis

AVA: Aortic Valve Area

iAVA: Indexed Aortic Valve Area

AVR: Aortic Valve Replacement

BSA: Body Surface Area

CAAS: Circumferential Ascending Aortic Strain

CAASR: Circumferential Ascending Aortic Strain Rate

D: Aortic Distensibility

ELI: Energy Loss Index

ICC: Intraclass Correlation Coefficient

LV: Left Ventricle

LVEF: Left Ventricular Ejection Fraction

LVOT: Left Ventricular Outflow Tract

MAP: Mean Arterial Pressure

PP: Pulse Pressure

ROI: Region of Interest

SAC: Systemic Arterial Compliance

SR: Strain Rate

SVI: Stroke Volume Index

TVR: Total Vascular Resistance

Z_{VA}: Valvulo arterial impedance

Abstract

Introduction: Evaluation of vascular mechanics through two-dimensional speckle-tracking echocardiography (2D-STE) is a feasible and accurate approach for assessing vascular stiffening. Degenerative aortic stenosis (AS) is currently considered a systemic vascular disease where rigidity of arterial walls increases. **Purpose:** To assess the circumferential ascending aorta strain rate (CAASR) in thoracic aortas of patients with AS, applying 2D-STE technology. **Population and methods:** 45 patients with indexed aortic valve areas (iAVA) ≤0.85 cm^2/m^2 were studied. Global CAASR served to assess vascular deformation. Clinical, echocardiographic, and non-invasive hemodynamic data were collected. A follow up (955 days) was also performed. **Results:** Average age of the cohort was 76.±10.3 years, with gender balance. Mean iAVA was 0.43±0.15 cm^2/m^2. Waveforms adequate for determining CAASR were found in 246 (91%) of the 270 aortic segments evaluated, for a mean global CAASR of 0.74±0.26 s^{-1}. Both intra- and inter-observer variability of global CAASR were deemed appropriate. CAASR correlated significantly with age (r=-0.49, *P*<0.01), the stiffness index (r=-0.59, *P*<0.01), systemic arterial compliance and total vascular resistance. There was a significant positive correlation between CAASR, body surface area (BSA), iAVA, and a negative relationship with valvulo-arterial impedance and E/e' ratio (r=-0.37, p=0.01). The stiffness index was (β=-0.41, *P*<0.01) independently associated with CAASR, in a model adjusted for age, BSA, iAVA and E/e'. Patients with a baseline CAASR ≤ 0.66 s^{-1} had a worse long-term outcome (survival 52.4 vs 83.3%, Log Rank *P*=0.04).**Conclusion**: CAASR is a promising echocardiographic tool for studying the vascular loading component of patients with AS.

Keywords: Two-Dimensional Speckle Tracking Echocardiography; Aortic Stenosis; Vascular Mechanics; Vascular Stiffness; Left Ventricular Afterload; Valvulo-Arterial Impedance; Systemic Arterial Compliance; Total Vascular Resistance; Follow-Up; Prognosis; Mortality

Introduction

Degenerative calcific aortic stenosis (AS) is currently viewed as a complex, multifaceted and systemic disease [1], displaying atherosclerotic-like and elastocalcinosis-like vascular changes that increase arterial wall rigidity [2]. Thus AS is not limited to valvular disease [2]. Arterial compliance is also reduced, and left ventricular (LV) geometry and function are altered [3].

Although the vascular component of AS is utmost importance, there is currently no gold standard method for determining local arterial stiffness. Available non-invasive methods show considerable differences in validity and reproducibility [4],[5]. Surrogates for arterial stiffness may be derived non-invasively from pulse transit time, arterial pressure waves, or relational changes in vessel diameter and distending pressure. The latter may be expressed as distensibility, compliance, elastic modulus, or stiffness index (β_1) [6].

Two-dimensional speckle-tracking echocardiography (2D-STE) involves identification of specific acoustic markers (ie, speckles) in grey-scale images, tracking them frame–by-frame throughout the cardiac cycle. This enables angle-independent calculations of motion and deformation variables, such as velocity, displacement, strain (ε), and strain rate (SR). A number of speckle-tracking algorithms have been developed, albeit aimed primarily at cardiac applications [7],[8]. Since 2008, 2D-STE studies have proved successful in assessing local vascular wall properties of proximal elastic arteries [9,10,11]. Apart from circumferential vascular ε, the rate of deformation, named the circumferential SR is other published index of vascular stiffening and aging [9].

The current study was designed to: i) assess circumferential ascending aorta strain rate (CAASR) using 2D-STE in patients with moderate to severe degenerative AS; ii) to identify predictors of CAASR; iii) to analyze the association of CAASR with LV afterload variables; iv) finally to study the CAASR prognostic significance.

Methodology

A total of 53 consecutive patients referred for echocardiography in a single laboratory were enrolled for a 2-month study, between January and February 2012. Each patient had a calculated aortic valve area ≤0.85 cm^2/m^2. Eight patients were eliminated due to poor-quality images. The final cohort consisted of 45 patients with moderate to severe AS, as previously detailed [12].

Informed consent was obtained from all participants. The local ethics committee approved this protocol.

Clinical data, systemic arterial hemodynamics and follow-up

Data recorded for each enrollee at admission included age, weight, height, and medical conditions (diabetes, hypertension, and congestive heart failure). The body surface area (BSA) was estimated according to the formula by DuBois and DuBois [13].

Systemic arterial pressure was measured using an arm cuff sphygmomanometer (right brachial artery) simultaneously with Doppler measurement of left ventricular outflow tract (LVOT) stroke volume. Indexed systemic arterial compliance (SAC) was calculated as follows: SAC= SVI/PP, where SVI is stroke volume index and PP is brachial pulse pressure. A low state of compliance was defined as SAC ≤0.6 $ml/mmHg/m^2$ [2]. Total vascular resistance (TVR) was estimated as follows: TVR = 80 × MAP/CO, where MAP is mean arterial pressure (ie, diastolic pressure plus one-third brachial pulse pressure) and CO is cardiac output [14]. Elevated TVR was defined as TVR >2000 $dynes/sec/cm^{-5}$ [2].

In November 2014, a clinical follow-up was performed by LL, who was blinded to the standard and advance echocardiographic data. The following outcomes were analysed: all cause mortality; cardiovascular mortality; aortic valve replacement (AVR); and heart failure hospitalization due to AS. We also assessed a combined endpoint of mortality + AVR + heart failure hospitalization.

Echocardiography

A Vivid 7 (GE Healthcare®, Horton, Norway) cardiovascular ultrasound device was used, with a 1.7/3.4 MHz tissue harmonic transducer. Complete echocardiographic studies called for standard views and techniques stipulated by established guidelines [15]. In addition, short-axis views of ascending aorta, past sinotubular junction (usually 2-3 cm above aortic valve), were obtained at a high frame rate (mean value, 71.1±5.3/s). For this purpose, machine settings were manually adjusted to optimize 2D aortic wall tracings and 2D-ST gray-scale

definition. All images were acquired at end-expiratory apnea. Loops of three cardiac cycles were stored digitally and analyzed offline via custom software (EchoPAC 9.0, GE Healthcare®, Horton, Norway).

Left ventricular assessment

Linear measurements of interventricular septum and posterior LV wall thickness and internal LV dimensions were acquired through a 2D long-axis parasternal window, in accord with accepted guidelines [16]. LV mass was calculated using a corrected formula of the American Society of Echocardiography and indexed for BSA [16].

LV end-systolic and end-diastolic volumes and LV ejection fraction (LVEF) were assessed using the modified Simpson's rule (method of disks) [16]. LV cardiac index was calculated as the product of heart rate and indexed stroke volume for body surface area. Stroke volume was obtained by LV outflow Doppler method as the product of LVOT area and LVOT time-velocity integral [17]. E/e' ratio (e' being an average of septal and lateral walls in tissue Doppler imaging) was used to estimate LV filling pressures [18].

Global LV afterload, elastic properties of aorta, and severity of aortic valvular stenosis

Valvuloarterial impedance (Z_{VA}), as a measure of global LV afterload, was calculated as follows: Z_{VA} = SAP+MG/SVI, where SAP is systolic arterial pressure and MG is mean transvalvular pressure gradient [2]. Significantly elevated Z_{VA} was signaled by values ≥4.5 mmHg/ml/m^2.

Aortic distensibility (D) and stiffness index (β_1) were calculated as follows: $D = 2(A_s - A_d)/[A_d (P_s - P_d)]$ in $cm^2 dyne^{-1} 10^{-6}$ and $\beta_1 = \ln(P_s / P_d)/(A_s - A_d)/A_d$ [19], where P_s and P_d are systolic and diastolic arterial pressures, and A_s and A_d are M-mode guided systolic and diastolic ascending aortic diameters, 2-3 cm above aortic valve. A_d was obtained as R wave peaked in simultaneously recorded electrocardiogram, and A_s was measured at maximal anterior aortic wall motion.

Classic Doppler echocardiographic indices of AS severity were assessed as well, including transvalvular (peak and mean) pressure gradients (by modified Bernoulli equation), indexed aortic valve area (iAVA) by continuity equation, and dimensionless velocity index (as ratio of LVOT time-velocity integral to aortic jet time-velocity integral). Energy loss index (ELI) was determined as follows: (AVA x AA/AA – AVA)/BSA, where AA is aortic cross-sectional area at level of sinotubular junction [20].

Two-dimensional speckle-tracking strain echocardiography

As in a prior publication of ours [12], calculations of regional and global thoracic ascending aortic mechanics relied on 2D-STE technology. With a line manually drawn along the inner aspect of aortic wall in short axis, additional lines were automatically generated (via 2D-STE) at the outer aspect of vessel wall. Considering the relative thinness of vascular walls (compared with cardiac walls), region of interest width was reduced to the minimal value allowable by software, as previously suggested [21]. The initial systolic frame generally served as the frame of interest, to include maximal aortic wall expansion and recoil. As in other instances [10,22], aortic wall was divided into six equidistant regions, all similar in size. In each region, numeric expressions of each 2D-STE variable represented mean values calculated from all points in arterial segments. These were color-coded and shown as a function of time throughout the cardiac cycle. Quantitative curves, depicting all regions, were possible for each 2D-ST variable. The tracking process and conversion to Lagrangian strains were performed offline, using dedicated software. CAASR curves generated here were aligned with those generated elsewhere [6,9] and included a positive early systolic peak. Global CAASR was then calculated as the mean of peak values for the six segments (Figure 1).

For the follow-up analysis we used data from our prior publication [12], regarding the global circumferential ascending aortic strain (CAAS).

We have also analyzed the LV global longitudinal ε with the 2D-STE. We calculated a mean value of 18 myocardial segments, 6 from each of the three standard apical views as previously reported [23].

Statistical analysis

The Kolmogorov-Smirnov test was used to confirm normal distribution of all continuous variables, expressed as mean and standard deviation. Student's *t* test was applied for group comparisons. Individual variables were checked for homogeneity of variance via Levene's test. Categorical variables were reported as frequencies and percentages, and χ^2 or Fisher exact tests were used when appropriate.

Based on stored images of 15 randomly selected patients, intra- and inter-observer reproducibility of CAASR values were assessed by Bland-Altman method [24] and intra-class correlation coefficient (ICC) [25].

Pearson's correlation was used to analyze the relationship between CAASR and an array of continuous variables. A linear regression analysis was performed thereafter to identify independent predictors of CAASR. We created three different models, one with clinical data,

one with afterload data, and one with valvular plus LV data. A final multivariate model including clinical, afterload and LV data was subsequently elaborated. Variables identified as significant on the bivariate analysis ($P<0.05$) and with clinical relevance, were included in the model.

A receiver-operating characteristic (ROC) curve analysis was used to compute the discriminatory power of CAASR to predict survival. The cumulative survival curves were constructed using the Kaplan-Meier method, and the groups were compared with the Log-Rank test.

A *P*-value <0.05 in two-tailed tests was considered statistically significant. All data calculations and analyses relied on SPSS® 15, Medcalc® 12.1.4 and GraphPad Prism® 6.05 statistical software packages.

Results

Average age of the 45 patients studied was 76.8±10.3 years, with gender balance. Mean iAVA was 0.43±0.15 cm^2/m^2.

Waveforms adequate for measuring CAASR were present in 246 (91%) of the 270 arterial segments evaluated. Mean global CAASR was 0.74±0.26 s^{-1} (Table 1).

CAASR correlated significantly with age (r=-0.49, *P*<0.01), BSA, and pulse pressure. It also showed significant associations with systemic arterial hemodynamic and aortic elastic variables such as SAC (r=0.54, *P*<0.01) (Figure 2, Panel A), TVR (r=-0.49, *P*<0.01), and β_1 (r=-0.59, *P* <0.01) (Figure 2, Panel B).

There was a significant positive correlation between CAASR and iAVA (r=0.44, *P* <0.01) and a negative correlation with Z_{VA} (r=-0.59, *P* <0.01).

With respect to LV performance variables, global CAASR correlated significantly with SVI (r=0.50, *P* <0.01)), with LVEF, and with E/e' ratio (r=-0.37, *P* =0.01) (Table 2).

We created three multivariate models to predict CAASR, based on clinical (Table 3.1), afterload (Table 3.2) and on valvular plus LV data (Table 3.3). We then constructed a new model that included the most relevant variables from each previous model. We demonstrated that the stiffness index was (β=-0.41, *P* <0.01) independently associated with CAASR, when adjusted for age, BSA, iAVA and estimated LV filling pressures (Table 3.4). This model had the highest R^2 (0.57) of all.

Agreement and reproducibility

Intra-observer variability of CAASR was 0.01 s^{-1} (95% confidence interval [CI]: 0.08-0.1 s^{-1}) (Figure 3, Panel A). The ICC of intra-observer CAASR variability was 0.97 (95% CI: 0.93-0.99).

Inter-observer variability of CAASR was -0.02 s^{-1} (95% CI: 0.16-0.11 s^{-1}) (Figure 3, Panel B). The ICC of inter-observer CAASR variability was 0.97 (95% CI: 0.91-0.98).

Follow up analysis

Data was available for all 45 patients, with a median follow-up time of 955 (536 – 1029) days. During this time 14 (31%) patients died. CAASR was significantly lower for the patients who died during follow up (0.61±0.18 vs 0.80±0.28 s^{-1}, *P* =0.03); conversely, no difference was identified regarding CAAS. A similar association was noted for CAASR to estimate cardiovascular mortality. No association was found with aortic mechanics (either strain or strain rate) regarding other endpoints, as AVR and admission for heart failure – Table 4. A CAASR cutpoint of 0.66 s^{-1} showed 71.4% sensitivity and 64.5 % specificity to predict

mortality during long-term follow up (AUC, 0.70; 95% CI: 0.54-0.82, *P* =0.02). Patients with a baseline global CAASR > 0.66 s^{-1} had a significant higher survival rate (83.3 vs 52.4%, Log Rank *P* =0.04) (Figure 4) than patients with values < 0.66 s^{-1}.

Utility of aortic strain rate in estimating vascular load

In 20 of our patients, SAC was ≤ 0.6 ml/mmHg/m^2. CAASR in these patients was significantly lower (0.63±0.21 vs 0.84±0.27 s^{-1}, *P* <0.01). In 14 of our patients, TVR was >2000 dynes/sec/cm^{-5}. CAASR in these patients was also significantly lower (0.82±0.25 vs 0.56±0.20 s^{-1}, p<0.01). Low SAC and elevated TVR were observed together in 11 patients. These subjects had the lowest CAASR values, compared with other patient subsets where SAC and TVR values were normal, or where SAC values alone were low and TVR normal (CAASR: 0.86±0.27, 0.74±0.19, and 0.54±0.19s^{-1}, respectively; *P* <0.01) (Figure 5).

Overall, we found that valvular and vascular components evolved in parallel. iAVA and CAASR values declined in tandem, along with increases in SVR (supplemental Table 1). However, SAC and stiffness index did not share this relationship.

Discussion

Our findings, based on 2D-STE technology, demonstrate the following concepts: (i) high feasibility and reproducibility of global CAASR determinations in patients with moderate to severe AS; (ii) correlation of CAASR and multiple parameters by univariate analysis, but β_1 index was independently associated with CAASR; (iii) association of CAASR with a SAC decline, a TVR elevation and with the LV remodeling process; (iv) prognostic influence of CAASR.

Circumferential ascending aorta strain rate

Declining arterial elasticity is largely attributable to progressive degeneration of elastin fibers within the media of arterial walls [26]. Collagen fibers gradually increase as a consequence, promoting stiffness and thickness of vessels. Such changes are especially important in proximal aorta, which is rich in the elastin fibers needed to support each systolic impulse and to accommodate stroke volume [27]. Arterial stiffness is one of the earliest detectable manifestations of adverse structural and functional changes within vascular walls. Stiffness increases with age in relatively healthy individuals and in the presence of hypertension, diabetes, and obesity [9].

This degenerative process is then bound to influence 2D-STE vascular mechanics [9]. In graphic depiction of the SR curve, circumferential SR assumes an early positive value during LV systole, as vessel wall expands to accommodate vascular flow. Large arteries are thus tasked

with providing adequate buffering during each ventricular contraction through arterial-ventricular coupling.

Vascular circumferential SR was first conceived by Oishi *et al.* in 2008 [9]. The original paper explores the vascular mechanics (ε and SR values) of abdominal aorta, asserting that vascular SR not only reflects the vascular degenerative aging process but also constitutes a better index within differing age groups, compared with the β_1 stiffness index [9]. Other studies have supported the feasibility and utility of circumferential vascular assessment as well, especially work by Bjallmark et al [6]. These investigators showed that in the common carotid artery, evaluation of vascular mechanics (including SR) via 2D-STE technology proved superior to conventional measures of vascular stiffness in assessing elastic properties of vessels [6]. Moreover, an important clinical implication of vascular ε and SR has been demonstrated recently. Parameters of carotid arterial vascular mechanics have served to predict past history of stroke in older subjects with existing increases in vascular stiffness [28]. It has also been shown that ε values of thoracic descending aorta, generated by velocity vector imaging software, are significantly lower in patients with AS, compared with values of patients with aortic regurgitation (AR); and that a bicuspid aortic valve negatively impacts aortic ε value in patients with either AS or AR [29].

To the best of our knowledge, this is the first effort to assess deformation of thoracic ascending aorta in terms of vascular SR. In related research on thoracic aortic mechanics, Vitarelli *et al.* [11] relied on tissue Doppler imaging and radial parameters. Radial deformation assesses the process of vascular thickening, which in our opinion is not conceptually equivalent with vascular wall deformation. Others have also demonstrated the poor performance of radial deformation in predicting vascular stiffening [6]. From our data, we found that locally assessed vascular stiffness was independently associated with CAASR, supporting vascular SR as best gauge of degenerative vascular remodeling.

Is CAASR useful for patients with aortic stenosis?

It is currently acknowledged that an imbalance in LV hemodynamic load increases and the capacity to overcome such increases is responsible for adverse outcomes in AS [3]. Not only is LV afterload increased by valvular obstruction, but vascular load is similarly increased. It is also well-established that reduced systemic compliance exists in >40% of patients with AS. This reduction in arterial compliance then exacerbates the LV afterload burden, culminating in adverse clinical events [2]. The changing face of this disease underscores a need for more

comprehensive assessment of AS, beyond classic variables, such as peak jet velocity, pressure gradients, valvular area, and LV function.

Through this investigation, we have shown that CAASR may be a useful non-invasively derived variable for studying the vascular component of AS, independent of blood pressure and LV performance measures, such as stroke volume. Lower CAASR correlated with increased vascular stiffness, thus indicating a higher global LV afterload. Importantly, CAASR was associated with both a pulsatile component of arterial load (SAC) and a static one (TVR). Contrary to other studies of vascular deformation, CAASR and blood pressure were unrelated [28]. Nevertheless, we believe our data are corroborated elsewhere in medical literature, where up to one-third of patients with AS have pseudo-normalized blood pressure due to reduced SAC and superimposed LV dysfunction [2,30]. Our data also indicate a significant correlation between CAASR, estimated LV filling pressures, and LVEF, all of which attest to the critical influence of vascular changes on the ventricular remodeling process, even in patients with moderate to severe AS.

In the setting of AS, we recently identified SVI as the most important determinant of circumferential ascending aortic ε, meaning that circumferential vascular deformation was dependent on change in vascular flow and not on local vascular wall properties [12]. Herein, we found that the vascular stiffness index (β_1) was strongly associated with CAASR, suggesting that the rate of circumferential vascular deformation corresponds with local arterial rigidity. CAAS and CAASR thus are complementary parameters that may aid in the non-invasive echocardiographic assessment of stroke flow and vascular load in patients with AS.

Although the primary aim of our study was to analyse the physiological determinants of CAASR in patients with degenerative AS, as an exploratory endpoint we also we also assessed clinical outcomes. We were able to demonstrate an association of thoracic ascending aortic mechanical parameters (namely CAASR, but not CAAS) with mortality during long-term follow-up. Therefore, we suggest that future research should focus on the clinical usefulness of aortic mechanics over classic outcome prediction variables, such as AVA, LV systolic and diastolic performance, flow, and vascular load.

Clinical Implications

Given the feasibility and reproducibility of 2D-STE global CAASR, we advocate its routine use in assessing the vascular loads of patients with AS. Of particular note, CAASR is a non-invasive echocardiographic parameter, unaffected by blood pressure and LV performance.

Limitations

Our analyses were based on a single centre, observational study, with a small number of patients. Brachial blood pressure was utilized, rather than central blood pressure. Brachial pressure is generally higher than central pressure, although recent data supports a reasonable clinical agreement between non-invasive brachial pressures and directly measured central aortic pressures in patients with AS [31]. To date, there is no gold standard for evaluating local arterial stiffness. As a matter of protocol, we chose vascular stiffness index [32] to validate CAASR. A recent study found no relationship between vascular mechanics and pulse wave velocity, suggesting that vascular ε and SR reflected local (not global) arterial stiffness [28]. We also had no invasive data regarding cardiac output, total systemic resistance and systemic vascular compliance.

Conclusions

CAASR determination showed high feasibility and excellent reproducibility in patients with moderate to severe AS. The stiffness index was independently associated with CAASR, and it had long-term prognostic influence, making CAASR a promising tool for studying the vascular loading component of patients with AS.

Contributions:

RT designed the study, performed data analysis, and generated the manuscript. Data was acquired by RT, AB and RMa. Post-processing imaging analysis was contributed by RT and RMo. LL preformed the clinical follow up. MR supervised all the post-processing analysis. RB consulted on methodology and results. NC and LG actively discussed and revised data. All authors participated in revision and acceptance of the finalized manuscript, confirming the accuracy of data.

Acknowledgments:

The authors thank Nélson Ribeiro BSc, and Ana Paula Oliveira BSc, for their help during initial echocardiographic patient evaluations, as well as Mrs Sónia Cancela for her logistic support.

Conflict of interest: The authors have no conflicts of interest.

Funding: none

Legends

Table 1: Circumferential ascending aorta strain rate

Table 2: Correlations of circumferential ascending aorta strain rate

Table 3.1: Model 1: Clinical parameters to predict CAASR

Table 3.2: Model 2: Afterload parameters to predict CAASR

Table 3.3: Model 3: Valvular and left ventricular parameters to predict CAASR

Table 3.4: Model 4: Final linear regression model to predict CAASR

Table 4: Follow up Data

Supplemental Table 1: Relationship between valvular and vascular loads

Figure 1: Global CAASR (s^{-1}) generated from short axis view of aorta, 2-3 cm above aortic valve. (A) Thoracic ascending aorta region of interest (short axis view). (B) Color M-mode of CAASR for all regions during cardiac cycle. (C) Color-coded curves of defined aortic segment (depicted in figure); global CAASR indicated by white dotted curve. Circumferential SR (first peak after ventricular systole) assumes early positive value due to vessel wall expansion.

Figure 2, Panel A: Correlation between global CAASR and SAC

Figure 2, Panel B: Correlation between global CAASR and β_1

Figure 3, Panel A: Bland-Altman plot of intra-observer global CAASR (s^{-1}) variability (Bias, $0.01s^{-1}$; 95% confidence interval: -0.08 to $0.1s^{-1}$).

Figure 3, Panel B: Bland-Altman plot of inter-observer global CAASR (s^{-1}) variability (Bias, -0.02 s^{-1}; 95% confidence interval: –0.16 to 0.11 s^{-1}).

Figure 4: Survival during long-term follow up stratified by CAASR cutpoint of 0.66 s^{-1}

Figure 5: CAASR in three patient subsets: normal SAC + normal TVR (n=22); low SAC + normal TVR (n=8); low SAC + elevated TVR (n=11) ($p<0.01$).

Table 1: Circumferential ascending aortic strain rate

	Total Population (n=45)
Global CAASR (s^{-1})	0.74±0.26
Segment 1 CAASR (s^{-1})	0.57±0.39
Segment 2 CAASR (s^{-1})	0.74±0.32
Segment 3 CAASR (s^{-1})	0.83±0.39
Segment 4 CAASR (s^{-1})	0.83±0.39
Segment 5 CAASR (s^{-1})	0.78±0.43
Segment 6 CAASR (s^{-1})	0.68±0.36

CAASR: circumferential ascending aortic strain rate

Table 2: Correlations of circumferential ascending aorta strain rate

	CAASR	
Clinical variables	***r***	***P***
Age (years)	-0.49	<0.01
Body surface area (m^2)	0.54	<0.01
Systolic arterial pressure (mmHg)	-0.28	0.71
Diastolic arterial pressure (mmHg)	0.05	0.42
Pulse pressure (mmHg)	-0.36	0.02
Heart rate (bpm)	-0.03	0.84
Aortic elastic properties – afterload data		
Maximal ascending aortic diameter (cm)	0.10	0.82
Minimal ascending aortic diameter (cm)	0.26	0.51
Stiffness index, β_1	-0.59	<0.01
Systemic arterial compliance (ml·mmHg^{-1}·m^{-2})	0.54	<0.01
Total vascular resistance (dyne·s·cm^{-5})	-0.49	<0.01
Aortic distensibility, D, (cm^{2}dyne^{-1}10^{-6})	0.21	0.17
Aortic valve data		
Indexed Aortic valve area (cm^2 / m^2)	0.44	<0.01
Dimensionless velocity index	0.34	0.02
Energy loss index (cm^2/m^2)	0.38	0.01
Mean aortic gradient (mmHg)	-0.28	0.07
Z_{VA} (mmHg / ml m^2)	-0.59	<0.01
Left ventricular data		
Stroke volume index (ml/m^2)	0.50	<0.01
LV ejection fraction by Simpson (%)	0.31	0.04
LV mass indexed (g/m^2)	-0.12	0.42
Relative wall thickness	-0.15	0.32
Global longitudinal ε (%)	-0.16	0.34
E/e’	-0.37	0.01

CAASR: circumferential ascending aortic strain rate ; LV: left ventricular; Z_{VA}: Valvulo-arterial impedance

Table 3.1 Model 1: Clinical parameters to predict CAASR

Variables	Beta	*T*	*P*
Age (years)	-0.29	-2.0	0.05
Body surface area (m^2)	0.32	2.13	0.04
Pulse pressure (mmHg)	-0.25	-2.0	0.052

F 9.0 ($p<0.01$); R^2=0.40

Table 3.2 Model 2: Afterload parameters to predict CAASR

Variables	Beta	*T*	*P*
Stiffness index, β_1	-0.42	-3.4	0.02
Systemic arterial compliance (ml $mmHg^{-1}$ m^{-2})	0.24	1.7	0.89
Total vascular resistance (dyne s cm^{-5})	-0.22	-1.7	0.10

F 13.0 ($p<0.01$); R^2=0.49

Table 3.3 Model 3: Valvular and left ventricular parameters to predict CAASR

Variables	Beta	*T*	*P*
Indexed aortic valve area (cm^2/m^2)	0.31	2.16	0.04
Stroke volume index (ml/m^2)	0.19	1.34	0.19
E/e’	-0.29	-2.23	0.03

F 6.3 ($p<0.01$); R^2=0.32

Table 3.4 Model 4: Final linear regression model to predict CAASR

Variables	**Beta**	***T***	***P***
Age (years)	-0.25	-1.88	0.07
Body surface area (m^2)	0.13	0.89	0.38
Stiffness index, β_1	-0.41	-3.55	<0.01
Indexed Aortic valve area (cm^2 / m^2)	0.21	1.95	0.06
E/e'	-0.16	-1.26	0.22

F 10,4 ($p<0.01$); R^2=0.57

Table 4: Follow-up data

Endpoints	CAASR (s^{-1})	CAS (%)
1.Mortality		
Yes (n=14)	0.61±0.18	5.9±2.9
No (n=31)	0.80±0.28	6.9±3.1
P Value	0.028	0.28
2.Cardiovascular Mortality		
Yes (n=10)	0.59±0.19	5.8±3.0
No (n=35)	0.78±0.27	6.4±3.0
P Value	0.05	0.55
3.Aortic valve replacement		
Yes (n=11)	0.76±0.26	6.0±2.7
No (n=34)	0.74±0.27	6.4±3.1
P Value	0.80	0.70
4.Heart failure admission		
Yes (n=14)	0.74±0.25	5.6±2.6
No (n=31)	0.75±0.27	6.6±3.1
P Value	0.94	0.34
5.Combined endpoint		
Yes (n=29)	0.73±0.25	5.9±2.9
No (n=16)	0.77±0.29	6.9±3.1
P Value	0.56	0.28

CAASR: circumferential ascending aortic strain rate; CAAS: circumferential ascending aortic strain

Supplemental Table 1: Relationship between the valvular and the vascular load

	Correlations	
	iAVA	*P*
Systolic arterial pressure (mmHg)	-0.14	0.35
Diastolic arterial pressure (mmHg)	-0.02	0.97
Pulse pressure (mmHg)	-0.17	0.26
Stroke volume index (ml/m^2)	0.41	<0.01
Systemic arterial compliance (ml / mmHg m^2)	0.28	0.06
Total vascular resistance (dyne s cm^{-5})	-0.53	<0.01
Aortic distensibility, D, ($cm^2 dyne^{-1} 10^{-6}$)	0.04	0.80
β_1 index	-0.22	0.14
CAASR (s^{-1})	0.44	<0.01
Z_{VA} (mmHg / ml m^2)	0.67	<0.01

CAASR: circumferential ascending aortic strain rate ; Z_{VA}: valvulo arterial impedance

Figure 1

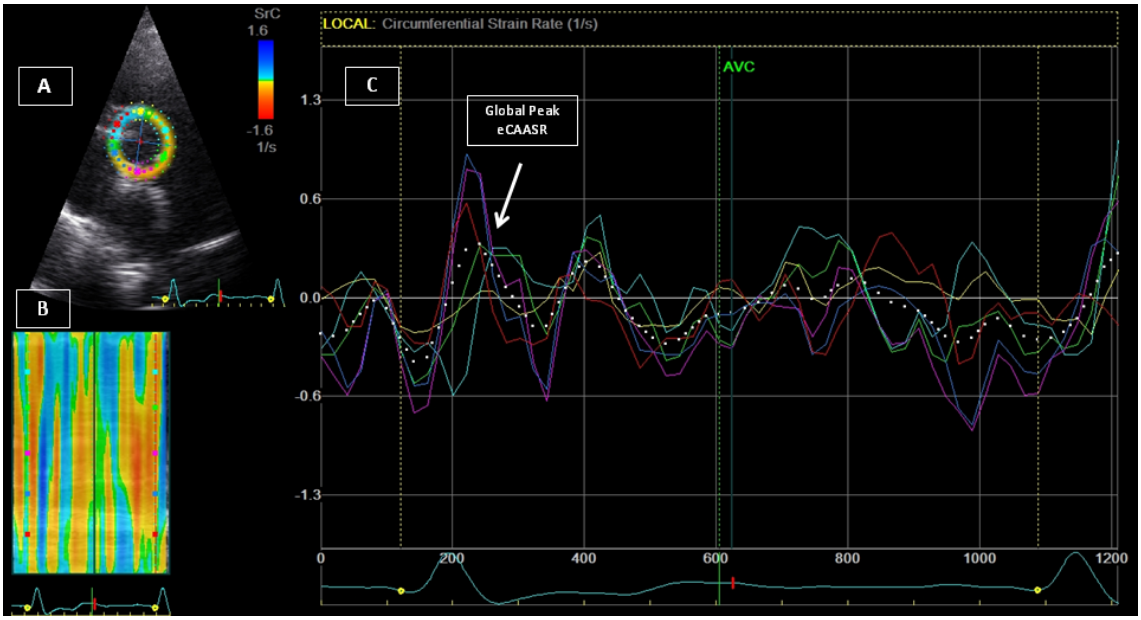
A
B
C
SrC
1.6
-1.6
1/s
LOCAL: Circumferential Strain Rate (1/s)
AVC
Global Peak
eCAASR
1.3
0.6
0.0
-0.6
-1.3
0
200
400
600
800
1000
1200

Figure 2, Panel A

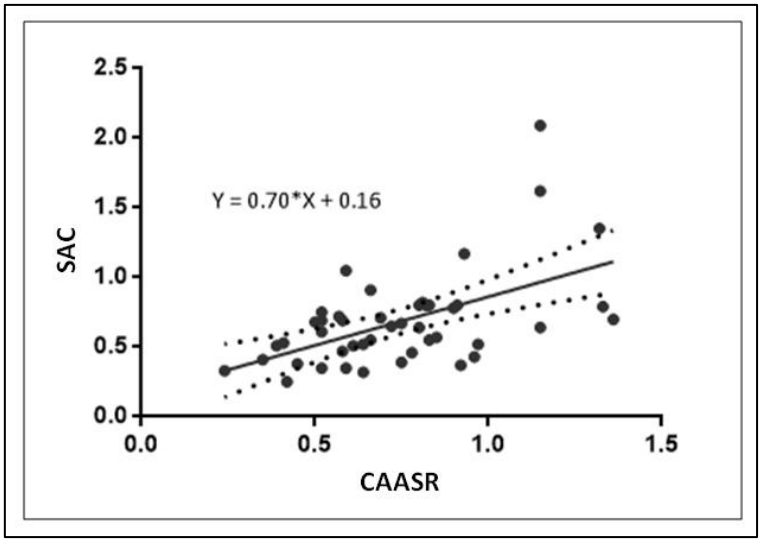

Figure 2, Panel B

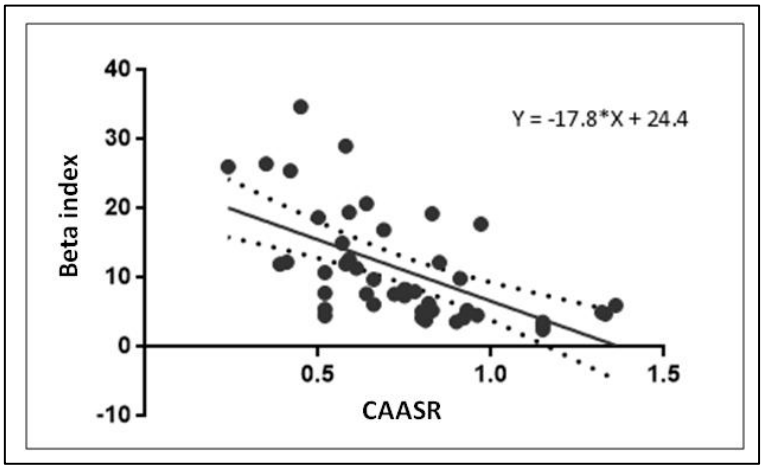

Figure 3, Panel A

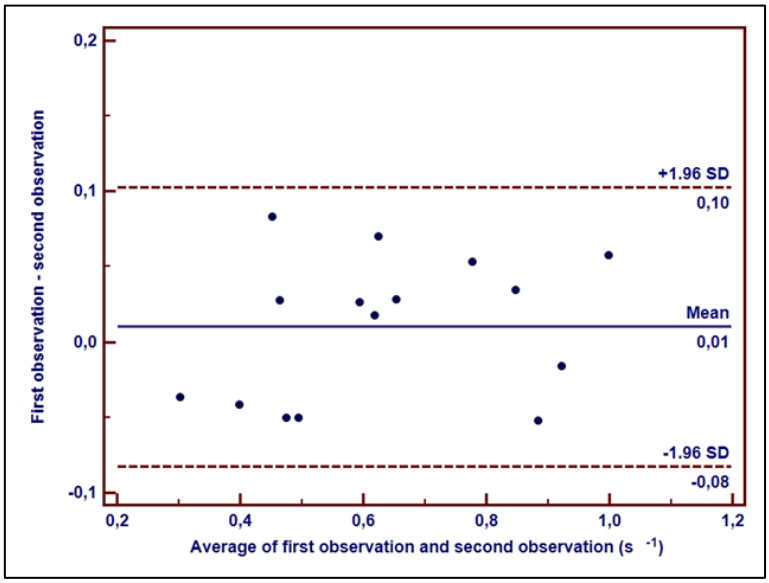

Figure 3, Panel B

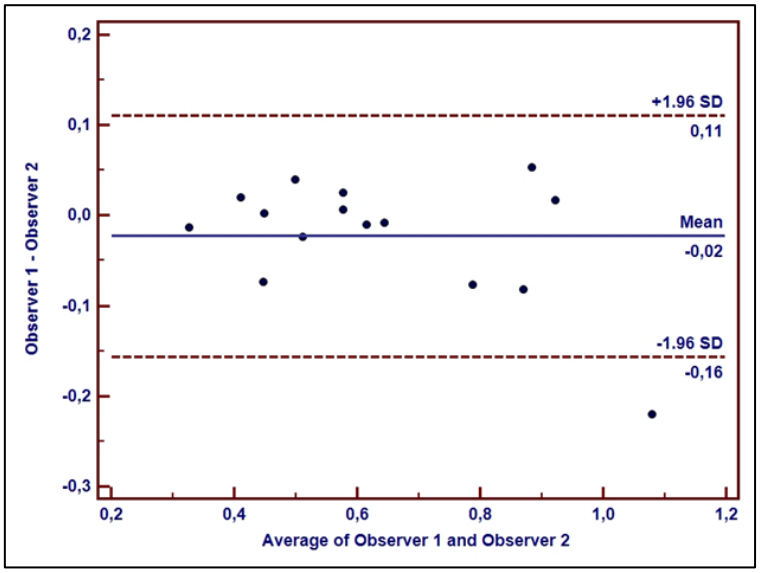

Figure 4

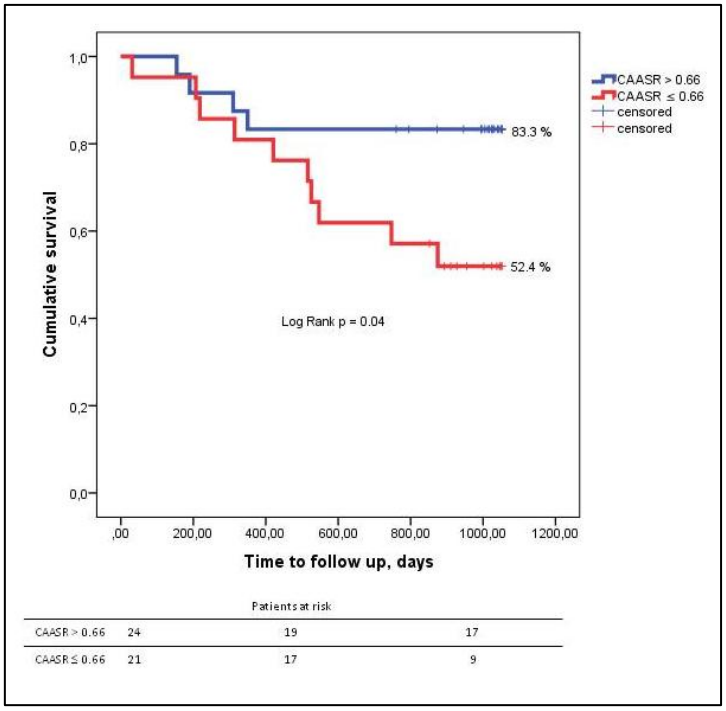
1,0
0,8
0,6
0,4
0,2
0,0
Cumulative survival
83.3 %
52.4 %
Log Rank p = 0.04
CAASR > 0.66
CAASR ≤ 0.66
censored
censored
,00
200,00
400,00
600,00
800,00
1000,00
1200,00
Time to follow up, days
Patients at risk
CAASR > 0.66 24 19 17
CAASR ≤ 0.66 21 17 9

Figure 5

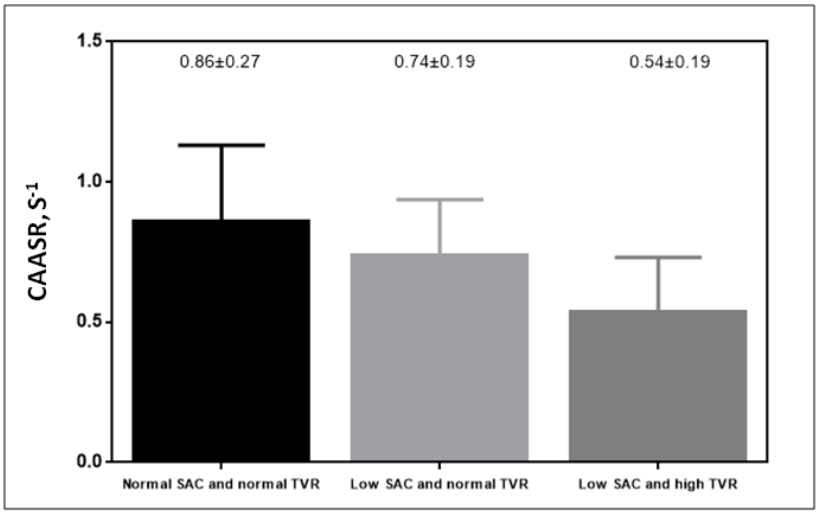
1.5
1.0
0.5
0.0
CAASR, S-1
0.86±0.27
0.74±0.19
0.54±0.19
Normal SAC and normal TVR
Low SAC and normal TVR
Low SAC and high TVR

References

1. Rajamannan NM, Evans FJ, Aikawa E, Grande-Allen KJ, Demer LL, et al. (2011) Calcific aortic valve disease: not simply a degenerative process: A review and agenda for research from the National Heart and Lung and Blood Institute Aortic Stenosis Working Group. Executive summary: Calcific aortic valve disease-2011 update. Circulation 124: 1783-1791.

2. Briand M, Dumesnil JG, Kadem L, Tongue AG, Rieu R, et al. (2005) Reduced systemic arterial compliance impacts significantly on left ventricular afterload and function in aortic stenosis: implications for diagnosis and treatment. J Am Coll Cardiol 46: 291-298.

3. Pibarot P, Dumesnil JG (2012) Improving assessment of aortic stenosis. J Am Coll Cardiol 60: 169-180.

4. Hamilton PK, Lockhart CJ, Quinn CE, McVeigh GE (2007) Arterial stiffness: clinical relevance, measurement and treatment. Clinical Science 113: 157-170.

5. Pannier BM, Avolio AP, Hoeks A, Mancia G, Takazawa K (2002) Methods and devices for measuring arterial compliance in humans. Am J Hypertens 15: 743-753.

6. Bjallmark A, Lind B, Peolsson M, Shahgaldi K, Brodin LA, et al. (2010) Ultrasonographic strain imaging is superior to conventional non-invasive measures of vascular stiffness in the detection of age-dependent differences in the mechanical properties of the common carotid artery. Eur J Echocardiogr 11: 630-636.

7. Becker M, Bilke E, Kuhl H, Katoh M, Kramann R, et al. (2006) Analysis of myocardial deformation based on pixel tracking in two dimensional echocardiographic images enables quantitative assessment of regional left ventricular function. Heart 92: 1102-1108.

8. Helle-Valle T, Crosby J, Edvardsen T, Lyseggen E, Amundsen BH, et al. (2005) New noninvasive method for assessment of left ventricular rotation: speckle tracking echocardiography. Circulation 112: 3149-3156.

9. Oishi Y, Mizuguchi Y, Miyoshi H, Iuchi A, Nagase N, et al. (2008) A novel approach to assess aortic stiffness related to changes in aging using a two-dimensional strain imaging. Echocardiography 25: 941-945.

10. Kim KH, Park JC, Yoon HJ, Yoon NS, Hong YJ, et al. (2009) Usefulness of aortic strain analysis by velocity vector imaging as a new echocardiographic measure of arterial stiffness. J Am Soc Echocardiogr 22: 1382-1388.

11. Vitarelli A, Giordano M, Germano G, Pergolini M, Cicconetti P, et al. (2010) Assessment of ascending aorta wall stiffness in hypertensive patients by tissue Doppler imaging and strain Doppler echocardiography. Heart 96: 1469-1474.

12. Teixeira R, Moreira N, Baptista R, Barbosa A, Martins R, et al. (2013) Circumferential ascending aortic strain and aortic stenosis. Eur Heart J Cardiovasc Imaging 14: 631-641.

13. Dubois D, Dubois E (1916) A formula to extimate the approximate surface area if height and weight are know. Arch Inter Med 17: 863-871.

14. Kadem L, Dumesnil JG, Rieu R, Durand LG, Garcia D, et al. (2005) Impact of systemic hypertension on the assessment of aortic stenosis. Heart 91: 354-361.

15. Evangelista A, Flachskampf F, Lancellotti P, Badano L, Aguilar R, et al. (2008) European Association of Echocardiography recommendations for standardization of performance, digital storage and reporting of echocardiographic studies. Eur J Echocardiogr 9: 438-448.

16. Lang RM, Bierig M, Devereux RB, Flachskampf FA, Foster E, et al. (2005) Recommendations for chamber quantification: a report from the American Society of Echocardiography's Guidelines and Standards Committee and the Chamber Quantification Writing Group, developed in conjunction with the European Association of Echocardiography, a branch of the European Society of Cardiology. J Am Soc Echocardiogr 18: 1440-1463.

17. Dubin J, Wallerson DC, Cody RJ, Devereux RB (1990) Comparative accuracy of Doppler echocardiographic methods for clinical stroke volume determination. American heart journal 120: 116-123.

18. Nagueh SF, Appleton CP, Gillebert TC, Marino PN, Oh JK, et al. (2009) Recommendations for the evaluation of left ventricular diastolic function by echocardiography. J Am Soc Echocardiogr 22: 107-133.

19. Stefanadis C, Stratos C, Boudoulas H, Kourouklis C, Toutouzas P (1990) Distensibility of the ascending aorta: comparison of invasive and non-invasive techniques in healthy men and in men with coronary artery disease. Eur Heart J 11: 990-996.

20. Garcia D, Pibarot P, Dumesnil JG, Sakr F, Durand LG (2000) Assessment of aortic valve stenosis severity: A new index based on the energy loss concept. Circulation 101: 765-771.

21. Catalano M, Lamberti-Castronuovo A, Catalano A, Filocamo D, Zimbalatti C (2011) Two-dimensional speckle-tracking strain imaging in the assessment of mechanical properties of carotid arteries: feasibility and comparison with conventional markers of subclinical atherosclerosis. Eur J Echocardiogr 12: 528-535.

22. Yuda S, Kaneko R, Muranaka A, Hashimoto A, Tsuchihashi K, et al. (2011) Quantitative measurement of circumferential carotid arterial strain by two-dimensional speckle tracking imaging in healthy subjects. Echocardiography 28: 899-906.

23. Mor-Avi V, Lang RM, Badano LP, Belohlavek M, Cardim NM, et al. (2011) Current and evolving echocardiographic techniques for the quantitative evaluation of cardiac mechanics: ASE/EAE consensus statement on methodology and indications endorsed by the Japanese Society of Echocardiography. J Am Soc Echocardiogr 24: 277-313.

24. Bland JM, Altman DG (1986) Statistical methods for assessing agreement between two methods of clinical measurement. Lancet 1: 307-310.

25. Shrout PE, Fleiss JL (1979) Intraclass correlations: uses in assessing rater reliability. Psychol Bull 86: 420-428.

26. Avolio A, Jones D, Tafazzoli-Shadpour M (1998) Quantification of alterations in structure and function of elastin in the arterial media. Hypertension 32: 170-175.

27. Cavalcante JL, Lima JA, Redheuil A, Al-Mallah MH (2011) Aortic stiffness: current understanding and future directions. J Am Coll Cardiol 57: 1511-1522.

28. Tsai WC, Sun YT, Liu YW, Ho CS, Chen JY, et al. (2013) Usefulness of vascular wall deformation for assessment of carotid arterial stiffness and association with previous stroke in elderly. Am J Hypertens 26: 770-777.

29. Petrini J, Jenner J, Rickenlund A, Eriksson P, Franco-Cereceda A, et al. (2014) Elastic properties of the descending aorta in patients with a bicuspid or tricuspid aortic valve and aortic valvular disease. J Am Soc Echocardiogr 27: 393-404.

30. Hachicha Z, Dumesnil JG, Bogaty P, Pibarot P (2007) Paradoxical low-flow, low-gradient severe aortic stenosis despite preserved ejection fraction is associated with higher afterload and reduced survival. Circulation 115: 2856-2864.

31. Rajani R, Chowienczyk P, Redwood S, Guilcher A, Chambers JB (2008) The noninvasive estimation of central aortic blood pressure in patients with aortic stenosis. J Hypertens 26: 2381-2388.

32. O'Rourke MF, Staessen JA, Vlachopoulos C, Duprez D, Plante GE (2002) Clinical applications of arterial stiffness; definitions and reference values. Am J Hypertens 15: 426-444.

Original Article Number 3

Aortic Arch Mechanics Measured With Two-Dimensional Speckle Tracking Echocardiography

J Hypertension. 2017. Accepted for publication 14th Februrary 2017

Rogério Teixeira[1,2,*] MD; Ricardo Monteiro[3] MSc; Rui Baptista[1,2] MD; Telmo Pereira[4] PhD; Miguel Ribeiro[5] MD; Alexandra Gonçalves[6,7] MD MMSc PhD; Nuno Cardim[8] MD PhD; Lino Gonçalves[1,2], MD PhD.

*Corresponding Author

[1] Serviço de Cardiologia, Centro Hospitalar e Universitário de Coimbra, Coimbra, Portugal

[2] Faculdade de Medicina Universidade de Coimbra, Coimbra, Portugal

[3] Lister Hospital, Stevenage, United Kingdom

[4] Escola Superior Tecnologia de Saúde Coimbra, Coimbra, Portugal

[5]Departamento de Medicina, Serviço de Cardiologia, Hospital Beatriz Ângelo, Loures, Portugal

[6] Cardiovascular Division, Brigham and Women's Hospital, Boston, MA, USA

[7] Faculdade de Medicina Universidade do Porto, Porto, Portugal

[8] Serviço de Cardiologia, Hospital da Luz, Lisboa, Portugal

Word Count: 3880 (without references or tables)

Abstract

Purpose: To study the feasibility of vascular mechanics at the aortic arch with two-dimensional speckle tracking echocardiography, as well as to define normal values and to compare results between hypertensive patients (HP) and "healthy" subjects (HS).

Methods: We included 107 subjects (61 HS and 46 HP) who underwent a complete echocardiographic exam, including a short axis view of the aortic arch. The speckle-tracking methodology was used to calculate aortic arch mechanics offline (EchoPAC; GE Healthcare®). The analysis was performed for circumferential aortic strain and for the early circumferential aortic strain rate, and we used an average result of the six equidistant segments of the arterial wall. We also assessed the aortic pulse wave velocity with the Complior® method.

Results: The 61 HS had a mean age of 33 ± 9 years, and 59% were women. Of the total 366 aortic arch wall segments, 344 (94%) had adequate waveforms for the speckle-tracking analysis. The HP had a mean age of 45 ± 12 years 54 % were women. Of the total 276 aortic wall segments, 261 (95%) had adequate waveforms for analysis. Aortic arch strain and strain rate were lower in the HP group than in the HS group (6.3±2.0% *vs*. 11.2±3.2% and 1.0±0.3 *vs.* 1.5±0.4 s^{-1}, respectively, both $P<0.01$). Aortic arch strain and strain were correlated with age (r=-0.62, r=-0.54, $P<0.01$), pulse pressure (r=-0.48; r=-0.39 $P<0.01$) and the pulse wave velocity (r=-0.57, r=-0.54, $P<0.01$). After adjustments for age, gender and body mass index, strain was significantly lower in HP, when compared to HS.

Conclusions: Speckle-tracking analysis of aortic arch images is feasible and might serve as a new approach to evaluate arterial function.

Key words: Two-dimensional speckle tracking echocardiography; vascular mechanics; aortic arch; vascular stiffness; hypertension;

Abbreviation List

2D-STE: Two-Dimensional Speckle Tracking Echocardiography

β_1: Aortic stiffness index

BP: Blood pressure

BMI: Body Mass Index

CAS: Circumferential Aortic Strain

CASR: Circumferential Aortic Strain Rate

CoV: Coefficient of Variation

e': LV Early diastolic velocity

HP: Hypertensive Patients

HS: Healthy Subjects

ICC: Intraclass Correlation Coefficient

LV: Left Ventricle

LVEF: Left Ventricular Ejection Fraction

PWV: Pulse Wave Velocity

Introduction

Two-dimensional speckle tracking echocardiography (2D-STE) is a semi automated analysis based on frame-by-frame tracking of tiny echo-dense speckles within the myocardium allowing the assessment of lengthening and shortening relative to the baseline – Lagrangian (1). This enables angle-independent calculations of motion and deformation variables, such as velocity, displacement, strain, and strain rate (2) (3). The deformation pattern can be analyzed in the longitudinal, radial and circumferential directions (2). The 2D-STE methodology has been validated by comparison with sonomicrometry (4) and tagged resonance imaging (5). The initial purpose of myocardial mechanics was the analysis of the left ventricular (LV) chamber. Subsequently it was expanded and validated for other cardiac chambers such as the right ventricle and the left ant the right atrium (1).

Vascular mechanics were first conceived by Oishi *et al*. (6) in 2008 at the level of the abdominal aorta, and since then others have demonstrated that the circumferential deformation of the proximal thoracic ascending aorta (7), the descending thoracic aorta, (7-9) and the carotid arteries (10) could be measured. Recently a three dimensional study of vascular mechanics also proved to be feasible (11). The focus of previous studies was the circumferential expansion and recoil of the vessel wall which enabled the assessment of a positive systolic strain plus a positive and negative strain rate (12). In 2015, two important validation studies of vascular mechanics (*in vivo* and *in vitro*) were reported, both based on sonomicrometry (13, 14). Moreover, an association between vascular mechanics and the collagen content of vascular wall has been demonstrated, promoting vascular mechanics as a new imaging surrogate of vascular stiffening (15). However, the assessment and reference patterns of the vascular mechanics at the aortic arch have not yet been explored. In that regard, this study has three main goals: 1) To study the feasibility and reproducibility of vascular mechanics at the aortic arch, using 2D-STE in a normal sample; 2) To compare the aortic arch mechanics between hypertensive patients (HP) and healthy subjects (HS) and 3) To access the association between aortic arch mechanics and LV early (e') diastolic velocity.

Methodology

We prospectively recruited a sample of apparently HS among hospital employees, with an age between 18 and 65 years. Participants were declared healthy after undergoing medical history and physical examination. Participants taking any cardiovascular medication, trained athletes and pregnant women were excluded. A total of 82 subjects were enrolled in the study. From these, 14 were excluded due to inadequate acoustic window and 3 by abnormal systolic blood pressure (> 140 mmHg). We also excluded 4 subjects due to poor tracking of the

short-axis view of the aortic arch. The final study population consisted of 61 HS. HS underwent anthropometric examinations, and the body surface area (BSA) was estimated according to the formula by DuBois and DuBois (16). All had normal findings on baseline echocardiography and electrocardiogram.

HP were selected from our outpatient echocardiographic referral population from January through March 2014. We excluded patients with heart failure, atrial fibrillation, recent (< 3 months) acute coronary syndrome or stroke, moderate to severe native valve disease, prosthetic heart valves, and pulmonary hypertension. During this period we received 94 requests for an outpatient echocardiographic assessment (initial or re-evaluation) for hypertensive heart disease, in patients younger than 65 years. From these, we excluded 41 due to evident co-morbidity (11, systolic heart failure; 7, atrial fibrillation; 15, moderate to severe aortic or mitral valve disease; 4, valve prosthesis; 3, recent myocardial infarction; and 1, moderate to severe pulmonary hypertension). We enrolled 53 HP in a complete echocardiographic study and excluded 7 due to poor tracking of the aortic wall in the suprasternal window. The final sample included 46 hypertensive patients.

Clinical data included age, weight, height, duration of hypertension, diabetes, dyslipidemia, smoking, prior history of acute myocardial infarction, stroke, coronary revascularization, and current medical therapy. Body mass index (BMI) was defined as the body mass divided by the square of the body height, and expressed as Kg/m^2.

Due to imbalances regarding the demographics of the HS and the HP groups, we subsequently selected 21 age-, gender- and BMI-matched case-controls from the 107 subjects included in the study.

Brachial blood pressure (BP) was measured in a supine position and after a 10-min resting period by an experienced operator and using a clinically validated (class A) sphygmomanometer (Colson MAM BP 3AA1-2®; Colson, Paris, France) (17). The mean of three measurements was used in the analysis. Brachial systolic (bSBP) and diastolic (dSBP) blood pressures were used to calculate the mean pulse pressure (bPP =bSBP −bDBP).

All subjects gave written informed consent before their participation in the study. The study protocol was approved by Comissão Nacional de Protecção de Dados (authorization 3611/2015); Hospital Beatriz Ângelo and Faculdade de Medicina da Universidade de Coimbra, ethics committee (protocol references: HBA 00762014 and CE – 005/2014).

Doppler Echocardiography

All echocardiograms were performed by 1 of 3 registered diagnostic cardiac sonographers with the same echocardiographic instrument (Vivid 7 GE Healthcare®; Horton,

Norway) and a 1.7 / 3.4 MHz tissue harmonics transducer. A complete echocardiographic study was performed with standard views, according to established guidelines (18), and data was digitally recorded for off-line analysis with software (Syngo Dynamics 9.0®; Siemens Medical Solutions, Ann Harbor, MI). All parameters were obtained after averaging three consecutive cycles. Blood pressure was measured with an arm-cuff sphygmomanometer.

Linear measurements of interventricular septum and posterior LV wall thickness and internal LV dimensions were acquired through a 2D long-axis parasternal window, in accord with accepted guidelines (19). LV and left atrial (LA) volumes were determined using the modified Simpson's rule, with images obtained from apical 4-chamber and 2-chamber views.

LV mass was calculated according to the Devereux's formula and indexed to BSA (19). Regarding the HP group, an LV mass index > 96 g/m^2 for the female gender, and > 116 g/m^2 for the male gender were considered abnormal (19).

The LA volume index (LAVI) was obtained after indexing for BSA. The left ventricular ejection fraction (LVEF) was assessed in all patients using the Simpson method (19) and the stroke volume was obtained using the LV outflow Doppler method, the product of the LV outflow area and the LV time-velocity integral (20). Pulse-wave Doppler was obtained in the apical 4-chamber view, and the peak early (E) and late (A) diastolic filling velocities, the E/A ratio and the E-wave deceleration time were obtained. Doppler tissue imaging of the mitral annular level was obtained at the septal and lateral positions. The early diastolic annular velocities showed are averages of the septal and lateral values. The LV filling pressure was estimated from the left side E/e' (e' was an average of septal and lateral walls in tissue Doppler imaging) ratio (21).

Thoracic ascending (tubular) aorta diameters were measured 2-3 cm above the level of the aortic valve, with the leading edge-to-leading edge diameter (19). We measured the aortic arch (short-axis) and the descending thoracic aorta (long-axis) at the suprasternal window. Aortic stiffness index (β_1) were calculated at the level of the aortic arch as follows $\beta_1 = \ln(P_s / P_d)/(A_s - A_d)/A_d$ (22), where P_s and P_d are systolic and diastolic arterial pressures, and A_s and A_d are M-mode guided systolic and diastolic aortic arch diameters. A_d was obtained as R wave peaked in simultaneously recorded electrocardiogram, and A_s was measured at maximal anterior aortic wall motion.

Two-dimensional speckle tracking echocardiography

The 2D-STE methodology was used to calculate the regional and global circumferential aortic arch strain (CAS) and strain rate (CASR). A short-axis view of the aortic arch, before the emergence of the brachiocephalic artery, recorded from the suprasternal notch, was selected

for this analysis. The images were acquired with a breath hold of 3 seconds, with a stable electrocardiography recording. Three consecutive heart cycles were recorded and averaged for sinus rhythm. The frame rate was >60 frames per second.

The tracking process and conversion to Lagrangian strains were performed offline using dedicated software (EchoPAC 9.0, GE Healthcare®; Horten, Norway). A line was manually drawn along the inner side of the aortic arch circumference. The software then automatically generated additional lines within a 15 mm wide region of interest . The shape and width of the regions of interest were manually adjusted. A cine loop preview feature allowed visual confirmation that the internal line followed the vascular expansion and recoil movements throughout the cardiac cycle (Supplemental Video 1 and Video 2). The initial systolic frame generally served as the frame of interest.

In agreement with previous publications on vascular mechanics (7, 10, 23), the aortic wall was divided into six equidistant regions, all similar in size. In each region, numeric expressions of each 2D-STE variable represented mean values calculated from all points in arterial segments. These were color-coded and shown as a function of time throughout the cardiac cycle. Quantitative curves, depicting all regions, were generated for each 2D-STE variable. Analyses were performed for CAS in percentages and for CASR in s^{-1}. For each, a global value was calculated, defined as the mean of the peak values of the six aortic wall segments (figure 1). The aortic arch mechanics were analyzed by one of the authors who was blinded to the clinical information.

Aortic Pulse Wave Velocity and carotid pulse wave analysis

Carotid-femoral pulse wave analysis (PWV), a measure of aortic stiffness, and carotid pulse wave analysis, were assessed simultaneously with the Complior® Analyse (Alam Medical, Paris, France) device according to a previously described technique (24). The measurements were made with the subjects in supine position with the neck in a slight hyperextension, and slightly rotated to the left, after a 10 minute resting period. Brachial BP was measured as previously described, entered on the Complior® Analyse software (Alam Medical, Paris, France), and then signal acquisition was launched. When the operator observed pulse waveforms of adequate quality, simultaneous carotid and femoral pressure curves were recorded for 15 seconds. (25). The distance travelled by the pulse waveforms was measured between the two recording sites directly on the body surface, and was automatically corrected according to the equation “0.8 x direct distance” (26). PWV was then calculated using measurements of transit time and distance travelled by the pulse wave, between the two recording sites. The carotid waveforms were calibrated with the brachial pressure, than were

averaged and mean values were extracted for the 15 seconds window of acquisition. The pressure curves were than analyzed, and morphological and temporal components of the waveforms were extracted. The following central hemodynamic parameters were calculated: central systolic blood pressure, central pulse pressure, augmentation index. All measurements were performed by a highly experienced operator (TP), with high reproducibility scores, as previously published (27) and a remarkable concordance between invasive arterial parameters and the Complior-based pulse wave analysis method, has also been previously documented (28).

In the sub-study of PWV and central hemodynamic parameters, we randomly enrolled 36 subjects. We included 22 HS and 14 HP. In these patients, the echocardiogram was performed after the PWV assessment and both operators were blinded to the clinical data and to other measurements.

Statistical analysis

The Kolmogorov-Smirnov test was used to confirm normal distribution of all continuous variables, expressed as mean and standard deviation. Variables with a non-normal distribution were transformed. Student's *t* test was applied for group comparisons. Individual variables were checked for homogeneity of variance via Levene's test.

Categorical variables were reported as frequencies and percentages, and χ^2 or Fisher exact tests were used when appropriate. Univariate and multivariate logistic regression analysis were performed to address the association between CAS and HP. Age, male gender and BMI (clinical variables) plus CAS were included in the model.

We elaborated a propensity score matching between HS and HP. The adjustment was performed for 3 clinical variables: age, gender and BMI. We selected 21 matched HP and HS, with score range ≤ 0.01 and compared CAS and CASR results.

The Pearson correlation coefficient was used to analyze the associations between CAS/CASR and age, pulse pressure, aortic arch dimensions and the Ln(β_1 index) for the 107 subjects included in the study. The association between CAS/CASR and LV e' was analyzed using two multivariate linear regression models, including age, pulse pressure, CAS and Ln(β_1 index).

Data analyses relied on SPSS® 15 (SPSS Inc, Chicago, IL), Medcalc® 12.1.4 (MedCalc Software, Mariakerke, Belgium) and GraphPad Prism® 6.05 (GraphPad Software Inc, La Jolla, CA) statistical software packages. A *P*-value <0.05 in two-tailed tests was considered statistically significant.

Inter- and intra-observer variability

The intra-observer and inter-observer variability of CAS and CASR were assessed with the Bland Altman method (29), interclass correlation coefficient (ICC) (30), and with the coefficient of variation (CoV). The analyses were performed in 30 randomly selected subjects from both the HS and HP groups.

The measurements were repeated one month later by the same echocardiographer to assess intra-observer reproducibility (RT). Inter-observer reproducibility was assessed by a second echocardiographer, who repeated the measurements (RM) in 30 participants. The values were compared with the first study. The reader could select the best cardiac cycle, but had to create a new region of interest. The readers were blinded to previous measurements.

Based on previous publications, CoV values < 10% were considered adequate (6, 31).

Results

Population sample description

We included 107 subjects (61 HS and 46 HP) and 642 aortic arch wall segments were analyzed. Among the 61 HS included, the mean age was 33 ± 9 years, and 59% were women. The HS' clinical and echocardiographic characteristics are summarized in table 1. All echocardiographic characteristics were within normal reference values.

The mean age of the HP cohort was 45 ± 12 years and 54% were women. Patients were known to be hypertensive for a median duration of 5 (range: 2-8) years, and were treated with a median of 2 (range: 1-3) antihypertensive agents. Half of the HP were medicated with calcium channel blockers, 41% with angiotensin converting enzyme inhibitors, 39% with diuretics, 35% with angiotensin II receptor blockers and 30% were medicated with beta-blockers. In the HP group, 22% (10/46) were diabetic, 20% (9/46) were smokers and almost half (48%, 22/46) had dyslipidemia, although only 39% (18/46) were on statin therapy.

HP were older but had a similar gender profile than the controls. As expected HP had a higher LV mass, a larger LA volume plus lower LV early diastolic velocities than HS (table 1).

Aortic arch mechanics: healthy subjects versus hypertensive patients

Among the HS, from a total of 366 aortic arch wall segments, 344 (94%) had adequate waveforms for 2D-STE analysis. The mean global CAS was 11.2 ± 3.2% and the mean global CASR was 1.5 ± 0.4s^{-1} (table 1). There were no significant gender differences regarding CAS (10.5 ± 2.8% for the 25 males and 11.7 ± 3.4% for the 36 females; P = 0.15).

Regarding the HP, from a total of 276 aortic wall segments, 261 (95%) had adequate waveforms for the 2D-STE analysis. The mean global CAS was 6.3 ± 2.0% and the mean global

CASR was 1.0 ± 0.3 s^{-1} (figure 2, panels A and B). HP had lower values of global and segmental aortic arch when compared with the HS group (table 1 plus supplemental table 1). In addition, by multivariate logistic regression analysis, CAS was independently associated with the hypertensive disease state, after adjustment for age, male gender and BMI (table 2).

When analyzing the 21 age-, gender- and BMI-matched case-controls, we found that CAS (7.1 ± 1.8 vs. 9.3 ± 2.4%; *P* < 0.01) and CASR (1.1 ± 0.3 vs. 1.4 ± 0.5 s^{-1}; *P*=0.03) were significantly lower among HP compared to the matched HS group (supplemental table 2).

Aortic arch mechanics associations

For the 107 subjects included in the study, we identified a negative correlation between CAS and age (r= –0.62; *P*<0.01), pulse pressure (r = –0.48; *P*<0.01), and the β_1 index (r= –0.43; *P*=0.01). The results were similar for the association of CASR (figure 4, panel B), and the previous described variables, although with a lower magnitude (table 3).

In the overall sample, aortic strain (r=-0.47, *P*<0.01) and strain rate were (r=-0.39; *P*<0.01) negatively correlated with the LV mass index. Moreover, CAS (r=0.61, *P*<0.01) and CASR (r=0.52, *P*<0.01) were also significantly correlated with LV e'. In a stepwise multivariate linear regression model, adjusted for age and systolic blood pressure, we found that CAS (β 0.27; *P*<0.01), remained independently associated with LV e' while β1 index did not (supplemental table 3).

HP with increased LV mass had lower values of CAS (5.0±1.0 vs 6.7±2.1%, *P* <0.01) and CASR (0.8±0.3 vs 1.0±0.3 s^{1}, *P* =0.049) than HP with normal LV mass (supplemental table 4).

Aortic stiffness

Data from the PVW was available for 14 HP and 22 HS. The mean PVW was 7.6 ± 2.2 m/s, and it was significantly higher for the selected HP (8.9 ± 2.9 vs. 6.8 ± 1.0 ms; *P* < 0.01). We found a negative correlation between the CAS and PWV (r = –0.57; *P* < 0.01) as well as the augmentation index (r = –0.47; *P* < 0.01). A similar association was also found for CASR (figure 3, panels A and B).

Measurement variability

Inter-observer bias of global CAS was 0.01 (limits of agreement [LA]: –1.2; 1.2). The ICC of inter-observer global CAS variability was 0.97 (95% confidence interval [CI] 0.94-0.99) and the CoV was 4.7%. The intra-observer bias of global CAS was 0.03 (LA: –0.54; 0.60). The ICC of intra-observer global CAS variability was 0.99 (95% CI: 0.94-0.99) and the CoV was 2.2%.

The inter-observer bias of the global CASR was 0.05 (LA: –0.26; 0.36). The ICC of inter-observer global CASR was 0.88 (95% CI: 0.78-0.94) and the CoV was 9.5%. The intra-observer bias of the global CASR was 0.02 (LA: –0.15; 0.18). The ICC of the intra-observer global CASR was 0.97 (0.94-0.98) and the CoV was 5.0%. Global strain and strain rate variability are presented in table 4, and segmental variability in supplemental table 5. The Bland Altman plots are presented in supplemental figure 1.

Discussion

Our findings demonstrate that 2D-STE for the evaluation of aortic arch vascular mechanics is highly feasible and reproducible. We also found that HP have lower values of aortic vascular mechanics than HS, and that aortic arch strain is independently associated with LV e'.

Aortic Arch Mechanics

To the best of our knowledge, this study addressed for the first time the assessment of aortic arch mechanics in the suprasternal window with 2D-STE. Our results are in agreement with previous literature regarding aortic mechanics, in that CAS and CASR can be used as surrogate markers of vascular stiffening (12). Aortic arch mechanics were influenced by age, and were significantly lower in hypertensive patients. Our results also showed that when CAS was added to a model with age and BMI, these later two variables were no longer a marker of disease. This suggests that CAS might capture the ageing effect of the central vasculature.

The feasibility of aortic arch 2D-STE was high, both in HP and HS, when selected by adequate image quality. Our results show a good agreement and reliability for the global result; however, the CoV was higher for the segmental mechanics. This can be explained by the lack of specific software for the 2D-STE vascular analysis, and also by the lack of standard reference points for the drawing of the region of interest.

Vascular stiffness

The arteries become stiffer with increasing age and with conditions such as hypertension (32). The increased stiffness results from structural changes, such as fragmentation of elastin, increased amount of collagen, calcification, glycation of both elastin and collagen, and cross linking of collagen by advanced glycation end-products (33).

The PWV has emerged as the gold standard method for the assessment of arterial stiffness, because of its relative ease in determination and its perceived reliability (24). The carotid-femoral PWV corresponds to the widely accepted propagative model of the arterial

system and it is supported by the large body of evidence demonstrating its association with incident cardiovascular disease, independently of traditional risk factors and in various populations (25).

In this study, CAS and CASR negatively correlated with PWV. Our results contrasted with a study by Tsai *et al*. in which the authors found no significant correlation of carotid mechanics with the PWV (34). Nevertheless, in that study the PWV was measured by photoplethysmography and included central and peripheral arteries stiffness (34). Moreover, contrary to the carotids, the aorta is a major vessel of interest when determining regional arterial stiffness, because the thoracic and abdominal aorta makes the largest contribution to the arterial buffering function (24).

Vascular mechanics and heart remodeling

We have demonstrated an association of vascular mechanics with tissue Doppler indices of myocardial relaxation – the LV e'. It has been previously demonstrated that the LV e' is a reliable non-invasive determinant of the LV constant of relaxation – *Tau* (35, 36). An increased afterload or late systolic load impairs myocardial relaxation and reduces the LV e' (37). Moreover HP with an increased LV mass had reduced values of aortic arch mechanics, also supporting the concept that aortic arch mechanics can be used as a surrogate for the vascular degenerative remodeling process in the context of aging and hypertension.

Increased stiffness of conduit arteries is associated with higher velocity of transmission of the pulse wave generated by LV ejection and an early return of reflected waves that return to the heart during LV systole; thus, increasing LV afterload and central pulse pressure (38). Moreover, an increased afterload may promote myocyte hypertrophy and slow LV relaxation (39). We believe that vascular strain and strain rate may reflect the ultrastructural changes of the vascular wall, which can have impact in LV diastolic function. In contrast to the abdominal and ascending aorta, the aortic arch is more superficial and more readily assessed. Moreover its assessment is not influenced by the surrounding structures.

We believe our currently proposed image acquisition of the aortic mechanics from the suprasternal window can be more convenient in the routine daily setting of a complete echocardiography study. Nevertheless we recognize that this new approach to evaluate arterial function is still investigational and further studies should be done to determine its clinical utility, especially over common echocardiographic measurements or the PWV. Moreover, it would be important to validate the association between vascular mechanics and the PWV more extensively, and to study its associations with other hypertensive target lesion markers, such as microalbuminuria.

Limitations

This is a single center, observational study, with a limited sample size, in a population consisted of healthy volunteers and hypertensive patients younger than 65 years. We report an adequate feasibility for the assessment of aortic arch mechanics, but we note that our results may not be reproduced in patients with difficult acoustic windows or in the elderly. The inter-observer variability, especially for the segmental values, may still represent a limitation for this assessment. At present, no other study has compared vascular mechanics with tagged magnetic resonance imaging. According to our experience the vascular speckle-tracking analysis is time consuming and increase the echocardiographic scan time. Moreover, measurements have to be taken off-line and the speckled tracking software may not be widely available.

Conclusions

Aortic arch mechanics assessed with two-dimensional speckle-tracking echocardiography is feasible and reproducible. We found that hypertensive patients have lower values of vascular mechanics than healthy subjects and we demonstrate an association between vascular stiffness and pulse wave velocity; however, further studies are warranted to evaluate the usefulness and the overall clinical utility of aortic arch mechanics.

Declaration of interest

The authors have nothing to declare.

Sources of Support: Dr. Gonçalves receives funds from Portuguese Foundation for Science and Technology, Grant HMSP-ICS/007/2012

Acknowledgments

The authors thank João Garcia BSc, Marisa Graça BSc, and Ana Silva BSc, for the echocardiographic evaluation of the patients,

Contributions:

RT conceptualized the study, performed the data analysis, wrote the manuscript and the revised manuscript. The two-dimensional echocardiographic study was performed by JG, MG and AS. Standard post-processing imaging analysis was contributed by RM. RT and RM performed the vascular mechanics analysis. TP did the PWV analysis. RB consulted on

methodology. MR supervised all the post-processing analysis. RT, RB, NC and LG actively discussed and revised data. AG gave important contributions to the revision process and to the elaboration of the revised manuscript. All authors participated in revision and acceptance of the finalized manuscript, confirming the accuracy of data.

Legends

Figures

Figure 1: Aortic arch mechanics generated from short axis view of the aortic arch in a patient with hypertension (Panels A and C) and in a healthy subject (Panels B and D). Global strain and strain rate are indicated by the white dotted curve.
Panel A: Analysis was performed for aortic arch strain, in a patient with hypertension. The value global of CAS was 7.6%.
Panel B: Analysis was performed for aortic arch strain, in a healthy subject. The value of global CAS was 15.9%.
Panel C: Analysis was performed for aortic arch strain rate, in a patient with hypertension. The global value of CASR was 0.7 s^{-1}.
Panel D: Analysis was performed for aortic arch strain rate, in a healthy subject. The value of global CASR was 1.3 s^{-1}.

Figure 2: Aortic arch mechanics for the Hypertensive Patients and the Healthy Subjects
Panel A: Circumferential Aortic Arch Strain
Panel B: Circumferential Aortic Arch Strain Rate

Figure 3: Association of aortic arch mechanics and stiffness
Panel A: Correlation of CAS and pulse wave velocity
Panel B: Correlation of CASR and pulse wave velocity

Supplemental Figure 1: Bland-Altman analysis
Panel A: Bland-Altman plot of inter-observer global CAS bias;
Panel B: Bland-Altman plot of intra-observer global CAS bias;
Panel C: Bland-Altman plot of inter-observer global CASR bias;
Panel D: Bland-Altman plot of intra-observer global CASR bias;

Supplemental Video 1: Short axis view of the aortic arch in a healthy subject
Supplemental Video 2: 2D-STE color-coded analyses of the aortic arch throughout the cardiac cycle.

Tables

Table 1: Clinical and 2D echocardiographic characteristics of the Healthy Subjects (n=61) and the Hypertensive Patients (n=46)

Clinical variables	**Healthy Subjects**	**Hypertensive Patients**	***P***
Age (years)	33±9	45±12	<0.01
Women (%)	36/61 (59)	25/46 (54)	0.63
Weight (Kg)	71±13	81±17	<0.01
Height (m)	1,69±0,09	1,66±0,11	0.23
Body mass index (Kg/m^2)	25±4	29±5	<0.01
Body surface area (m^2)	1.8±0.2	1.9±0.3	0.07
Pulse pressure (mmHg)	52±10	62±17	<0.01
Heart rate (bpm)	68±12	73±9	0.04
Echocardiographic Data			
Thoracic ascending aorta (cm)	2.9±0.3	3.1±0.4	<0.01
Aortic Arch (cm)	2.8±0.5	3.1±0.4	<0.01
Aortic stiffness, β_1 index	3.4±1.9	4.7±2.9	<0.01
Left ventricular diastolic diameter (cm)	4.7±0.5	4.8±4.8	0.21
Left ventricular mass indexed (g/m^2)	63.4±15.7	117.9±31.0	<0.01
Left ventricular ejection fraction (%)	63.5±4.3	60.6±7.4	0.02
Left atrium volume index (ml/m^2)	23.1±4.5	29.1±6.9	<0.01
e' (average septal/lateral)	14.2±2.9	9.9±3.2	<0.01
E/e'	5.9±1.4	8.8±3.1	<0.01
Global circumferential aortic strain (%)	11.2±3.2	6.3±2.0	<0.01
Global circumferential aortic strain rate (s^{-1})	1.5±0.4	1.0±0.3	<0.01

Table 2: Multivariate logistic regression analysis to study the association between hypertensive disease state and aortic strain (n=107 subjects)

Variables	Adjusted OR	95% CI	*P*
Global circumferential aortic strain, %	0.41	0.27 – 0.63	<0.01
Age, years	0.98	0.92 – 1.05	0.98
Male gender	0.85	0.26 – 2.78	0.79
Body mass index, Kg/m^2	1.12	0.99 – 1.28	0.08

Chi square: 74.0; *P*<0.01; C-statistic 0.92 (95%CI 0.86– 0.97)

Table 3: Correlations of vascular mechanics at the aortic arch for the 107 subjects

	Global Circumferential Aortic Strain		Global Circumferential Aortic Strain Rate	
Variables	***r***	***P***	***r***	***P***
Age, years	-0.62	<0.01	-0.54	<0.01
Pulse pressure, mmHg	-0.48	<0.01	-0.39	<0.01
Aortic arch, cm	-0.29	0.01	-0.29	0.01
Aortic stiffness (Ln (β_1 index))	-0.43	0.01	-0.26	0.01

Table 4: Variability of global and segmental vascular aortic arch mechanics (n=30)

	Inter-observer variability			Intra-observer variability		
	Bias (limitis of agreement)	**ICC (95% CI)**	**CoV (%)**	**Bias (limits of agreement)**	**ICC (95% CI)**	**CoV (%)**
Global CAS	0.01 (-1.2; 1.2)	0.97 (0.94 – 099)	4.7	0.03 (-0.54; 0.60)	0.99 (0.94 – 0.99)	2.2
Global CASR	0.05 (-0.26;0.36)	0.88 (0.78 – 0.94)	9.5	0.02 (-0.15; 0.18)	0.97 (0.94 – 0.98)	5.0

CAS: circumferential aortic strain; CASR: circumferential aortic strain rate; ICC – intraclass correlation coefficient;

Supplemental Table 1: Vascular mechanics at the aortic arch

	Healthy Subjects (n=61)	**Hypertensive Patients (n=46)**	***P***
CAS segment 1 (%)	10.2±4.9	4.6±2.4	<0.01
CAS segment 2 (%)	11.9±5.4	5.2±3.3	<0.01
CAS segment 3 (%)	9.9±4.3	6.2±3.6	<0.01
CAS segment 4 (%)	11.8±3.8	7.6±3.8	<0.01
CAS segment 5 (%)	12.0±6.1	7.4±3.5	<0.01
CAS segment 6 (%)	11.9±6.2	6.6±3.3	<0.01
CASR segment 1 (s^{-1})	1.6±0.6	0.8±0.4	<0.01
CASR segment 2 (s^{-1})	1.8±0.7	1.1±0.6	<0.01
CASR segment 3 (s^{-1})	1.4±0.6	1.1±0.5	<0.01
CASR segment 4 (s^{-1})	1.5±0.7	1.1±0.6	<0.01
CASR segment 5 (s^{-1})	1.4±0.6	0.9±0.5	<0.01
CASR segment 6 (s^{-1})	1.5±0.7	0.9±0.4	<0.01

CAS – circumferential aortic strain; CASR – circumferential aortic strain rate;

Supplemental Table 2: Aortic arch mechanics, an age and gender matched analysis

	Healthy Subjects (n=21)	**Hypertensive Patients (n=21)**	***P***
Age (years)	40±10	40±12	0.93
Male gender (%)	11/21 (52)	9/21 (43)	0.54
Weight (Kg)	75±14	74±16	0.75
Height (m)	1.67±0.10	1.63±0.12	0.34
Body mass index (Kg/m^2)	27±5	27±4	0.84
Body surface area (m^2)	1.8±0.2	1.8±0.3	0.54
Heart rate (bpm)	70±12	73±9	0.22
Pulse Pressure (mmHg)	55±13	57±13	0.69
Aortic Arch (cm)	2.9±0.3	2.9±0.4	0.84
Left ventricular mass indexed (g/m^2)	64.6±16.7	91.3±25.4	<0.01
Left ventricular ejection fraction (%)	63.5±4.7	58.1±6.6	<0.01
Left atrium volume index (ml/m^2)	24.1±5.4	26.4±7.3	0.26
Aortic stiffness, β_1 index	4.6±2.8	6.0±3.4	0.17
Global circumferential aortic strain (%)	9.3±2.4	7.1±1.8	<0.01
Global circumferential aortic strain rate (s^{-1})	1.4±0.5	1.1±0.3	0.03

Supplemental Table 3: Multivariate linear regression models for the LV e'

Model 1			
Variables	**Beta**	***T***	***P***
Age, years	-0.66	-8.9	<0.01
R^2=0.43			
Model 2			
Variables	**Beta**	***T***	***P***
Age, years	-0.48	-6.1	<0.01
Systolic blood pressure, mmHg	-0.34	-4.4	<0.01
R^2=0.52; R^2 change=0.09, *P*<0.01			
Model 3			
Variables	**Beta**	***T***	***P***
Age, years	-0.37	-4.3	<0.01
Systolic blood pressure, mmHg	-0.24	-2.9	<0.01
Global circumferential aortic strain, %	0.27	2.9	<0.01
R^2=0.56; R^2 change from Model 2=0.04, *P*<0.01			
Model 4			
Variables	**Beta**	***T***	***P***
Age, years	-0.49	-6.0	<0.01
Systolic blood pressure, mmHg	-0.35	-4.4	<0.01
Aortic stiffness (Ln (β_1 index))	0.04	0.6	0.57
R^2=0.52; R^2 change from Model 2=0.01, *P*=0.57			

Supplemental Table 4: Hypertensive patients with normal versus increased LV mass

	Normal LV Mass (N=34)	**Increased LV Mass (N=12)**	***P* Value**
Age (years)	43±13	50±9	<0.01
Male gender (%)	17/34 (50)	4/12 (44)	0.32
Body mass index (Kg/m^2)	29±5	29±3	0.72
Body surface area (m^2)	1.9±0.2	1.7±0.2	0.01
Pulse pressure (mmHg)	62±18	62±16	0.99
Heart rate (bpm)	73±9	73±10	0.89
Left ventricular ejection fraction (%)	62±6	58±10	0.18
e' (average septal/lateral)	11±3	7±3	<0.01
E/e'	8±3	11±4	<0.01
Left atrial volume index (ml/m^2)	28±6	33±7	0.02
Aortic stiffness, β_1 index	4.8±3.3	4.3±1.8	0.57
Global circumferential aortic strain (%)	6.7±2.1	5.0±1.0	<0.01
Global circumferential aortic strain rate (s^{-1})	1.0±0.3	0.8±0.3	0.049

Supplemental Table 5: Variability of segmental vascular aortic arch mechanics (n=30)

	Inter-observer variability			Intra-observer variability		
	Bias (limitis of agreement)	**ICC (95% CI)**	**CoV (%)**	**Bias (limits of agreement)**	**ICC (95% CI)**	**CoV (%)**
CAS segment 1	0.1 (-2.8; 3.0)	0.92 (0.83 – 0.96)	13.2	0.2 (-1.5; 1.8)	0.97 (0.95 – 0.99)	7.7
CAS segment 2	-0.3 (-3.2; 2.7)	0.93 (0.86 – 0.97)	12.9	-0.1 (-2.0; 1.8)	0.97 (0.94 – 0.99)	8.4
CAS segment 3	-0.1 (-2.9; 2.8)	0.92 (0.84 – 0.96)	10.7	0.04 (-1.5; 1.6)	0.97 (0.95 – 0.99)	5.9
CAS segment 4	0.0 (-3.7; 3.6)	0.89 (0.79 – 0.95)	12.6	0.1 (-2.2; 2.3)	0.96 (0.91; 0.98)	7.9
CAS segment 5	0.0 (-2.7; 2.7)	0.94 (0.88 – 0.97)	9.8	0.02 (-1.9; 1.9)	0.97 (0.94 – 0.99)	6.9
CAS segment 6	0.3 (-2.1; 2.6)	0.96 (0.92 – 0.98)	8.8	0.0 (-1.9; 2.0)	0.97 (0.95 – 0.99)	7.0
CASR segment 1	0.02 (-0.64;0.61)	0.86(0.71 – 0.93)	20.7	0.02 (-0.25;0.29)	0.97 (0.95 – 0.99)	8.9
CASR segment 2	0.01 (-0.61;0.59)	0.94 (0.88 – 0.97)	15.9	-0.04(-0.26;0.18)	0.97 (0.96 – 0.99)	6.2
CASR segment 3	0.07 (-0.54;0.67)	0.86 (0.70 – 0.93)	16.8	0.01(-0.26;0.27)	0.97 (0.95 – 0.99)	7.0
CASR segment 4	0.08 (-0.42;0.58)	0.92 (0.84 – 0.96)	15.9	0.06(-0.30;0.42)	0.96 (0.92 – 0.98)	10.4
CASR segment 5	0.04 (-0.43;0.51)	0.95 (0.88 – 0.97)	15.9	0.03(-0.34;0.39)	0.97 (0.93 – 0.98)	12.2
CASR segment 6	0.07 (-0.29;0.43)	0.97 (0.92 – 0.98)	12.3	0.02(-0.33;0.36)	0.97(0.93 – 0.99)	10.8

CAS: circumferential aortic strain; CASR: circumferential aortic strain rate; ICC – intraclass correlation coefficient;

Figure 1

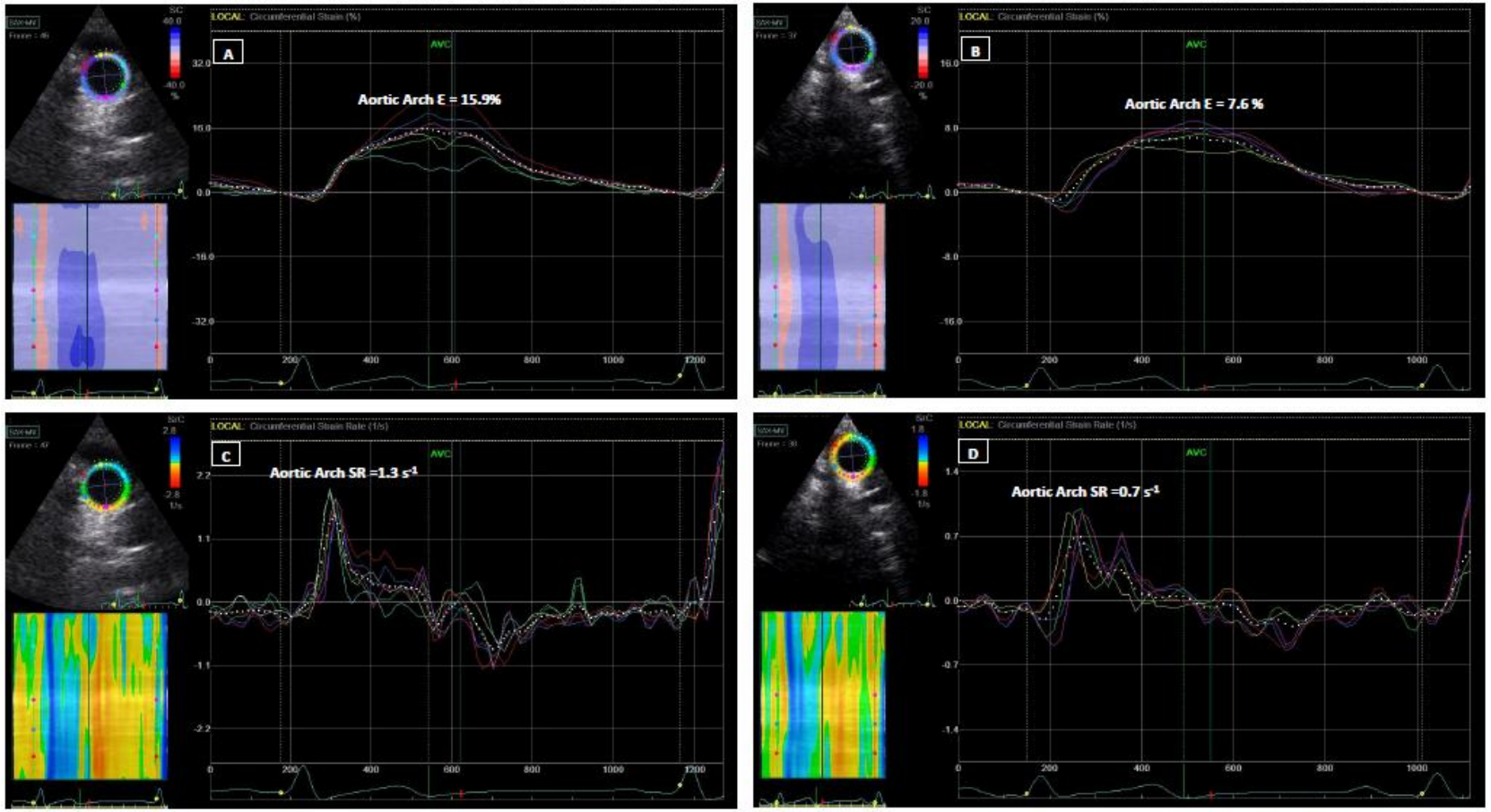
A
Aortic Arch E = 15.9%
B
Aortic Arch E = 7.6 %
C
Aortic Arch SR =1.3 s-1
D
Aortic Arch SR =0.7 s-1

Figure 2 Panel A

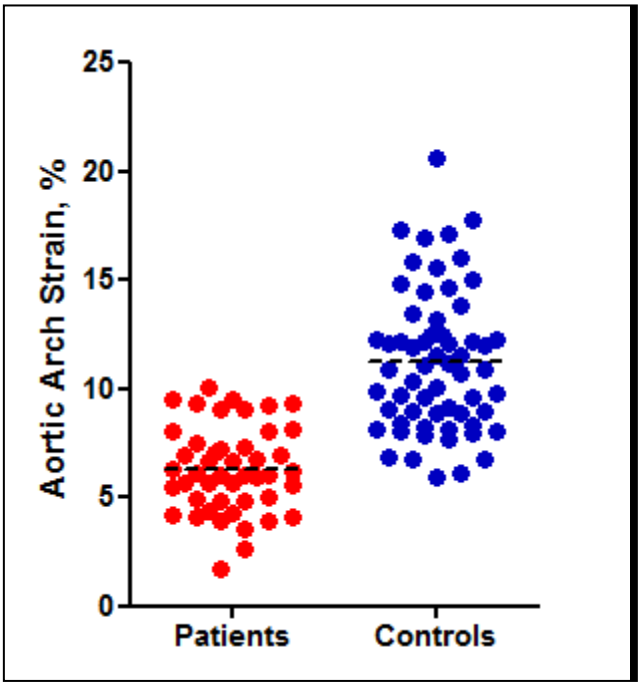

Figure 2 Panel B

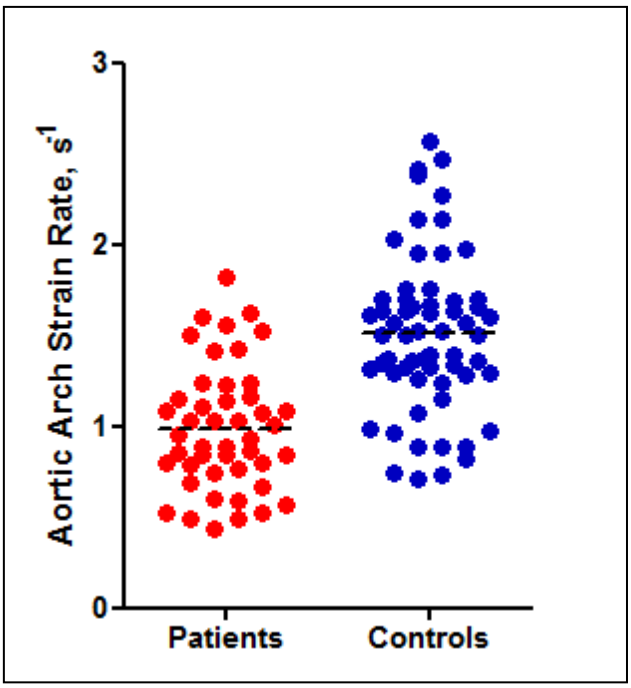

Figure 3 Panel A **Figure 3 Panel B**

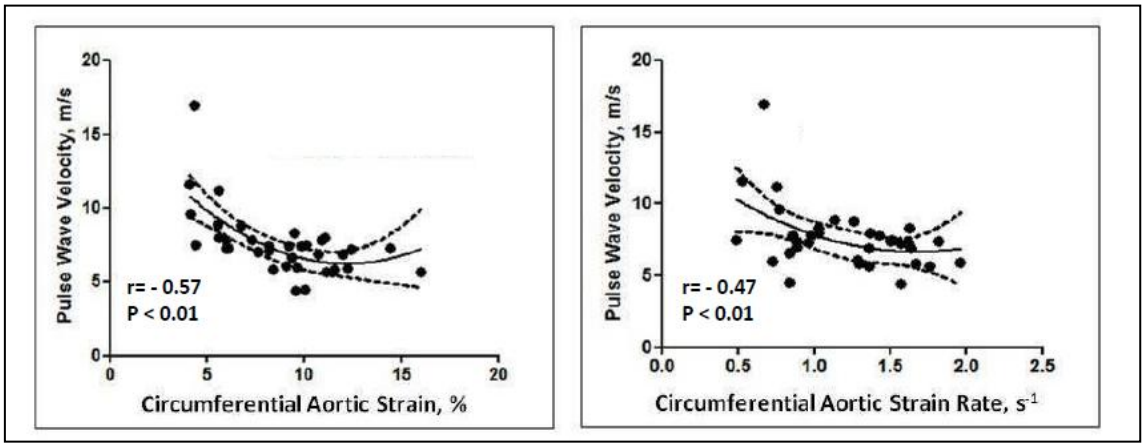

Supplemental Figure 1

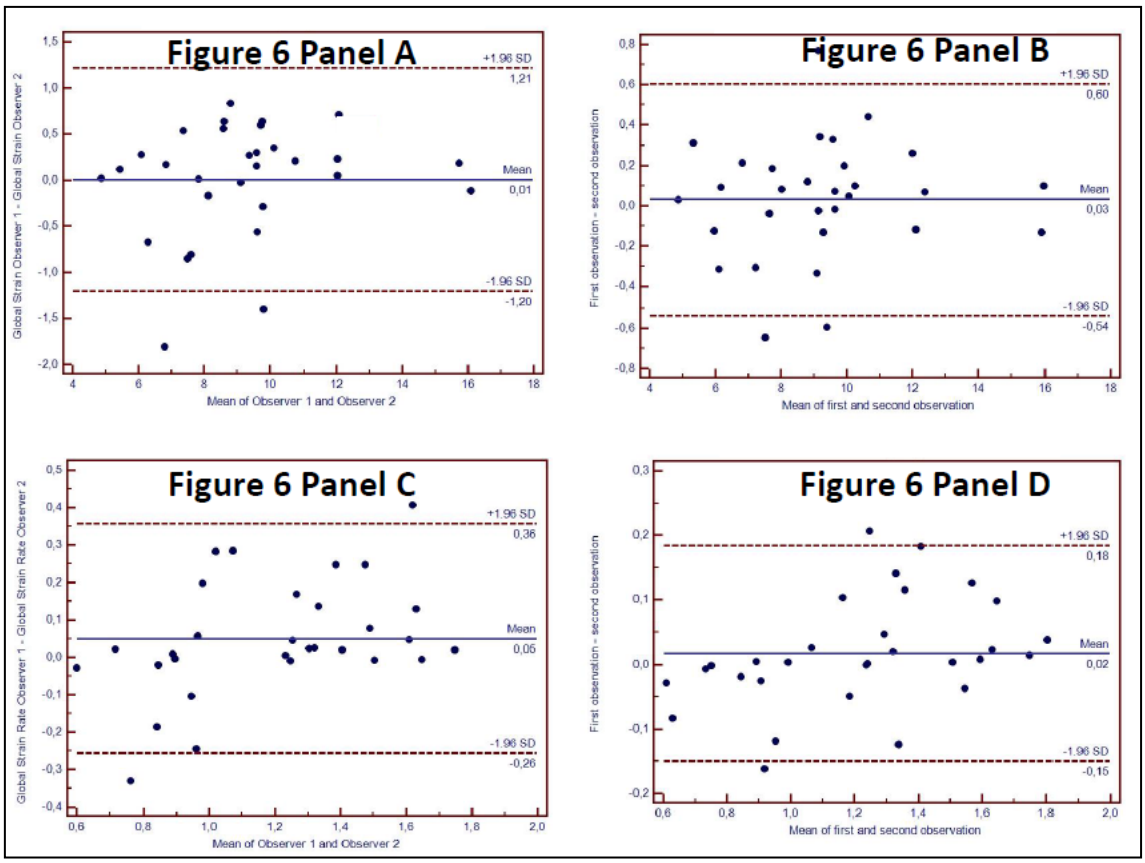

References

1. Mor-Avi V, Lang RM, Badano LP, Belohlavek M, Cardim NM, Derumeaux G, et al. Current and evolving echocardiographic techniques for the quantitative evaluation of cardiac mechanics: ASE/EAE consensus statement on methodology and indications endorsed by the Japanese Society of Echocardiography. J Am Soc Echocardiogr. 2011 Mar;24(3):277-313.
2. Leitman M, Lysyansky P, Sidenko S, Shir V, Peleg E, Binenbaum M, et al. Two-dimensional strain-a novel software for real-time quantitative echocardiographic assessment of myocardial function. J Am Soc Echocardiogr. 2004 Oct;17(10):1021-9.
3. Reisner SA, Lysyansky P, Agmon Y, Mutlak D, Lessick J, Friedman Z. Global longitudinal strain: a novel index of left ventricular systolic function. J Am Soc Echocardiogr. 2004 Jun;17(6):630-3.
4. Korinek J, Wang J, Sengupta PP, Miyazaki C, Kjaergaard J, McMahon E, et al. Two-dimensional strain--a Doppler-independent ultrasound method for quantitation of regional deformation: validation in vitro and in vivo. J Am Soc Echocardiogr. 2005 Dec;18(12):1247-53.
5. Cho GY, Chan J, Leano R, Strudwick M, Marwick TH. Comparison of two-dimensional speckle and tissue velocity based strain and validation with harmonic phase magnetic resonance imaging. Am J Cardiol. 2006 Jun 1;97(11):1661-6.
6. Oishi Y, Mizuguchi Y, Miyoshi H, Iuchi A, Nagase N, Oki T. A novel approach to assess aortic stiffness related to changes in aging using a two-dimensional strain imaging. Echocardiography. 2008 Oct;25(9):941-5.
7. Teixeira R, Moreira N, Baptista R, Barbosa A, Martins R, Castro G, et al. Circumferential ascending aortic strain and aortic stenosis. Eur Heart J Cardiovasc Imaging. 2013 Jul;14(7):631-41.
8. Kim KH, Park JC, Yoon HJ, Yoon NS, Hong YJ, Park HW, et al. Usefulness of aortic strain analysis by velocity vector imaging as a new echocardiographic measure of arterial stiffness. Journal of the American Society of Echocardiography : official publication of the American Society of Echocardiography. 2009 Dec;22(12):1382-8.
9. Petrini J, Jenner J, Rickenlund A, Eriksson P, Franco-Cereceda A, Caidahl K, et al. Elastic properties of the descending aorta in patients with a bicuspid or tricuspid aortic valve and aortic valvular disease. J Am Soc Echocardiogr. 2014 Apr;27(4):393-404.
10. Yuda S, Kaneko R, Muranaka A, Hashimoto A, Tsuchihashi K, Miura T, et al. Quantitative measurement of circumferential carotid arterial strain by two-dimensional speckle tracking imaging in healthy subjects. Echocardiography. 2011 Sep;28(8):899-906.
11. Karatolios K, Wittek A, Nwe TH, Bihari P, Shelke A, Josef D, et al. Method for aortic wall strain measurement with three-dimensional ultrasound speckle tracking and fitted finite element analysis. Ann Thorac Surg. 2013 Nov;96(5):1664-71.
12. Teixeira R, Vieira MJ, Goncalves A, Cardim N, Goncalves L. Ultrasonographic vascular mechanics to assess arterial stiffness: a review. Eur Heart J Cardiovasc Imaging. 2015 Nov 6.
13. Larsson M, Verbrugghe P, Smoljkic M, Verhoeven J, Heyde B, Famaey N, et al. Strain assessment in the carotid artery wall using ultrasound speckle tracking: validation in a sheep model. Phys Med Biol. 2015 Feb 7;60(3):1107-23.
14. Larsson M, Heyde B, Kremer F, Brodin LA, D'Hooge J. Ultrasound speckle tracking for radial, longitudinal and circumferential strain estimation of the carotid artery--an in vitro validation via sonomicrometry using clinical and high-frequency ultrasound. Ultrasonics. 2015 Feb;56:399-408.
15. Kim SA, Lee KH, Won HY, Park S, Chung JH, Jang Y, et al. Quantitative assessment of aortic elasticity with aging using velocity-vector imaging and its histologic correlation. Arterioscler Thromb Vasc Biol. 2013 Jun;33(6):1306-12.
16. Dubois D, Dubois E. A formula to extimate the approximate surface area if height and weight are know. Arch Inter Med. 1916;17:863-71.

17. Pereira T, Maldonado J. Performance of the Colson MAM BP 3AA1-2 automatic blood pressure monitor according to the European Society of Hypertension validation protocol. Rev Port Cardiol. 2005(24):1341-51.
18. Evangelista A, Flachskampf F, Lancellotti P, Badano L, Aguilar R, Monaghan M, et al. European Association of Echocardiography recommendations for standardization of performance, digital storage and reporting of echocardiographic studies. Eur J Echocardiogr. 2008 Jul;9(4):438-48.
19. Lang RM, Badano LP, Mor-Avi V, Afilalo J, Armstrong A, Ernande L, et al. Recommendations for cardiac chamber quantification by echocardiography in adults: an update from the American Society of Echocardiography and the European Association of Cardiovascular Imaging. J Am Soc Echocardiogr. 2015 Jan;28(1):1-39 e14.
20. Dubin J, Wallerson DC, Cody RJ, Devereux RB. Comparative accuracy of Doppler echocardiographic methods for clinical stroke volume determination. Am Heart J. 1990 Jul;120(1):116-23.
21. Ommen SR, Nishimura RA, Appleton CP, Miller FA, Oh JK, Redfield MM, et al. Clinical utility of Doppler echocardiography and tissue Doppler imaging in the estimation of left ventricular filling pressures: A comparative simultaneous Doppler-catheterization study. Circulation. 2000 Oct 10;102(15):1788-94.
22. Stefanadis C, Stratos C, Boudoulas H, Kourouklis C, Toutouzas P. Distensibility of the ascending aorta: comparison of invasive and non-invasive techniques in healthy men and in men with coronary artery disease. Eur Heart J. 1990 Nov;11(11):990-6.
23. Kim KH, Park JC, Yoon HJ, Yoon NS, Hong YJ, Park HW, et al. Usefulness of aortic strain analysis by velocity vector imaging as a new echocardiographic measure of arterial stiffness. J Am Soc Echocardiogr. 2009 Dec;22(12):1382-8.
24. Laurent S, Cockcroft J, Van Bortel L, Boutouyrie P, Giannattasio C, Hayoz D, et al. Expert consensus document on arterial stiffness: methodological issues and clinical applications. Eur Heart J. 2006 Nov;27(21):2588-605.
25. Determinants of pulse wave velocity in healthy people and in the presence of cardiovascular risk factors: 'establishing normal and reference values'. Eur Heart J. 2010 Oct;31(19):2338-50.
26. Van Bortel LM, Laurent S, Boutouyrie P, Chowienczyk P, Cruickshank JK, De Backer T, et al. Expert consensus document on the measurement of aortic stiffness in daily practice using carotid-femoral pulse wave velocity. J Hypertens. 2012 Mar;30(3):445-8.
27. Pereira T, Maldonado J, Andrade I, Cardoso E, Laranjeiro M, Coutinho R, et al. Reproducibility of aortic pulse wave velocity as assessed with the new Complior Analyse. Blood Press Monit. 2014 Jun;19(3):170-5.
28. Pereira T, Maldonado J, Coutinho R, Cardoso E, Laranjeiro M, Andrade I, et al. Invasive validation of the Complior Analyse in the assessment of central artery pressure curves: a methodological study. Blood Press Monit. 2014 Oct;19(5):280-7.
29. Bland JM, Altman DG. Statistical methods for assessing agreement between two methods of clinical measurement. Lancet. 1986 Feb 8;1(8476):307-10.
30. Shrout PE, Fleiss JL. Intraclass correlations: uses in assessing rater reliability. Psychol Bull. 1979 Mar;86(2):420-8.
31. Petrini J, Yousry M, Rickenlund A, Liska J, Hamsten A, Eriksson P, et al. The feasibility of velocity vector imaging by transesophageal echocardiography for assessment of elastic properties of the descending aorta in aortic valve disease. J Am Soc Echocardiogr. 2010 Sep;23(9):985-92.
32. Janic M, Lunder M, Sabovic M. Arterial stiffness and cardiovascular therapy. Biomed Res Int. 2014;2014:621437.
33. Laurent S, Boutouyrie P, Lacolley P. Structural and genetic bases of arterial stiffness. Hypertension. 2005 Jun;45(6):1050-5.

34. Tsai WC, Sun YT, Liu YW, Ho CS, Chen JY, Wang MC, et al. Usefulness of vascular wall deformation for assessment of carotid arterial stiffness and association with previous stroke in elderly. Am J Hypertens. 2013 Jun;26(6):770-7.
35. Nagueh SF, Sun H, Kopelen HA, Middleton KJ, Khoury DS. Hemodynamic determinants of the mitral annulus diastolic velocities by tissue Doppler. J Am Coll Cardiol. 2001 Jan;37(1):278-85.
36. Oki T, Tabata T, Yamada H, Wakatsuki T, Shinohara H, Nishikado A, et al. Clinical application of pulsed Doppler tissue imaging for assessing abnormal left ventricular relaxation. Am J Cardiol. 1997 Apr 1;79(7):921-8.
37. Nagueh SF, Appleton CP, Gillebert TC, Marino PN, Oh JK, Smiseth OA, et al. Recommendations for the evaluation of left ventricular diastolic function by echocardiography. J Am Soc Echocardiogr. 2009 Feb;22(2):107-33.
38. O'Rourke MF. Diastolic heart failure, diastolic left ventricular dysfunction and exercise intolerance. J Am Coll Cardiol. 2001 Sep;38(3):803-5.
39. Leite-Moreira AF, Correia-Pinto J, Gillebert TC. Afterload induced changes in myocardial relaxation: a mechanism for diastolic dysfunction. Cardiovasc Res. 1999 Aug 1;43(2):344-53.

Original Article Number 4

Descending Aortic Mechanics and Atrial Fibrillation: A Two-Dimensional Speckle Tracking Transesophageal Echocardiography Study

Int J Cardiovasc Imaging. 2016 Apr; 33(4): 509-519

Rogério Teixeira[1,2]* MD; Ricardo Monteiro[3] MSc; Paulo Dinis[1] MD, Maria José Santos[1] BSc; Ana Botelho[1] MD; Nuno Quintal[1] MD; Nuno Cardim[4] MD PhD; Lino Gonçalves[1,2] MD PhD.

*Corresponding Author

[1] Serviço de Cardiologia, Centro Hospitalar e Universitário de Coimbra – Hospital Geral, Coimbra, Portugal

[2] Faculdade de Medicina Universidade de Coimbra, Coimbra, Portugal

[3] Lister Hospital, Stevenage, United Kingdom

[4] Serviço de Cardiologia, Hospital da Luz, Lisboa, Portugal

Word Count: 3071

Abbreviation List

2D-STE: Two-Dimensional Speckle Tracking Echocardiography

β_1: Aortic stiffness index

ε: Strain

AF: Atrial Fibrillation

BSA: Body Surface Area

CAS: Circumferential Aortic Strain

CASR: Circumferential Aortic Strain Rate

CHA_2DS_2-VASc score: C-congestive heart failure; H-Hipertension; A_2-Age >75; S_2-Stroke; V-vascular disease; A-Age 65-75; Sc- sex category

CoV: Coefficient of Variation

EHRA: European Heart Rhythm Association

HF: Heart Failure

LA: Left Atrium

LAA: Left Atrial Appendage

LAVI: Lef Atrial Volume Index

LV: Left Ventricle

LVEF: Left Ventricular Ejection Fraction

NYHA: New York Heart Association

PWV: Pulse Wave Velocity

ROI: Region of Interest

SR: Strain Rate

TEE: Transesophageal Echocardiography

Abstract

Introduction: Vascular mechanics assessed with two-dimensional speckle tracking echocardiography (2D-STE) could be used as a new imaging surrogate of vascular stiffening. The CHA_2DS_2-VASc score is considered accurate as an estimate of stroke risk in non-valvular AF, althought many potential stroke risk factors have not been included in this scoring method. **Purposes:** The purpose of this research is to study the feasibility of evaluating vascular mechanics at the descending aorta in non-valvular AF patients using transesophageal 2D-STE and to analyze the association between descending aortic mechanics and stroke. **Methods:** We prospectively recruited a group of 44 patients referred for a transesophageal echocardiogram (TEE) in the context of cardioversion for non-valvular AF. A short-axis view of the descending aorta, one to two centimeters after the aortic arch was selected for the vascular mechanics assessment with the 2D-STE methodology. The vascular mechanics parameters analyzed were circumferential aortic strain (CAS) and early circumferential aortic strain rate (CASR). A clinical assessment was performed with focus on the past stroke history and the CHA_2DS_2-VASc score. **Results:** The mean age of our cohort was 65 ± 13 years and 75% were men; AF was known for 2.8±2.5 years and it was considered paroxystic in 41% of cases. Waveforms adequate for measuring 2D-STE were present in 85% of the 264 descending aortic wall segments. The mean CAS was 3.5±1.2% and the mean CASR was 0.7±0.3 s^{-1}. The inter- and intra-observer variability for aortic mechanics was considered adequate. The median CHA_2DS_2VASc score was 2 (2 – 3). As the score increased we noted that both the CAS (r=-0.38, *P*=0.01) and the CASR (r=-0.42, *P*<0.01) decreased. Over 16% of the AF patients had a past history of stroke. These patients had lower values of both descending aortic strain (2.2 [1.8 – 2.6] vs 3.9[3.3 – 4.9]%, *P*<0.01) and strain rate (0.4 [0.3 – 0.4] vs 0.7 [0.6 – 1.1] s^{-1}, *P*<0.01). CAS remained independently associated with a past history of stroke after adjustment for the CHA_2DS_2VASc score. **Conclusions:** Our data showed that non-valvular AF patients with a past history of stroke had lower values of aortic mechanics assessed with transesophageal 2D-STE.

Keywords: Transesophageal Echocardiogram; Two-Dimensional Speckle-Tracking Echocardiography; Strain, Strain Rate; Atrial Fibrillation; Left Atrial Appendage; Stroke; CHA_2DS_2VASc score

Introduction

Ultrasound technology is capable of delivering dynamic images of the heart and central arteries (1). Two-dimensional speckle tracking echocardiography (2D-STE) has evolved in recent years. It's a semi-automated analysis based on frame-by-frame tracking of tiny echo-dense speckles within the myocardium, from which motion and deformation variables, such as velocity, displacement, strain (ε), and strain rate (SR) can be assessed (2).

The early applications of these new methodologies involved the study of 4 cardiac chambers, but its usage has been expanded and validated by sonomicrometry (3, 4) for the assessment of the aortic vascular wall mechanics (1). Moreover, an association between vascular mechanics by 2D-STE and the collagen content of vascular wall has been demonstrated, promoting vascular mechanics as a new imaging surrogate of vascular stiffening (5).

Atrial fibrillation (AF) is one of the most prevalent arrhythmias and is associated with a five-fold increased risk of stroke and a higher mortality (6). The left atrial appendage (LAA) is the main site of thrombus formation in patients suffering from AF (7). The CHA_2DS_2-VASc score is a clinical prediction rule for estimating the risk of stroke in patients with non-rheumatic valvular AF and is based on demographic and clinical variables. The CHA_2DS_2-VASc score has since been validated in multiple cohorts (8) and it is considered accurate to estimate the stroke risk in non-valvular AF, although many potential stroke risk factors have not been included (9).

This study had the following goals: 1) To determine the feasibility and reproducibility of evaluation of vascular mechanics at the descending thoracic aorta using two-dimensional speckle tracking transesophageal echocardiography in patients with non-valvular AF; 2) To study the association of vascular mechanics with the stroke risk score and with history of prior stroke in patiens with non-valvular AF; and 3) To analyze the association of vascular mechanics with left atrial appendage function and with the presence of a LAA thrombus in the same group of patients.

Methods

We prospectively recruited a group of patients referred for a transesophageal echocardiogram (TEE) in the context of cardioversion for AF. They were enrolled between January and June of 2015. During this period, we received 216 orders for a TEE. Of these, 58 requests were for a TEE prior to a cardioversion. Four patients were excluded for poor visualization of the descending aortic wall in the TEE, 3 patients were excluded for rheumatic mitral valve disease, 3 patients were excluded due to atrial flutter, 2 patients were excluded because they were in sinus rhythm and 2 patients were excluded because they were referred for a repeat procedure during the study period. The final sample included 44 non-valvular AF patients referred for a TEE prior to cardioversion.

All subjects gave written informed consent before their participation in the study. The study protocol was approved by *Comissão Nacional de Protecção de Dados* (authorization 3611/2015); and *Faculdade de Medicina da Universidade de Coimbra*, ethics committee (protocol reference CE – 005/2014).

Clinical data

AF patients underwent anthropometric examinations, and the body surface area (BSA) was estimated according to the formula by DuBois and DuBois (10).

Clinical data included age, weight, height, blood pressure and heart rate. We collected data regarding the type of AF (paroxystic, persistent and permanent), the duration of the episode (more than one month) and the year of the AF diagnosis. The history of hypertension, diabetes, dyslipidemia, smoking habits, prior acute myocardial infarction, coronary revascularization, were recorded. Heart failure (HF) diagnosis was done according to the 2012 guidelines, based on symptoms, signs and evidence of cardiac structural abnormalities (11). We noted if it was an acute or chronic episode and the phenotype of HF: preserved or reduced left ventricular systolic function. We also recorded the *NYHA* class and the *EHRA* functional class. The CHA_2DS_2-VASc score (C-congestive heart failure; H-Hipertension; A_2-Age >75; S_2-Stroke; V-vascular disease; A-Age 65-75; Sc-sex category) was calculated. Patients were grouped according to the score as following: Score = 1; Score = 2; Score = 3 or 4; Score > 4. Previous stroke history was defined by an hospital admission for ischemic stroke.

Data also included the current medical therapy (particularly focusing on hipocoagulation and antiarrhythmics) and the response to cardioversion.

Transthoracic echocardiography

Transthoracic echocardiography was performed using a Vivid 7 (GE Healthcare®, Horton, Norway) cardiovascular ultrasound device, with a 1.7/3.4 MHz tissue harmonic transducer. Complete echocardiographic studies called for standard views and techniques stipulated by established guidelines (12). All parameters were obtained after averaging five consecutive cycles. Blood pressure was measured with an arm-cuff sphygmomanometer.

In the 2D long-axis parasternal window we assessed the 2D linear measurements of the interventricular septum, the posterior LV wall thickness and the internal LV dimensions in accord with accepted guidelines (13). LV mass was calculated according to the Devereux's formula (14). The LV and left atrial (LA) volumes were determined using the modified Simpson's rule, with images obtained from apical 4-chamber and 2-chamber views. The LA volume index (LAVI) was obtained after indexing for BSA. The left ventricular ejection fraction (LVEF) was assessed in all patients using the Simpson method (13). The LV filling pressure was estimated from the left side E/e' ratio (e' was based on the septal wall in tissue Doppler imaging) (15).

Transesophageal echocardiography

The TEE was performed in all patients using local anesthesia (spray lidocaine) and mild sedation (2 to 4 mg of intravenous midazolam). We used a 6 T phased array multiplane transesophageal probe and the images were obtained at a frequency of 5.0 MHz.

A standard TEE exam was performed carefully and in agreement with current guidelines for performing a comprehensive TEE (16). A careful survey of the entirety of both atria, including the appendages, was performed. LAA thrombi were recognized by identifying a mobile or sessile, irregularly shaped, grey, textured density that was clearly separate from the lining of the atrial appendage.

Maximal LAA areas were measured by tracing a line from the top of the upper pulmonary vein limbus along the entire endocardial LAA border. The maximum and minimum main lobe LAA areas were obtained, independent of the QRS time, in a range between 60 and 90 degrees. The LAA fractional area change was calculated as a percentage: (LAA max – LAA min)/LAA max×100 (17).

LAA flow velocities were assessed with a pulsed Doppler sample placed 1 cm from the entry of the LAA into the body of the left atrium. Emptying and filling velocities were estimated by averaging five well-defined emptying and filling waves.

The aortic stiffness index (β_1) was calculated at the level of the thoracic descending aorta according to the formula: $\ln(P_s/P_d)/(A_s - A_d)/A_d$ (18). A_s and A_d are M-mode guided

systolic and diastolic descending aorta diameters, respectively. A_s was measured at the maximal anterior aortic wall motion and A_d was obtained at the R wave peak in a simultaneously recorded electrocardiogram. P_s and P_d are systolic and diastolic arterial pressures, respectively.

RM performed all of the classic echocardiographic measures and was blinded to the clinical situation and the vascular mechanics.

Two-dimensional speckle tracking transesophageal echocardiography

A short-axis view of the descending aorta, one to two centimeters after the aortic arch was selected for the vascular mechanics assessment with the 2D-STE methodology. The analysis was performed in places with no significant vascular plaques. The images were acquired with a breath hold of 3 seconds, with a stable electrocardiography recording. As all patients were in AF and an average of five consecutive heart cycles were recorded. The frame rate was >60 frames per second.

The tracking process and conversion to Lagrangian strains were performed offline using dedicated software (EchoPAC 9.0; GE Healthcare®, Horten, Norway). A line alongside the inner side of the descending aortic circumference was drawn by the operator. The software then automatically generated additional lines within a 15 mm wide region of interest (ROI), which was manually adjusted. A cine loop preview feature allowed visual confirmation that the internal line followed the vascular expansion and recoil movements throughout the cardiac cycle. The initial systolic frame generally served as the frame of interest to include maximal aortic wall expansion and recoil.

In agreement with previous publications on 2D-STE analysis of vascular mechanics (19-21), the aortic circumference was divided into six equidistant regions, all similar in size. In each region, numeric expressions of each 2D-STE variable represented mean values calculated from all points in arterial segments. Quantitative curves, depicting all regions, were generated for each 2D-STE variable. Analyses were performed for CAS in percentages and for CASR in s^{-1}. For each, a global value was calculated, defined as the mean of the peak values of the six aortic wall segments – Figure 1, Panels A and B.

Inter- and intra-observer variability

The inter-observer reproducibility was assessed by having a second echocardiographer (PD) repeat the aortic strain and strain rate measurements. The measurements were

performed on stored images of 11 randomly selected patients and were compared with the first observer's measurements.

To evaluate the intra-observer variability, the measurements were repeated one month later by the same observer (RT) in the same 11 subjects. Readers were blinded to previous measurements and had to create a new region of interest of the aortic wall.

Statistical analysis

The Kolmogorov-Smirnov test was used to assess the distribution of the continuous variables. Variables with normal distribution are expressed as mean and standard deviation, and the Student's *t* test was applied for group comparisons. Individual variables were checked for homogeneity of variance via Levene's test. Variables with a non-normal distribution were expressed as median and interquartile range, and groups were compared with the Mann-Whitney and the Kruskal-Wallis test.

Categorical variables are reported as frequencies and percentages, and χ^2 or Fisher exact tests were used when appropriate.

The Spearmen correlation coefficient (*rho*) was used to analyze the associations between vascular mechanics and the LAA velocities, LAA area fraction exchange, LAVI and LVEF.

A logistic regression analysis was performed for the categorical variable previous history of stroke. The CHA_2DS_2-VASc score, CAS, CASR and age were combined and included in different models. Non-normal distributed variables were transformed.

We used the Bland-Altman method (22), the intraclass correlation coefficient (ICC) (23), and the coefficient of variation (CoV) to assess the inter- and intra-observer variability of global and segmental CAS and CASR.

A *P*-value <0.05 in two-tailed tests was considered statistically significant. All data calculations and analyses relied on SPSS® 15, Medcalc® 12.1.4 and GraphPad Prism® 6.05 statistical software packages.

Results

Population sample description

We included 44 AF patients referred for TEE and cardioversion. The mean age of our cohort was 65 ± 13 years and 75% of the patients were men.

AF was a known diagnosis for 2.8±2.5 years amongst the study patients. It was considered paroxysmal in 41% and persistent in 48% of cases. The echocardiogram was performed on an urgent basis in 27% of these patients.

All patients were anticoagulated; 57% were on a new oral anticoagulant, 16% were on warfarin and 27% were on subcutaneous enoxaparin. The most commonly used anti-arrhythmics in these patients were beta-blockers (64%), amiodarone (50%), and propafenone (7%).

A thrombus was identified in 11% of cases and in these patients the cardioversion was cancelled. Out of the remaining 39 patients, sinus rhythm was immediately restored after cardioversion in 95% of cases. No complications were noted.

Inter- and intra-observer variability in evaluation of descending thoracic aortic mechanics

Waveforms adequate for measuring 2D-STE were present in 85% of the 264 visualized descending aortic wall segments. The mean global CAS was 3.5±1.2% and the median value was 3.6 (2.7 – 4.5)%. The mean global CASR was 0.7±0.3 s^{-1} and the median was 0.6 (0.4 – 0.9)s^{-1}. Table 1 shows the segmental values for both vascular strain and strain rate.

Regarding the inter-observer variability, the CoV for global strain was 11.4% and for the strain rate was 15%. With respect to the intra-observer analysis, the CoV for global strain was 13.9% and for the strain rate was 15.0%. Data regarding bias, limits of agreement and the ICC for global aortic strain and strain rate is presented in Table 2 and Figure 2.

Aortic mechanics and risk of stroke

The median CHA_2DS_2VASc score for our sample was 2 (2 – 3). As the score increased, we noted that both the descending aortic strain (r=-0.38, *P*=0.01) and strain rate (r=-0.42, *P*<0.01) decreased. Moreover, patients with a lower CHA_2DS_2VASc score (=1) had significantly higher values of vascular strain and strain rate than patients with a higher score (>4). This difference was not identified for the Beta-1 index (Figure 3, Panels A, B and C).

In our sample, 16% of patients had a history of prior stroke (Table 3). These patients had lower values of both descending aortic strain (2.2 [1.8 – 2.6] vs 3.9[3.3 – 4.9]%, *P*<0.01)

and strain rate (0.4 [0.3 – 0.4] vs 0.7 [0.6 – 1.1] s^{-1}, *P*<0.01) as compared to patients with no history of cerebrovascular disease.

Contrary to CASR, CAS remained independently associated with a past history of stroke after adjustment for both the CHA2DS2VASc score and age as a continuous variable (Table 4).

Left atrial appendage

Regarding the LAA velocities, we noted a significant positive correlation between the LAA filling (*rho*=0.36; *P*=0.02) and emptying (*rho*=0.34; *P*=0.02) velocities with the CASR (Table 5). Moreover, both CAS (*rho*=0.62; *P*<0.01) and CASR (*rho*=0.48; *P*<0.01) correlated with the LAA area fraction change – Figure 4, Panels A and B. On the contrary, we identified a negative correlation between aortic strain (*rho*=-0.44, *P*<0.01) and strain rate (*rho*=-0.33, *P*=0.04) with the E/'e (Table 5).

We identified a LAA thrombus in 5 patients. These patients' demographic and type of AF were comparable to those of the patients with no LAA thrombus. They had a larger LA (LAVI: 79[68 – 108] vs 49[43 – 58], *P*<0.01) and they were more often medicated with warfarin (60.0 vs 10.3%, *P*<0.04). Patients with a LAA thrombus had numerically lower values of CAS (2.9 [1.8 – 3.4] vs 3.8 [2.8 – 4.8]% *P*=0.05) and CASR (0.45[0.39 – 0.60] vs 0.64[0.52 – 1.06], s^{-1} *P*=0.05), but the difference was at the upper limit of statistical significance. Pulse pressure and the Beta1 index were similar for both groups. – Supplemental Table 1. A CAS cutoff of 3.6% had 100% sensitivity and 56% specificity for identification of LAA thrombus, and a CASR cutoff of 0.51 s^{-1} had a sensitivity of 80% and a specificity of 76.9% for identification of LAA thrombus.

Discussion

i) Evaluation of thoracic aortic descending mechanics using 2D-ST TEE was feasible in non-valvular AF patients; ii) Non-valvular AF patients with a higher CHA_2DS_2-VASc score had lower values of aortic vascular mechanics; iii) In non-valvular AF patients, descending aortic strain remained independently associated with a past history of stroke after adjustment using the CHA_2DS_2-VASc score or age as a continuous variable; iv) Vascular mechanics influenced the LAA velocities and LAA fraction change.

Descending aortic mechanics

Previous authors have studied descending aortic mechanics using transesophageal 2D-STE (1). In 2009, Kim *et al.* evaluated 137 patients referred for a TEE due to stroke and valvular heart disease. An important association between vascular strain and the brachial-ankle pulse wave velocity (PWV) was shown, supporting the use of vascular mechanics as an imaging marker of global arterial stiffness (19). Petrini *et al*. also studied descending aortic mechanics in patients with aortic stenosis and aortic regurgitation. They demonstrated that patients with aortic stenosis had higher vascular stiffness when compared with patients with aortic regurgitation (24).

When compared to previous studies regarding the use of vascular mechanics by 2D-STE in the descending aorta, our study showed lower feasibility and reproducibility. Our analysis was the first study to focus on patients with AF; this may have influenced the reproducibility values, as all patients in our study had an irregularly irregular rhythm.

Vascular mechanics and stroke

Our study demonstrated that patients with AF and a past history of stroke had reduced values of vascular mechanics. We have also noted that a higher stroke risk (as assessed with the CHA_2DS_2-VASc score) was associated with reduced values of aortic strain and strain rate. Our data corroborated the findings of the Tsai *et al.* study (25). Those authors enrolled 89 patients (>60 years of age) from a community health survey program and studied vascular deformation with 2D-STE at the level of the carotids. They showed that after adjustment for age, heart rate, systolic blood pressure, and cholesterol levels, vascular strain and strain rate values were correlated with a prior history of stroke in older subjects with existing vascular stiffening (25).

It has been established that the carotid-femoral PWV is independently associated with stroke in middle aged hypertensive patients (26). Arterial stiffness may favor the occurrence of

cerebrovascular events through an increase in central pulse pressure (26). Moreover, aortic stiffness influences the remodeling of cerebral vasculature in stroke patients. Mechanisms of this influence on remodeling include fibrosis, medial smooth muscle necrosis, breaks in elastin fibers, calcifications, and diffusion of macromolecules within the arterial wall (27, 28).

Left atrial appendage

It has been established that the presence of LAA thrombi (29), spontaneous echo contrast (30) and low LAA velocities (≤20 cm/s) (31) on TEE in patients with AF are independent predictors of stroke and thromboembolism.

Prior studies have indicated that circumferential vascular mechanics may serve as a surrogate marker of arterial vascular stiffening, due to their significant association PWV, the gold standard marker of arterial rigidity (19). Increased stiffness of conduit arteries is associated with higher velocity of transmission of the pulse wave generated by LV ejection and an early return of reflected waves that return to the heart during LV systole; thus, increasing LV afterload and central pulse pressure, promoting myocyte hypertrophy and interstitial fibrosis, causing LV diastolic dysfunction (32).

Our data showed that in AF, an increase in aortic rigidity identified using transesophageal 2D-STE influenced LAA performance, assessed with either the inflow or LAA outflow velocities or with the LAA area change. In addition, patients with AF plus a LAA thrombus had numerically lower aortic mechanics values.

The rational for the association between the parameters of aortic mechanics and the function of the LAA, could be the influence of aortic stiffness on the LV diastolic function. Moreover, we also noted a significant negative association of aortic mechanics with the LV E/e', which is a surrogate for the LV filling pressure and LA pressure.

The influence of vascular mechanics on LAA function may also explain the association of lower values of descending aortic vascular mechanics with a prior stroke history and with a higher CHA_2DS_2-VASc score in patients with non-valvular AF.

Limitations

This was a single center, observational study of non-valvular AF patients referred for a TEE prior to cardioversion. We note that the reported values of aortic mechanics with TEE 2D-STE were obtained from high quality images TEE images and our results may not be reproduced in patients with difficult acoustic windows. The design of the study made it impossible to analyze the longitudinal association of aortic mechanics assessed by TEE 2D-STE with stroke in non-valvular AF patients.

Conclusions:

The study of vascular mechanics at the descending thoracic aorta using transesophageal 2D-STE in non-valvular AF patients was feasible and had adequate reproducibility. Lower values of aortic strain were associated with a past history of stroke and with higher values of the CHA_2DS_2-VASc score. Our study was not powered to study associations between the four subgroups of CHA_2DS_2-VASc score patients, aortic mechanics and the β_1 index.

Declaration of interest: the authors have nothing to declare.

Legends

Table 1: Circumferential descending aortic mechanics

Table 2: Inter and intra-observer variability of global vascular mechanics at the descending aorta (n=11)

Table 3: Characteristics of patients with a previous history of stroke

Table 4: Logistic regression analysis for previous history of stroke

Table 5: Correlations of vascular mechanics of the descending aorta (N=44)

Supplemental Table 1: Characteristics of patients with a left atrial appendage thrombus

Figure 1: Descending thoracic aortic mechanics generated from short axis view of the descending aorta with transesophageal 2D-STE. Global strain (Panel A) and strain rate (Panel B) are indicated by the white dotted curve.

Figure 2, Panel A: Inter- and intra-observer bias and limits of agreement for global strain.

Figure 2, Panel B: Inter and intra-observer bias and limits of agreement for global strain rate.

Figure 3, Panel A: Aortic strain and the CHA_2DS_2-VASc score: Aortic Strain decreased across the four groups. Score 1: 4.1 (3.6 – 5.1) %; Score 2: 3.7 (2.6 – 5.3) %; Score 3-4: 3.6 (3.0 – 5.0) %; Score >4: 2.7 (2.1 – 3.7) %. *P* value for all group comparisons = 0.08. *P* value for Score 1 vs Score >4 = 0.01.

Figure 3, Panel B: Aortic strain rate and the CHA_2DS_2-VASc score. Aortic Strain Rate decreased across the four groups. Score 1: 0.79 (0.59 – 1.11) s^{-1}. Score 2: 0.82 (0.49 – 1.23) s^{-1}. Score 3-4: 0.68 (0.50 – 0.82) s^{-1}. Score >4: 0.42 (0.39 – 0.64) s^{-1} . *P* value for all group comparisons = 0.38. *P* value for Score 1 vs Score >4 = 0.24.

Figure 3, Panel C: Beta-1 index and the CHA_2DS_2-VASc score. The Beta-1 index, numerically increased across the four groups. Score 1: 9.9 (5.5 – 16.9). Score 2: 0.82 (7.6 – 16.3). Score 3-4:

0.68 (10.5 – 25.5). Score >4: 0.42 (7.6 – 34.1). *P* value for all group comparisons = 0.38. *P* value for Score 1 vs Score >4 = 0.24

Figure 4, Panel A: Correlation of aortic strain and the LAA fractional area change.

Figure 4, Panel B: Correlation of aortic strain rate and the LAA fractional area change.

Table 1: Circumferential descending aortic mechanics

	Total Population (n=44)	
	Mean ± SD	Median and IQ range
Segment 1 Strain (%)	3.7±2.2	3.2 (2.3 – 5.2)
Segment 2 Strain (%)	4.2±1.9	4.5 (3.0 – 5.8)
Segment 3 Strain (%)	3.1±1.6	3.4 (1.6 – 4.5)
Segment 4 Strain (%)	2.8±1.3	2.2 (1.6 – 5.0)
Segment 5 Strain (%)	3.4±2.0	3.4 (1.9 – 5.0)
Segment 6 Strain (%)	3.7±2.2	3.5 (2.1 – 5.3)
Global Strain (%)	3.5±1.2	3.6 (2.7 – 4.5)
Segment 1 Strain Rate (s^{-1})	0.8±0.5	0.6 (0.4 – 1.1)
Segment 2 Strain Rate (s^{-1})	0.8±0.5	0.7 (0.4 – 1.0)
Segment 3 Strain Rate (s^{-1})	0.5±0.3	0.5 (0.4 – 0.6)
Segment 4 Strain Rate (s^{-1})	0.6±0.4	0.6 (0.2 – 0.9)
Segment 5 Strain Rate (s^{-1})	0.8±0.4	0.6 (0.4 – 1.0)
Segment 6 Strain Rate (s^{-1})	0.8±0.4	0.7 (0.5 – 1.1)
Global Strain Rate(s^{-1})	0.7±0.3	0.6 (0.4 – 0.9)

SD: standard deviation; IQ: interquartile

Table 2: Inter and intra-observer variability of global vascular mechanics at the descending aorta (n=11)

	Inter-observer variability			Intra-observer variability		
	Bias (limits of agreement)	ICC (95% CI)	CoV (%)	Bias (limits of agreement)	ICC (95% CI)	CoV (%)
Global Strain	-0.06 (-1.05 – 0.93)	0.89 (0.67 – 0.97)	11.4	-0.30 (-1.41; 0.81)	0.89 (0.67 – 0.97)	13.9
Global Strain Rate	-0.06 (-0.3 – 0.17)	0.87 (0.62 – 0.96)	15.0	-0.03 (-0.29; 0.22)	0.87 (0.62 – 0.96)	15.0

ICC – intraclass correlation coefficient;

Table 3 : Characteristics of patients with a previous history of stroke

	Previous Stroke History (N=7)	No Previous Stroke History (N=37)	*P*
Age (years)	77±12	63±12	<0.01
Male gender (%)	3/7 (42.9)	30/37 (81.1)	0.03
Paroxystic Atrial Fibrillation (%)	3/7 (42.9)	15/37 (40.5)	0.91
Heart Failure (%)	6/7 (85.7)	21/37 (56.8)	0.15
CHA_2DS_2VASc	6 (3 – 7)	2 (2 – 3)	<0.01
Left ventricular ejection fraction (%)	46 (29 – 60)	47 (36 – 57)	0.73
Left atrium volume index (ml/m^2)	67±27	53±15	0.61
E/e' ratio	16±6	13±7	0.32
E-Wave decelation time (ms)	121±23	125±63	0.87
CAS (%)	2.2 (1.8 – 2.6)	3.9 (3.3 – 4.9)	<0.01
CASR (s^{-1})	0.4 (0.3– 0.4)	0.7 (0.6 – 1.1)	0.01
Aortic stiffness (β_1 index)	10.8 (6.9 – 40.4)	12.9 (7.5 – 19.6)	0.85
Pulse pressure (mmHg)	54±20	55±17	0.93
New oral antiocoagulants (%)	3/7 (43)	22/37 (60)	0.42

CAS: circumferential aortic strain; CASR: circumferential aortic strain rate; LAA: left atrial appendage

Table 4: Logistic regression analysis for previous history of stroke

Model 1			
Variables	**OR**	**95% CI**	***P***
Ln (CHA_2DS_2VASc)	33.8	3.1 – 370.9	<0.01
C-statistics: 0.89 (0.76 – 0.96)			
Model 2			
Variables	**OR**	**95% CI**	***P***
Ln (CHA_2DS_2VASc)	33.5	2.1 – 526.4	0.01
Ln (CAS)	0.014	0.00 – 0.89	0.04
C-statistics: 0.96 (0.85 – 0.99)			
Model 3			
Variables	**OR**	**95% CI**	***P***
Age (per 1 year increase)	1.1	0.99	0.07
Ln (CAS)	0.04	0.002-0.68	0.03
C-statistics: 0.97 (0.85 – 0.99)			
Model 4			
Variables	**OR**	**95% CI**	***P***
Ln (CHA_2DS_2VASc)	13.5	1.21 – 152.1	0.04
Ln (CASR)	0.02	0.01 – 1.52	0.08
C-statistics: 0.95 (0.87 – 0.99)			

Table 5: Correlations of vascular mechanics of the descending aorta (N=44)

	CAS		CASR	
	r	***P***	***r***	***P***
Left atrial indexed volume, ml/m^2	-0.29	0.14	-0.26	0.09
E/e’	-0.44	<0.01	-0.32	0.04
Left ventricular ejection fraction, %	0.28	0.07	0.22	0.14
Left atrial appendage area fraction change, %	0.62	<0.01	0.48	<0.01
Left atrial appendage filling velocities, cm/s	0.23	0.14	0.36	0.02
Left atrial appendage emptying velocities, cm/s	0.26	0.09	0.34	0.02

Supplemental Table 1: Characteristics of patients with a left atrial appendage thrombus

	LAA Thrombus (N=5)	No LAA Thrombus (N=39)	*P*
Age (years)	65±13	65±13	0.96
Male gender (%)	3/5 (60)	30/39 (77)	0.41
Paroxystic Atrial Fibrillation (%)	2/5 (40.0)	16/39 (41.0)	0.80
Heart Failure (%)	5/5 (100)	22/39 (56.4)	0.06
CHA_2DS_2VASc	3 (2 -5)	2 (2 -2)	0.23
Left ventricular ejection fraction (%)	36 (28 – 50)	50 (37 – 58)	0.14
Left atrium volume index (ml/m^2)	79 (68 – 108)	49 (43 – 58)	<0.01
E-wave decelaration time (ms)	116±45	125±61	0.75
E/e'	16±5	13±7	0.28
CAS (%)	2.9 (1.8 – 3.4)	3.8 (2.8 – 4.8)	0.05
CASR (s^{-1})	0.45 (0.39 – 0.60)	0.64 (0.52 -1.10)	0.05
Aortic stiffness (β_1 index)	9.7 (6.1 – 38.7)	12.9 (7.1 – 20.0)	0.97
Pulse pressure (mmHg)	50 (27 – 70)	55 (40 – 65)	0.67
New oral antiocoagulants (%)	2/5 (40.0)	23/39 (59.0)	0.42
Warfarin (%)	3/5 (60.0)	4/39 (10.3)	0.04
Average INR of patients with Warfarin	1.6 (1.1 – 3.8)	1.2 (1.1 – 1.3)	0.82
Low molecular weight heparin (%)	0/5 (0.0)	12/39 (30.8)	0.15

CAS: circumferential aortic strain; CASR: circumferential aortic strain rate; LAA: left atrial appendage

Figure1 Panel A

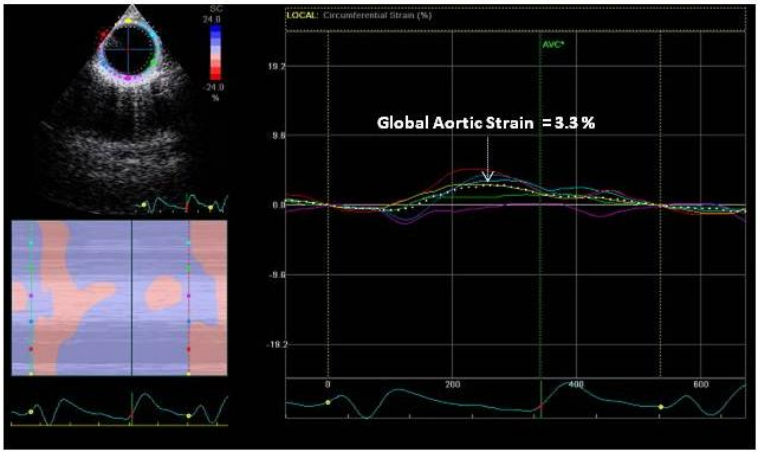

Figure 1 Panel B

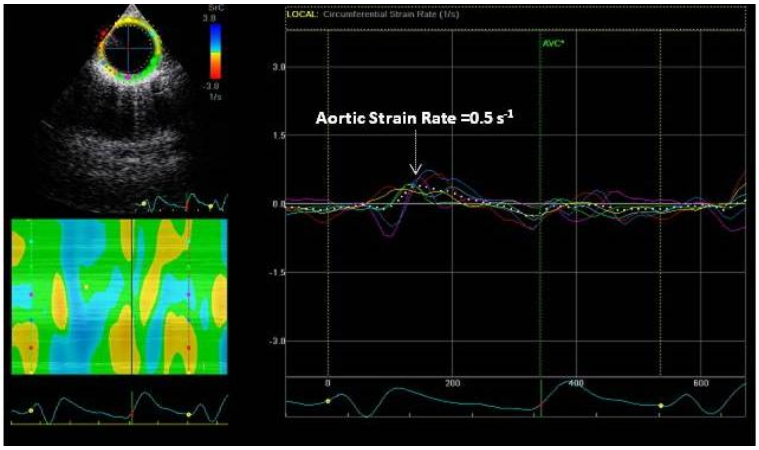

Figure 2 Panel A

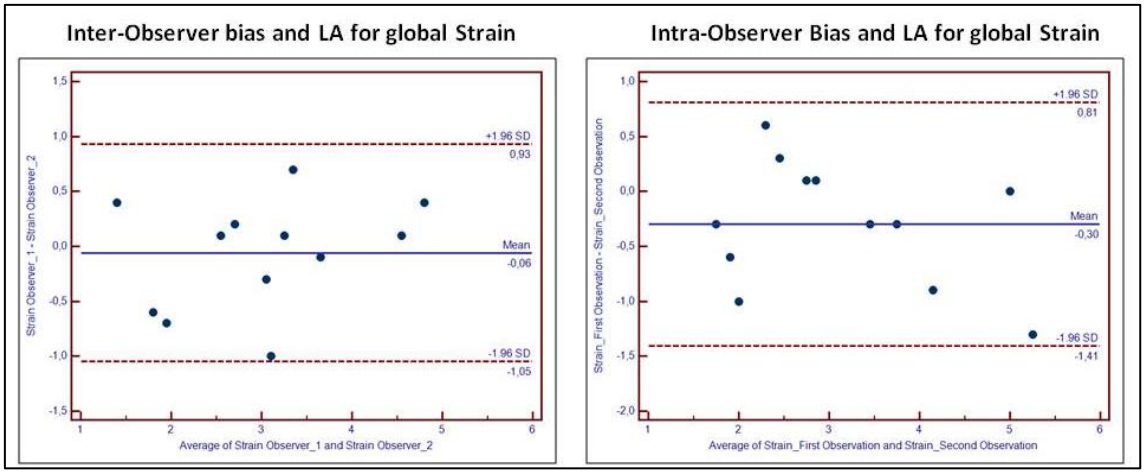

Figure 2 Panel B

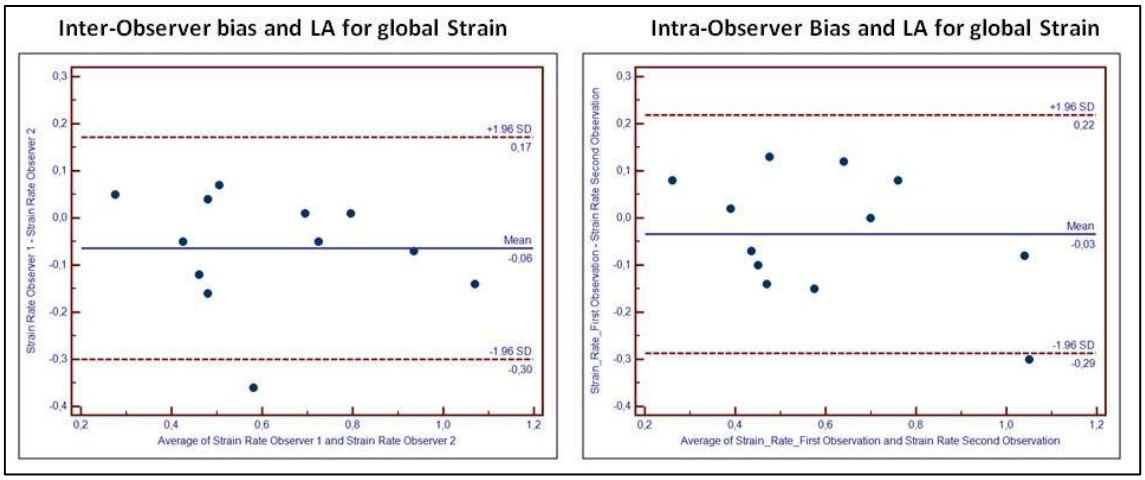

Figure 3 Panel A

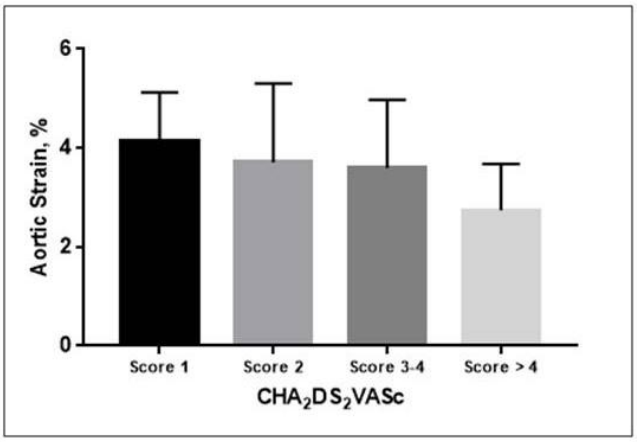

Figure 3 Panel B

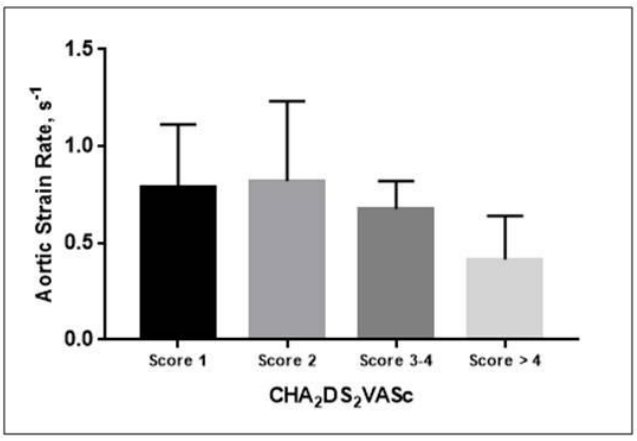

Figure 3 Panel C

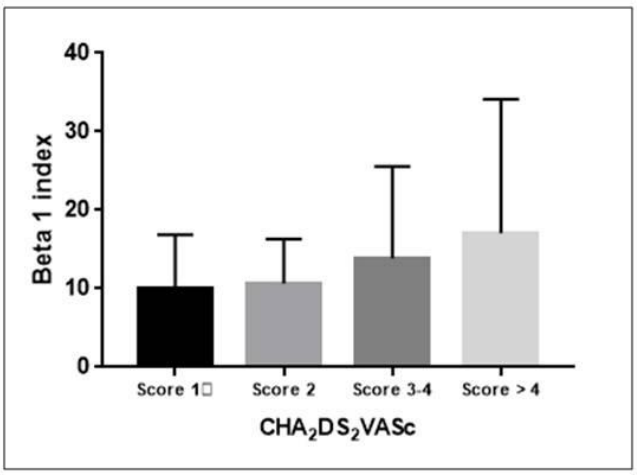

Figure 4 Panel A

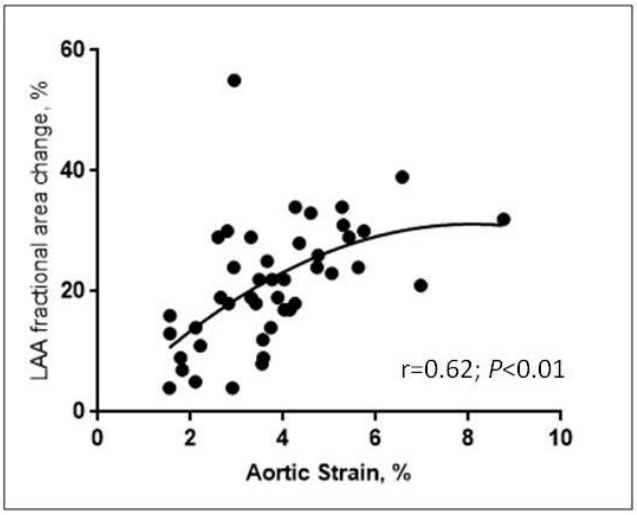

Figure 4 Panel B

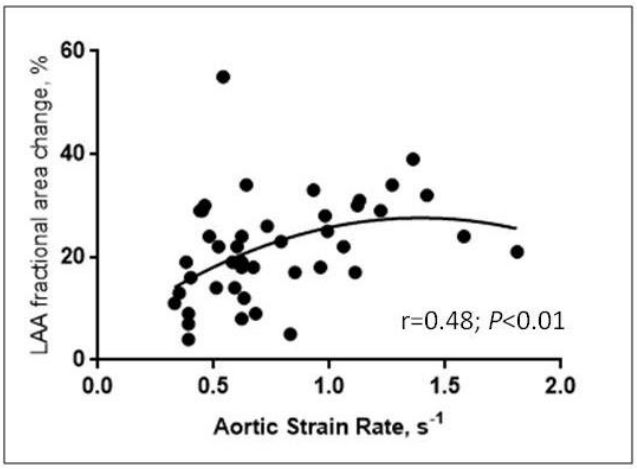

References

1. Teixeira R, Vieira MJ, Goncalves A, Cardim N, Goncalves L. Ultrasonographic vascular mechanics to assess arterial stiffness: a review. Eur Heart J Cardiovasc Imaging. 2016 Mar;17(3):233-46.
2. Mor-Avi V, Lang RM, Badano LP, Belohlavek M, Cardim NM, Derumeaux G, et al. Current and evolving echocardiographic techniques for the quantitative evaluation of cardiac mechanics: ASE / EAE consensus statement on methodology and indications. J Am Soc Echocardiogr. 2011 Mar;24(3):277-313.
3. Larsson M, Verbrugghe P, Smoljkic M, Verhoeven J, Heyde B, Famaey N, et al. Strain assessment in the carotid artery wall using ultrasound speckle tracking: validation in a sheep model. Phys Med Biol. 2015 Feb 7;60(3):1107-23.
4. Larsson M, Heyde B, Kremer F, Brodin LA, D'Hooge J. Ultrasound speckle tracking for radial, longitudinal and circumferential strain estimation of the carotid artery--an in vitro validation via sonomicrometry using clinical and high-frequency ultrasound. Ultrasonics. 2015 Feb;56:399-408.
5. Kim SA, Lee KH, Won HY, Park S, Chung JH, Jang Y, et al. Quantitative assessment of aortic elasticity with aging using velocity-vector imaging and its histologic correlation. Arterioscler Thromb Vasc Biol. 2013 Jun;33(6):1306-12.
6. Camm AJ, Lip GY, De Caterina R, Savelieva I, Atar D, Hohnloser SH, et al. 2012 Focused update of the ESC Guidelines for the management of atrial fibrillation: an update of the 2010 ESC Guidelines for the management of atrial fibrillation. Developed with the special contribution of the European Heart Rhythm Association. Eur Heart J. 2012 Nov;33(21):2719-47.
7. Camm AJ, Kirchhof P, Lip GY, Schotten U, Savelieva I, Ernst S, et al. Guidelines for the management of atrial fibrillation: the Task Force for the Management of Atrial Fibrillation of the European Society of Cardiology (ESC). Eur Heart J. 2010 Oct;31(19):2369-429.
8. Lip GY. Stroke in atrial fibrillation: epidemiology and thromboprophylaxis. J Thromb Haemost. 2011 Jul;9 Suppl 1:344-51.
9. Lip GY, Nieuwlaat R, Pisters R, Lane DA, Crijns HJ. Refining clinical risk stratification for predicting stroke and thromboembolism in atrial fibrillation using a novel risk factor-based approach: the euro heart survey on atrial fibrillation. Chest. 2010 Feb;137(2):263-72.
10. Dubois D, Dubois E. A formula to extimate the approximate surface area if height and weight are know. Arch Inter Med. 1916;17:863-71.
11. McMurray JJ, Adamopoulos S, Anker SD, Auricchio A, Bohm M, Dickstein K, et al. ESC Guidelines for the diagnosis and treatment of acute and chronic heart failure 2012: The Task Force for the Diagnosis and Treatment of Acute and Chronic Heart Failure 2012 of the European Society of Cardiology. Developed in collaboration with the Heart Failure Association (HFA) of the ESC. Eur Heart J. 2012 Jul;33(14):1787-847.
12. Evangelista A, Flachskampf F, Lancellotti P, Badano L, Aguilar R, Monaghan M, et al. European Association of Echocardiography recommendations for standardization of performance, digital storage and reporting of echocardiographic studies. Eur J Echocardiogr. 2008 Jul;9(4):438-48.
13. Lang RM, Badano LP, Mor-Avi V, Afilalo J, Armstrong A, Ernande L, et al. Recommendations for cardiac chamber quantification by echocardiography in adults: an update from the american society of echocardiography and the European association of cardiovascular imaging. J Am Soc Echocardiogr. 2015 Jan;28(1):1-39 e14.
14. Lang RM, Bierig M, Devereux RB, Flachskampf FA, Foster E, Pellikka PA, et al. Recommendations for chamber quantification: a report from the American Society of Echocardiography's Guidelines and Standards Committee and the Chamber Quantification Writing Group, developed in conjunction with the European Association of Echocardiography, a branch of the European Society of Cardiology. J Am Soc Echocardiogr. 2005 Dec;18(12):1440-63.
15. Sohn DW, Song JM, Zo JH, Chai IH, Kim HS, Chun HG, et al. Mitral annulus velocity in the evaluation of left ventricular diastolic function in atrial fibrillation. J Am Soc Echocardiogr. 1999 Nov;12(11):927-31.
16. Flachskampf FA, Badano L, Daniel WG, Feneck RO, Fox KF, Fraser AG, et al. Recommendations for transoesophageal echocardiography: update 2010. Eur J Echocardiogr. 2010 Aug;11(7):557-76.
17. Ito T, Suwa M, Hirota Y, Otake Y, Moriguchi A, Kawamura K. Influence of left atrial function on Doppler transmitral and pulmonary venous flow patterns in dilated and hypertrophic cardiomyopathy: evaluation of left atrial appendage function by transesophageal echocardiography. Am Heart J. 1996 Jan;131(1):122-30.

18. Stefanadis C, Stratos C, Boudoulas H, Kourouklis C, Toutouzas P. Distensibility of the ascending aorta: comparison of invasive and non-invasive techniques in healthy men and in men with coronary artery disease. Eur Heart J. 1990 Nov;11(11):990-6.

19. Kim KH, Park JC, Yoon HJ, Yoon NS, Hong YJ, Park HW, et al. Usefulness of aortic strain analysis by velocity vector imaging as a new echocardiographic measure of arterial stiffness. J Am Soc Echocardiogr. 2009 Dec;22(12):1382-8.

20. Yuda S, Kaneko R, Muranaka A, Hashimoto A, Tsuchihashi K, Miura T, et al. Quantitative measurement of circumferential carotid arterial strain by two-dimensional speckle tracking imaging in healthy subjects. Echocardiography. 2011 Sep;28(8):899-906.

21. Teixeira R, Moreira N, Baptista R, Barbosa A, Martins R, Castro G, et al. Circumferential ascending aortic strain and aortic stenosis. Eur Heart J Cardiovasc Imaging. 2013 Jul;14(7):631-41.

22. Bland JM, Altman DG. Statistical methods for assessing agreement between two methods of clinical measurement. Lancet. 1986 Feb 8;1(8476):307-10.

23. Shrout PE, Fleiss JL. Intraclass correlations: uses in assessing rater reliability. Psychol Bull. 1979 Mar;86(2):420-8.

24. Petrini J, Yousry M, Rickenlund A, Liska J, Hamsten A, Eriksson P, et al. The feasibility of velocity vector imaging by transesophageal echocardiography for assessment of elastic properties of the descending aorta in aortic valve disease. J Am Soc Echocardiogr. 2010 Sep;23(9):985-92.

25. Tsai WC, Sun YT, Liu YW, Ho CS, Chen JY, Wang MC, et al. Usefulness of vascular wall deformation for assessment of carotid arterial stiffness and association with previous stroke in elderly. Am J Hypertens. 2013 Jun;26(6):770-7.

26. Laurent S, Katsahian S, Fassot C, Tropeano AI, Gautier I, Laloux B, et al. Aortic stiffness is an independent predictor of fatal stroke in essential hypertension. Stroke. 2003 May;34(5):1203-6.

27. Masawa N, Yoshida Y, Yamada T, Joshita T, Sato S, Mihara B. Morphometry of structural preservation of tunica media in aged and hypertensive human intracerebral arteries. Stroke. 1994 Jan;25(1):122-7.

28. Heistad DD, Armstrong ML, Baumbach GL, Faraci FM. Sick vessel syndrome. Recovery of atherosclerotic and hypertensive vessels. Hypertension. 1995 Sep;26(3):509-13.

29. Bernhardt P, Schmidt H, Hammerstingl C, Luderitz B, Omran H. Atrial thrombi-a prospective follow-up study over 3 years with transesophageal echocardiography and cranial magnetic resonance imaging. Echocardiography. 2006 May;23(5):388-94.

30. Leung DY, Black IW, Cranney GB, Hopkins AP, Walsh WF. Prognostic implications of left atrial spontaneous echo contrast in nonvalvular atrial fibrillation. J Am Coll Cardiol. 1994 Sep;24(3):755-62.

31. Zabalgoitia M, Halperin JL, Pearce LA, Blackshear JL, Asinger RW, Hart RG. Transesophageal echocardiographic correlates of clinical risk of thromboembolism in nonvalvular atrial fibrillation. Stroke Prevention in Atrial Fibrillation III Investigators. J Am Coll Cardiol. 1998 Jun;31(7):1622-6.

32. O'Rourke MF. Diastolic heart failure, diastolic left ventricular dysfunction and exercise intolerance. J Am Coll Cardiol. 2001 Sep;38(3):803-5.

Part III: Discussion and Future Perspectives

Abbreviation List

2D-STE: Two-Dimensional Speckle Tracking Echocardiography

β_1: Aortic stiffness index

ε: Strain

AF: Atrial fibrillation

AS: Aortic stenosis

AR: Aortic regurgitation

CHA_2DS_2-VASc score: C-congestive heart failure; H-Hypertension; A_2-Age >75; S_2-Stroke; V-vascular disease; A-Age 65-75; Sc- sex category

LA: Left atrial

LAA: Left atrial appendage

SR: Strain Rate

TEE: Transesophageal Echocardiography

Word Count: 3603

Discussion

Ultrasound delivers dynamic images of the heart and central arteries. A new semiautomated technique, two-dimensional speckle tracking echocardiography (2D-STE), has improved over the past few years. Two-dimensional speckle tracking echocardiography is based on the tracking of tiny echo-dense speckles of the B-mode ultrasound image. It allows the assessment of motion and deformation parameters such as velocity, displacement, strain (ε), and strain rate (SR) in either the longitudinal, radial, or circumferential axis (1).

The 2D-STE has been used to evaluate all 4 cardiac chambers, but the numbers of applications has increased, and 2D-STE has been validated for assessing the mechanics of the walls of the aortic and carotid arteries (2). The assessment of vascular mechanics by 2D-STE was first conceived in 2008 for the abdominal aorta (3). The circumferential expansion and recoil of the wall of the abdominal aorta could be assessed by 2D-STE as positive circumferential systolic ε plus positive and negative circumferential SR values. Two-dimensional speckle tracking echocardiography was then proved feasible for evaluating the circumferential deformation of the proximal thoracic ascending aorta (4), the descending thoracic aorta, (4-6) and the carotid arteries (7) (2).

In vivo and in vitro studies have used sonomicrometry to validate 2D-STE for assessing vascular mechanics (8, 9). In addition, an in vivo animal study found a significant association between the parameters of vascular mechanics and the collagen content of the vascular wall (10). The results of these studies suggest that the parameters of vascular mechanics might be used as imaging surrogates of vascular stiffening (2).

Two-dimensional speckle tracking echocardiography is beneficial because it can perform circumferential assessments of the entire aorta or carotid artery and account for local variations in wall motion and deformation (2). These findings suggest the limitations of M-mode echocardiography, because it is a one-dimensional assessment. Two-dimensional speckle tracking echocardiography enables the instantaneous assessment of vessel wall motion, which provides an accurate estimation of the structural and functional circumferential changes in the vessel wall (11).

Given the results of these preliminary studies of 2D-STE, we decided to use 2D-STE to assess the vascular mechanics of various cardiovascular pathologies, including aortic stenosis (AS), hypertensive heart disease, and atrial fibrillation (AF). Moreover, to the best of our knowledge, we also used 2D-STE for the first time to perform assessments of vascular mechanics at the level of the aortic arch.

Vascular mechanics and aortic stenosis

Degenerative AS is currently viewed as a complex, multifaceted, and systemic disease that manifests atherosclerotic-like and elastocalcinosis-like vascular changes that lead to increases in arterial wall rigidity (12). The reduction in arterial compliance as a result of increased vascular stiffness then contributes to the left ventricular (LV) burden, culminating in adverse clinical events (13). The changing face of this disease underscores a need for a more comprehensive assessment of AS beyond the classic variables of peak jet velocity, pressure gradients, valvular area, and LV function.

We first used 2D-STE to study the mechanics of the ascending aorta in patients with moderate to severe degenerative AS. We demonstrated that the stroke volume index was the most important determinant of the circumferential strain of the ascending aorta, indicating that circumferential vascular deformation was dependent on changes in vascular flow and not on localized characteristics of the vascular wall (4). The impact of systolic flow on vascular mechanics was also later demonstrated by Petrini *et al.* in a study of 140 patients with isolated AS and 52 patients with isolated aortic regurgitation (AR) (6).

Studying the same cohort of patients with degenerative AS, we subsequently proved that the index of vascular stiffness (β_1) was strongly associated with the circumferential strain rate of the ascending aorta, suggesting that the rate of circumferential vascular deformation corresponds with local rigidity of the arterial wall. We suggested that strain in the ascending aorta and strain rate were complementary parameters that may be used for the noninvasive echocardiographic assessment of stroke flow and vascular load in patients with AS.

The primary aims of our initial study using 2D-STE to assess the ascending aorta were to analyse the physiological determinants of aortic strain and strain rate in patients with degenerative AS, but we also assessed as secondary aims clinical outcomes. As an exploratory endpoint we were able to demonstrate over a long follow-up period that the mechanics of the ascending aorta (namely strain rate, but not strain) were associated with mortality. Although the 2D-STE assessment of aortic mechanics is a difficult and time-consuming methodology, the data may have prognostic value, which may support the use of 2D-STE for the assessment of patients with AS.

Another study from our group by Leite *et al*. recently demonstrated that differences in the parameters of aortic mechanics derived from 2D-STE images obtained at the level of the ascending aorta between patients with AS, AR, and healthy participants were significant, after age and gender matching. These parameters were lower in patients with AS, probably

indicating that the elastic properties of the aorta were changed to a significantly greater extent in the patients with AS compared with the AR patients and healthy controls (14).

Aortic arch mechanics

To the best of our knowledge, we used 2D-STE for the first time to study vascular mechanics at the level of the aortic arch. We enrolled a cohort of 61 apparently healthy participants, and we reported normal values. We demonstrated the feasibility of 2D-STE to assess the aorta at the level of the aortic arch and found that both the inter- and intraobserver variabilities were acceptable. We showed that the mechanics of the aortic arch (strain and strain rate) were significantly lower for a group of hypertensive patients, after adjustments for age and pulse pressure, than for the healthy participants. Furthermore, our data also showed an association of strain and strain rate as determined by 2D-STE, with the pulse wave velocity as assessed by the gold standard method used to study vascular stiffness (Complior method). Finally, since we hypothesized that the parameters of vascular mechanics can be used as surrogate markers for vascular stiffening, we also demonstrated that the parameters of vascular mechanics are associated with the velocities of left ventricular relaxation.

We and other investigators (2) have used 2D-STE to study the vascular mechanics of the aorta at different levels. The aortic arch is a more superficial structure than the ascending or descending aorta, making it a more convenient image acquisition site for studying aortic mechanics during a complete echocardiography study. However, we note that this echocardiographic window is difficult to access in older individuals and in obese patients with a large neck. At the same time, the parasternal view can be harder to obtain in younger patients with the heart in a more vertical position. The possibility of these structural roadblocks suggests that the vascular location for performing an assessment of aortic vascular mechanics should be tailored to the patient. A faster assessment of younger patients with a history of hypertension or other risk factors for cardiovascular disease might be performed at the level of the aortic arch.

The arteries of an individual stiffen with aging and with conditions such as hypertension (15). The stiffening is a result of structural changes in the vessel wall (16). Previous studies on vascular mechanics demonstrated decreasing vascular strain and strain rate with increasing age, regardless of the location of assessment (at the level of the carotids (7, 17) abdominal aorta (3), or the thoracic aorta (18)). Moreover, hypertensive patients have also been found to have lower values of the parameters of vascular mechanics (19). Our data were in general agreement with the previous studies, although our results also support the

theory that circumferential strain of the aortic arch may be a parameter that reflects the effect of aging on the vasculature. Our supposition was based on the results of multivariate analysis, which found that when strain was added to a model that included pulse pressure and age, these latter 2 variables were no longer markers of hypertensive disease.

As the stiffness of conduit arteries increase, the left ventricular afterload increases because of an early return of the reflected vascular wave (20). This can affect left ventricular diastolic function. We demonstrated that the parameters of vascular mechanics are associated with the early diastolic velocity of the left ventricle, supporting the use of 2D-STE to assess vascular mechanics at the level of the aortic arch, for measurements of parameters that can be used as markers of the degenerative remodeling process of the vasculature in the context of aging and hypertension.

Atrial fibrillation and aortic mechanics

For the final stage of our investigation, we studied aortic mechanics at the level of the descending aorta in a cohort of patients with atrial fibrillation (AF) who needed cardioversion and were referred for transesophageal echocardiography (TEE). The results led us to conclude that the transesophageal 2D-STE assessment of these patients was feasible and obtained adequate reproducibility. The results showed that patients with nonvalvular AF and a higher CHA_2DS_2-VASc score had lower values of the parameters of aortic vascular mechanics than patients with a lower score. Aortic strain remained independently associated with a past history of stroke after adjustment for the CHA_2DS_2VASc score. Finally, we identified an association between the parameters of aortic mechanics and the function of the left atrial appendage.

Increased arterial rigidity has been found to lead to increased central pulse pressure and to promote the occurrence of cerebrovascular events (21). Moreover, aortic stiffness may stimulate vascular remodeling, which includes fibrosis, smooth muscle necrosis, breaks in elastin fibers, calcifications, and diffusion of macromolecules within the arterial wall (22, 23). The pulse wave velocity, as assessed by the gold standard method, is an independent risk factor for stroke in middle-aged hypertensive patients (21). We believe that our data are in agreement with these findings, because we think that the parameters of vascular mechanics are imaging surrogates of aortic stiffness. Our results also showed that the classic β_1 index could not identify AF patients with a past history of stroke, which was in contrast to the results of 2D-STE assessments of vascular mechanics.

We were unable to demonstrate an association between 2D-STE assessments of aortic mechanics and the response to cardioversion. This might be attributed to the following

problems: i) our sample size was too small to determine the predictive power of the parameters ii) our study patients with AF were heterogeneous; we enrolled patients with either paroxysmal or persistent AF. We also included acute, unstable patients and patients with heart failure; iii) the response to cardioversion varies because of such variables as LA remodeling, upstream pharmacological therapy, and hydroelectrolytic homeostasis.

Limitations

We proposed a new application for 2D-STE, namely its use for assessing the vascular mechanics of vessel walls. Similar to the atrium, the vascular wall is a thin structure, and therefore image quality should be optimal (24, 25). The validation of 2D-STE for assessment of vascular mechanics was obtained by *in vivo* and *in vitro* sonomicrometry (8, 9). That, plus the histological evidence of an association between the parameters of vascular mechanics and the collagen content of the vascular wall (10) were extremely important for supporting our proposed use of 2D-STE to assess vascular walls. However, and contrary to studies of 2D-STE used to assess ventricular and atrial myocardial mechanics (1, 24), no study has yet demonstrated an association between vascular mechanics assessed by echocardiography and tagged magnetic resonance imaging.

The feasibility and reproducibility of the parameters of vascular mechanics as determined by 2D-STE in our studies and by others were high (2). We note that the results of the 2D-STE assessments were obtained from high-quality images of patients and healthy participants. Moreover, patients with inadequate images or with poor tracking of the vascular wall were excluded. Therefore, the values of the parameters of vascular mechanics that we obtained and our conclusions might not be consistent with results obtained from a broader range of participants.

The speckle-tracking methodology can be complex and time-consuming. To illustrate this, our group recently reported on the usefulness of 2D-STE for differentiating between restrictive and constrictive physiology. We noted that some indexes, such as left ventricular rotational displacement, were difficult to assess, were time-consuming, and could only be obtained from high-quality images (26), highlighting a global limitation of speckle tracking echocardiography.

Another important limitation of this methodology is the overlap of values between the different study groups. The overlap in the values for aortic arch strain and strain rate in the hypertensive vs healthy participants suggests that 2D-STE assessments of vascular mechanics is

unlikely to add definite value to clinical practice. Finally, there is no data regarding the normal and pathological variability of vascular mechanics obtained with 2D-STE across the aorta.

Future Perspectives

A future focus of research on 2D-STE should focus on comparing the clinical usefulness of the parameters of vascular mechanics with the classical variables that are known predictors of outcome in different clinical contexts. For example, in aortic valve disease, the parameters of aortic mechanics should be evaluated for prognostic utility in patients with moderate-to-severe disease before valve replacement therapy and compared with classic variables such as age, aortic valve area, peak aortic valve gradient, and left ventricular systolic function. Moreover, since we have found associations between the parameters of vascular mechanics and systolic flow and aortic valve rigidity, the assessment of vascular mechanics before and after aortic valve replacement (either surgically or percutaneously) would be of interest. Finally, an interesting question needing clarification is whether or not an assessment of vascular mechanics at the ascending aortic level could identify patients with an increased risk of a clinical event after an aortic valve replacement.

Our assessment of vascular mechanics at the aortic arch should be corroborated by other groups of investigators for feasibility and reference values. In the setting of hypertensive disease, we have suggested the use of parameters of vascular mechanics as imaging markers of disease in target vascular organs. In this context, a prospective and longitudinal study to determine if assessment of vascular mechanics by 2D-STE could identify hypertensive patients with increased risk of a clinical event such as stroke, heart failure, myocardial infarction, atrial fibrillation, renal failure, or mortality..

Assessments of pulse wave velocity in hypertensive patients has demonstrated that angiotensin-converting enzyme inhibitors, beta blockers, and calcium channel antagonists reduce arterial rigidity (27). The evaluation of antihypertensive medication and nonpharmacological interventions such as aerobic training for their effect on vascular mechanics would be of interest. Namely, does antihypertensive medication have an effect on vascular mechanics? Is this effect independent of the blood pressure? Can we rely on 2D-STE as an imaging vascular risk marker?

Our group recently reported a retrospective study of patients with aortic valve disease who took statins and found that they had lower values of the parameters of the mechanics of the ascending aorta than the group of patients not taking statins. This paradoxical result may

indicate that these patients on statins had a higher vascular load and a more advanced state of arteriosclerosis but nevertheless is certainly a topic of interest for future analysis (28).

Regarding the study of descending aortic mechanics in patients with AF, a prospective analysis of the rigidity values obtained by imaging as predictors of stroke would be important to strengthen the retrospective association we have reported. Moreover, it would be possible to determine if assessments of vascular mechanics can improve the accuracy of the CHA_2DS_2-VASc score.

The answers to these research questions may provide compelling arguments for the widespread use of 2D-STE assessments of aortic mechanics.. We look forward to additional advances in ultrasound technology that might improve the assessment of localized arterial stiffness, and reveal clinically relevant associations between vascular mechanics and cardiovascular disease.

References

1. Mor-Avi V, Lang RM, Badano LP, Belohlavek M, Cardim NM, Derumeaux G, et al. Current and evolving echocardiographic techniques for the quantitative evaluation of cardiac mechanics: American Society Echocardiography / European Association of Echocardiography consensus statement on methodology and indications endorsed by the Japanese Society of Echocardiography. J Am Soc Echocardiogr. 2011 Mar;24(3):277-313.
2. Teixeira R, Vieira MJ, Goncalves A, Cardim N, Goncalves L. Ultrasonographic vascular mechanics to assess arterial stiffness: a review. Eur Heart J Cardiovasc Imaging. 2016 Mar;17(3):233-46.
3. Oishi Y, Mizuguchi Y, Miyoshi H, Iuchi A, Nagase N, Oki T. A novel approach to assess aortic stiffness related to changes in aging using a two-dimensional strain imaging. Echocardiography. 2008 Oct;25(9):941-5.
4. Teixeira R, Moreira N, Baptista R, Barbosa A, Martins R, Castro G, et al. Circumferential ascending aortic strain and aortic stenosis. Eur Heart J Cardiovasc Imaging. 2013 Jul;14(7):631-41.
5. Kim KH, Park JC, Yoon HJ, Yoon NS, Hong YJ, Park HW, et al. Usefulness of aortic strain analysis by velocity vector imaging as a new echocardiographic measure of arterial stiffness. Journal of the American Society of Echocardiography : official publication of the American Society of Echocardiography. 2009 Dec;22(12):1382-8.
6. Petrini J, Jenner J, Rickenlund A, Eriksson P, Franco-Cereceda A, Caidahl K, et al. Elastic properties of the descending aorta in patients with a bicuspid or tricuspid aortic valve and aortic valvular disease. J Am Soc Echocardiogr. 2014 Apr;27(4):393-404.
7. Yuda S, Kaneko R, Muranaka A, Hashimoto A, Tsuchihashi K, Miura T, et al. Quantitative measurement of circumferential carotid arterial strain by two-dimensional speckle tracking imaging in healthy subjects. Echocardiography. 2011 Sep;28(8):899-906.
8. Larsson M, Verbrugghe P, Smoljkic M, Verhoeven J, Heyde B, Famaey N, et al. Strain assessment in the carotid artery wall using ultrasound speckle tracking: validation in a sheep model. Phys Med Biol. 2015 Feb 7;60(3):1107-23.
9. Larsson M, Heyde B, Kremer F, Brodin LA, D'Hooge J. Ultrasound speckle tracking for radial, longitudinal and circumferential strain estimation of the carotid artery--an in vitro validation via sonomicrometry using clinical and high-frequency ultrasound. Ultrasonics. 2015 Feb;56:399-408.
10. Kim SA, Lee KH, Won HY, Park S, Chung JH, Jang Y, et al. Quantitative assessment of aortic elasticity with aging using velocity-vector imaging and its histologic correlation. Arterioscler Thromb Vasc Biol. 2013 Jun;33(6):1306-12.
11. Bjallmark A, Lind B, Peolsson M, Shahgaldi K, Brodin LA, Nowak J. Ultrasonographic strain imaging is superior to conventional non-invasive measures of vascular stiffness in the detection of age-dependent differences in the mechanical properties of the common carotid artery. Eur J Echocardiogr. 2010 Aug;11(7):630-6.
12. Rajamannan NM, Evans FJ, Aikawa E, Grande-Allen KJ, Demer LL, Heistad DD, et al. Calcific aortic valve disease: not simply a degenerative process: A review and agenda for research from the National Heart and Lung and Blood Institute Aortic Stenosis Working Group. Executive summary: Calcific aortic valve disease-2011 update. Circulation. 2011 Oct 18;124(16):1783-91.
13. Briand M, Dumesnil JG, Kadem L, Tongue AG, Rieu R, Garcia D, et al. Reduced systemic arterial compliance impacts significantly on left ventricular afterload and function in aortic stenosis: implications for diagnosis and treatment. J Am Coll Cardiol. 2005 Jul 19;46(2):291-8.
14. Leite L, Teixeira R, Oliveira-Santos M, Barbosa A, Martins R, Castro G, et al. Aortic Valve Disease and Vascular Mechanics: Two-Dimensional Speckle Tracking Echocardiographic Analysis. Echocardiography. 2016 Apr 16.
15. Janic M, Lunder M, Sabovic M. Arterial stiffness and cardiovascular therapy. Biomed Res Int. 2014;2014:621437.
16. Laurent S, Boutouyrie P, Lacolley P. Structural and genetic bases of arterial stiffness. Hypertension. 2005 Jun;45(6):1050-5.
17. Yang EY, Brunner G, Dokainish H, Hartley CJ, Taffet G, Lakkis N, et al. Application of speckle-tracking in the evaluation of carotid artery function in subjects with hypertension and diabetes. J Am Soc Echocardiogr. 2013 Aug;26(8):901-9 e1.
18. Kim KH, Park JC, Yoon HJ, Yoon NS, Hong YJ, Park HW, et al. Usefulness of aortic strain analysis by velocity vector imaging as a new echocardiographic measure of arterial stiffness. J Am Soc Echocardiogr. 2009 Dec;22(12):1382-8.

19. Saito M, Okayama H, Inoue K, Yoshii T, Hiasa G, Sumimoto T, et al. Carotid arterial circumferential strain by two-dimensional speckle tracking: a novel parameter of arterial elasticity. Hypertens Res. 2012 Sep;35(9):897-902.

20. O'Rourke MF. Diastolic heart failure, diastolic left ventricular dysfunction and exercise intolerance. J Am Coll Cardiol. 2001 Sep;38(3):803-5.

21. Laurent S, Katsahian S, Fassot C, Tropeano AI, Gautier I, Laloux B, et al. Aortic stiffness is an independent predictor of fatal stroke in essential hypertension. Stroke. 2003 May;34(5):1203-6.

22. Masawa N, Yoshida Y, Yamada T, Joshita T, Sato S, Mihara B. Morphometry of structural preservation of tunica media in aged and hypertensive human intracerebral arteries. Stroke. 1994 Jan;25(1):122-7.

23. Heistad DD, Armstrong ML, Baumbach GL, Faraci FM. Sick vessel syndrome. Recovery of atherosclerotic and hypertensive vessels. Hypertension. 1995 Sep;26(3):509-13.

24. Vieira MJ, Teixeira R, Goncalves L, Gersh BJ. Left atrial mechanics: echocardiographic assessment and clinical implications. J Am Soc Echocardiogr. 2014 May;27(5):463-78.

25. Teixeira R, Monteiro R, Garcia J, Baptista R, Ribeiro M, Cardim N, et al. The relationship between tricuspid regurgitation severity and right atrial mechanics: a speckle tracking echocardiography study. Int J Cardiovasc Imaging. 2015 Aug;31(6):1125-35.

26. Madeira M, Teixeira R, Costa M, Goncalves L, Klein AL. Two-dimensional speckle tracking cardiac mechanics and constrictive pericarditis: systematic review. Echocardiography. 2016 Aug 19.

27. Cavalcante JL, Lima JA, Redheuil A, Al-Mallah MH. Aortic stiffness: current understanding and future directions. J Am Coll Cardiol. 2011 Apr 5;57(14):1511-22.

28. Leite L, Teixeira R, Baptista R, Barbosa A, Ribeiro N, Castro G, et al. Statins and vascular load in aortic valve disease patients, a two dimensional speckle tracking echocardiographic study. Eur Heart J Cardiovasc Imaging. 2015;16(Suppl 2):S102-S29

Part IV: Supplements

Supplements Table of Contents

Supplement Number 1:

Protocol Approval*: Comissão Nacional de Protecção de Dados*

COMISSÃO NACIONAL
DE PROTECÇÃO DE DADOS

AUTORIZAÇÃO N.º 3611 /2015

I. Pedido

Rogério Paiva Cardoso Teixeira, no âmbito de Doutoramento em Medicina pela Universidade de Coimbra, notificou à Comissão Nacional de Protecção de Dados (CNPD) um tratamento de dados pessoais com a finalidade de elaborar um estudo intitulado "*Ultrassonographic vascular mechanics: Feasibility, usefulness and clinical applications*".

O estudo tem como principal objetivo a identificação de alterações na artéria aorta, que poderão ser mais evidentes em doentes com antecedentes de hipertensão arterial, enfarte do miocárdio e doença das válvulas do coração.

O estudo decorrerá nos serviços de Cardiologia do Centro Hospitalar Universitário de Coimbra e do Hospital Beatriz Ângelo. Serão recrutados os pacientes referenciados para uma ecocardiografia.

A participação no estudo consistirá na recolha de dados clínicos, exame físico e no estudo mais detalhado da artéria aorta aquando da ecocardiografia.

Os dados serão recolhidos num "caderno de recolha de dados" no qual não há identificação nominal do titular, sendo aposto um código de doente. A chave desta codificação só pode ser conhecida do responsável.

Os destinatários são ainda informados sobre a natureza facultativa da sua participação e garantia de confidencialidade no tratamento, caso decidam participar, recolhendo responsável o seu consentimento informado para o efeito.

COMISSÃO NACIONAL
DE PROTECÇÃO DE DADOS

II. Análise

A CNPD já se pronunciou na sua Deliberação n.º 227/2007 sobre o enquadramento legal, os fundamentos de legitimidade, os princípios orientadores para o correto cumprimento da LPD, bem como as condições gerais aplicáveis ao tratamento de dados pessoais para a finalidade de estudos de investigação na área da saúde.
Porque em grande parte referentes à vida privada e também à saúde, os dados recolhidos pela requerente têm a natureza de sensíveis, nos termos do disposto no n.º 1 do artigo 7.º da LPD.

Em regra, o tratamento de dados sensíveis é proibido, de acordo com o disposto no n.º 1 do artigo 7.º da LPD. Todavia, nos termos do n.º 2 do mesmo artigo, o tratamento de dados da vida privada e de saúde é permitido, quando haja uma disposição legal que consagre esse tratamento de dados, quando por motivos de interesse público importante o tratamento for indispensável ao exercício das atribuições legais ou estatutárias do seu responsável ou quando o titular dos dados tiver prestado o seu consentimento.

Não estando preenchidas as duas primeiras condições de legitimidade, o fundamento de legitimidade só pode basear-se no consentimento dos titulares dos dados ou dos representantes legais, quando os titulares dos dados sejam incapazes.

Assim, é necessário o «consentimento expresso do titular», entendendo-se por consentimento qualquer manifestação de vontade, livre, específica e informada, nos termos da qual o titular aceita que os seus dados sejam objeto de tratamento (cf. artigo 3.º, alínea *h*), da LPD), o qual deve ser obtido através de uma "declaração de consentimento informado" onde seja utilizada uma linguagem clara e acessível.

Nos termos do artigo 10.º da LPD, a declaração de consentimento tem de conter a identificação do responsável pelo tratamento e a finalidade do tratamento, devendo ainda conter informação sobre a existência e as condições do direito de acesso e de retificação por parte do respetivo titular.

COMISSÃO NACIONAL
DE PROTECÇÃO DE DADOS

Os titulares dos dados, de acordo com a declaração de consentimento informado junta aos autos, apõem as suas assinaturas na mesma, deste modo satisfazendo as exigências legais.

Cabe ao Investigador assegurar a confidencialidade dos dados pessoais e da informação tratada, conforme o estatuído na alínea *g*) do artigo 10.º da Lei n.º 21/2014, de 16 de abril (Lei da investigação clínica).
Assim, apenas poderão ter acesso aos registos médicos originais, ou seja, a dados que identificam os participantes, o investigador e um monitor, (nos termos do artigo 11.º da Lei da investigação clínica), e apenas na medida do estritamente necessário, também recaindo sobre este a obrigação de confidencialidade.

A informação tratada é recolhida de forma lícita (artigo 5.º, n.º1 alínea *a*) da Lei n.º 67/98), para finalidades determinadas, explícitas e legítimas (cf. alínea *b*) do mesmo artigo) e não é excessiva.

O fundamento de legitimidade é o consentimento expresso do titular dos dados.

III. Conclusão

Assim, nos termos das disposições conjugadas do n.º 2 do artigo 7.º, n.º 1 do artigo 27.º, alínea *a*) do n.º 1 do artigo 28.º e artigo 30.º da Lei de Proteção de Dados, com as condições e limites fixados na referida Deliberação n.º 227/2007, que se dão aqui por reproduzidos e que fundamentam esta decisão, autoriza-se o tratamento de dados *supra* referido, consignando-se o seguinte:

Responsável pelo tratamento: Rogério Paiva Cardoso Teixeira;
Finalidade: estudo *"Ultrassonographic vascular mechanics: Feasibility, usefulness and clinical applications"*;
Categoria de Dados pessoais tratados: código do participante; Idade, género, peso, altura, tensão arterial, frequência cardíaca, doenças cardiovasculares prévias,

COMISSÃO NACIONAL
DE PROTECÇÃO DE DADOS

doenças não cardiovasculares prévias, medicação habitual, ritmo cardíaco, frequência cardíaca e por último múltiplos dados da ecocardiografia: dimensões das câmaras, fracção de ejecção, mecânica ventricular e vascular.

Entidades a quem podem ser comunicados: Não há.

Formas de exercício do direito de acesso e retificação: Junto do responsável.

Interconexões de tratamentos: Não há.

Transferências de dados para países terceiros: Não há.

Prazo de conservação: A chave de codificação dos dados do titular deve ser destruída um mês após o fim do estudo.

Dos termos e condições fixados na Deliberação n.º 227/ 2007 e na presente Autorização decorrem obrigações que o responsável deve cumprir. Deve, igualmente, dar conhecimento dessas condições a todos os intervenientes no circuito de informação.

Lisboa, 17 de abril de 2015

Filipa Calvão (Presidente)

Supplement Number 2:

Protoco Approval: *Faculdade de Medicina da Universidade de Coimbra*

· U C ·

FMUC FACULDADE DE MEDICINA
UNIVERSIDADE DE COIMBRA

COMISSÃO DE ÉTICA DA FMUC

Of. Refª **013-CE-2014**

Data 31 / 03 /**2014**

C/conhecimento ao aluno

Exmo Senhor

Prof. Doutor Joaquim Neto Murta

Presidente do Conselho Científico

Assunto: Projecto de Investigação no âmbito do Programa de Doutoramento em Ciências da Saúde. (refª CE-005/2014)

Candidato(a): Rogério Paiva Cardoso Teixeira

Titulo do Projecto: *"Ultrassonographic vascular mechanics: feasibility, usefulness and clinical applications"*

A Comissão de Ética da Faculdade de Medicina, após análise do projecto de investigação supra identificado, decidiu emitir o parecer que a seguir se transcreve: ***"Parecer Favorável".***

Queira aceitar os meus melhores cumprimentos,

O Presidente,

Prof. Doutor João Manuel Pedroso de Lima

GC

SERVIÇOS TÉCNICOS DE APOIO À GESTÃO - STAG - COMISSÃO DE ÉTICA
Pólo das Ciências da Saúde • Unidade Central
Azinhaga de Santa Comba, Celas, 3000-354 COIMBRA - PORTUGAL
Tel.: +351 239 857 707 (Ext. 542707) | Fax: +351 239 823 236
E-mail: comissaoetica@fmed.uc.pt | www.fmed.uc.pt

Supplement Number 3:

Protocol Approval: *Comissão Ética da Hospital Beatriz Ângelo*

HOSPITAL BEATRIZ ÂNGELO

Exmo. Senhor

Dr. Miguel Almeida Ribeiro

Diretor do Serviço de Cardiologia

Hospital Beatriz Ângelo

Loures, 17 de fevereiro de 2014

N/Ref. *0698/2014_RM*

Estudo HBA N.º 0076

Assunto: Estudo – "Ultrassonographic vascular mechanics: Feasibility, usefulness and clinical applications"

Caro Dr. Miguel Almeida Ribeiro,

Temos o prazer de informar V. Exa. de que o estudo em epígrafe foi aprovado pela Comissão de Ética para a Saúde e Comissão de Investigação Clínica do Hospital Beatriz Ângelo.

Com os melhores cumprimentos,

O Presidente das Comissões

Professor Doutor Rui Maio

Supplement Number 4:

Informed Consent: Final Version

FORMULÁRIO DE INFORMAÇÃO E CONSENTIMENTO INFORMADO

Título do Projeto:

Ultrassonographic vascular mechanics:
Feasibility, usefulness and clinical applications

PROTOCOLO Nº	
PROMOTOR	Rogério Paiva Cardoso Teixeira
INVESTIGADOR COORDENADOR	Rogério Paiva Cardoso Teixeira
CENTRO DE ESTUDO	Faculdade de Medicina Universidade de Coimbra
INVESTIGADOR PRINCIPAL	Rogério Paiva Cardoso Teixeira
MORADA	Rua Maria Vitória Bobone 22-3 3 Ap 332 3030 Coimbra
CONTACTO TELEFÓNICO	936740242

NOME DO DOENTE
(LETRA DE IMPRENSA) _____

É convidado(a) a participar voluntariamente neste estudo porque foi referenciado pelo seu clínico assistente para a realização de uma ecocardiografia para estudar o seu problema de saúde.

Este procedimento é chamado consentimento informado e descreve a finalidade do estudo, os procedimentos, os possíveis benefícios e riscos.

A sua participação poderá contribuir para melhorar o conhecimento sobre uma nova metodologia ecocardiográfica para avaliar a doença e o processo de envelhecimento da artéria aorta.

Receberá uma cópia deste Consentimento Informado para rever e solicitar aconselhamento de familiares e amigos. O Investigador ou outro membro da sua equipa irá esclarecer qualquer dúvida que tenha sobre o termo de consentimento e também alguma palavra ou informação que

possa não entender.

Depois de compreender o estudo e de não ter qualquer dúvida acerca do mesmo, deverá tomar a decisão de participar ou não. Caso queira participar, ser-lhe-á solicitado que assine e date este formulário. Após a sua assinatura e a do Investigador, ser-lhe-á entregue uma cópia. Caso não queira participar, não haverá qualquer penalização nos cuidados que irá receber.

1. INFORMAÇÃO GERAL E OBJECTIVOS DO ESTUDO

Este estudo faz parte do projecto de Doutoramento em Medicina do Dr. Rogério Teixeira, Cardiologista do Hospital Beatriz Ângelo, e Assistente da Faculdade de Medicina da Universidade de Coimbra. Este projecto é orientado pelo Professor Doutor Lino Gonçalves da Faculdade de Medicina da Universidade de Coimbra e pelo Professor Doutor Nuno Cardim, da Faculdade de Ciências Médicas da Universidade Nova de Lisboa. O estudo irá decorrer no Serviço de Cardiologia do Centro Hospital e Universitário de Coimbra, e no Serviço de Cardiologia do Hospital Beatriz Ângelo.

O processo de envelhecimento e desgaste também pode atingir as artérias que conduzem o sangue do coração para os vasos sanguíneos mais periféricos. Estas alterações podem ser mais precoces e graves na presença de algumas doenças como a hipertensão arterial, um enfarte do miocárdio e doença das válvulas do coração. O objectivo geral desta investigação prende-se com a identificação de alterações da artéria aorta, que poderão ser mais evidentes em doentes com os antecedentes referidos.

A ecografia cardíaca é predominantemente focada na análise do músculo cardíaco e das válvulas. Num primeiro tempo, são adquiridas diferentes imagens (fotografias e pequenos vídeos) do seu coração, para posterior análise numa estação de trabalho. A fase inicial tem uma duração habitual de 20 a 30 minutos. Num segundo tempo, na estação de trabalho são realizadas várias medições, e é elaborado o relatório final que será entregue ao seu médico assistente. Tal processo demora habitualmente entre 10 e 15 minutos.

Com o presente estudo temos como objectivo aproveitar a referenciação que foi efectuada para uma ecocardiografia, e estender a análise ao estudo mais detalhado da artéria aorta. Isso provavelmente prolongará a fase de aquisição do exame em 5 a 10 minutos. Posteriormente, será realizado na estação de trabalho sem a sua presença, o estudo mais detalhado das suas imagens. Esse estudo não influenciará o relatório dito clássico do exame a que está a ser submetido. É também importante que saiba que os seus dados serão recolhidos para uma base de dados, e que durante este processo será sempre mantida a sua confidencialidade.

Importa também assinlar que trata-se de um estudo observacional, e como tal não não será feita nenhuma alteração na sua medicação ou tratamentos habituais.

Este estudo foi aprovado pela Comissão de Ética da Faculdade Medicina da Universidade de Coimbra (FMUC) de modo a garantir a protecção dos direitos, segurança e bem-estar de todos os doentes ou outros participantes incluídos e garantir prova pública dessa protecção.

Como participante neste estudo beneficiará da vigilância e apoio do seu médico, garantindo assim a sua segurança.

2. PROCEDIMENTOS E CONDUÇÃO DO ESTUDO

2.1. Procedimentos

2.1.1. Realização de história clínica

Um médico do estudo realizará uma revisão da sua história médica recente e registará a sua medicação atual.

2.1.2. Realização do exame físico

Será realizada uma exame físico, que consiste na avaliação do seu peso, da sua altura, dos valores de pressão arterial e da pulsação.

2.1.3. Realização da ecocardiografia

Um médico ou um técnico realizarão a sua ecocardiografia de acordo com as recomendações internacionais em vigor. Ao autorizar participar neste estudo, o médico ou o técnico irão prolongar a fase de aquisição de imagens, em cerca de 5 a 10 minutos por forma a captar imanges mais detalhadas da sua artéria aorta.

2.1.4.Outros Procedimentos

É importante referir que as imagens adquiridas durante a ecocardiografia, serão trabalhadas em maior detalhe numa estação de trabalho – a denominda análise de pós-processamento de imagem. É desta forma que serão obtidos os parâmetros a analisar no presente estudo.

Poderá também ser convidade a participar numa análise do envelecimento das artérias por um outro método não ecocardiográfico. Este método baseia-se na avaliação do sinal do pulso com uma pequena sonda na artéria femoral (coxa) e na artéria carótida (pescoço).

2.2. Calendário das visitas

Este estudo consiste numa visita única com duração de cerca de 15-30 minutos, que será feita previamente à realização da ecocardiografia.

Com o presente estudo temos como objectivo aproveitar a referenciação que foi efectuada para uma ecocardiografia, e estender a análise ao estudo mais detalhado da artéria aorta. Isso provavelmente prolongará a fase de aquisição do exame em 5 a 10 minutos. Ou seja a ecocardiografia que tem um tempo previsto para realização de 30 minutos, poderá passar para 35-40 minutos. Posteriormente, será realizado na estação de trabalho sem a sua presença, o estudo mais detalhado das suas imagens. Esse estudo não influenciará o relatório clássico do exame a que está a ser submetido

2.3. Tratamento de dados

É também importante que saiba que os seus dados serão recolhidos para uma base de dados, e que durante este processo será sempre mantida a sua confidencialidade.

3. RISCOS E POTENCIAIS INCONVENIENTES PARA O DOENTE

A ecografia é um exame sem radiação, e portanto sem risco acrescido para a sua saúde. Quer isto dizer que prolongar o exame 5 a 10 minutos não terá influência no seu estado de saúde.

4. POTENCIAIS BENEFÍCIOS

A participação no presente estudo não lhe trará nenhum benefício imediato. No entanto, importa referir que este estudo pode melhorar a forma como se diagnosticam complicações da doença vascular através da ecocardiografia. Isso poderá no futuro melhorar o conhecimento e assim melhorar os cuidados clínicos a prestar aos doentes com situações idênticas à sua.

5. NOVAS INFORMAÇÕES

Ser-lhe-á dado conhecimento de qualquer nova informação que possa ser relevante para a sua condição ou que possa influenciar a sua vontade de continuar a participar no estudo.

8. PARTICIPAÇÃO/ ABANDONO VOLUNTÁRIO

É inteiramente livre de aceitar ou recusar participar neste estudo. Pode retirar o seu consentimento em qualquer altura sem qualquer consequência para si, sem precisar de explicar as razões, sem qualquer penalidade ou perda de benefícios e sem comprometer a sua relação com o

Investigador que lhe propõe a participação neste estudo. Ser-lhe-á pedido para informar o Investigador se decidir retirar o seu consentimento.

O Investigador do estudo pode decidir terminar a sua participação neste estudo se entender que não é do melhor interesse para a sua saúde continuar nele. O médico do estudo notificá-lo-á e falará consigo a respeito da mesma.

9. CONFIDENCIALIDADE

Sem violar as normas de confidencialidade, serão atribuídos a auditores e autoridades reguladoras acesso aos registos médicos para verificação dos procedimentos realizados e informação obtida no estudo, de acordo com as leis e regulamentos aplicáveis. Os seus registos manter-se-ão confidenciais e anonimizados de acordo com os regulamentos e leis aplicáveis. Se os resultados deste estudo forem publicados a sua identidade manter-se-á confidencial.

Ao assinar este Consentimento Informado autoriza este acesso condicionado e restrito.

Pode ainda em qualquer altura exercer o seu direito de acesso à informação. Pode ter também acesso à sua informação médica directamente ou através do seu médico neste estudo. Tem também o direito de se opor à transmissão de dados que sejam cobertos pela confidencialidade profissional.

Os registos médicos que o identificarem e o formulário de consentimento informado que assinar serão verificados para fins do estudo pelo promotor e/ou por representantes do promotor, e para fins regulamentares pelo promotor e/ou pelos representantes do promotor e agências reguladoras noutros países. A Comissão de Ética responsável pelo estudo pode solicitar o acesso aos seus registos médicos para assegurar-se que o estudo está a ser realizado de acordo com o protocolo. Não pode ser garantida confidencialidade absoluta devido à necessidade de passar a informação a essas partes.

Ao assinar este termo de consentimento informado, permite que as suas informações médicas neste estudo sejam verificadas, processadas e relatadas conforme for necessário para finalidades científicas legítimas.)

Confidencialidade e tratamento de dados pessoais

Os dados pessoais dos participantes no estudo, incluindo a informação médica ou de saúde recolhida ou criada como parte do estudo, serão utilizados para condução do estudo, designadamente para fins de investigação científica relacionados com a sua doença em estudo.

Ao dar o seu consentimento à participação no estudo, a informação a si respeitante, designadamente a informação clínica, será utilizada da seguinte forma:

1. Os investigadores e as outras pessoas envolvidas no estudo recolherão e utilizarão os seus dados pessoais para as finalidades acima descritas.
2. Os dados do estudo, associados às suas iniciais ou a outro código que não o (a) identifica directamente (e não ao seu nome) serão comunicados pelos investigadores e outras pessoas envolvidas no estudo ao promotor do estudo, que os utilizará para as finalidades acima descritas.
3. Os dados do estudo, associados às suas iniciais ou a outro código que não permita identificá-lo(a) directamente, poderão ser comunicados a autoridades de saúde nacionais e internacionais.
4. A sua identidade não será revelada em quaisquer relatórios ou publicações resultantes deste estudo.
5. Todas as pessoas ou entidades com acesso aos seus dados pessoais estão sujeitas a sigilo profissional.
6. Ao dar o seu consentimento para participar no estudo autoriza o promotor ou empresas de monitorização de estudos/estudos especificamente contratadas para o efeito e seus colaboradores e/ou autoridades de saúde, a aceder aos dados constantes do seu processo clínico, para conferir a informação recolhida e registada pelos investigadores, designadamente para assegurar o rigor dos dados que lhe dizem respeito e para garantir que o estudo se encontra a ser desenvolvido correctamente e que os dados obtidos são fiáveis.
7. Nos termos da lei, tem o direito de, através de um dos médicos envolvidos no estudo/estudo, solicitar o acesso aos dados que lhe digam respeito, bem como de solicitar a rectificação dos seus dados de identificação.
8. Tem ainda o direito de retirar este consentimento em qualquer altura através da notificação ao investigador, o que implicará que deixe de participar no estudo/estudo. No entanto, os dados recolhidos ou criados como parte do estudo até essa altura que não o(a) identifiquem poderão continuar a ser utilizados para o propósito de estudo/estudo, nomeadamente para manter a integridade científica do estudo, e a sua informação médica não será removida do arquivo do estudo.

9. Se não der o seu consentimento, assinando este documento, não poderá participar neste estudo. Se o consentimento agora prestado não for retirado e até que o faça, este será válido e manter-se-á em vigor.

10. COMPENSAÇÃO

Este estudo é da iniciativa do investigador e, por isso, se solicita a sua participação sem uma compensação financeira para a sua execução, tal como também acontece com os investigadores. Não haverá portanto qualquer custo para o participante pela sua participação neste estudo.

11. CONTACTOS

Se tiver perguntas relativas aos seus direitos como participante deste estudo, deve contactar:

Presidente da Comissão de Ética da FMUC,
Azinhaga de Santa Comba, Celas – 3000-548 Coimbra
Telefone: 239 857 707
e-mail: comissaoetica@fmed.uc.pt

Se tiver questões sobre este estudo deve contactar:

Rogério Paiva Cardoso Teixeira
Rua Maria Vitória Bobone, 22-3, 3 Ap 332, 3030 Coimbra
TLM: 962499758
e-mail: rogeriopteixeira@gmail.com

NÃO ASSINE ESTE FORMULÁRIO DE CONSENTIMENTO INFORMADO A MENOS QUE TENHA TIDO A OPORTUNIDADE DE PERGUNTAR E TER RECEBIDO RESPOSTAS SATISFATÓRIAS A TODAS AS SUAS PERGUNTAS.

CONSENTIMENTO INFORMADO

De acordo com a Declaração de Helsínquia da Associação Médica Mundial e suas actualizações:

1. Declaro ter lido este formulário e aceito de forma voluntária participar neste estudo.

2. Fui devidamente informado(a) da natureza, objectivos, riscos, duração provável do estudo, bem como do que é esperado da minha parte.

3. Tive a oportunidade de fazer perguntas sobre o estudo e percebi as respostas e as informações que me foram dadas. A qualquer momento posso fazer mais perguntas ao médico responsável do estudo. Durante o estudo e sempre que quiser, posso receber informação sobre o seu desenvolvimento. O médico responsável dará toda a informação importante que surja durante o estudo que possa alterar a minha vontade de continuar a participar.

4. Aceito que utilizem a informação relativa à minha história clínica e os meus tratamentos no estrito respeito do segredo médico e anonimato. Os meus dados serão mantidos estritamente confidenciais. Autorizo a consulta dos meus dados apenas por pessoas designadas pelo promotor e por representantes das autoridades reguladoras.

5. Aceito seguir todas as instruções que me forem dadas durante o estudo. Aceito em colaborar com o médico e informá-lo(a) imediatamente das alterações do meu estado de saúde e bem-estar e de todos os sintomas inesperados e não usuais que ocorram.

6. Autorizo o uso dos resultados do estudo para fins exclusivamente científicos e, em particular, aceito que esses resultados sejam divulgados às autoridades sanitárias competentes.

7. Aceito que os dados gerados durante o estudo sejam informatizados pelo investigador ou outrem por si designado. Eu posso exercer o meu direito de rectificação e/ ou oposição.

8. Tenho conhecimento que sou livre de desistir do estudo a qualquer momento, sem ter de justificar a minha decisão e sem comprometer a qualidade dos meus cuidados médicos. Eu tenho conhecimento que o médico tem o direito de decidir sobre a minha saída prematura do estudo e que me informará da causa da mesma.

9. Fui informado que o estudo pode ser interrompido por decisão do investigador, do promotor ou das autoridades reguladoras.

Nome do Participante_____

Assinatura : _____ ***Data:***_____/____/____

Nome de Testemunha / Representante Legal:_____

Assinatura: _____ ***Data:***_____/____/____

Confirmo que expliquei ao participante acima mencionado a natureza, os objectivos e os potenciais riscos do Estudo acima mencionado.

Nome do Investigador:_____

Assinatura: _____ ***Data:***_____/____/____

Supplement Number 5:

Informed Consent: First Version

Consentimento informado

Estudo da deformação vascular da artéria aorta por ecocardiografia

Está a ser convidado a participar num estudo clínico sobre a utilidade da deformação vascular determinada por ecocardiografia. Este estudo faz parte do projecto de Doutoramento em Medicina do Dr. Rogério Teixeira, Cardiologista do Hospital Beatriz Ângelo, e Assistente da Faculdade de Medicina da Universidade de Coimbra. Este projecto é orientado pelo Professor Doutor Lino Gonçalves da Faculdade de Medicina da Universidade de Coimbra e pelo Professor Doutor Nuno Cardim, da Faculdade de Ciências Médicas da Universidade Nova de Lisboa. Este projecto foi aprovado pela Comissão de Ética da Faculdade de Medicina da Universidade de Coimbra.

Foi referenciado pelo seu clínico assistente para a realização de uma ecocardiografia para estudar o seu problema de saúde. A ecografia cardíaca é predominantemente focada na análise do músculo cardíaco e das válvulas. Num primeiro tempo, são adquiridas diferentes imagens (fotografias e pequenos videos) do seu coração, para posterior análise numa estação de trabalho. A fase inicial tem uma duração habitual de 20 a 30 minutos. Num segundo tempo, na estação de trabalho são realizadas várias medições, e é elaborado o relatório final que será entregue ao seu médico assistente. Tal processo demora habitualmente entre 10 e 15 minutos.

O processo de envelhecimento e desgaste também pode atingir as artérias que conduzem o sangue do coração para os vasos sanguíneos mais periféricos. Estas alterações podem ser mais precoces e graves na presença de algumas doenças como a hipertensão arterial, um enfarte do miocárdio e doença das válvulas do coração. O objectivo geral desta investigação prende-se com a identificação de alterações da artéria aorta, que poderão ser mais evidentes em doentes com os antecedentes referidos.

Com o presente estudo temos como objectivo aproveitar a referenciação que foi efectuada para uma ecocardiografia, e estender a análise ao estudo mais detalhado da artéria aorta. Isso provavelmente prolongará a fase de aquisição do exame em 5 a 10 minutos. Posteriormente, será realizado na estação de trabalho sem a sua presença, o estudo mais detalhado das suas imagens. Esse estudo não influenciará o relatório dito clássico do exame a que está a ser submetido. É também importante que saiba que os seus dados serão recolhidos para uma base de dados, e que durante este processo será sempre mantida a sua confidencialidade.

Deverá também saber que:

- se recusar participar não será prejudicado. O seu exame será realizado, relatado e enviado para o seu médico assistente normalmente .
- a participação no presente estudo não lhe trará nenhum benefício imediato.
- a participação do presente estudo não lhe trará qualquer custo adicional.
- a ecografia é um exame sem radiação, e portanto sem risco acrescido para a sua saúde. Quer isto dizer que prolongar o exame 5 a 10 minutos não terá influência no seu estado de saúde.
- a informação obtida da análise mais pormenorizada da aorta não será comunicada no relatório final, porque o seu impacto na prática clínica ainda é desconhecido.

Declaro que li e compreendi o que me foi pedido. Tive também oportunidade para esclarecer dúvidas com o médico e com a equipa de investigação sobre o exame ecográfico. Em face disso:

- autorizo e cedo as imagens do exame ecográfico que me foi solicitado à equipa de investigação clínica liderada pelo Dr. Rogério Teixeira;
- autorizo que sejam adquiridas imagens adicionais da aorta torácica para posterior análise, sabendo que isso prolongará o tempo de exame entre 5 e 10 minutos;
- autorizo que os dados clínicos e ecográficos resultantes sejam incluídos numa base de dados para serem devidamente estudados.

Médico Assistente:

Nome:_____

Data:_____

Assinatura:_____

Doente:

Nome:_____

Data:_____

Assinatura:_____

Informação para o doente

A ecocardiografia é uma técnica que permite a visualização do coração em tempo real. É um método considerado não invasivo, e sem riscos para a saúde.

A ecografia permite a obtençao de imagens paradas (tipo fotografias) e vídeos do coração, e assim fornece informações muito importantes sobre o músculo, e as válvulas no coração, e os fluxos de sangue dentro de cada cavidade cardíaca.

Para além do coração é possível com a ecocardiografia a obtenção de imagens da artéria aorta. Esta é a principal artéria do corpo humano, e tem como função permitir o fluxo de sangue do coração para o resto do corpo.

O projecto de investigação em que está aceitar participar foca-se principalmente no estudo da artéria aorta na proximidade do coração. É sabido que com o envelhecimento e em certas doenças, há um atingimento também das paredes que forma a aorta, tornado a artéria mais rija.

Hoje em dia estão disponíveis formas para estudar mais detalhadamente as imagens obtidas na ecocardiografia por um técnica de imagem especial chamada "speckle tracking". O objectivo principal deste estudo é precisamente aplicar esta nova metodologia nas imagens da aorta obtidas por ecocardiografia.

Esperamos aplicar com sucesso esta nova metodologia imagiológica, e perceber as consequências para o coração, e as associações com diferentes doenças, nomedamente com a hipertensão, com as doenças da válvula aórtica e com a doença coronária. Muito obrigado pela sua participação.

A equipa de investiagadores

Rogério Teixeira, Nuno Cardim, Lino Gonçalves.

Se tiver dúvidas ou necessitar de algum esclarecimento pode contactar o Dr Rogério Teixeira através do número: 936740242 ou do email: rogerio.teixeira@hbeatrizangelo.pt

14

Supplement number 6

Letter To The Editor: Vascular Mechanics And Stroke – A Critical Appraisal: Study The Arteries But Do Not Forget The Flow

Letter to the Editor

Vascular mechanics and stroke – a critical appraisal: study the arteries but do not forget the flow

Am J Hypertens. 2013 Jul;26(7):946

Rogério Teixeira[1,2]* MD, Maria João Vieira[2] PHD, Miguel Almeida Ribeiro[1] MD, Nuno Cardim[3] MD, PHD, Lino Gonçalves [2,4] MD, PHD

1 Departamento de Medicina, Serviço de Cardiologia, Hospital Beatriz Ângelo, Loures, Portugal 2 Faculdade de Medicina Universidade de Coimbra, Coimbra, Portugal 3 Serviço de Cardiologia, Hospital da Luz, Lisboa, Portugal 4 Serviço de Cardiologia, Centro Hospitalar e Universitário de Coimbra, Coimbra, Portugal *

Total word count: 369. Number of references: 4

Dear editor in chief, **Dr. Michael Alderman,**

We have read with interest the paper of Tsai et al (1) regarding the usefulness of carotid vascular mechanics to assess carotid arterial stiffness, and its association with a previous history of stroke in patients 60 years old or more, from a community health survey program. Since the first publication from Oishi in 2008 (2), a number of studies have been performed to validate vascular circumferential strain and strain rate both in the ascending, descending thoracic aorta, the abdominal aorta or in the carotid arteries. Locally assessed carotid stiffness can influence carotid strain (CS) and carotid strain rate (CSR), but it is also conceivable that both vascular deformation indexes could be influenced by blood flow. In fact, we have recently demonstrated in a group of consecutive patients with moderate to severe aortic stenosis, that the most important determinant of circumferential ascending aortic strain was the stroke volume index (3). It remained the strongest predictor of aortic circumferential strain, when adjusted for covariates such as the stiffness index, systemic resistance, vascular compliance and impedance. This means that circumferential vascular strain was highly dependent on the aortic flow, in a similar way as the left atrial and the left ventricular (LV) longitudinal strain are influenced by phasic volume changes (3). In the study of Tsai et al (1) CS and CSR were significantly correlated with local vascular stiffness, but the influence of blood flow was not taken into account. We believe that noninvasive, echo-Doppler derived, carotid blood flow, should have been performed, as it could probably influence CS and CSR. Moreover a number of echocardiographic variables such as LV ejection fraction, LV diastolic function and filling pressures, and LV mass index could have been assessed, as they influence LV myocardial performance, stroke volume, carotid blood flow, and Manuscript consequently CS and CSR. This information would have been especially important in elderly hypertensive patients with a history of stroke. In fact, approximately 25% of all ischemic strokes are due to cardiac embolism with heart failure and hypertension being two major risk factors for stroke (4). We therefore believe that the adjustment for those covariates should have been done to validate and improve the quality of the multivariate model for the prediction of stroke. Key words: vascular mechanics The authors declare they have no conflict of interests.

References

1. Tsai W, Sun Y, Liu Y, Ho C, Chen J, Wang M, Tsai, L. Usefulness of cascular wall deformation for assessment of carotid arterial stiffness and association with previous stroke in elderly. Am J Hypertens. 2013 Mar 11.

2. Oishi Y, Mizuguchi Y, Miyoshi H, Iuchi A, Nagase N, Oki T. A novel approach to assess aortic stiffness related to changes in aging using a two-dimensional strain imaging. Echocardiography. 2008 25(9):941-5.

3. Teixeira R, Moreira N, Baptista R, Barbosa A, Martins R, Castro G, Providencia L. Circumferential ascending aortic strain and aortic stenosis. Eur Heart J Cardiovasc Imag. 2012 Nov 2.

4. Endres M, Heuschmann PU, Laufs U, Hakim AM. Primary prevention of stroke: blood pressure, lipids, and heart failure. Eur Heart J. 2011 32(5):545-52

Supplement number 7

Original Article:Aortic valve disease and vascular mechanics: two-dimensional spekle tracking echocardiographic analysis

Original Article

Aortic valve disease and vascular mechanics: two-dimensional speckle tracking echocardiographic analysis

Echocrdiography. 2016 Apr 16. doi: 10.1111/echo.13236.

Luís Leite, MD;[1§] Rogério Teixeira, MD;[2,3§] Manuel Oliveira-Santos, MD;[1] António Barbosa, BSc;[1] Rui Martins, MD;[1] Graça Castro, MD;[1] Lino Gonçalves, PhD;[2,3] Mariano Pego, MD[1]

[§] Both authors contributed equally to this work

[1] Centro Hospitalar e Universitário de Coimbra, Hospitais da Universidade de Coimbra

[2] Centro Hospitalar e Universitário de Coimbra, Hospital Geral

[3] Faculdade de Medicina da Universidade de Coimbra

Word Count: 3004 (without references or tables)

Author contributions: LL and RT: conception and design, analysis and interpretation of data, drafting of article. MOS: analysis of data, critical manuscript revision. AB, RM, GC, JG and MP: interpretation of data, critical manuscript revision. All authors have read and approved the final draft.

Abstract

Purpose: Degenerative aortic valve disease (AVD) is a complex disorder that goes beyond valve itself, also undermining aortic wall. We aimed to assess the ascending aortic mechanics with two-dimensional speckle-tracking echocardiography (2D-STE) in patients with aortic regurgitation (AR) and hypothesized a relationship with degree of AR. Aortic mechanics were then compared with those of similarly studied healthy controls and patients with aortic stenosis (AS); finally we aimed to assess the prognostic significance of vascular mechanics in AVD. **Methods**: Overall, 73 patients with moderate-to-severe AR and 22 healthy subjects were enrolled, alongside a previously examined cohort (N=45) with moderate-to-severe AS. Global circumferential ascending aortic strain (CAAS) and strain rate (CAASR) served as indices of aortic deformation; corrected CAAS was calculated as CAAS/pulse pressure (PP). Median clinical follow-up was 438 days. **Results:** In patients with severe (vs moderate) AR, CAASR (1.53±0.29 s^{-1} vs 1.90±0.62 s^{-1}, P<0.05) and corrected CAAS (0.14 ±0.06 %/mmHg vs 0.19±0.08%/mmHg, P<0.05) were significantly lower, whereas CAAS did not differ significantly. Measurers of aortic mechanics (CAAS, corrected CAAS, CAASR) differed significantly (all P<0.01) in patients with AS, AR and in healthy subjects, with lower values seen in patients with AS. In follow-up, survival rate of AVD patients with baseline CAASR >0.88 s^{-1} was significantly higher (log rank, 97.4% vs 73.0%; P=0.03).**Conclusions**: Quantitative measures of aortic mechanics were lower for AS patients, suggesting a more significant derangement of aortic elastic properties. In the context of AVD, vascular mechanics assessment proved useful in gauging clinical prognosis.

Keywords: Two-Dimensional Speckle Tracking Echocardiography; Aortic Mechanics; Strain; Strain Rate; Aortic Regurgitation; Aortic Stenosis.

Abbreviation List:

AVD – Aortic valve disease; AS – Aortic stenosis; AR – Aortic regurgitation; AVR – Aortic valve replacement; BMI – Body mass index; BSA – Body surface area; CAAS – Circumferential ascending aortic strain; CAASR – Circumferential ascending aortic strain rate; CO – Cardiac output; CoV – Coefficient of variation; CV – Cardiovascular; CW – Continuous wave; EROA – Effective regurgitant orifice area; HF – Heart failure; iAVA – Indexed aortic valve area; ICC – Interclass correlation coefficient; IQR – Interquartile range; LV – Left ventricle; LVEF – Left ventricle ejection fraction; LVOT – Left ventricular outflow tract; MAP – Mean arterial pressure; MG – Mean transvalvular pressure gradient; NYHA – New York Heart Association; PISA – Proximal isovelocity surface area; PP – Pulse pressure; PHT – Pressure half-time; R Vol – Regurgitant volume; SAC – Systemic arterial compliance; SAP – Systolic arterial pressure; SVI – Stroke volume index; TVI – Time Velocity Integral; TVR – Total vascular resistance; VC – Vena contracta; Zva – Valvulo-arterial impedance; β – Stiffness index (1 or 2); 2D-STE – Two-dimensional speckle-tracking echocardiography.

Introduction

Degenerative aortic valve disease (AVD) is highly prevalent in developed countries[1,2] and it is increasing given the aging of the population.[3] Transthoracic echocardiography is a widely available non-invasive exam, and it is the most commonly used imaging modality for detecting and evaluating valvular heart disease.

Speckle tracking echocardiography uses standard B-mode images to track blocks of speckles frame-to-frame, measuring dimensional lengthening/shortening relative to baseline.[4] This method enables angle-independent calculations of motion and deformation variables, such as velocity, displacement, strain and strain rate, that can be assessed in the longitudinal, radial and circumferential directions. Initially the study was confined to left ventricle (LV), but with further validation, scope was expanded to include other cardiac chambers. Since 2008, use of two-dimensional speckle tracking echocardiography (2D-STE) has been demonstrated for examining vascular walls,[5,6] first at abdominal aorta, and then along ascending[7] and descending aorta,[8] aortic arch,[9] and carotid arteries[10]. Vascular mechanics similarly have been validated *in vivo*[11] and *in vitro*[12], using sonomicrometry. Moreover, an association of the collagen content of the vessels and vascular mechanics has also been proved, promoting aortic mechanics as a new imaging surrogate of vascular stiffening.[13]

Degenerative AVD is currently viewed as a systemic disease evoking changes in arterial wall rigidity and compliance, a concept borne out mainly in aortic stenosis (AS).[14,15] Although a gold standard method of determining local vascular stiffness has yet to be approved, our group has recently shown[7,16] the utility of 2D-STE for this purpose in patients with degenerative AS. The association of vascular mechanics and aortic regurgitation (AR) is less established, but previous studies[17] do indicate that a reduction in aortic distensibility hastens the need for aortic valve replacement in patients with chronic AR.

The purposes of this 2D-STE study were as follows: (1) assess circumferential ascending aorta strain (CAAS) and strain rate (CAASR) in patients with moderate-to-severe AR; (2) explore a potential association between CAAS and CAASR, and the severity of AR; (3) compare aortic mechanics in patients with AR or AS, relative to healthy controls; (4) examine the prognostic significance of CAAS and CAASR in the setting of degenerative AVD.

Material and Methods

a) Study population

A total of 73 consecutive patients with isolated AR with vena contracta (VC) >3 mm from a single laboratory were prospectively enrolled in a 3-month study, conducted between December 2013 and February 2014. Isolated AR was defined as mean transvalvular pressure

gradient <20 mm Hg. AR in patients was considered severe if VC >6 mm, plus one of the following quantitative criteria:[18,19] effective regurgitant orifice area (EROA) ≥30 mm^2, regurgitant volume (R Vol) ≥60 mL, diastolic flow reversal in descending aorta with end-diastolic velocity >20 cm/s or Time Velocity Integral (TVI) of reverse flow >15 cm.

A cohort of 45 consecutive patients with an indexed aortic valvular area (iAVA) ≤0.85 cm^2/m^2, as previously detailed by our group,[7] was also included in this data analysis.

Additionally, we included 22 apparently healthy subjects referred for echocardiography due to suspected cardiac structural disease. These subjects had a normal echocardiography and electrocardiogram.

The study protocol was approved by *Comissão Nacional de Protecção de Dados* (authorization 3611/2015) and by *Faculdade de Medicina da Universidade de Coimbra* ethics comitee (protocol reference CE – 005/2014).

b) Clinical data

Data recorded for each patient at admission included age, weight, height and cardiovascular risk factors (such as hypertension, diabetes, dyslipidemia and smoking habits). Histories of acute myocardial infarction, stroke, chronic kidney disease and congestive heart failure (HF) were documented. Body surface area (BSA)[20] and body mass index (BMI)[21] were estimated according to applicable formula. Clinical status was assessed in accord with the New York Heart Association (NYHA) classification.[22] Current medications were recorded.

c) Systemic arterial hemodynamics

Systemic arterial pressure was measured using an arm cuff sphygmomanometer simultaneously with Doppler measurement of left ventricular outflow tract (LVOT) stroke volume. Indexed systemic arterial compliance (SAC) was calculated as follows: SAC = SVI/PP, where SVI is stroke volume index and PP is brachial pulse pressure.[14] Total vascular resistance (TVR) was estimated as follows: TVR = 80 x MAP/CO, where MAP is mean arterial pressure (ie, diastolic pressure plus one-third brachial pulse pressure) and CO is cardiac output.[23]

d) Echocardiography

Transthoracic echocardiography was performed using a Vivid 7 (GE Healthcare®, Horton, Norway) cardiovascular ultrasound device, with a 1.7/3.4 MHz tissue harmonic transducer. Complete echocardiographic studies called for standard views and techniques stipulated by established guidelines.[24] In addition, short-axis views of ascending aorta, distal to sino-tubular junction, 2–3 cm above aortic valve, were obtained at a frame rate > 50 frames

per second. Machine settings were manually adjusted to optimize 2D aortic wall tracings and 2D-STE gray-scale definition. All images were acquired at end-expiratory apnea. Loops of three cardiac cycles were stored digitally and analyzed offline using a customized software package (EchoPAC 9.0, GE Healthcare®, Horton, Norway).

Aortic regurgitation assessment:

The etiology and mechanism of AR, either from aortic leaflets disease or from aortic root dilatation, were analyzed. Assessment of AR severity was based on the recommended integration of qualitative and quantitative parameters,[18,19] including: VC width; proximal isovelocity surface area (PISA) method; diastolic flow reversal in the descending aorta (end-diastolic velocity, TVI of the reverse flow, ratio of reverse to forward TVI); and pressure half-time (PTH) of continuous wave (CW) Doppler.

Left ventricular assessment:

Left ventricular dimensions were acquired through a 2D long-axis parasternal window, in accord with current guidelines.[25] The LV mass was calculated via American Society of Echocardiography corrected formula and indexed for BSA. LV end-systolic and end-diastolic volumes and LV ejection fraction (LVEF) were assessed using the modified Simpson's rule.[25] LV cardiac index was calculated as the product of heart rate and indexed stroke volume for BSA. Stroke volume was obtained by LV outflow Doppler method as the product of LVOT area and time-velocity integral [26]. The calculation of E/e' ratio (e' being an average of septal and lateral walls in tissue Doppler imaging) was used to estimate LV filling pressures.[27]

Global LV afterload and elastic properties of aorta:

Valvulo-arterial impedance (Z_{VA}), as a measure of global LV afterload, was calculated as follows: Z_{VA} = SAP + MG/ SVI, where SAP is systolic arterial pressure and MG is mean transvalvular pressure gradient.[14]

The aortic stiffness index (β1) was calculated as: $\beta 1 = \ln(P_s/P_d)/(A_s-A_d)/A_d$,[28] where P_s and P_d are systolic and diastolic arterial pressures, and A_s and A_d are M-mode guided systolic and diastolic ascending aortic diameters, 2–3 cm above aortic valve. A_d was obtained as R wave peaked in simultaneously recorded electrocardiograms, and A_s was measured at maximal anterior aortic wall motion. Aortic stiffness index (β2) was also assessed using 2D-STE peak systolic circumferential strain according to the equation: $\beta 2 = \ln(P_s/P_d)$/global CAAS.[5]

Two-dimensional speckle tracking strain echocardiography:

The 2D-STE technique was used to calculate regional and global thoracic ascending aorta mechanics. With a line manually drawn along inner aspect of aortic wall in short axis, additional lines were automatically generated digitally at the outer aspect of vessel wall. Due to the thinness of vascular walls, relative to cardiac walls, region of interest width was reduced to the minimal value allowable by software, as previously suggested.[29] The initial systolic frame generally served as the frame of interest, to include maximal aortic wall expansion and recoil. As suggested previously,[8,30] aortic wall was divided into six equidistant regions, all similar in size. In each region, numeric expressions of each 2D-STE variable represented mean values calculated from all points in the segment. These were color-coded and shown as a function of time throughout the cardiac cycle. The tracking process and conversion to Lagrangian strains were performed offline, using dedicated software (EchoPAQ 9.0; GE Healthcare®, Horten, Norway). CAAS and CAASR were then determined. The CAAS curve peak value was usually appeared in proximity to (late peak) aortic valvular closure; global CAAS represented the mean of the six segmental peak values. Corrected CAAS was calculated as global CAAS/PP.[30] CAASR curves, as in previously published data,[10,5] included a positive early systolic peak, with global CAASR representing the mean of the six segmental peak values. Quantitative curves reflecting all regions could be expressed for each 2D-ST variable (Fig. 1).

The intra-observer and inter-observer variability of CAAS and CAASR were assessed in 10% randomly selected subjects from both AR and control groups. These measurements were repeated one month later by the same echocardiographer (LL) to assess intra-observer reproducibility. Inter-observer reproducibility was assessed by a second echocardiographer (MOS), and all values were compared with those of the first study.

e) Follow-up

Clinical follow-up was performed targeting the following outcomes: all-cause mortality; cardiovascular (CV) mortality; aortic valve replacement (AVR); and HF hospitalization. We also assessed a combined endpoint of CV mortality, AVR or HF hospitalization.

f) Statistical analysis

Normality of continuous variables was tested by histogram observation and Kolmogorov-Smirnov test. Continuous variables were expressed as mean ± standard deviation and categorical variables as percentage. Student's t-test or Anova were applied for group comparisons. Individual variables were checked for homogeneity of variance via Levene's test. For categorical variables, Chi-square or Fisher's exact tests were used as appropriate.

Pearson's correlation was used to analyze relationships between CAAS or CAASR and continuous variables. Linear regression analysis was performed thereafter to identify variables independently associated with CAAS and CAASR. A final multivariate model was subsequently elaborated, assessing all clinically relevant significant (P<0.25) variables identified in univariate analysis.

In order to control effects of age and gender on vascular mechanics, we also performed one-to-one matching in comparing aortic mechanics in AR and AS patients with healthy control subjects.

Based on stored images of 10% randomly selected patients, intra and inter-observer reproducibility of CAAS and CAASR values were assessed by intra-class correlation coefficient (ICC) and by coefficient of variation (CoV).[31]

A receiver-operating characteristic (ROC) curve analysis was used to compute the discriminatory power of CAASR to predict survival in AVD patients. Cumulative survival curves were constructed using Kaplan–Meier method, and group comparisons relied on log-rank test.

A P value <0.05 in two-tailed tests was considered statistically significant. Statistical analysis relied on standard software, specifically SPSS v20.0 (SPSS Inc, Chicago, IL, USA), MedCalc 12.2.1 (freeware), and GraphPad Prism 5.00 (GraphPad Software, In, La Jolla, CA, USA).

Results

a) Ascending aortic mechanics in AR

Mean age of patients with AR was 72±10 years, with gender balance. In most patients, the etiology of AR was either degenerative or unclear/mixed. Mean values of global CAAS, corrected global CAAS, and global CAASR were 10.81±3.95%, 0.17±0.08%/mmHg, and 1.81±0.58 s^{-1}, respectively.

a1) Patient stratification by degree of AR (moderate vs severe)

Baseline demographic data, previous cardiovascular histories, and medication use were relatively balanced between groups (Table 1). Patients were also homogenous in terms of SAC, although severe AR patients had a higher PP and a lower TVR. Both groups also displayed similar etiologies, aortic diameters, and elastic proprieties (Table 2). LV diastolic dimension and volume were significantly higher in patients with severe AR, as were indexed LV mass and SVI. However, values of LVEF, cardiac index, and E/E' ratio were similar for both groups.

In analysis of ascending aortic mechanics, global CAAS was similar in both groups, whereas corrected global CAAS (0.14 ± 0.06 %/mmHg vs. 0.19 ± 0.08 %/mmHg, P<0.05) and

global CAASR (1.53 ± 0.29 s^{-1} vs. 1.90 ± 0.62 s^{-1}, *P*<0.05) were significantly lower in patients with severe AR (Table 3).

a2) Variability of vascular mechanics in AR

Global CAASR correlated significantly with VC width (r =-0.35, *P*<0.01) and with TVI of reverse flow (r=-0.44, *P*<0.01) (Table 4). Multiple linear regression analysis revealed an independent association between E/E' ratio and global CAAS (β=0.28, *P*=0.04), when adjusted for end-diastolic velocity of reverse flow and cardiac index (Table 5). After adjustment for SAC, only TVI of reverse flow (β=-0.05, *P*<0.01) remained significantly predictive of CAASR (Table 6).

b) Ascending aortic mechanics in AR vs. AS vs. healthy controls

Aortic mechanics (CAAS, corrected CAAS, and CAASR) differed significantly in AS, AR and in healthy control subjects (all *P*<0.01) (Figure 2). Because mean age also differed significantly among groups (AS, 77±10 years; AR, 72±10 years; controls, 53±17 years; *P*<0.01), age- and gender-matched analysis was conducted, with no change in outcome (*P*<0.01) (Supplemental Table 1).

The β1 (AS, 7.25±4.42; AR, 4.05±2.90; controls, 3.25±2.99) and β2 stiffness index (AS, 12.44±5.92; AR, 7.16±4.64; controls, 5.08±2.75) also differed significantly by group (*P*<0.01). Unlike vascular mechanics, SAC (*P*=0.99) and TVR (*P*=0.43) in all groups were similar.

c) Agreement and reproducibility

Waveforms adequate for measuring CAAS and CAASR were present in 778 (92.6%) of the 840 arterial segments evaluated. Results of intra-observer variability assessment were as follows: global CAAS, ICC=0.96 (95% CI, 0.84-0.99) and CoV=6.9%; global CAASR, ICC=0.96 (95% CI, 0.85-0.99) and CoV=7.4%. In assessing inter-observer variability, results were as follows: global CAAS, ICC=0.89 (95% CI, 0.60-0.98) and CoV=10.4%; global CAASR, ICC=0.90 (95% CI 0.64-0.98) and CoV=10.5%.

d) Follow up analysis

Data was available for all 118 patients with AVD, who were followed for a median period of 438 (IQR 386–539) days. During this time, global mortality was 16.1% and CV mortality was 10.2%. Global CAAS, corrected global CAAS, and global CAASR were significantly lower in all-cause or CV mortality subsets (Table 7).

A CAASR cutpoint of 0.88 s^{-1} showed 83.3% sensitivity and 73.5% specificity for estimating global mortality in patients with degenerative AVD during follow up (AU=0.79, 95%

CI: 0.66-0.93, *P*<0.01). Patients with a baseline global CAASR > 0.88 s^{-1} had a significant higher survival rate (97.4% vs 73.0%, long-rank *P*=0.03) (Fig. 3).

Discussion

Based on 2D-STE study, the following were demonstrated: (1) high feasibility and reproducibility of global CAAS and CAASR determinations in patients with moderate-to-severe AR; (2) significantly lower global CAASR, albeit not global CAAS, in patients with severe (vs moderate) AR; (3) independent associations between global CAAS and E/E' ratio and between global CAASR and TVI of reverse flow in patients with AR; (4) significant differences in aortic mechanics (CAAS, corrected CAAS, and CAASR) in AS, AR and in the control subjects; and (5) the clinical prognostic significance of aortic mechanics in degenerative AVD.

Moderate-to-severe AR

To the best of our knowledge, this is the first effort to examine the utility of quantifying ascending aortic mechanics by 2D-STE in patients with AR. In our prior report on patients with AS, SVI emerged as the most important determinant of CAAS,[7] whereas stiffness index β1 was strongly associated with CAASR,[16] suggesting that the rate of circumferential vascular deformation depends more on local arterial wall properties and is less influenced by systolic flow.

The concept that degenerative AVD alters arterial wall rigidity and compliance is also valid in the setting of AR. In patients with severe AR, higher vascular load and lower global CAASR were evident, likely reflecting more advanced arteriosclerosis. Wilson et al.[17] demonstrated that a decrease in distensibility of aorta imposes a higher afterload and may contribute to deterioration of chronic heart failure over time.

In instances of severe AR, higher SVI (due to increased regurgitant volume) is balanced by significant impairment of vascular elastic properties, perhaps explaining why global CAAS does not differ substantially by grade (moderate vs severe) of AR. The corrected CAAS, which includes also the PP, was significantly different in moderate vs. severe AR patients.

Comparing to the other aortic elastic proprieties analyzed (β1 and β2 stiffness index) which did not significantly differ by AR severity, CAASR and corrected CAAS seemed to be more sensitive parameters.

AR vs. AS vs. healthy controls

Aortic mechanics (CAAS, corrected CAAS and CAASR) derived from 2D-STE images differed significantly in AS, AR and healthy subjects, even after age and gender matching.

These parameters were lower in patients with AS, so in this context, elastic properties of aorta are seemingly altered to a significantly greater extent. The groups also differed significantly in β1 and β2 stiffness index, although not in terms of SAC and TVR, supporting the hypothesis that vascular differences are mainly localized.

In an investigation by Petrini et al.,[32] transesophageal echocardiography was performed in patients with isolated severe AS or AR, all prior to surgery in the operating room. Images of descending aorta were analyzed using software developed expressly for speckle-tracking imaging (VVI; Siemens Healthcare, Erlangen, Germany), thus enabling automatic frame-by-frame recording of area change, with VVI strain corresponding to maximal systolic circumferential strain. Strain was considerably higher in patients with AR than in those with AS, which corroborates our findings.

Clinical prognostic significance of aortic mechanics

In degenerative AS, it is acknowledged that LV afterload increases due not only to valvular obstruction but also to increased vascular load.[33] Reduction in arterial compliance as a consequence increased vascular stiffness then contributes to LV burden, culminating in adverse clinical events.[14] This relationship with vascular load has also been reported in the setting of AR, linking decreased distensibility with faster progression to surgery.[17]

According to our exploratory analysis, aortic mechanics seems to have a prognostic impact in patients with degenerative AVD. Lower values of global CAAS, corrected global CAAS, and global CAASR showed significant associations with higher global mortality and CV death, with lesser differences found for AVR and HF hospitalization endpoints. In long-term follow-up, a significant relationship between CAASR >0.88 s^{-1} and global mortality was also demonstrable.

Limitations

This was a single-center study, based on a relatively small patient sampling (N=140). Rather than monitoring central blood pressure, brachial pressures were recorded, which typically are overestimated. Furthermore, no invasive data on cardiac output, total systemic resistance, or systemic vascular compliance were available. Although age disparity among groups was potentially problematic, outcomes of age- and gender-matched subgroup analysis upheld our initial findings. The incremental value of 2D-STE aortic mechanics in AVD evaluation, in addition to conventional methods, was not assessed. Further studies should be designed to explore it.

Conclusions

In patients with AVD, use of 2D-STE to assess ascending aortic mechanics was feasible and proved highly reproducible. Global CAASR was significantly lower in patients with severe (vs moderate) AR, and measured parameters indicated significantly greater impairment of aortic elastic properties in patients with AS. The prognostic influence of ascending aortic mechanics in AVD was also demonstrable, underscoring the value of studying the vascular component with 2D-STE.

Acknowledgments:

The authors thank Ana Paula Oliveira BSc and Nélson Ribeiro BSc for their help during initial echocardiographic patient evaluations.

Legends

Table 1: Baseline information, risk factors, medication and systemic arterial hemodynamics of AR patients

Table 2: Aortic regurgitation etiology and severity, LV geometry and function, aortic diameters and elastic properties

Table 3: Circumferential ascending aortic strain and strain rate

Table 4: Correlations with global CAAS and global CAASR

Table 5: Linear regression model to predict global CAAS in AR

Table 6: Linear regression model to predict global CAASR in AR

Table 7: Follow-up data regarding ascending aortic mechanics

Figure 1: Assessment of ascending aorta mechanics via 2D-ST echocardiography generated from short axis view of aorta, 2–3 cm above aortic valve: quantitative curves representing all regions in a control subject *(A)*, in a patient with isolated AR *(B)* or isolated AS *(C)*. Peaks of CAAS (in proximity to aortic valvular closure) and CAASR (first peak after ventricular systole) both assume positive values due to expansion of vessel wall.

Figure 2: Ascending aorta mechanics in patients with AS, AR and in control subjects: comparisons by global CAAS *(A)*, corrected global CAAS *(B)* and global CAASR *(C).*

Figure 3: Patient survival in follow-up, stratified by global CAASR cutpoint (0.88 s^{-1}).

Table 1: Baseline information, risk factors, medication and systemic arterial hemodynamics of AR patients

	Total AR patients (n=73)	**Moderate AR (n=55)**	**Severe AR (n=18)**	***P***
Age (years)	71.5 ± 9.5	71.9 ± 9.7	70.2 ± 9.0	0.48
Male gender (%)	42 (57.5)	30 (54.5)	12 (66.7)	0.37
BMI (kg/m^2)	26.3 ± 3.4	26.4 ± 3.4	25.8 ± 3.4	0.47
Cardiovascular risk factors and medical conditions:				
- Hypertension (%)	57 (78.1)	13 (76.4)	15 (83.3)	0.75
- Diabetes (%)	13 (17.8)	11 (20.0)	2 (11.1)	0.50
- Dyslipidemia (%)	47 (64.4)	38 (69.1)	9 (50.0)	0.14
- Smoker (%)	2 (2.7)	2 (3.6)	0 (0.0)	0.56
- Ex-smoker (%)	5 (6.8)	3 (5.5)	2 (11.1)	0.59
- Chronic kidney disease (%)	13 (17.8)	9 (16.4)	4 (22.2)	0.72
- Previous MI (%)	9 (4.1)	8 (14.5)	1 (5.6)	0.44
- Previous stroke (%)	3 (4.1)	2 (3.6)	1 (5.6)	0.58
- Current CHF admission (%)	7 (9.6)	3 (5.5)	4 (22.2)	0.06
NYHA class				
- Class I (%)	44 (60.3)	36 (65.5)	8 (44.4)	
- Class II (%)	22 (30.1)	16 (29.1)	6 (33.3)	0.08
- Class III (%)	7 (9.6)	3 (5.5)	4 (22.2)	
- Class IV (%)	0 (0.0)	0 (0.0)	0 (0.0)	
Current medication:				
- ACE inhibitor (%)	33 (45.2)	26 (47.3)	7 (38.9)	0.54
- ARB (%)	26 (35.6)	17 (30.9)	9 (50.0)	0.14
- MRA (%)	5 (6.8)	4 (7.3)	1 (5.6)	0.64
- CCB (%)	14 (19.2)	11 (20.0)	3 (16.7)	0.53
- Beta-blockers (%)	30 (41.1)	21 (38.2)	9 (50.0)	0.38
- Diuretics (%)	43 (58.9)	29 (52.7)	14 (77.8)	0.10
- Statin (%)	35 (47.9)	27 (49.1)	8 (44.4)	0.73
Systemic arterial hemodynamics:				
- Systolic arterial pressure (mmHg)	138.1 ± 16.9	137.6 ± 16.2	139.4 ± 18.2	0.72
- Diastolic arterial pressure (mmHg)	72.6 ± 14.2	76.0 ± 12.3	62.1 ± 15.1	<0.01
- Pulse pressure (mmHg)	65.5 ± 18.8	61.7 ± 15.1	77.3 ± 24.0	<0.01
- Heart rate (bpm)	67.8 ± 13.7	68.9 ± 14.8	64.2 ± 8.9	0.21
- Systemic arterial compliance (mL mmHg^{-1} m^{-2})	0.68 ± 0.30	0.67 ± 0.30	0.71 ± 0.29	0.66
- Total vascular resistance (mmHg min L^{-1})	1748.2 ± 640.3	1868.9 ± 651.5	1351.7 ± 413.0	<0.01

Table 2: Aortic regurgitation etiology and severity, LV geometry and function, aortic diameters and elastic properties

	Total AR patients (n=73)	Moderate AR (n=55)	Severe AR (n=18)	*P*
AR etiology:				
- Degenerative (%)	14 (19.2)	10 (18.2)	4 (22.2)	0.15
- Bicuspid aortic valve (%)	2 (2.7)	1 (1.8)	1 (5.6)	
- Cusp rupture (%)	1 (1.4)	0 (0.0)	1 (5.6)	
- Aortic root pathology (%)	13 (17.8)	8 (14.5)	5 (27.8)	
- Unclear mechanism (%)	43 (58.9)	36 (65.5)	7 (38.9)	
AR severity:				
- Vena contracta width (mm)	5.0 ± 1.6	4.3 ± 0.7	7.3 ± 1.3	<0.01
- EROA (mm^2)	28.2 ± 15.5	20.3 ± 7.1	39.9 ± 17.5	<0.01
- R Vol (mL)	61.5 ± 38.8	39.8 ± 15.0	92.4 ± 41.7	<0.01
- End-diastolic velocity of the reversal flow (cm/s)	11.0 ± 7.3	9.4 ± 7.2	14.9 ± 6.0	<0.01
- TVI of the reversal flow (cm)	13.8 ± 5.6	12.3 ± 4.5	17.4 ± 6.4	<0.01
- Ratio of reversal to forward TVI	1.2 ± 0.6	1.1 ± 0.6	1.4 ± 0.7	0.16
- PTH of CW Doppler AR jet (ms)	435.6 ± 141.3	471.0 ± 129.8	285.1 ± 73.6	<0.01
LV assessment:				
- LV diastolic dimension (mm)	57.8 ± 7.9	56.3 ± 7.5	62.4 ± 7.7	<0.01
- LV systolic dimension (mm)	39.7 ± 9.1	38.6 ± 9.0	42.9 ± 8.8	0.09
- LV EDV indexed (mL/m^2)	76.8 ± 28.0	72.1 ± 35.5	91.0 ± 31.3	0.01
- LV ESV indexed (mL/m^2)	35.0 ± 21.9	32.6 ± 21.5	42.1 ± 22.4	0.11
- LVEF biplane (%)	56.2 ± 11.6	56.3 ± 12.1	55.8 ± 10.3	0.87
- LV mass indexed (g/m^2)	72.7 ± 20.2	68.7 ± 18.7	83.7 ± 20.8	0.01
- Stroke volume index (mL/m^2)	42.0 ± 14.9	39.2 ± 14.1	51.1 ± 14.2	<0.01
- Cardiac index ($L/min/m^2$)	2.8 ± 1.1	2.7 ± 1.2	3.2 ± 1.0	0.11
- E/E' ratio	11.9 ± 5.3	12.2 ± 5.5	10.5 ± 4.5	0.30
LA volume indexed (mL/m^2)	39.0 ± 17.1	38.1 ± 17.0	41.8 ± 17.6	0.44
Valvulo-arterial impedance ($mmHg\ mL^{-1}\ m^{-2}$)	3.9 ± 1.4	4.1 ± 1.5	3.1 ± 1.0	<0.01
Aortic diameters:				
- Valve annulus (mm)	34.9 ± 4.9	34.8 ± 4.5	35.5 ± 6.1	0.62
- Aortic sinus (mm)	36.8 ± 5.6	36.4 ± 5.3	38.3 ± 6.3	0.25
- Sinotubular junction (mm)	34.8 ± 5.7	34.5 ± 5.7	36.0 ± 6.0	0.33
- Proximal ascending aorta (mm)	39.4 ± 5.9	39.0 ± 5.6	40.5 ± 6.7	0.40
Aortic elastic properties:				
- Stiffness index β1	4.1 ± 7.3	3.9 ± 7.7	4.6 ± 5.9	0.66
- Stiffness index β2	7.2 ± 4.6	6.8 ± 4.6	8.3 ± 4.8	0.24

AR, aortic regurgitation; EROA, effective regurgitant orifice area; R Vol, regurgitant volume; TVI, tissue velocity index; PTH, pressure half-time; CW, continuous wave; LV, left ventricle; EDV, end-diastolic volume; ESV, end-systolic volume; LVEF, left ventricular ejection fraction; LA, left atrium

Table 3: Circumferential ascending aortic strain and strain rate

	Total AR patients (n=73)	**Moderate AR (n=55)**	**Severe AR (n=18)**	***P***
Global CAAS (%)	10.81 ± 3.95	10.91 ± 4.22	10.50 ± 3.10	0.72
Corrected global CAAS (%/mmHg)	0.17 ± 0.08	0.19 ± 0.08	0.14 ± 0.06	<0.05
Global CAASR (s^{-1})	1.81 ± 0.58	1.90 ± 0.62	1.53 ± 0.29	<0.05

AR, aortic regurgitation; CAAS, circumferential ascending aorta strain; CAASR, circumferential ascending aorta strain rate

Table 4: Correlations with global CAAS and global CAASR

Variables	**Global CAAS**		**Global CAASR**	
	r	**P value**	**r**	**P value**
Age (years)	0.79	0.54	0.11	0.42
Systemic arterial hemodynamics:				
- Systolic arterial pressure (mmHg)	-0.01	0.93	0.03	0.83
- Systemic arterial compliance (mL $mmHg^{-1}$ m^{-2})	-0.10	0.49	-0.17	0.25
- Total vascular resistance (mmHg min L^{-1})	-0.02	0.92	0.11	0.45
AR severity:				
- Vena contracta width (mm)	-0.15	0.26	-0.35	<0.01
- End-diastolic velocity of the reversal flow (cm/s)	-0.18	0.20	-0.24	0.10
- TVI of the reversal flow (cm)	0.03	0.81	-0.44	<0.01
LV assessment:				
- LVEF biplane (%)	0.12	0.34	-0.04	0.79
- Cardiac index (L/min/m^2)	0.23	0.10	-0.07	0.64
- E/E' ratio	0.16	0.25	-0.03	0.86
Aortic elastic properties:				
- Stiffness index β1	0.01	0.99	-0.08	0.56

Table 5: Linear regression model to predict global CAAS in AR

Variables	β	T value	P value
E/E' ratio	0.28	2.01	0.04
End-diastolic velocity of the reversal flow (cm/s)	-0.11	-1.56	0.13
Cardiac index (L/min/m^2)	0.80	1.75	0.09

B_0 = 7.3 (P<0.01); F 3.0 (p<0.05); R^2 = 0.23.

Table 6: Linear regression model to predict global CAASR in AR

Variables	β	T value	P value
TVI of the reversal flow (mm)	-0.05	-2.29	<0.01
Systemic arterial compliance (mL $mmHg^{-1}$ m^{-2})	-0.43	-1.86	0.07

B_0 = 2.7 (P<0.01); F 5.7 (P<0.01); R^2 = 0.26.

Table 7: Follow-up data regarding ascending aortic mechanics

	Global CAAS (%)	**Corrected global CAAS** (%/mmHg)	**Global CAASR** (s^{-1})
Global mortality			
- Yes (n=19)	6.99 ± 4.05	0.11 ± 0.06	0.86 ± 0.50
- No (n=99)	9.30 ± 4.15	0.16 ± 0.08	1.45 ± 0.70
- P value	0.03	0.04	<0.01
Cardiovascular mortality			
- Yes (n=12)	6.45 ± 3.38	0.09 ± 0.04	0.77 ± 0.44
- No (n=106)	9.23 ± 4.21	0.15 ± 0.08	1.42 ± 0.70
- P value	0.03	0.02	<0.01
Aortic valve replacement			
- Yes (n=17)	7.70 ± 3.55	0.14 ± 0.08	0.99 ± 0.45
- No (n=101)	9.13 ± 4.29	0.15 ± 0.08	1.41 ± 0.73
- P value	0.21	0.52	0.03
Heart failure hospitalization			
- Yes (n=19)	6.93 ± 3.72	0.13 ± 0.09	1.08 ± 0.72
- No (n=99)	9.34 ± 4.20	0.15 ± 0.08	1.40 ± 0.69
- P value	0.02	0.33	0.06
Combined endpoint			
- Yes (n=29)	7.21 ± 3.87	0.12 ± 0.08	1.08 ± 0.66
- No (n=89)	9.52 ± 4.17	0.16 ± 0.08	1.44 ± 0.70
- P value	0.01	0.08	0.02

Figure 1

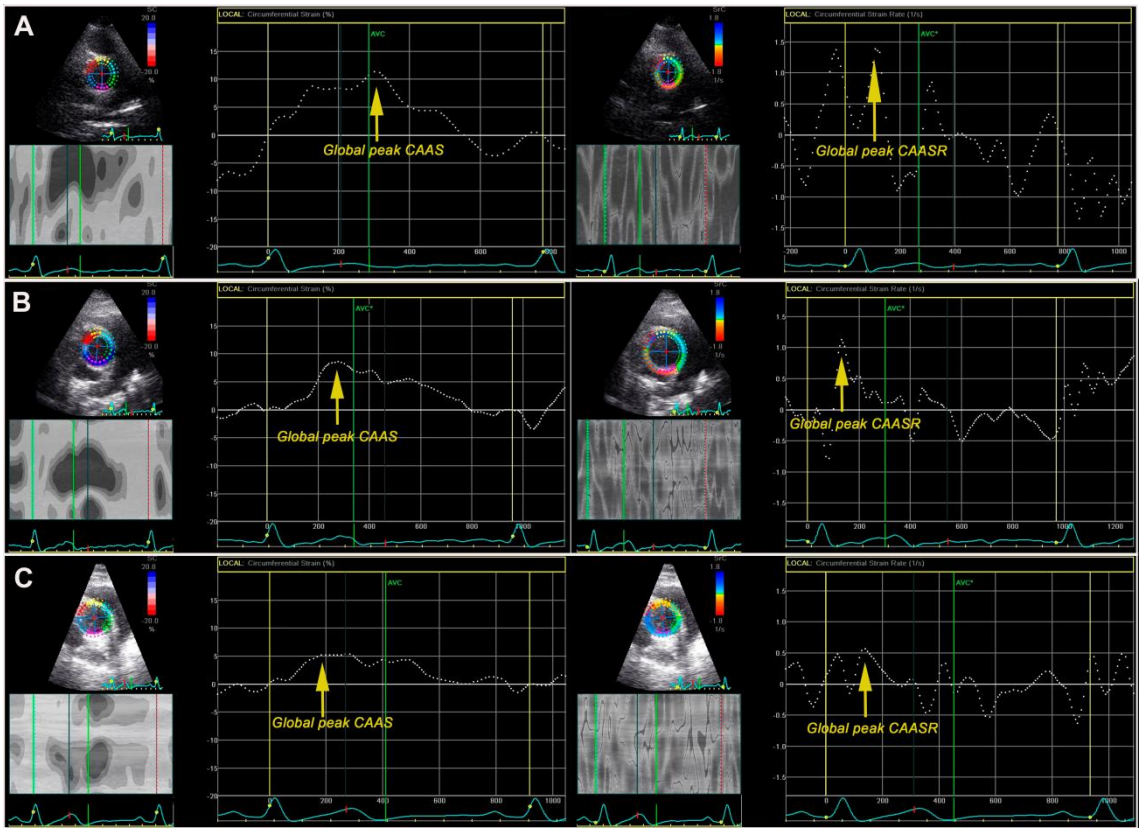
A
Global peak CAAS
Global peak CAASR
B
Global peak CAAS
Global peak CAASR
C
Global peak CAAS
Global peak CAASR

Figure 2

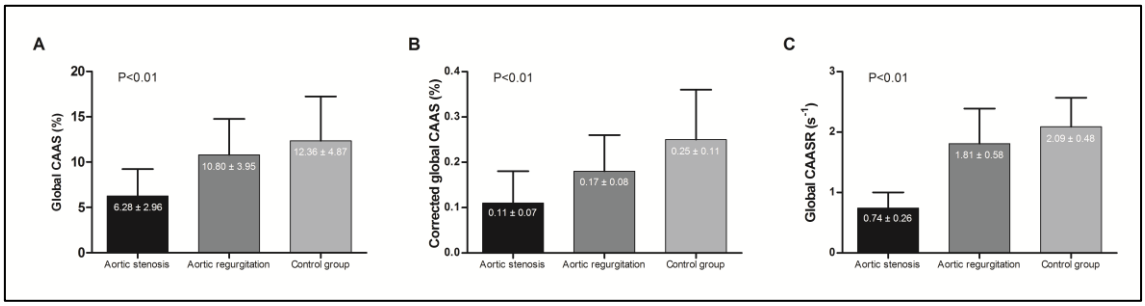

Figure 3

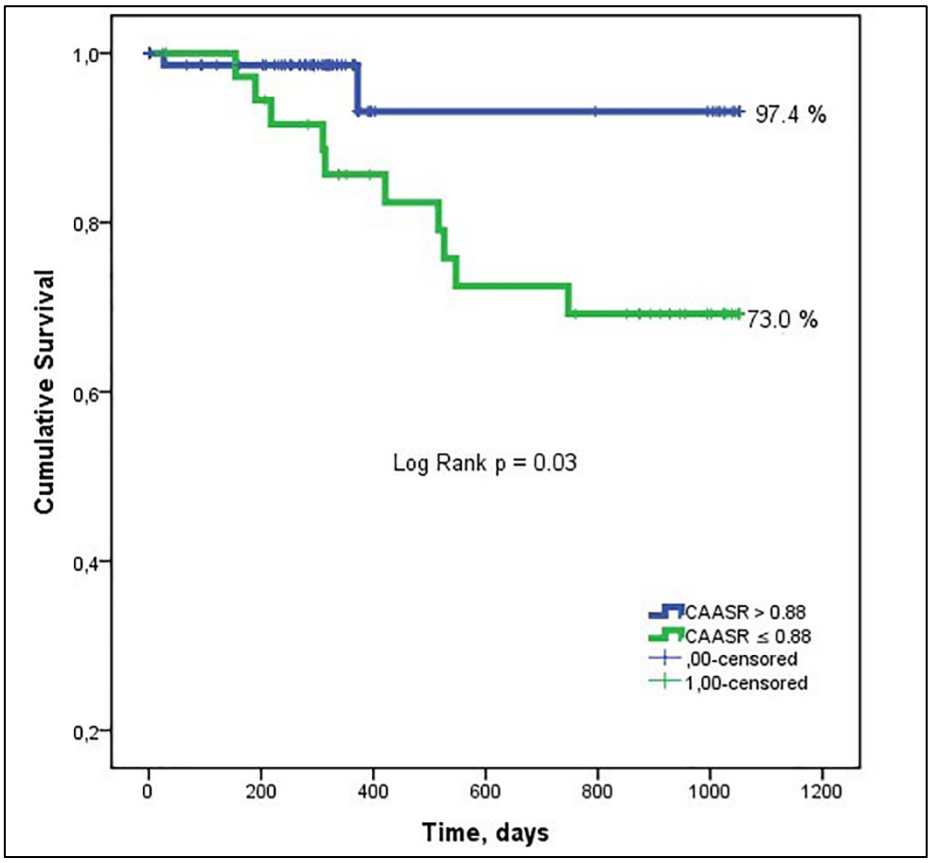

References

1. Iung B, Baron G, Butchart EG, et al: A prospective survey of patients with valvular heart disease in Europe: The Euro Heart Survey on Valvular Heart Disease. Eur. Heart J. 2003:24(13):1231–43.
2. Nkomo VT, Gardin JM, Skelton TN, et al: Burden of valvular heart diseases: a population-based study. Lancet. 2006:368(9540):1005–11.
3. Leibowitz D, Stessman J, Jacobs JM, et al: Prevalence and prognosis of aortic valve disease in subjects older than 85 years of age. Am. J. Cardiol. 2013:112(3):395–9.
4. Mor-Avi V, Lang RM, Badano LP, et al: Current and evolving echocardiographic techniques for the quantitative evaluation of cardiac mechanics: ASE/EAE consensus statement on methodology and indications endorsed by the Japanese Society of Echocardiography. Eur. J. Echocardiogr. 2011:12(3):167–205.
5. Oishi Y, Mizuguchi Y, Miyoshi H, et al: A novel approach to assess aortic stiffness related to changes in aging using a two-dimensional strain imaging. Echocardiography. 2008:25(9):941–5.
6. Teixeira R, Vieira MJ, Gonçalves A, et al: Ultrasonographic vascular mechanics to assess arterial stiffness: a review. Eur. Heart J. Cardiovasc. Imaging. 2015: doi:10.1093/ehjci/jev287
7. Teixeira R, Moreira N, Baptista R, et al: Circumferential ascending aortic strain and aortic stenosis. Eur. Heart J. Cardiovasc. Imaging. 2013:14(7):631–41.
8. Kim KH, Park JC, Yoon HJ, et al: Usefulness of aortic strain analysis by velocity vector imaging as a new echocardiographic measure of arterial stiffness. J. Am. Soc. Echocardiogr. 2009:22(12):1382–8.
9. Teixeira R, Monteiro R, Garcia J, et al: Feasibility of aortic arch mechanics; a study in normal subjects. Eur. Heart J. Cardiovasc. Imaging. 2014:15:ii9–ii12.
10. Bjällmark A, Lind B, Peolsson M, et al: Ultrasonographic strain imaging is superior to conventional non-invasive measures of vascular stiffness in the detection of age-dependent differences in the mechanical properties of the common carotid artery. Eur. J. Echocardiogr. 2010:11(7):630–6.
11. Larsson M, Verbrugghe P, Smoljkić M, et al: Strain assessment in the carotid artery wall using ultrasound speckle tracking: validation in a sheep model. Phys. Med. Biol. 2015:60(3):1107–23.
12. Larsson M, Heyde B, Kremer F, et al: Ultrasound speckle tracking for radial, longitudinal and circumferential strain estimation of the carotid artery--an in vitro validation via sonomicrometry using clinical and high-frequency ultrasound. Ultrasonics. 2015:56:399–408.
13. Kim S-A, Lee KH, Won H-Y, et al: Quantitative assessment of aortic elasticity with aging using velocity-vector imaging and its histologic correlation. Arterioscler. Thromb. Vasc. Biol. 2013:33(6):1306–12.
14. Briand M, Dumesnil JG, Kadem L, et al: Reduced systemic arterial compliance impacts significantly on left ventricular afterload and function in aortic stenosis: implications for diagnosis and treatment. J. Am. Coll. Cardiol. 2005:46(2):291–8.
15. Pibarot P, Dumesnil JG: Assessment of aortic stenosis severity: check the valve but don't forget the arteries! Heart. 2007:93(7):780–2.
16. Teixeira R, Monteiro R, Baptista R, et al: Circumferential vascular strain rate to estimate vascular load in aortic stenosis: a speckle tracking echocardiography study. Int. J. Cardiovasc. Imaging. 2015:31(4):681-9.
17. Wilson RA, McDonald RW, Bristow JD, et al: Correlates of aortic distensibility in chronic aortic regurgitation and relation to progression to surgery. J. Am. Coll. Cardiol. 1992:19(4):733–8.
18. Lancellotti P, Tribouilloy C, Hagendorff A, et al: European Association of Echocardiography recommendations for the assessment of valvular regurgitation. Part 1: aortic and pulmonary regurgitation (native valve disease). Eur. J. Echocardiogr. 2010:11(3):223–44.
19. Zoghbi WA, Enriquez-Sarano M, Foster E, et al: Recommendations for evaluation of the severity of native valvular regurgitation with two-dimensional and Doppler echocardiography. J. Am. Soc. Echocardiogr. 2003:16(7):777–802.
20. Dubois D, Dubois E: A formula to estimate the approximate surface area if height and weight are known. Arch Inter Med. 1916:17:863–871.
21. Keys A, Fidanza F, Karvonen MJ, et al: Indices of relative weight and obesity. J. Chronic Dis. 1972:25(6):329–43.
22. McMurray JJ V, Adamopoulos S, Anker SD, et al: ESC Guidelines for the diagnosis and treatment of acute and chronic heart failure 2012: The Task Force for the Diagnosis and Treatment of Acute and Chronic Heart Failure 2012 of the European Society of Cardiology. Developed in collaboration with the Heart. Eur. Heart J. 2012:33(14):1787–847.

23. Kadem L, Dumesnil JG, Rieu R, et al: Impact of systemic hypertension on the assessment of aortic stenosis. Heart. 2005:91(3):354–61.

24. Evangelista A, Flachskampf F, Lancellotti P, et al: European Association of Echocardiography recommendations for standardization of performance, digital storage and reporting of echocardiographic studies. Eur. J. Echocardiogr. 2008:9(4):438–48.

25. Lang RM, Badano LP, Mor-Avi V, et al: Recommendations for Cardiac Chamber Quantification by Echocardiography in Adults: An Update from the American Society of Echocardiography and the European Association of Cardiovascular Imaging. J. Am. Soc. Echocardiogr. 2015:28(1):1–39.e14.

26. Dubin J, Wallerson DC, Cody RJ, et al: Comparative accuracy of Doppler echocardiographic methods for clinical stroke volume determination. Am. Heart J. 1990:120(1):116–23.

27. Ommen SR, Nishimura RA, Appleton CP, et al: Clinical utility of Doppler echocardiography and tissue Doppler imaging in the estimation of left ventricular filling pressures: A comparative simultaneous Doppler-catheterization study. Circulation. 2000:102(15):1788–94.

28. Stefanadis C, Stratos C, Boudoulas H, et al: Distensibility of the ascending aorta: comparison of invasive and non-invasive techniques in healthy men and in men with coronary artery disease. Eur. Heart J. 1990:11(11):990–6.

29. Catalano M, Lamberti-Castronuovo A, Catalano A, et al: Two-dimensional speckle-tracking strain imaging in the assessment of mechanical properties of carotid arteries: feasibility and comparison with conventional markers of subclinical atherosclerosis. Eur. J. Echocardiogr. 2011:12(7):528–35.

30. Yuda S, Kaneko R, Muranaka A, et al: Quantitative measurement of circumferential carotid arterial strain by two-dimensional speckle tracking imaging in healthy subjects. Echocardiography. 2011:28(8):899–906.

31. Shrout PE, Fleiss JL: Intraclass correlations: uses in assessing rater reliability. Psychol. Bull. 1979:86(2):420–8.

32. Petrini J, Jenner J, Rickenlund A, et al: Elastic properties of the descending aorta in patients with a bicuspid or tricuspid aortic valve and aortic valvular disease. J. Am. Soc. Echocardiogr. 2014:27(4):393–404.

33. Pibarot P, Dumesnil JG: Improving assessment of aortic stenosis. J. Am. Coll. Cardiol. 2012:60(3):169–80.

Supplement number 8

Original Article: The Relationship Between Tricuspid Regurgitation Severity And Right Atrial Mechanics: A Speckle Tracking Echocardiography Study

Original Article

The relationship between tricuspid regurgitation severity and right atrial mechanics: A speckle tracking echocardiography study

Int J Cardiovasc Imaging. 2015 Aug; 31(6): 1125-35.

Rogério Teixeira*[1,2,4] MD, Ricardo Monteiro[3] BSc, João Garcia[1] BSc, Rui Baptista[2,4] MD, Miguel Ribeiro[1] MD, Nuno Cardim[5] MD, PhD, FESC Lino Gonçalves [2,6] MD, PhD, FESC

*****Corresponding author

[1] Departamento de Medicina, Serviço de Cardiologia, Hospital Beatriz Ângelo, Loures, Portugal;

[2] Faculdade de Medicina, Universidade de Coimbra, Coimbra, Portugal;

[3] Hertfordshire Cardiac Centre, Lister Hospital, Stevenage, United Kingdom;

[4] Serviço de Cardiologia, Centro Hospitalar e Universitário de Coimbra, Coimbra, Portugal;

[5] Serviço de Cardiologia, Hospital da Luz, Lisboa, Portugal;

[6] Serviço de Cardiologia, Centro Hospitalar e Universitário de Coimbra – Hospital Geral, Coimbra, Portugal;

Total word count: 3857

*****

Abstract

Purpose: The aim at this study was to assess the influence of the tricuspid regurgitation volume (TRvol) in right atrium (RA) reservoir phase myocardial mechanics **Methodology:** We included 55 heart failure (HF) patients referred for transthoracic echocardiography during a 2-month period. 18 had HF with a reduced ejection fraction (HFREF) and 37 HF with a preserved ejection fraction (HFPEF). TR was chronic and functional. TRvol was calculated according to the PISA method. This study of RA used 2D-speckle tracking echocardiography to measure strain ($r\varepsilon_R$) and strain rate (rSR_R). The reference frame coincided with the onset of the QRS. RA stiffness was assessed as the ratio: (rE/e') / $r\varepsilon_R$ **Results:** The median age of the sample was 78 (64 – 84) years, with female gender predominance (63.6%). The median value of $r\varepsilon_R$ was 16% (range, 12.7 – 24.0) and of rSR_R was 1.57 s^{-1} (range, 1.09 – 2.05). We observed a significant negative correlation between $r\varepsilon_R$ ($r=-0.68$, $p<0.01$) and rSR_R ($r=-0.58$, $p<0.01$) and TRvol. RA mechanics decreased significantly with an increase in the TR grade. We created two multivariate linear regression models for $r\varepsilon_R$ and rSR_R, separately for the patients with sinus rhythm or atrial fibrillation. The TRvol was independently associated with $r\varepsilon_R$ after adjusting to the RA area, right ventricular (RV) longitudinal systolic function and the estimated pulmonary vascular resistance. We demonstrated an increase in RA stiffness with an increase in TR severity, and an association for functional status (NYHA class) and RA compliance. The HFREF group had a significantly lower $r\varepsilon_R$ and rSR_R that the HFPEF patients. **Conclusions:** According to our study, in HF patients, a chronic volume overload state significantly reduced the RA reservoir phase mechanics.

Key words: Right Atrium; Echocardiography; Speckle Tracking; Mechanics; Strain; Strain Rate; Tricuspid Regurgitation; Compliance; Stiffness; heart failure

Introduction

The right atrium (RA) has an important role to modulate right ventricular (RV) filling, accomplished by three basic functions: reservoir, conduit, and booster pump phases [1]. In the presence of tricuspid regurgitation (TR) static and dynamic RA volumes are increased. Besides, the atrial performance is significantly modified, as seminal studies with an impedance catheter demonstrated a shift from the figure of eight loop to a single clockwise loop, consistent with a ventricularization of the RA[2].

Echocardiographic parameters such as two and three dimensional measurements and Doppler flow assessment have proved to be useful to study the atrial performance, but they have a number of limitations such as foreshortening, lack of gold standard measurement of atrial function, difficulties with the echocardiographic window and with the timing of various atrial events[3].

Two-dimensional speckle tracking echocardiography (2D-STE) revolutionized cardiovascular imaging in the past decade. The methodology is based on standard B-mode images to track the motion of speckles over time and to measure lengthening and shortening relative to the baseline – Lagrangian[1]. This enables angle-independent assessment of myocardial mechanics, from which displacement, velocity, strain (Ɛ) and strain rate (SR) can be derived [4]′ [5].

Myocardial mechanics have been used to study primarily left ventricular (LV) performance, but since 2007 they have been applied to analyze thin wall structures, such as the left atrium (LA) [6] in different clinical settings [7]′[8]′[9]. Subsequently, the analysis of right atrium (RA) mechanics using 2D-STE proved feasible [10], and normal references values have recently been published [11]′[12]. Myocardial atrial mechanics are significantly influenced by atrial phasic volume changes [13]. During the reservoir atrial phase, both atrial Ɛ and SR increases and reach a peak value, just before atrio-ventricular valve opening, reflecting passive RA filling. In this context, the influence of a chronic volume overload on RA mechanics, such as TR, has not been analyzed. Therefore, the primary aim of this study was to assess the influence of the tricuspid regurgitation volume (TRvol) on the RA reservoir phase myocardial mechanics in patients with heart failure (HF).

Methods

Study Population

A total of 81 consecutive patients referred for echocardiography due to HF were enrolled in a 2-month study, between May and June 2013. Patients had optimal apical and parasternal views allowing precise quantification of TR and the study of myocardial mechanics.

Eleven patients were excluded due to moderate to severe left sided valve disease, 7 due to clinical instability and 3 for trivial TR. Moreover, 5 patients were excluded due to poor quality speckle tracking images, yielding 55 patients for the final sample. It was possible to calculate the TR volume (TRvol) according to the proximal isovelocity surface area (PISA) method and subsequently to assess RA mechanics in all patients. The TR was functional (secondary) and chronic in all patients.

We included as a control group, 15 subjects with no or trivial TR (no PISA). These subjects were referred to an echocardiogram due to suspected HF but no significant structural cardiac abnormalities were recorded, such as left ventricular systolic dysfunction, moderate to severe atrial enlargement, moderate to severe left sided valvular heart disease, and pulmonary hypertension. All controls were in sinus rhythm.

Clinical Data

Clinical data included age, weight, height and prior history of acute myocardial infarction, stroke, diabetes, hypertension, atrial fibrillation, coronary revascularization, NYHA classification and current admission for congestive HF.

Heart failure diagnosis was performed according to recent guidelines, based on symptoms, signs and evidence of cardiac structural abnormalities. HF with reduced ejection fraction (HFREF) patients had an LVEF < 50%. HF with preserved ejection fraction (HFPEF) had an LVEF > 50%, and evidence of LV hypertrophy, LA enlargement or diastolic dysfunction[14].

Systemic arterial pressure was measured using an arm cuff sphygmomanometer (right brachial artery). Informed consent was obtained from all patients. The local ethics committee approved the protocol (reference number HBA-0059).

Echocardiography

Echocardiography was performed using a Vivid 7 ultrasound scanner (GE Healthcare®, Horten, Norway) and a 1.7 / 3.4 MHz tissue harmonics transducer. A complete echocardiographic study was performed using standard views according to established guidelines, and data was digitally recorded for off-line analysis [15]. The study used a modified apical four-chamber view optimized for the right ventricle (RV) and the RA[16].

Three consecutive heart cycles were acquired during breath holding with stable ECG tracings, to minimize respiratory movements and obtain images suitable for RA size quantification and 2D-STE analysis for sinus rhythm patients. For AF patients, five consecutive heart cycles were acquired. The grayscale second-harmonic 2D imaging technique was used,

and the image contrast, frequency, depth and sector size were adjusted to achieve adequate frame rates and optimize the RA border visualization.

Two-dimensional and Doppler echocardiographic variables

Right and left chamber dimensions and function

The RA diastolic area (RADA), the RA systolic area (RASA) and the inlet RV dimensions were assessed from a modified apical 4-chamber view. Basal linear measurements and systolic and diastolic RV areas were obtained. From these areas, we calculated the RV fractional area change according to recent guidelines [16]. From the subcostal view, we measured the RV free wall thickness and inferior vena cava (IVC) dimensions [16]. Patients were in the supine position, and measurements were performed during expiration and maximal inspiration, avoiding Valsalva like maneuvers. The IVC collapsibility index (IVCCI) was calculated as: (IVC_{max} – IVC_{min}) / IVC_{max}[17]. We calculated the RA maximum (RA V_{max}) prior to tricuspid valve opening, and minimum (RA V_{min}) volume, immediately after tricuspid valve closure, according to the area-length method. Then we calculated the RA emptying fraction (RAEF) as (RA V_{max} - RA V_{min})/ RA $V_{max[18]}$.

The longitudinal RV function was also assessed from a 4-chamber view with the tricuspid annular plane systolic excursion (TAPSE)[19] method. Using Doppler tissue imaging with an apical 4-chamber view, we analyzed the RV basal lateral systolic (RV S') peak velocity [20]. We used the right-sided E/e' ratio (rE/e') to estimate RV filling pressures [21].

The left ventricular ejection fraction (LVEF) was assessed in all patients using the Simpson method [18]. The left ventricular (LV) cardiac index was calculated as the product of the heart rate and the stroke volume indexed for body surface area (BSA). Stroke volume was obtained using the LV outflow Doppler method, the product of the LV outflow area and the LV time-velocity integral (TVI)[22]. LV mass was calculated according to the Devereux's formula [18]. The LV filling pressure was estimated from the left side E/e' (e' was an average of septal and lateral walls in tissue Doppler imaging) ratio[23].

Tricuspid regurgitation assessment

Tricuspid regurgitation was assessed using color-flow Doppler, with the anterograde velocity of the tricuspid inflow and the hepatic vein flow pattern, according to recent guidelines[24]. Although only a limited number of studies have validated the methodology, we quantified TR according to the flow convergence method. The radius of the PISA was obtained from an apical 4 –chamber view, tricuspid zoomed, systolic frame during end-expiratory apnea. As functional TR is dynamic through the cardiac cycle, with early and late systolic peaks,

we used the systolic frame with the maximum radius of the PISA. Afterwards, we calculated the TR effective regurgitant orifice (TERO) and the tricuspid regurgitant volume (TRVol) as previously described[24].

In agreement with the European guidelines [24], TR severity was classified in three groups (mild, moderate and severe), based on the PISA radius (mild TR ≤ 5mm; moderate TR 6 – 9mm; severe TR >9 mm). We have also performed an integrative approach of the TR severity that included qualitative, semi-quantitative and quantitative variables, which corroborated the TR severity stratification. Two observers graded TR. Discordant cases were solved by consensus.

Right ventricular hemodynamics – pulmonary circulation assessment

The pulmonary artery systolic pressure (PASP) was estimated according to the formula: 4 x V^2 + RA pressure (RAP), where V is the TR jet peak velocity (TRJPV)[25]. The RAP was estimated from the IVC diameter and respiratory changes, following recent guidelines[16].

The pulmonary vascular resistance (PVR) was estimated according to the formula: (TR peak velocity / RVOT TVI) x 10 + 0.16[26].

Two-dimensional speckle tracking echocardiography

The 2D-STE methodology was used to calculate the regional and global longitudinal RA reservoir Ɛ ($r\varepsilon_R$) and SR (rSR_R). Modified apical 4-chamber views images, obtained using conventional echocardiography, were used for this analysis. The images were acquired with a breath hold of 3 seconds, with a stable electrocardiography recording. Three consecutive heart cycles were recorded and averaged for sinus rhythm and 5 cycles for AF patients. The frame rate was >60 frames per second.

The tracking process and conversion to Lagrangian strains were performed offline using dedicated software (EchoPAQ 9.0, GE Healthcare®, Horten, Norway). A line was manually drawn along the inner side of the RA wall. The software then automatically generated additional lines within a 15 mm wide region of interest (ROI). The shape and width of the ROI were manually adjusted. A cine loop preview feature allowed visual confirmation that the internal line followed the RA endocardium movements throughout the cardiac cycle. If the tracking of the RA endocardium was unsatisfactory, the ROI was adjusted manually to ensure optimal tracking. As previously reported,[10,12] we also divided the RA wall into 6 equidistant regions, with similar sizes. In each region, numeric values for each 2D-STE variable represented the mean values calculated from all the points in the segment. These were color-coded and presented as a function of time throughout the cardiac cycle. Quantitative curves representing

all regions could be expressed for each 2D-STE variable. Because we included patients with AF and sinus rhythm (SR), we used the first RV systolic frame as the frame of interest – QRS timed analysis.

Analyses were performed for peak $r\varepsilon_R$ in percentages and for rSR_R in s^{-1}. For each, a global value was calculated, defined as the mean of the peak values of the six RA wall segments (Figure 1). As previously reported for the LA, we estimated the RA stiffness index (RASI) as the ratio of the rE/e' and $r\varepsilon_R$ [27]. RA mechanics analysis were performed by two authors (RM and JG), who were blinded to standard echocardiographic data.

We subsequently divided our study population in two groups, based on the median value (0.35) of the RASI.

We have also analyzed the RV global longitudinal mechanics with the 2D-ST. We calculated a mean value of 6 myocardial segments, from an apical 4-chamber, RV focused view [1].

Inter and intraobserver variability

Intraobserver and interobserver variability of $r\varepsilon_R$ and rSR_R were assessed with the Bland Altman method[28] (Supplemental Figure 1), interclass correlation coefficient (ICC)[29] and with the mean percentage error.

Eleven patients were randomly selected, 6 were in AF and 5 in sinus rhythm. For the AF patients the RA mechanics were averaged over 5 cardiac cycles, and for the sinus rhythm for 3 cardiac cycles.

The measurements were repeated after 1 month by the same operator to measure intraobserver reproducibility. Interobserver reproducibility was assessed by having a second operator repeat the measurements. Observers selected the best cardiac cycles and had to create a new ROI by themselves. They were blinded to previous measurements."

We also assessed the interobserver variability of TRvol with the same methodology.

Statistics

The Kolomogorov-Smirnov test was used to evaluate the distribution of the continuous variables. Both $r\text{Ɛ}_R$ and rSR_R were not normally distributed. According to their distribution, continuous data are presented as mean and standard deviation (SD) or as median and interquartile (IQ) range. Groups were compared using the Student's t-test or the ANOVA, for normal distributed variables and using the Mann-Whitney or the Kruskal-Wallis for non-normal variables.

Categorical variables are reported as frequencies and percentages, and the chi-square or the Fisher exact tests were used when appropriate.

A post-hoc power analysis was performed. Based on the data collected, the sample had a power of 99% to identify a significant correlation between the TRvol and $r\text{Ɛ}_R$.

The Spearman correlation coefficient was used to analyze the associations between $r\text{Ɛ}_R$ and rSR_R and a number of continuous variables. Afterwards, a linear regression analysis was performed for $Ln(r\text{Ɛ}_R)$ and for $Ln(rSR_R)$. Variables that were significant in the bivariate analysis, such as the RASA, TRVol, PVR, and RV S' were included in the multivariate models. For the dependent variables $Ln(r\text{Ɛ}_R)$ and $Ln(rSR_R)$, we created two separate multivariate linear regression models, one for the AF patients and the other for patients with sinus rhythm.

For $r\text{Ɛ}_R$, rSR_R and TRvol Bland Altman plots were derived to identify possible bias (mean divergence) and the limits of agreement (2 standard deviation of the divergence). ICC was calculated for testing measurement variability. The mean percentage error was calculated as the absolute difference between two sets of observations divided by the mean of the observations: $|X_1 - X_2| / \text{mean}\ (X_1 - X_2) \times 100$.

A two-tailed p value <0.05 was considered statistically significant. Data analyses and calculations were performed with SPSS®15, Medcalc®12.1.4, G-Power®3.13 and GraphPad Prism® 6.05.

Results

The median age of the sample was 78 (64 – 84) years, with female gender predominance (63.6%).

Right atrial reservoir strain

For the 55 patients, $r\varepsilon_R$ had a median value of 16.0%, with an interquartile range of 12.7 to 24.0%. The $r\varepsilon_R$ was not influenced by age, gender, BSA or blood pressure. We observed a negative correlation of $r\varepsilon_R$ with right chamber dimensions, such as the RADA (r=-0.51, p<0.01), RASA (r=-0.65, p<0.01), and the RV diastolic diameter. RAEF correlated positively with $r\varepsilon_R$ (r=0.54, p<0.01). TR related variables, such as TRvol (r=-0.68, p<0.01) and TERO were significantly associated with $r\varepsilon_R$. Finally, $r\varepsilon_R$ correlated negatively with PASP and with the estimated PVR (Table 1).

Intraobserver variability of $r\varepsilon_R$ was 0.01 % (95% confidence interval [CI]: -1.29; 1.32%) (Supplemental figure 1, panel A). The ICC of $r\varepsilon_R$ for intraobserver variability was 0.98 (95% CI: 0.96;0.99) and the mean error was 5.2%. Interobserver variability of $r\varepsilon_R$ was -0.1 % (95% CI: -3.30, 3.10%) (Supplemental figure 1, panel B). The ICC was 0.92(95% CI: 0.74 – 0.98) and the mean error was 9.9%.

We fit two multivariate linear regression models to estimate $Ln(r\varepsilon_R)$, either for the AF patients or for the patients with sinus rhythm. In both models, we included the following variables: RASA, TRV, RV S', and the estimated PVR. For the AF patients, only TRvol (β -0.64; p<0.01) was independently associated with $Ln(r\varepsilon_R)$. For the patients with sinus rhythm, in addition to TRvol (β -0.43; p<0.01), both RV S' (β 0.41; p=0.02) and RASA (β -0.36; p=0.02) were found to be independently associated with $Ln(r\varepsilon_R)$ (Table 2).

Right atrial reservoir strain rate

In the study sample, the median rSR_R was 1.6 s^{-1}, with an interquartile range from 1.1 to 2.1 s^{-1}. Similar to $r\varepsilon_R$, there was a negative correlation between rSR_R and the RA dimensions, RAEF, RV longitudinal systolic function and the IVC diameter. A positive correlation was observed between the IVC collapsibility index and rSR_R (r=0.54, p<0.01). In addition, we found important associations between rSR_R and TRvol (r=-0.58, p<0.01), TERO and PVR (r=-0.61, p<0.01) (Table 1).

Intraobserver variability of rSR_R was -0.02 s^{-1} (95% CI: -0.24; 0.19 s^{-1}) (supplemental figure 1, panel C). The ICC of rSR_R for intra-observer variability was 0.90 (95% CI: 0.68; 0.97) and the mean error was 7.3%. Interobserver variability of $r\varepsilon_R$ was -0.03 s^{-1} (95% CI: -0.28; 021 s^{-}

^{1}) (Supplemental figure 1, panel D). The ICC was 0.88 (95% CI: 0.63 – 0.97) and the mean error was 8.5%.

Using multivariate analysis, we found that in the sinus rhythm patients only the RV S' wave (β 0.41, p<0.01) was independently associated with Ln(rSR_R) in a model adjusted for RA dimensions, estimated PVR and TRvol – Table 3.

Right atrium stiffness

The RASI (rE/e' / $r\varepsilon_R$) correlated positively with the RA dimensions, TRvol (r=0.56, p<0.01); PASP and estimated PVR (r=0.53, p<0.01). In contrast, the stiffness index was negatively correlated with the IVC collapsibility index, LVEF and RV S' (r=-0.65, p<0.01) (Table 2).

A history of HRREF was more frequent in patients with a higher RASI (>0.35). These patients also had higher right sided chamber dimensions, a lower RV systolic performance, and more severe TR – Table 4. A higher NYHA class was also associated with the group of patients with a RASI >0.35. Moreover, these patients had both a higher PASP and estimated PRV – Figure 2 Panels A and B.

Tricuspid regurgitation severity

We noted that $r\varepsilon_R$ decreased significantly across TR severity groups (mild TR: 22.9 [17.0 – 26.9]; moderate TR: 15.4 [12.9 – 17.2]; severe TR patients 9.6 [7.7 – 10.7]%, p<0.01). A similar decrease was noted for rSR_R (mild TR: 1.9 [1.5 – 2.5]; moderate TR: 1.6 [1.2 – 1.9]; severe TR patients 1.0 [0.8 – 1.1]s^{-1}, p<0.01) – Figure 3 Panel A and B respectively.

Contrary, we observed a significant increase in RA stiffness with a grading severity in TR (mild TR: 0.18 [0.13 – 0.29]; moderate TR: 0.38 [0.23 – 0.47]; severe TR: 0.66 [0.41 – 0.89]; p< 0.01 – Figure 3 Panel C.

Our control group had a median age of 67 (62 – 73) years, male gender predominance and no or trivial TR – Supplemental Table 1. The RA reservoir mechanics were significantly higher, and the RASI was significantly lower than the mild TR group patients – Figure 3, Panels A-C.

There were no significant differences regarding RV myocardial mechanics, but the difference between $r\varepsilon_R$ and |RV ε| was lower for the severe TR patients – Supplemental Figure 2.

Regarding interobserver variability of TRvol: bias was 1.5 ml (95% CI: -4.6; 7.6 ml); the ICC was 0.97 (95% CI: 0.88; 0.99) and the mean error was 9.6%.

Heart Failure with preserved versus reduced ejection fraction

From our sample 37 patients had HFPEF and 18 HFRF. Groups were similar regarding age, and AF prevalence. HFREF was more frequently associated with male gender and with a current admission for HF. As expected HFPEF patients had smaller LVs and a higher LVEF (58.3±4.1 vs 36.4±12.2%, $p<0.01$). Groups were balanced regarding RA dimensions, but HFREF patients had a higher TRvol and PASP. RA reservoir phase mechanics ($r\varepsilon_R$, rSR_R) were significantly lower for the HFREF patients (Table 5).

Discussion

Our findings demonstrate the following: (i) RA reservoir phase mechanics decreased significantly with an increase in TRvol; (ii) TRvol was independently associated with $r\varepsilon_R$ for both the AF and sinus rhythm patients; (iii) an increase in RA stiffness (non-invasively assessed with 2D-ST) was observed with an increase in TR severity;

Tricuspid regurgitation

It is well established that atrial reservoir phase ε is significantly influenced by phasic volume changes [13]. Previous studies have shown significant negative correlations between LA ε during the reservoir phase and mitral regurgitation (MR). Cameli *et al.* demonstrated that asymptomatic mild MR patients had a higher LA ε_R than the control group, supporting the important contribution of volume changes to positively influence LA mechanics during the reservoir phase[7]. Contrarily, same study proved that LA ε_R was reduced for moderate and severe asymptomatic MR patients, when compared to controls[7]. We believe our data agrees with the study from Cameli *et al.*, because we demonstrated a progressive reduction in the RA mechanics values as the grade of TR severity increased. On the contrary, our mild TR patients had lower values of RA mechanics than our control group. We note that we could not match our control group for all the variables that influenced the RA reservoir phase mechanics such as the rhythm, RV longitudinal function and RA chamber dimensions.

Chronic atrial volume overload leads not only to chamber enlargement but also to chronic inflammatory changes, cellular hypertrophy, decrease metalloproteinase expression and interstitial fibrosis[30]. It has been demonstrated that LA ε_R correlated significantly with the extent of LA wall fibrosis assessed by cardiac magnetic resonance imaging[31] and with LA interstitial fibrosis in patients with mitral valve disease[32] in pathological specimens. This means that LA ε_R reflects not only phasic volume changes, but also ultrastructural changes of the myocardium, supporting its use to evaluate chamber stiffness and compliance.

The ratio of the LV filling pressures (invasive and non-invasively estimated) to the LA ε_R was proven to be an accurate index to distinguish diastolic HF patients from those with asymptomatic diastolic dysfunction [27]. A recent publication with data invasively obtained and a larger sample size, demonstrated that for the same LA pressure, HFPEF patients had a smaller LA volume but a higher LA stiffness, than HFREF patients [33]. In our study, the RASI (our surrogate marker of RA stiffness) was significantly higher for HF patients than controls, and we identified an association of a higher RASI with a higher NYHA functional class.

Right atrium mechanics

The investigation of RA mechanics with 2D-STE has been previously performed by several authors. The first report was published by D'Andrea *et al.* [10] in a cohort of HF patients submitted to cardiac resynchronization therapy. Subsequently, normal values for RA $r\mathcal{E}_R$ and rSR_R in the adult population were published either using a P-wave [11] or a QRS [12] timed analysis, all supporting the feasibility of the assessment. Recently, normal values and maturational changes have also been published for the pediatric population[34].

Padeletti *et al.* demonstrated a significantly correlation of RA mechanics with invasive hemodynamic data [35]. In 40 advanced HF patients from a cardiac transplantation program underwenting right heart catheterization, significant negative correlations between $r\mathcal{E}_R$ and systolic (r=-0.81) and mean (r=-0.80) pulmonary pressures and PVR (r=-0.61) were observed [35]; these findings were similar to the associations that we observed non-invasively.

Besides the influence of TRvol, our data also supported the influence of AF and RV systolic longitudinal function in RA phase mechanics. The hypothesis that RA reservoir mechanics reflect ultrastructural changes of the myocardium is probably common to many pathological conditions, such as AF, TV disease, increased PVR, and RV systolic dysfunction; we believe that our data also corroborate these cumulative ultrastructural abnormalities in the reservoir phase RA mechanical indexes. Future studies to address the usefulness of RA reservoir phase mechanics to assess prognosis in different clinical settings must take in consideration these covariates.

Limitations

We note that our conclusions were based on a single centre study, with a small number of patients. Our patients were older and had a diagnosis of HF, and almost half had AF, which made it difficult to find a complete matched control group with no or trivial TR. All of these findings could limit extrapolating of our results more widely.

We have included patients in AF, and for that we do not report the atrial boost pump function mechanics. Moreover, we do not report data on the conduit phase atrial mechanics because the curves were noisy, and the results were not consistent.

The PISA method to quantify TR has been validated in a small number of studies and it could underestimate the severity of the regurgitation. To study RA mechanics, we used software that was developed for LV analysis because dedicated software for RA analysis has not been released. Due to the cross-sectional design of our study, it was not possible to evaluate the prognostic implications of RA mechanics.

We did not perform any invasive hemodynamic measurement. This seems particularly important for the assessment of the RA compliance / stiffness, as the index we used (the RASI) is not yet invasively validated.

Conclusions

According to our study, in HF patients, a chronic volume overload state significantly reduced the RA reservoir phase mechanics. The underlying rhythm, chamber dimensions, and RV function also modulated the RA reservoir phase mechanical indexes.

Acknowledgments

The authors thank Solange Fernandes, BSc and Susana Pinto, BSc for their help in the echocardiographic evaluation of the patients.

Conflict of interest: The authors have no conflicts of interest.

Funding: none

Contributions for the manuscript:

RT conceptualized the research, analyzed the data and wrote the manuscript. RM performed the strain analysis and JG performed the strain rate analysis. RM elaborated the database. RT and MAR supervised the standard and advanced echocardiographic measurements. RB, NC and LG actively discussed the results, interpreted the data and reviewed the draft manuscript. RT elaborated the revised manuscript. All the authors have read and approved the manuscript version submitted.

Legends

Table 1: Correlations of right atrial reservoir phase mechanics and right atrial stiffness index

Table 2: Multivariate linear regression model to estimate $r\varepsilon_R$

Table 3: Multivariate linear regression model to estimate rSR_R

Table 4: Compliant RA (RASI ≤ 0.35) versus stiff RA (RASI > 0.35) patients

Table 5: HFPEF vs HFREF patients

Supplemental Table 1: Comparison of the Controls vs the HF patients

Figure 1: RA mechanics and TR – examples.

Panels A-C: Mild TR patient with a TRvol of 9.3 ml, a $r\varepsilon_R$ of 44.2% and a rSR_R of 2.7 s^{-1}

Panels D-E: Moderate TR patient with a TRvol of 21.7 ml, a $r\varepsilon_R$ of 12.6% and a rSR_R of 1.0 s^{-1}

Panels G-I: Severe TR patient with a TRvol of 44.2 ml, a $r\varepsilon_R$ of 9.2% and a rSR_R of 0.89 s^{-1}

Figure 2:

Panel A: Pulmonary systolic artery pressure for lower and higher RASI patients.

Panel B: Estimated pulmonary vascular resistance for lower and higher RASI patients.

Figure 3:

Panel A: Median and interquartile range of $r\varepsilon_R$ for mild (n=23), moderate (n=20), severe (n=12) TR patients and controls (n=15). Controls $r\varepsilon_R$ 31.7 (23.7 – 44.0); Mild TR: $r\varepsilon_R$ 22.9 (17.0 – 26.9); Moderate TR: $r\varepsilon_R$ 15.4 (12.9 – 17.2); Severe TR: $r\varepsilon_R$ 9.6 (7.7 – 10.7)%. P value for Mild vs Moderate vs Severe TR group comparisons < 0.01. P value for controls vs Mild TR patients = 0.02.

Panel B: Median and interquartile range of rSR_R for mild (n=23), moderate (n=20), severe (n=12) TR patients and controls (n=15). Controls rSR_R: 2.5 (2.1 – 2.9) s^{-1}; Mild TR: rSR_R 1.9 (1.5 – 2.5) s^{-1}; Moderate TR: rSR_R 1.6 (1.2 – 1.9) s^{-1}; Severe TR: rSR_R 1.0 (0.8 – 1.1) s^{-1}. P value for Mild vs Moderate vs Severe TR group comparisons < 0.01. P value for controls vs Mild TR patients = 0.03.

Panel C: Median and interquartile range of RA stiffness index for mild (n=23), moderate (n=20) severe (n=12) TR patients and controls (n=15). Controls: 0.14(0.11 – 0.21); Mild TR: 0.18 (0.13 – 0.29); Moderate TR: 0.38 (0.23 – 0.47); Severe TR: rSR_R 0.66 (0.41 – 0.89). P value for Mild vs Moderate vs Severe TR group comparisons < 0.01. P value for controls vs Mild TR patients = 0.049.

Supplemental Figure 1: Bland-Altman plot of inter and intra-observer variability.

Panel A: Intraobserver variability for $r\varepsilon_R$. The bias was 0.01%, with a 95% CI: -1.29 to 1.34%.

Panel B: Interobserver variability for $r\varepsilon_R$. The bias was -0.1% with a 95% CI: -3.3 to 3.1%.

Panel C: Intraobserver variability for rSR_R. The bias was -0.02 s^{-1} with a 95% CI: -0.24 to 0.19 s^{-1}.

Panel D: Interobserver variability for rSR_R The bias was -0.03 s^{-1} with a 95% CI: -0.28 to 0.21 s^{-1}.

Supplemental Figure 2:

Panel A: Median and interquartile range of RV systolic ε for mild (n=23), moderate (n=20) and severe (n=12) TR patients.

Panel B: Median and interquartile range of RV systolic SR for mild (n=23), moderate (n=20) and severe (n=12) TR patients.

Panel C: Median and interquartile range of (RA reservoir ε – RV systolic SR) for mild (n=23), moderate (n=20) and severe (n=12) TR patients.

Table 1: Correlations of right atrial reservoir phase mechanics and right atrial stiffness index

	$r\varepsilon_R$ (%)		rSR_R (s^{-1})		RASI	
Variables	***r***	***P***	***r***	***P***	***r***	***P***
Age (years)	-0.17	0.23	0.02	0.91	0.01	0.95
Heart rate (bpm)	-0.15	0.26	-0.27	0.04	0.28	0.04
RADA (cm^2)	-0.51	<0.01	-0.40	<0.01	0.30	0.24
RASA (cm^2)	-0.65	<0.01	-0.55	<0.01	0.46	<0.01
RAEF (%)	0.54	<0.01	0.59	<0.01	-0.42	<0.01
IVC collapsibility (%)	0.56	<0.01	0.54	<0.01	-0.45	<0.01
RV fraction area exchange (%)	0.18	0.20	0.24	0.08	-0.29	0.03
TAPSE (mm)	0.53	<0.01	0.63	<0.01	-0.63	<0.01
RV S' (cm/s)	0.60	<0.01	0.60	<0.01	-0.65	<0.01
rE/e'	-0.46	<0.01	-0.43	<0.01	-	
PASP (mmHg)	-0.34	0.01	-0.28	0.04	0.42	<0.01
PVR (W)	-0.50	<0.01	-0.61	<0.01	0.53	<0.01
TRvol(ml)	-0.68	<0.01	-0.58	<0.01	0.59	<0.01
TERO (mm^2)	-0.61	<0.01	-0.53	<0.01	0.48	<0.01

IVC – inferior vena cava; LA – left atrial; LV – left ventricular; LVEF – left ventricular ejection fraction; LVEDV – LV end-diastolic volume; LVESV – LV end-systolic volume; LAVI – left atrial volume index; PASP – pulmonary artery systolic pressure; PVR – pulmonary vascular resistance; RA – right atrial; RADA – RA end-diastolic area; RASA – RA end-systolic area; RASI – RA stiffness index; RAEF – RA emptying fraction; RVDD – RV end-diastolic diameter 4c; RVOT – right ventricular outflow tract; RVOT_SE: right ventricular outflow tract systolic excursion; RVFAE – RV fraction area exchange; $r\varepsilon_R$ – right atrial peak strain reservoir strain; rSR_R – right atrial peak strain rate reservoir phase; SVI – stroke volume index; TAPSE – tricuspid annular plane systolic excursion; TERO – tricuspid effective regurgitant orifice; TR – tricuspid regurgitation; TRV – tricuspid regurgitant volume; TRJV – tricuspid regurgitant jet velocity.

Table 2: Multivariate linear regression model to predict Ln($r\varepsilon_R$)

For atrial fibrillation patients (n=30)			
Variables	**Beta**	***T***	***P***
RASA (cm^2)	-0.06	-0.29	0.77
TRvol (ml)	-0.64	-3.19	<0.01
RV S' (cm/s)	0.15	1.01	0.32
PVR (W)	-0.15	-1.00	0.33
F= 10.3 (P<0.01); R^2=0.63			
For sinus rhythm patients (n=25)			
Variables	**Beta**	***T***	***P***
RASA (cm^2)	-0.36	-2.60	0.02
TRvol (ml)	-0.43	-3.79	<0.01
RV S' (cm/s)	0.41	3.51	0.02
PVR (W)	-0.08	-0.58	0.57
F= 18.1 (P<0.01); R^2=0.78			

PVR – pulmonary vascular resistance; RASA – RA end-systolic area; $r\varepsilon_R$ – right atrial peak strain reservoir phase; RV – right ventricle; TRvol – tricuspid regurgitant volume

Table 3: Multivariate linear regression model to predict Ln(rSR_R)

For atrial fibrillation patients (n=30)			
Variables	**Beta**	***T***	***P***
RASA (cm^2)	-0.10	-0.39	0.70
TRvol (ml)	-0.33	-1.31	0.20
RV S' (cm/s)	0.29	1.67	0.11
PVR (W)	-0.19	-1.02	0.32
F= 4.5 (P<0.01); R^2 0.42			
For sinus rhythm patients (n=25)			
Variables	**Beta**	***T***	***P***
RASA (cm^2)	-0.30	-1.95	0.07
TRvol(ml)	-0.23	-1.87	0.08
RV S' (cm/s)	0.41	3.20	<0.01
PVR (W)	-0.27	-1.74	0.10
F= 13.8 (P<0.01); R^2=0.73			

PVR – pulmonary vascular resistance; RASA – RA end-systolic area; rSR_R – right atrial peak strain rate reservoir phase; RV – right ventricle; TRvol – tricuspid regurgitant volume

Table 4: Compliant RA (RASI ≤ 0.35) versus stiff RA (RASI > 0.35) patients

	RA stiffnex index ≤ 0.35	**RA stiffnex index > 0.35**	***P***
Age (years)	78 (64 – 83)	79 (71 – 85)	0.56
Male gender (%)	6/28 (21.4)	14/27 (51.9)	0.02
NYHA class	1 (1 – 2)	2 (2 – 3)	<0.01
Diabetes (%)	5/28 (17.9)	9/27 (33.3)	0.19
Heart failure reduced EF (%)	4/28 (14.3)	14/27 (51.9)	<0.01
Current heart failure admission (%)	8/28 (28.6)	24/27 (88.9)	<0.01
Systemic arterial hemodynamics			
Systolic arterial pressure (mmHg)	139±25	124±19	0.02
Diastolic arterial pressure (mmHg)	66±10	73±12	0.01
Heart rate (bpm)	77±13	70±13	0.04
Atrial fibrillation (%)	12/28 (42.9)	18/27 (66.7)	0.08
Standard echocardiographic data			
RADA (cm^2)	22.8±4.6	28.6±9.3	<0.01
RASA (cm^2)	16.6±5.6	23.8±8.5	<0.01
RAEF (%)	46.7±20.0	30.7±15.3	<0.01
RVDD (mm)	4.0 (3.7 – 4.4)	4.9 (4.4 – 5.1)	<0.01
IVC collapsability (%)	43.8±18.7	22.5±18.9	<0.01
TAPSE (mm)	20.0 (17.0 – 25.4)	15.0 (12.0 – 17.0)	<0.01
RV S' (cm/s)	12.1±3.3	8.7±2.1	<0.01
TRvol (ml)	21.7±8.3	34.7±13.9	<0.01
PVR (W)	1.9 (1.6 – 2.4)	2.9 (2.2 – 3.7)	<0.01
PASP (mmHg)	32.5 (31.0 – 37.6)	49.0 (40.0 – 68.0)	<0.01
LAVI (ml/m^2)	49.5±17.2	54.1±21.7	0.39
LVEF (%)	56.1±9.2	45.6±14.4	0.02
Stroke volume index (ml/m^2)	62.2±21.4	54.7±13.9	0.13
Cardiac index ($ml/min\ m^2$)	2.4±0.8	2.3±0.5	0.39

HFREF – heart failure with reduced ejection fraction; HFPEF – heart failure with preserved ejection fraction; LAVI – left atrial volume index; LV – left ventricle; LVEF – left ventricular ejection fraction; LVEDV – LV end-diastolic volume; LVESV – LV end-systolic volume; MI – myocardial infarction; PASP – pulmonary artery systolic pressure; RA – right atrial; RADA – RA end-diastolic area; RASA – RA end-systolic area; RAEF – right atrium emptying fraction; $r\varepsilon_R$ – right atrial peak strain reservoir strain; rSR_R – right atrial peak strain rate reservoir phase; TAPSE – tricuspid annulus plane systolic excursion; TRvol – tricuspid regurgitant volume.

Table 5: HFPEF vs HFREF patients

	HFPEF (n=37)	**HFREF (n=18)**	***P***
Age (years)	80 (64 – 85)	75 (66 – 83)	0.43
Male gender (%)	9/37 (24.3)	11/18 (61.1)	<0.01
NYHA class	1.7±0.8	2.3±0.8	0.02
Risk factors and concomitant diseases, %			
Diabetes (%)	12/37 (34.2)	2/18 (11.1)	0.09
Hypertension (%)	28/37 (75.7)	15/18 (83.3)	0.52
Previous myocardial infarction (%)	3/37 (8.1)	8/18 (44.4)	<0.01
Current heart failure admission (%)	15/37 (40.5)	17/18 (94.4)	<0.01
Systemic arterial hemodynamics			
Systolic arterial pressure (mmHg)	139±23	118±18	<0.01
Diastolic arterial pressure (mmHg)	71±12	67±10	0.32
Heart rate (bpm)	70±12	80±13	<0.01
Atrial fibrillation (%)	22/37 (59.5)	8/18 (44.4)	0.29
Standard echocardiographic data			
RADA (cm^2)	26.0±7.9	20.3±8.5	0.66
RASA (cm^2)	20.0±7.9	20.3±8.5	0.93
RAEF (%)	41.0±21.1	35.0±15.4	0.26
LVEDV (ml/m^2)	81.0 (67.5 – 92.8)	121.0 (97.5 – 155.5)	<0.01
LVESV (ml/m^2)	32.5 (26.5 – 40.8)	76.0 (58.3 – 112.8)	<0.01
LV mass index (g/m^2)	91.2±22.7	112.7±26.7	<0.01
LAVI (ml/m^2)	52.6±22.0	50.1±13.6	0.66
LVEF (%)	58.3±4.1	36.4±12.2	<0.01
TAPSE (mm)	17.0 (15.0 – 22.5)	15.0 (12.0 – 20.0)	0.08
Stroke volume index (ml/m^2)	35.1±11.1	27.9±5.4	0.02
Cardiac index ($ml/min\ m^2$)	2.4±0.7	2.2±0.5	0.19
TRvol (ml)	25.9±12.4	32.5±13.5	0.08
PASP (mmHg)	35.0 (31.5 – 48.5)	49.5 (40.0 – 53.3)	0.04
RA reservoir phase mechanics			
$r\varepsilon_R$ (%)	16.8 (13.6 – 26.0)	14.1 (10.1 – 17.1)	<0.01
rSR_R (s^{-1})	1.8 (1.3 – 2.4)	1.1 (1.0 – 1.6)	<0.01
RA stiffness index	0.28 (0.16 – 0.43)	0.42 (0.33 – 0.79)	<0.01

HFREF – heart failure with reduced ejection fraction; HFPEF – heart failure with preserved ejection fraction; LAVI – left atrial volume index; LV – left ventricle; LVEF – left ventricular ejection fraction; LVEDV – LV end-diastolic volume; LVESV – LV end-systolic volume; MI – myocardial infarction; PASP – pulmonary artery systolic pressure; RA – right atrial; RADA – RA end-diastolic area; RASA – RA end-systolic area; RAEF – right atrium emptying fraction; $r\varepsilon_R$ – right atrial peak strain reservoir strain; rSR_R – right atrial peak strain rate reservoir phase; TAPSE – tricuspid annulus plane systolic excursion; TRvol – tricuspid regurgitant volume.

Supplemental Table 1: Comparison of the Controls vs the HF patients

	Controls (N=15)	HF patients (N=55)	P value
Age, years	67 (62 – 73)	78 (64 – 84)	0.10
Male Gender (%)	12/15 (80)	20/55 (36.4)	<0.01
Body surface area, m^2	1.8±0.2	1.8±0.2	0.89
Atrial fibrillation (%)	0/15 (0)	30/55 (54.5)	<0.01
RADA, cm^2	15.6±3.8	25.6±7.8	<0.01
RVDD, cm	3.5 (3.4 – 4.1)	4.4 (4.0 – 5.0)	<0.01
RV S' , cm/s	12.7±1.7	10.4±3.2	0.01
$r\varepsilon_R$, %	31.8 (23.1 – 44.0)	16.2 (12.6 – 24.2)	<0.01
rSR_R , s^{-1}	2.5 (2.1 – 2.9)	1.6 (1.1 – 2.0)	<0.01
RA stiffness index	0.14 (0.11 – 0.21)	0.35 (0.17 – 0.49)	<0.01

Figure 1

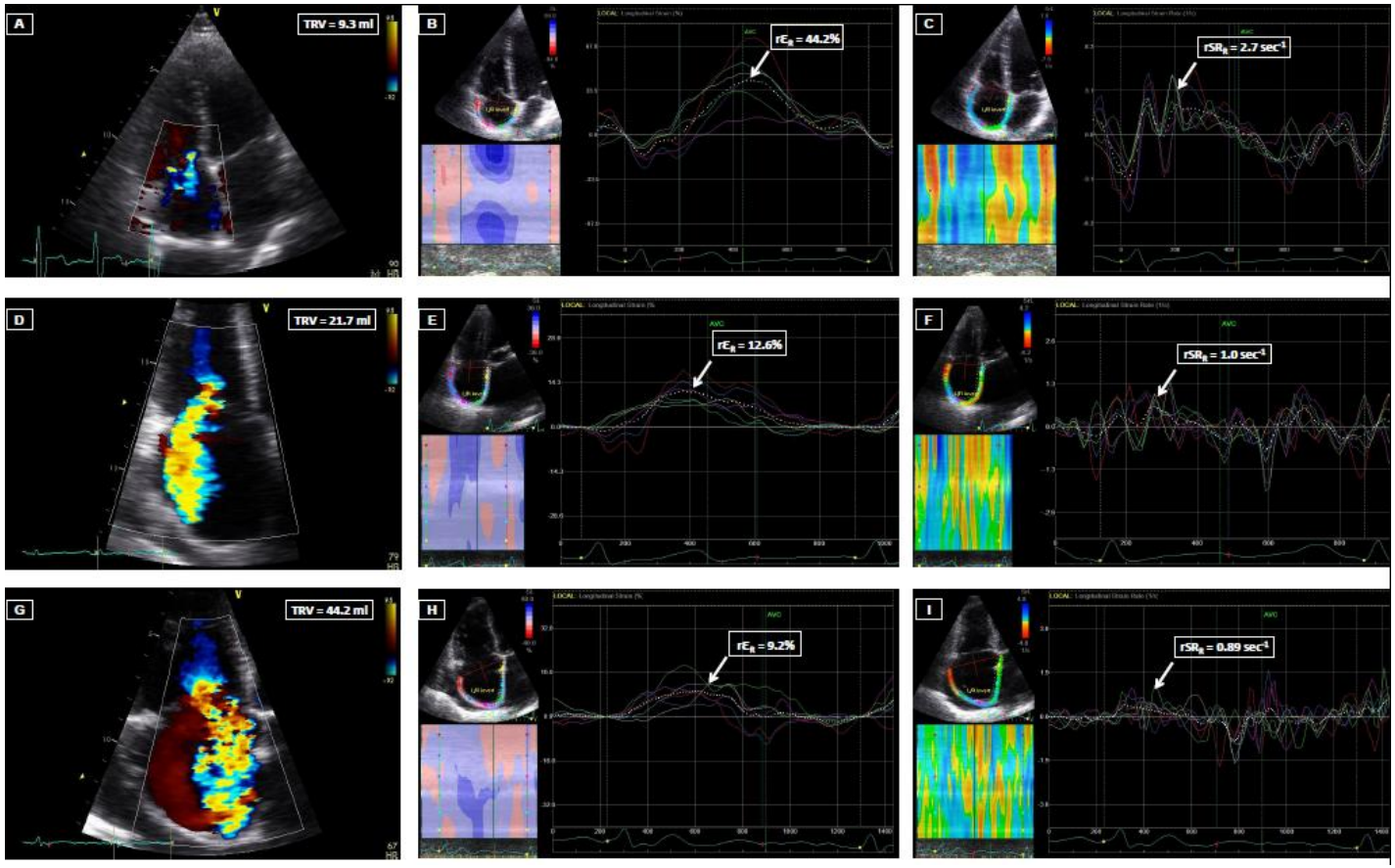
A
TRV = 9.3 ml
B
rE$_R$ = 44.2%
C
rSR$_R$ = 2.7 sec^{-1}
D
TRV = 21.7 ml
E
rE$_R$ = 12.6%
F
rSR$_R$ = 1.0 sec^{-1}
G
TRV = 44.2 ml
H
rE$_R$ = 9.2%
I
rSR$_R$ = 0.89 sec^{-1}

Figure 2 Panel A

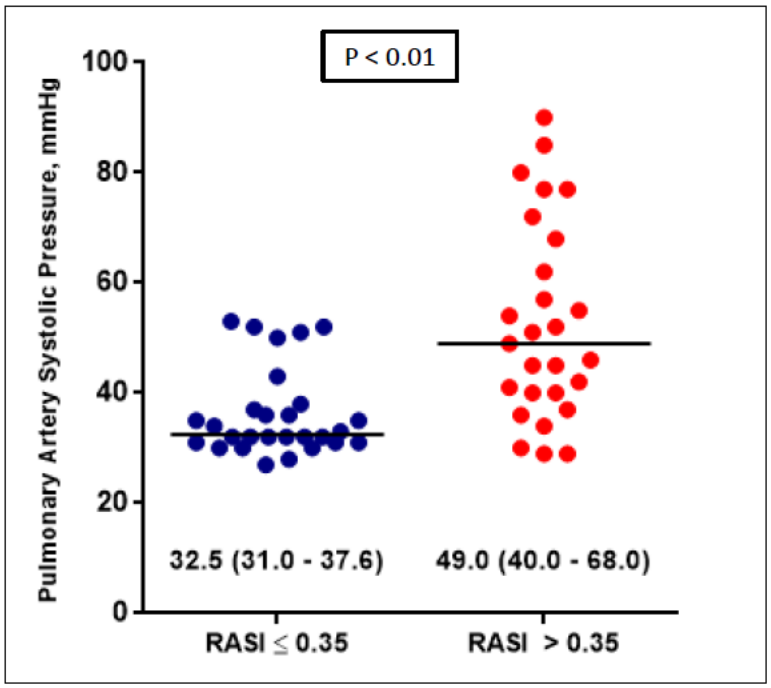

Figure 2 Panel B

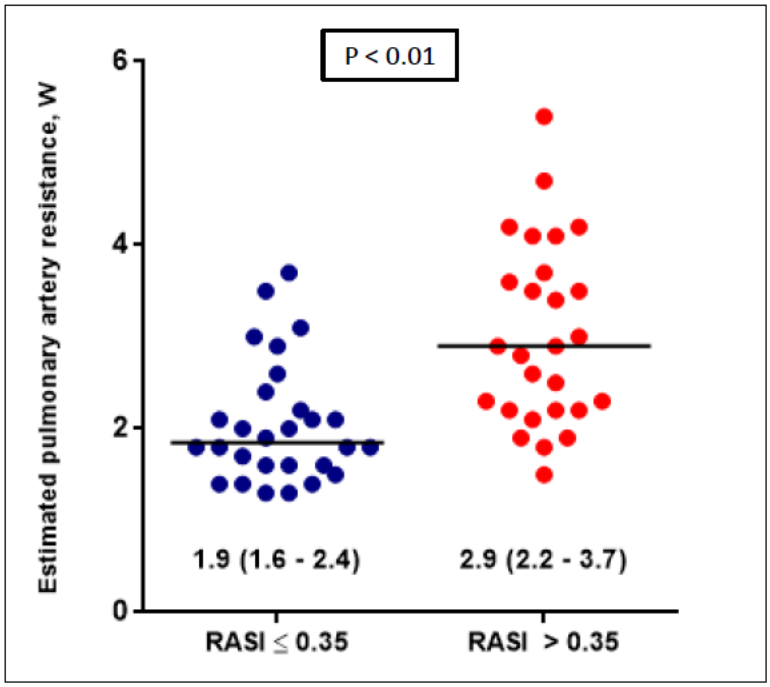

Figure 3 Panel A

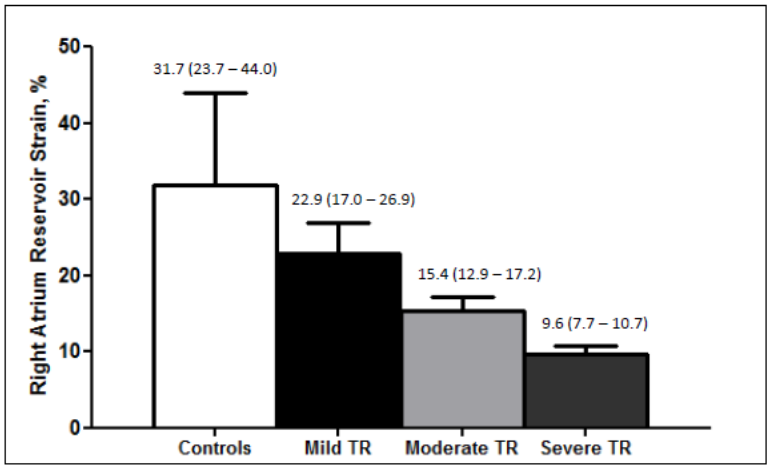

Figure 3 Panel B

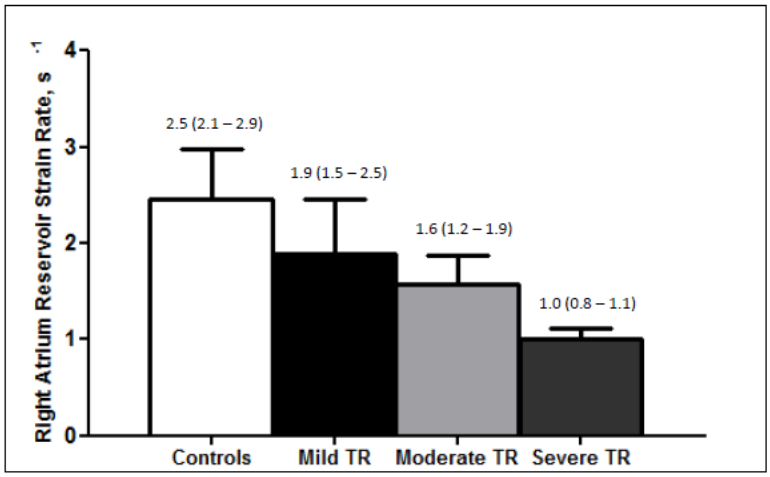

Figure 3 Panel C

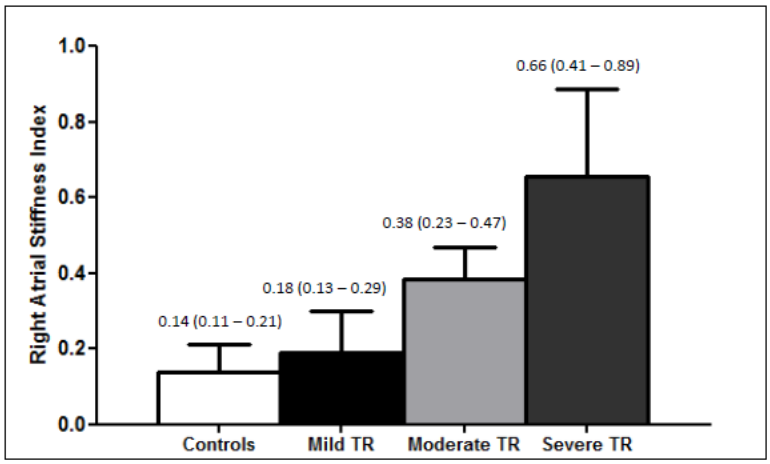

Supplemental Figure 1

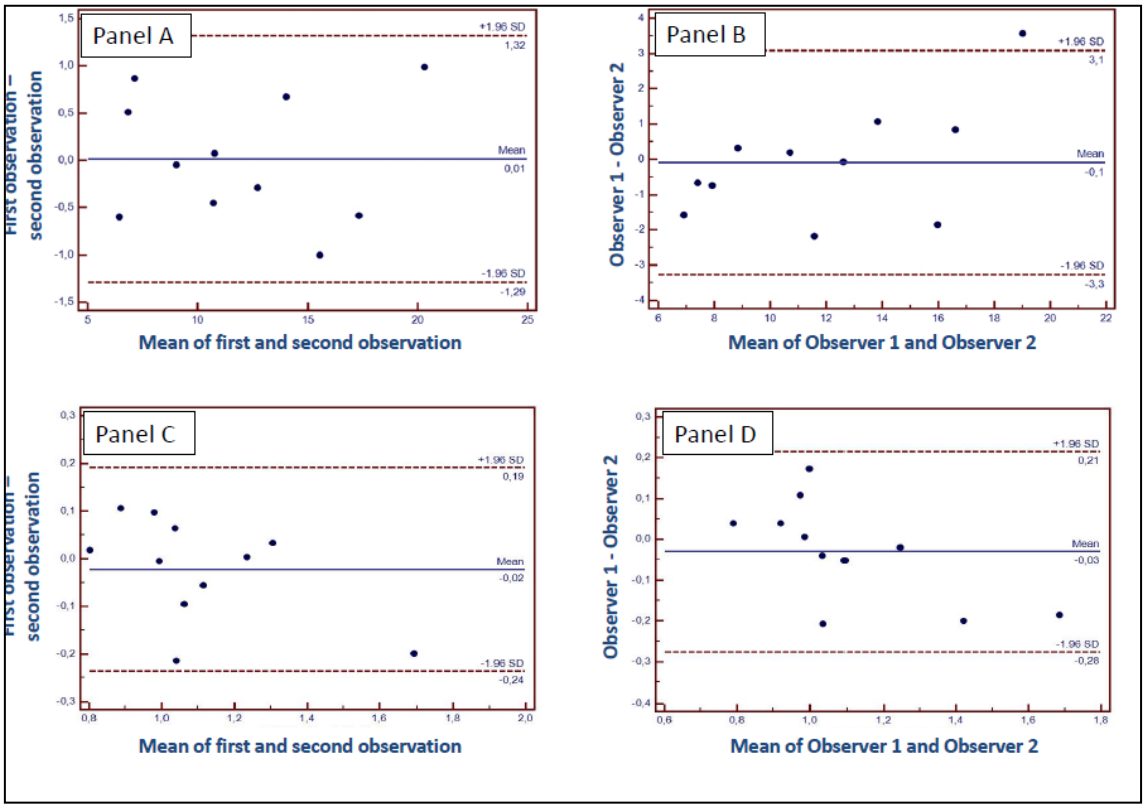

Supplemental Figure 2

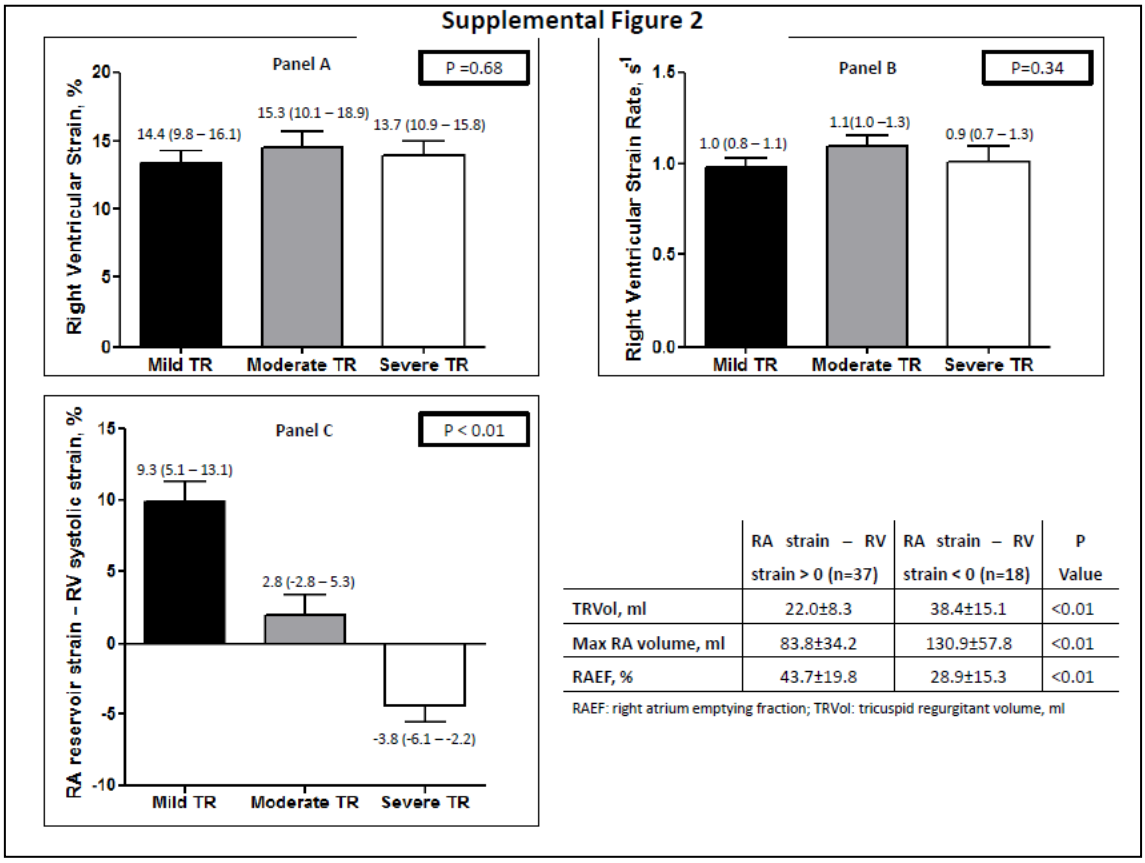

	RA strain – RV strain > 0 (n=37)	RA strain – RV strain < 0 (n=18)	P Value
TRVol, ml	22.0±8.3	38.4±15.1	<0.01
Max RA volume, ml	83.8±34.2	130.9±57.8	<0.01
RAEF, %	43.7±19.8	28.9±15.3	<0.01

RAEF: right atrium emptying fraction; TRVol: tricuspid regurgitant volume, ml

References

1. Mor-Avi V, Lang RM, Badano LP, Belohlavek M, Cardim NM, et al. (2011) Current and evolving echocardiographic techniques for the quantitative evaluation of cardiac mechanics: ASE/EAE consensus statement on methodology and indications endorsed by the Japanese Society of Echocardiography. J Am Soc Echocardiogr 24: 277-313.

2. Miller MJ, McKay RG, Ferguson JJ, Sahagian P, Nakao S, et al. (1986) Right atrial pressure-volume relationships in tricuspid regurgitation. Circulation 73: 799-808.

3. Vieira MJ, Teixeira R, Goncalves L, Gersh BJ (2014) Left atrial mechanics: echocardiographic assessment and clinical implications. J Am Soc Echocardiogr 27: 463-478.

4. Leitman M, Lysyansky P, Sidenko S, Shir V, Peleg E, et al. (2004) Two-dimensional strain-a novel software for real-time quantitative echocardiographic assessment of myocardial function. J Am Soc Echocardiogr 17: 1021-1029.

5. Reisner SA, Lysyansky P, Agmon Y, Mutlak D, Lessick J, et al. (2004) Global longitudinal strain: a novel index of left ventricular systolic function. J Am Soc Echocardiogr 17: 630-633.

6. Sirbu C, Herbots L, D'Hooge J, Claus P, Marciniak A, et al. (2006) Feasibility of strain and strain rate imaging for the assessment of regional left atrial deformation: a study in normal subjects. Eur J Echocardiogr 7: 199-208.

7. Cameli M, Lisi M, Giacomin E, Caputo M, Navarri R, et al. (2011) Chronic mitral regurgitation: left atrial deformation analysis by two-dimensional speckle tracking echocardiography. Echocardiography 28: 327-334.

8. Tops LF, Delgado V, Bertini M, Marsan NA, Den Uijl DW, et al. (2011) Left atrial strain predicts reverse remodeling after catheter ablation for atrial fibrillation. J Am Coll Cardiol 57: 324-331.

9. Ersboll M, Andersen MJ, Valeur N, Mogensen UM, Waziri H, et al. (2013) The prognostic value of left atrial peak reservoir strain in acute myocardial infarction is dependent on left ventricular longitudinal function and left atrial size. Circ Cardiovasc Imaging 6: 26-33.

10. D'Andrea A, Scarafile R, Riegler L, Salerno G, Gravino R, et al. (2009) Right atrial size and deformation in patients with dilated cardiomyopathy undergoing cardiac resynchronization therapy. Eur J Heart Fail 11: 1169-1177.

11. Padeletti M, Cameli M, Lisi M, Malandrino A, Zaca V, et al. (2012) Reference values of right atrial longitudinal strain imaging by two-dimensional speckle tracking. Echocardiography 29: 147-152.

12. Peluso D, Badano LP, Muraru D, Dal Bianco L, Cucchini U, et al. (2013) Right atrial size and function assessed with three-dimensional and speckle-tracking echocardiography in 200 healthy volunteers. Eur Heart J Cardiovasc Imaging 14: 1106-1114.

13. Saraiva RM, Demirkol S, Buakhamsri A, Greenberg N, Popovic ZB, et al. (2010) Left Atrial Strain Measured by Two-Dimensional Speckle Tracking Represents a New Tool to Evaluate Left Atrial Function. J Am Soc Echocardiogr 23: 172-180.

14. McMurray JJ, Adamopoulos S, Anker SD, Auricchio A, Bohm M, et al. (2012) ESC Guidelines for the diagnosis and treatment of acute and chronic heart failure 2012: The Task Force for the Diagnosis and Treatment of Acute and Chronic Heart Failure 2012 of the European Society of Cardiology. Developed in collaboration with the Heart Failure Association (HFA) of the ESC. Eur Heart J 33: 1787-1847.

15. Evangelista A, Flachskampf F, Lancellotti P, Badano L, Aguilar R, et al. (2008) European Association of Echocardiography recommendations for standardization of performance, digital storage and reporting of echocardiographic studies. Eur J Echocardiogr 9: 438-448.

16. Rudski LG, Lai WW, Afilalo J, Hua L, Handschumacher MD, et al. (2010) Guidelines for the echocardiographic assessment of the right heart in adults: a report from the American Society of Echocardiography endorsed by the European Association of Echocardiography, a registered branch of the European Society of Cardiology, and the Canadian Society of Echocardiography. J Am Soc Echocardiogr 23: 685-713; quiz 786-688.

17. Natori H, Tamaki S, Kira S (1979) Ultrasonographic evaluation of ventilatory effect on inferior vena caval configuration. Am Rev Respir Dis 120: 421-427.

18. Lang RM, Bierig M, Devereux RB, Flachskampf FA, Foster E, et al. (2005) Recommendations for chamber quantification: a report from the American Society of Echocardiography's Guidelines and Standards Committee and the Chamber Quantification Writing Group, developed in conjunction with the European Association of Echocardiography, a branch of the European Society of Cardiology. J Am Soc Echocardiogr 18: 1440-1463.

19. Kaul S, Tei C, Hopkins JM, Shah PM (1984) Assessment of right ventricular function using two-dimensional echocardiography. Am Heart J 107: 526-531.

20. Lindqvist P, Waldenstrom A, Henein M, Morner S, Kazzam E (2005) Regional and global right ventricular function in healthy individuals aged 20-90 years: a pulsed Doppler tissue imaging study: Umea General Population Heart Study. Echocardiography 22: 305-314.

21. Nageh MF, Kopelen HA, Zoghbi WA, Quinones MA, Nagueh SF (1999) Estimation of mean right atrial pressure using tissue Doppler imaging. Am J Cardiol 84: 1448-1451, A1448.

22. Dubin J, Wallerson DC, Cody RJ, Devereux RB (1990) Comparative accuracy of Doppler echocardiographic methods for clinical stroke volume determination. Am Heart J 120: 116-123.

23. Ommen SR, Nishimura RA, Appleton CP, Miller FA, Oh JK, et al. (2000) Clinical utility of Doppler echocardiography and tissue Doppler imaging in the estimation of left ventricular filling pressures: A comparative simultaneous Doppler-catheterization study. Circulation 102: 1788-1794.

24. Lancellotti P, Moura L, Pierard LA, Agricola E, Popescu BA, et al. (2010) European Association of Echocardiography recommendations for the assessment of valvular regurgitation. Part 2: mitral and tricuspid regurgitation (native valve disease). Eur J Echocardiogr 11: 307-332.

25. Yock PG, Popp RL (1984) Noninvasive estimation of right ventricular systolic pressure by Doppler ultrasound in patients with tricuspid regurgitation. Circulation 70: 657-662.

26. Abbas AE, Fortuin FD, Schiller NB, Appleton CP, Moreno CA, et al. (2003) A simple method for noninvasive estimation of pulmonary vascular resistance. J Am Coll Cardiol 41: 1021-1027.

27. Kurt M, Wang J, Torre-Amione G, Nagueh SF (2009) Left atrial function in diastolic heart failure. Circ Cardiovasc Imaging 2: 10-15.

28. Bland JM, Altman DG (1986) Statistical methods for assessing agreement between two methods of clinical measurement. Lancet 1: 307-310.

29. Shrout PE, Fleiss JL (1979) Intraclass correlations: uses in assessing rater reliability. Psychol Bull 86: 420-428.

30. Anne W, Willems R, Roskams T, Sergeant P, Herijgers P, et al. (2005) Matrix metalloproteinases and atrial remodeling in patients with mitral valve disease and atrial fibrillation. Cardiovasc Res 67: 655-666.

31. Kuppahally SS, Akoum N, Burgon NS, Badger TJ, Kholmovski EG, et al. (2010) Left Atrial Strain and Strain Rate in Patients With Paroxysmal and Persistent Atrial Fibrillation / CLINICAL PERSPECTIVE. Circulation Cardiovasc Imaging 3: 231-239.

32. Her A-Y, Choi E-Y, Shim CY, Song BW, Lee S, et al. (2012) Prediction of Left Atrial Fibrosis With Speckle Tracking Echocardiography in Mitral Valve Disease: A Comparative Study With Histopathology. Korean Circ J 42: 311-318.

33. Melenovsky V, Hwang SJ, Redfield MM, Zakeri R, Lin G, et al. (2015) Left atrial remodeling and function in advanced heart failure with preserved or reduced ejection fraction. Circ Heart Fail 8: 295-303.

34. Kutty S, Padiyath A, Li L, Peng Q, Rangamani S, et al. (2013) Functional maturation of left and right atrial systolic and diastolic performance in infants, children, and adolescents. J Am Soc Echocardiogr 26: 398-409 e392.

35. Padeletti M, Cameli M, Lisi M, Zaca V, Tsioulpas C, et al. (2011) Right atrial speckle tracking analysis as a novel noninvasive method for pulmonary hemodynamics assessment in patients with chronic systolic heart failure. Echocardiography 28: 658-664.

Supplement Number 9

Review Article: Two-dimensional Speckle Tracking Cardiac Mechanics and Constrictive Pericarditis: Systematic Review

Review Article

Two-dimensional Speckle Tracking Cardiac Mechanics and Constrictive Pericarditis: Systematic Review

Echocardiography 2016 Jul; 1-11. Doi: 10.1111/echo.13293

Marta Madeira[1*] MD, Rogério Teixeira[1,2*+] MD, Marco Costa[1] MD, Lino Gonçalves[1,2] MD, PhD, Allan L. Klein[3] MD

* Both authors contributed equally to the paper

+ Corresponding Author

[1]Serviço de Cardiologia, Centro Hospitalar e Universitário de Coimbra – Hospital Geral, Coimbra, Portugal

[2] Faculdade de Medicina da Universidade de Coimbra, Coimbra, Portugal

[3]Heart and Vascular Institute, Center for the Diagnosis and Treatment of Pericardial Diseases, Cleveland Clinic, Cleveland, Ohio, USA

Word Count: 3339 (without references or tables)

Abstract

Transthoracic echocardiography has a pivotal role in the diagnosis of constrictive pericarditis (CP). In addition to the classic M-mode, two-dimensional and Doppler indices, newer methodologies designed to evaluate myocardial mechanics, such as two-dimensional speckle-tracking echocardiography (2D-STE), provide additional diagnostic and clinical information in the context of CP. Research has demonstrated that cardiac mechanics can improve echocardiographic diagnostic accuracy of CP and aid in differentiating between constrictive and restrictive ventricular physiology. 2D-STE can also be used to assess the success of pericardiectomy and its impact on atrial and ventricular mechanics.

In the course of this review we describe cardiac mechanics in patients with CP and summarize the influence of pericardiectomy on atrial and ventricular mechanics assessed using 2D-STE.

Keywords: constrictive pericarditis; restrictive cardiomyopathy; cardiac mechanics; two-dimensional speckle tracking echocardiography

Abbreviation List

ε: strain;

2D-STE: two-dimensional speckle tracking echocardiography;

CMR: cardiac magnetic resonance;

CP: constrictive pericarditis;

GLS: global longitudinal strain;

IVS: interventricular septum;

LA: left atrial;

LV: left ventricular;

LVLW: left ventricular lateral wall;

LVSW: left ventricular septal wall;

RCM: restrictive cardiomyopathy;

RVFW: right ventricle free wall;

SR: strain rate;

TDI: tissue Doppler imaging.

Introduction

Constrictive pericarditis (CP) is characterized by impaired diastolic cardiac filling and elevated ventricular filling pressures, results from the external constraint of a fibrotic or inflamed pericardium, with fused visceral and parietal layers.[1–3] It usually presents as right-sided heart failure with significant systemic congestion, such as elevated jugular venous pressure, peripheral edema, hepatomegaly and ascites.[4]

Pericarditis, cardiac surgery and mediastinal radiotherapy are the leading identifiable causes of CP in the developed world.[4] Pericardiectomy is the definitive treatment in patients who are refractory to medical treatment; it relieves pericardial restraint and, in the absence of concomitant myocardial dysfunction, effectively restores diastolic filling.[5–8]

Restrictive cardiomyopathy (RCM), an intrinsic myocardial disease, has a hemodynamic profile similar to CP.[9–11] Distinguishing between this two entities can be challenging and the correct differential diagnosis is extremely important because their management differs considerably; CP has a curative treatment.[7]

Diastolic dysfunction in CP is related to epicardial tethering, pericardial constraint and involvement of the adjacent myocardium by the pericardial fibrotic process, whereas RCM is predominantly characterized by subendocardial diastolic dysfunction.[12,15] Because the subendocardial region is responsible for longitudinal shortening, diseases that affect predominantly the subendocardial fibers will alter the longitudinal deformation of the ventricular wall.[16–18] In contrast, diseases that affect the subepicardial myofibers are expected to decrease circumferential shortening and torsion of the left ventricle (LV).[16–18]

Echocardiography

Because noninvasive imaging techniques continue to advance, the clinical differentiation of CP from RCM is based on the recognition of a cluster of structural, mechanical and hemodynamic changes rather than a single structural or functional variable used in isolation.[12] Although not a gold standard for the diagnosis of CP, transthoracic echocardiography is an important method for evaluating this entity. According to a recent study, the three most important echocardiographic parameters for the diagnosis of CP were the presence of respiration-related ventricular septal shift, preserved or increased medial mitral annular e' velocity, and prominent hepatic vein expiratory diastolic flow reversals.[13] Table 1 summarizes diagnostic performance data that compares the relative usefulness of the echocardiographic data used to diagnose CP.

Two-dimensional speckle tracking echocardiography (2D-STE) is a recent angle-independent, semi-automated technique used to evaluate the myocardium.[14] It uses standard

B-mode images to track blocks of speckles from frame to frame and measures lengthening and shortening relative to the baseline – *Lagrangian* method. 2D-STE provides local myocardial information, from which displacement, velocity, strain (ε) and strain rate (SR) can be derived, allowing an accurate assessment of longitudinal, radial and circumferential myocardial mechanics.[14]

This review aims to comprehensively describe ventricular and atrial mechanics in CP and to discuss the incremental clinical importance of such mechanics for differentiating CP from RCM. We also review the impact of pericardiectomy on ventricular and atrial mechanics and its correlation with symptomatic improvement.

Methods

The authors searched electronic databases for articles published in English until August 2015. Databases included MEDLINE and the Cochrane Central Register of Controlled Trials. The search was conducted using the keywords “constrictive pericarditis” and “cardiac mechanics” or “speckle tracking echocardiography”. Citations were screened at the title/abstract level and full texts were manually obtained for all potentially relevant articles. This search strategy yielded fourteen publications. Seven publications were excluded because it was clear about the title and abstract that they did not fulfil the selection criteria.

Additional publications were identified by searching the reference lists of the relevant publications and the main international guidelines concerning the subject of this review. Forty-five publications were finally included in the review (Figure 1).

The quality assessment of the studies was performed using the Newcastle-Ottawa scale – Table 2 and Supplemental Table 1.[19]

Ventricular Mechanics

The helical nature of the heart muscle determines its wringing motion during the cardiac cycle, with counterclockwise rotation of the apex and clockwise rotation of the base around the LV long axis.[14] The absolute apex-to-base difference in LV rotation, counterclockwise in systole, is referred to as twist or torsion (twist normalized to length) and results in storage of potential energy.[14,18] Subsequent recoil of twist (or untwisting) during early diastole is associated with the release of restoring forces that contribute to diastolic suction and early LV filling.[14] During this process, the magnitude of circumferential and longitudinal expansion of the LV is modulated by the stiffness of pericardial layers.[20,21] Loss of normal compliance of pericardial layers is expected to alter the circumferential pattern of diastolic recoil and, to a lesser degree, the pattern of myocardial motion in the longitudinal

direction.[15,22] Furthermore, especially in CP due to cardiac surgery and mediastinal irradiation, the process of scarring and inflammation of the pericardial layers sometimes extends into the myocardial wall,[4,23,24] which further attenuates the circumferential recoil of the LV.[15] In contrast, patients with RCM and intrinsic myocardial diseases that manifest endocardial dysfunction have reduced longitudinal deformation, while LV circumferential deformation and twist are relatively preserved.[6,15]

Circumferential LV mechanics

LV expansion in CP may be more limited in the circumferential rather than in the longitudinal direction because of pericardial restraint[25] and potential epicardial involvement.[26–28]

Accordingly, a study conducted by Sengupta *et al.*[15] that evaluated longitudinal, circumferential and radial LV mechanics using 2D-STE in 26 patients with CP, 19 patients with RCM and 21 controls found that patients with CP had lower global and segmental LV circumferential ε than both control subjects and patients with RCM. These results were corroborated by two additional studies that found similar results[6,9] and reinforced previous observations of significantly reduced circumferential shortening of the LV in CP when evaluated by cineangiographic techniques .[29,30]

In contrast, a study conducted by Amaki *et al.*[12] to assess the consistency of diagnostic information between cardiac magnetic resonance (CMR) tissue tracking analysis and 2D-STE, which included 28 patients with CP, 30 patients with RCM and 34 control subjects, showed that patients with RCM had marginally lower circumferential ε when compared with patients with CP and controls when evaluated by CMR tissue tracking analysis. However, circumferential ε was similar between CP and RCM patients based on 2D-STE analysis.[12] The differences from previous studies may be related to the selective sampling in the Amaki *et a.l*[12] study from the subendocardial region, which is a layer spared from myocardial tethering.[9]

Longitudinal LV mechanics

Pericardial to myocardial tethering along the ventricular free walls in CP results in reduction of longitudinal deformation of the ventricular free walls, with preserved deformation of interventricular septal wall.[31,32]

Using 2D-STE, Amaki *et al.*[12] observed that global longitudinal ε was significantly lower in RCM patients than in CP patients and control subjects. Furthermore, using a multivariable model, they verified that global longitudinal ε added diagnostic value to left ventricle ejection

fraction, left ventricle mass, e' and respiratory septal shift as echocardiographic predictors for differentiating RCM from CP.[12]

Sengupta *et al.*[15] also hypothesized that segmental LV cardiac mechanics were heterogenous in CP. Specifically, the authors analyzed the longitudinal ε in different LV segments and demonstrated that longitudinal ε recorded in the LV basal segments was significantly higher in controls and CP patients than in RCM patients. However, in the LV apical region, longitudinal ε was equally reduced for both CP and RCM patients.[15] The LV longitudinal ε heterogeneity among LV segments could be explained by the continuity of the subendocardial and subepicardial apical myofibers,[18] such that the tethering of the subepicardial region in CP might also influence longitudinal subendocardial deformation of the LV apex.[15]

Kusunose *et al.*[9] stated that the tethering effect of pericardial thickening could be patchy,[32] sparing the annulus and thus reducing the reliability of annular velocities to differentiate constriction from restriction.[20,23] It was proposed that the assessment of longitudinal ε would be an ideal method to evaluate the impact of tethering along the entire LV free wall and not just the annulus.[9] Furthermore, they expected that in CP the LV lateral wall (LVLW) and right ventricle free wall (RVFW) systolic longitudinal ε would be decreased, but the septal wall systolic ε would be preserved as a result of a local constraint on LVLW and RVFW.[9] These differences could result from perimyocardial adhesions and involvement of the adjacent myocardium by the pericardial fibrotic process, which could reduce the deformation of the adjacent LVLW and RVFW, sparing septal wall deformation.[26–28,33] However, because RCM is a diffuse process, analysis of ventricular mechanics will reveal no such regional variation, allowing these two entities to be distinguished.[9] Accordingly, a study conducted by Kusunose *et al.*[9] that compared myocardial mechanics of CP (52 patients), RCM (35 patients) and controls (26 subjects) found that global longitudinal, radial and circumferential strains were significantly more reduced in RCM than in both CP patients and controls and that this reduction was uniform. In contrast, when compared to RCM patients, CP patients had higher ε values in the septum than in the RVFW or LVLW, but lower than in the healthy age and gender matched control group.[9] Furthermore, the LVLW/LV septal wall (LVSW) ε ratio was more accurate for differentiating between CP and RCM patients than the e' and the S' obtained from the LV anterolateral/LV septal segments.[9] The RVFW/LVSW ε ratio was also able to differentiate CP from RCM and the ε ratio (LVLW/LVSW) correlated with the degree of increased pericardial thickness.[9]

Furthermore, tissue tracking analysis in patients with CP is not limited to echocardiography as demonstrated in a study comparing the diagnostic concordance of

echocardiography and CMR.[12] In this study, CMR-measured global longitudinal ε had diagnostic value similar to that of echocardiography-derived global longitudinal ε for distinguishing CP from RCM (Figure 2). This study's findings demonstrate the value of extracting more diagnostic variables from a single modality, thereby increasing its cost efficacy.[12]

Radial LV mechanics

Quantum mechanics suggest that shortening in the longitudinal and circumferential directions would result in thickening in the radial direction due to conservation of mass.[14] According to this principle, radial ε can be derived as the sum of longitudinal and circumferential ε.[14] The radial movement of epicardial surface of the LV is greatest at the base and least at the mid level.[34] Hence, tethering of the epicardial surface in CP might limit the radial motion of myocardium, particularly near the LV base.[15] Segupta *et al.* demonstrated that radial ε in CP is markedly attenuated at the LV base, but radial ε of apical and mid LV segments is similar for CP patients, RCM patients and healthy controls.[15]

Torsional LV mechanics

Reduced apical rotation have been demonstrated in CP, but not in RCM, in which apical rotation did not differ significantly from controls.[15,35] However, peak LV rotation and rates of rotation during ejection, early diastole and late diastole were similar in CP patients, RCM patients and control subjects in the basal and mid segments.[15] On the other hand, a study conducted by Alharthi *et al.*[35], which characterized the impact of pericardial adhesions induced in nine pigs on epicardial and endocardial LV rotational mechanics, observed a trend towards an increase in basal rotation magnitude (epicardial and endocardial) following patchy adhesion induction. These results may reflect a functional compensatory effect on rotational mechanics of the LV base. The reduction of apical rotation in CP could be due to a lack of normal pericardium, which usually enables swift and friction-free apical motion, and potential scarring and inflammation extending into the epicardial layer of the myocardial wall.[26–28,33,35] Furthermore, Alharthi *et al.*[35] demonstrated that the apical endocardial and epicardial rotations were significantly reduced by simulated adhesions; nevertheless, their gradients did not significantly change, which suggests a proportional reduction in rotation with a preserved transmural gradient.

Apical rotation appears to be the determining factor of LV twisting, which is derived from the net difference of apical and basal rotations.[36] Sengupta *et al.*[15] demonstrated that the net LV twist was significantly lower in CP patients compared with RCM patients and controls and that peak global circumferential shortening ε was positively correlated with the magnitude

of net LV twist, whereas the longitudinal shortening ε was inversely correlated. In a study of an animal model of pericardial adhesions, LV twist magnitude in the endocardial layer decreased, whereas the decrease in the epicardial twist magnitude was not significant, although the gradient of endocardial to epicardial twist did not significantly change after the intervention.[35] Alharthi *et al.*[35] also showed that after induction of patchy adhesions endocardial LV torsion (LV twist magnitude normalized to LV length)[14,36] decreased and epicardial LV torsion had a decreasing trend, but the gradient of endocardial to epicardial torsion was not changed significantly.

In 2015 Negishi *et al.*[37] published the results of a study of 83 CP patients and 20 controls with 2D-STE. They confirmed previous findings that LV global longitudinal and circumferential ε were significantly reduced in CP patients compared to controls. Moreover, the authors focused on the LV displacement, and proved that CP patients had lower lateral but similar septal LV longitudinal displacement than controls. Regarding rotational displacement it was assessed the longitudinal septal-to-lateral rotational displacement, which can quantify the rocking or swinging motion of the whole heart. It was showed that there were no significant differences between groups regarding the rotational displacement, although CP patients had values close to zero, which could be explained by the encasement of the rigid pericardium.[37]

Atrial Mechanics

The left atrium (LA) has a pivotal role in the sequence of events that modulate LV filling.[38] Hence, analysis of LA mechanics is relevant to pathologies such as CP and RCM in which diastolic dysfunction is the cornerstone of their physiopathology.[10,11] LA ε during the reservoir phase has been demonstrated to correlate significantly with LV end-diastolic pressure and found to be more accurate for assessing LV end-diastolic pressure than the LA indexed volume.[38]

The impact of a tethered pericardium on LA mechanics was evaluated in study published by Motoki *et al*.[39] that included 52 CP patients and 19 controls. In this study, CP patients had a depressed LA reservoir ε in the lateral wall. Probably due to a compensatory mechanism similar to the LV (which has exaggerated longitudinal septal motion), CP patients had a higher septal reservoir phase ε wall than the control group.[39]

It has also been demonstrated in a group of 30 CP patients, that the LA reservoir, conduit and contractile phase mechanics were significantly reduced when compared to a control group.[40]

In 2015, Liu *et al*.[41] assessed LA mechanics in 35 patients with CP, 30 patients with RCM and 30 controls. The authors showed that LA global and regional ε and SR during the LA

reservoir phase were significantly reduced in patients with CP and RCM compared with controls.[41] Furthermore, patients with RCM had a significantly lower LA septal reservoir ε and SR compared with CP patients, although the reservoir ε and SR of the LA lateral wall of patients with CP and patients with RCM were not significantly different.[41] Moreover, compared to LA septal reservoir ε, the LA lateral reservoir ε seems to be more reduced in patients with CP, which may result from the influence of the pericardial disease process, on the lateral wall of the atrium .[41] Importantly, a worse NYHA class was associated with a more reduced LA reservoir ε, indicating that the LA performance may play a role in the functional capacity of CP patients.[41]

In Table 3, we summarized studies that assessed cardiac mechanics in patients with CP.

Effects of Pericardiectomy on ventricular and atrial mechanics

The relief from pericardial restraint using pericardiectomy is the only curative treatment for patients with CP.[7,28,42] The results published by Kusunose *et al.*[9] showed that circumferential and longitudinal LV mechanics improved after pericardiectomy, but radial mechanics remained unchanged. The improvement of ε was greater in RV and LV free walls, with an increase of LVLW/LVSW ε ratio. Immediately after pericardiectomy, Sengupta *et al.*[15] demonstrated a reduction in early diastolic mitral annular velocity, but LV rotation and untwisting velocities remained unchanged, which suggests that pericardiectomy might not immediately normalize LV mechanics in patients with CP. The differences between the results of Sengupta *et al.*[15] and Kusunose *et al.*[9] might be explained by a larger population and a different etiologic profile in the later study (75% idiopathic cause, 4% radiation cause and 19% previous cardiac surgery *versus* 31% idiopathic cause, 31% radiation cause and 19% previous cardiac surgery, respectively). Previous studies have shown that after pericardiectomy, LV circumferential shortening and velocity remained abnormal and the majority of patients had persistent signs of constriction on echocardiography, although symptoms of heart failure improved.[30,43] Furthermore, patients with congenital absence of pericardium have a markedly decrease in LV torsion,[44] which indicates that pericardiectomy might not restore the frictionless surface that is required for normal cardiac rotation. In addition, because the epicardial dysfunction and fibrosis might be chronic processes,[4,23,24] post-operative recovery of LV function may not occur immediately .

Recently, it has been demonstrated for a group of 27 CP that after pericardiectomy, LV septal longitudinal displacement decreased and lateral longitudinal displacement increased.[37] Regarding rotational displacement, it significantly increased after surgery. This means that after the release of the pericardial constraint, the whole heart swung more counterclockwise

during systole.[37] Importantly, the authors observed that the increase in rotational displacement after pericardiectomy was associated with a reduction of the diuretic dose.[37]

Regarding LA mechanics, Motoki *et al.*[39] reported that LA ε during the reservoir and the contractile phases significantly improved after pericardiectomy, which was in contrast to the LA ε during the conduit phase (Figure 3). Moreover, these changes were heterogeneous; after surgery, the lateral wall had a more significant improvement in all components of LA function than did the septal walls.[39] Furthermore, in patients with New York Heart Association classification improvement, LA mechanics improved significantly more than in patients without this degree of symptomatic alleviation.

Clinical Implications

The differentiation of CP from RCM can be challenging, due to similarities in their hemodynamic profile.[9–11] However, correct differentiation of these two entities is extremely important, as pericardiectomy can be curative in patients with CP.[5–8] In the modern era, different patterns of atrial and ventricular mechanics aid in distinguishing CP from other conditions, such as RCM – Table 4. In addition, in the presence of a mixed physiology (pericardial constraint combined with myocardial dysfunction), assessment of LV longitudinal, circumferential and torsional mechanics by 2D-STE can describe the extent of myocardial involvement and potentially predict the response to pericardiectomy.[6]

The outcome after pericardiectomy is variable for reasons that are not well understood, such as concomitant myocarditis or myocardial damage, incomplete pericardial stripping and the severity of pericardial calcification.[37] Cardiac mechanics can provide useful information after surgery allowing the quantification of the effect of the loss of pericardial support. Furthermore, changes in the ε pattern after pericardiectomy may be used to evaluate pericardiectomy success in patients with persistent diastolic heart failure in whom inadequate stripping of pericardium is suspected.[9]

The presented studies excluded patients with inadequate image quality or poor tracking, which means that the reported values should not expect to be obtained in unselected subjects. Moreover, some of the parameters are hard to assess and can be time consuming.

According to the Newcastle–Ottawa quality score,[19] 5 of 7 studies were considered high quality (score > 6), nevertheless, the number of studies in this field of knowledge is sparse and further prospective studies are needed to validate the potential clinical utility of such diagnostic algorithms.

Conclusions

In CP, the thickened, fused and frequently calcified shell-like pericardial membranes tethers the epimyocardial region.[26,27] In contrast, in RCM, infiltrative deposits and fibrosis predominate throughout the subendocardial region.[45,46] Because the myocardial region affected in these two conditions differs, the patterns of LV circumferential and longitudinal mechanics are expected to differ. RCM is characterized by abnormal longitudinal LV mechanics with relative sparing of the LV rotation; conversely, patients with CP have relatively preserved longitudinal LV mechanics but markedly abnormal circumferential deformation, torsion and untwisting velocity (Figure 4).[6,12,15,35]

CP patients have a unique cardiac mechanics profile and, although time consuming, 2D-STE can be used to differentiate CP from RCM patients because the study of cardiac mechanics contributes more to diagnostic accuracy than other echocardiographic parameters. Furthermore, 2D-STE provides data non-invasively to better evaluate the efficacy and response to pericardiectomy.

Acklnowlegments: The authors would like to thank Maria João Vieira MD PhD, for the quality assessment of the studies.

Compliance With Ethical Standards:

Funding: The authors have nothing to declare;

Conflict of interest: The authors have no conflict of interest to declare;

Ethical approval: This article does not contain any studies with human participants or animals performed by any of the authors.

Legends:

Table 1: Summary of the classic echocardiographic parameters used to diagnose constrictive pericarditis (adapted from Dal-Bianco J *et al*.[6]).

Table 2: Characteristics and Quality of Included Studies.

Table 3: Cardiac mechanics in constrictive pericarditis: summary of most relevant studies.

Table 4: Echocardiographic differences between constriction and restriction.

Supplemental Table 1: Newcastle–Ottawa quality score.

Figure 1: Flow diagram depicting the selection of the articles included in this systematic review.

Figure 2: Longitudinal left ventricular ε measured from both echocardiogram and cardiac magnetic resonance using an apical 4-chamber view in a patient with constrictive pericarditis (A and B), restrictive cardiomyopathy (C and D) and in a control (E and F). Longitudinal left ventricular ε was significantly reduced in the restrictive cardiomyopathy compared with the constrictive pericarditis patients and with controls. Reprinted from Amaki M. *et al*.[12] with permission from Elsevier®.

Figure 3: Measurement of left atrial longitudinal strain using two-dimensional speckle tracking echocardiography in patients before and after pericardiectomy. Graphical displays of deformation parameters for each segment were generated automatically and were used for the measurement of left atrial strain values. (A) This patient showed depressed left atrial ε in the lateral walls (yellow and sky blue) and high variables in the septal walls (red and blue). (B) Lateral left atrial ε was increased, septal ε was decreased, and global ε (black) improved after the procedure. Reprinted from Motoki H. *et al.*[39] with permission from Elsevier®.

Figure 4: Cardiac mechanics in constrictive pericarditis patients.

Table 1: Summary of the classic echocardiographic parameters used to diagnose constrictive pericarditis (adapted from Dal-Bianco J *et al.*[6]; Welch T *et al.*[13])

Echocardiographic parameter	Sensitivity	Specificity
Doppler echocardiography		
≥25% respiratory variation of peak early diastolic MV inflow velocity; augmented hepatic vein diastolic flow reversals after the onset of expiration; ≥25% of forward diastolic velocity	88%	67%
≥10% respiratory variation of peak early diastolic MV inflow velocity	84%	91%
Color M-mode MV inflow propagation; first aliasing contour 100 cm/s	74%	91%
Respiratory variation in PV systolic/diastolic flow ratio ≥65% in inspiration + % change of early mitral peak diastolic flow ≥40%	86%	94%
Respiratory variation in PV peak diastolic flow velocity ≥18%	79%	91%
Dilated hepatic veins, "W" wave pattern (reverse flow in late systole and diastasis)	68%	100%
LV septal/posterior wall radial motion		
IVS bounce, M-mode	40-88%	80%
IVS bounce, 2-dimensional	62%	93%
Biphasic early diastolic IVS motion by color TDI (≥7 cm/s) motion	82%	93%
Biphasic early diastolic IVS motion by pulsed tissue Doppler	100%	100%
LV posterior wall flattening, M-mode	64-92%	82-100%
Miscellaneous echocardiographic findings		
Pericardial thickening, M-mode	53-100%	50-100%
Pericardial thickening, 2-dimensional	36%	-
Left atrial enlargement, M-mode	75%	100%
Premature PV opening, M-mode	14%	100%
Tissue Doppler echocardiography		
Medial e' velocity ≥ 9 cm/s	83%	81%
Medial e' / Lateral e' ≥ 0.91	75%	85%

DTI: tissue Doppler imaging; IVS: interventricular septum; LV: left ventricle; MV: mitral valve;PV: pulmonary valve

Table 2: Characteristics and Quality of Included Studies

			Nº of Subjects			Study Quality (Newcastle-Ottawa Scale)			
Study	**Design**	**Time Period**	**CP**	**RCM**	**Controls**	**Selection**	**Comparability**	**Outcome**	**Total Score**
Sengupta et al, 2008	Prospective	2005-2007	26	19	21	****	*	***	8
Kusunose et al, 2013	Retrospective	2005-2012	52	35	26	****	*	***	8
Motoki et al, 2013	Retrospective	2007-2010	52	--	19	****	--	**	6
Liu et al, 2013	Prospective	2007-2011	30	--	30	****	*	**	7
Amaki et al, 2014	Retrospective	2006-2013	28	30	34	****	*	***	8
Negishi et al, 2015	Retrospective	2007-2010	83	--	20	****	--	***	7
Liu et al, 2015	Prospective	---	35	30	39	****	--	**	6

Each asterisk represents if an individual criterion within the subsection was fulfilled.

CP: constrictive pericarditis; RCM: restrictive cardiomyopathy

Table 3: Cardiac mechanics in constrictive pericarditis: summary of most relevant studies.

Study and Year	Population	Methodology	Main findings
Sengupta *et al.*[15], 2008	26 patients with CP (31% idiopathic, 31% radiotherapy, 19% previous cardiac surgery and 19% viral pericarditis), + 19 patients with RCM + 21 controls	Longitudinal, radial and circumferential mechanics of the LV were quantified by 2D-STE.	• In comparison with controls, CP patients had impaired LV circumferential ε (base; -16±6 vs -9±6%; *P*<0.016), torsion (3±1 vs 1±1°/cm; *P*<0.016), and untwisting velocities (116±62 vs 36±50°/s; *P*<0.016). • RCM patients had impaired LV longitudinal displacement (base: 14.7±2.5 cm vs 9.8±2.8 cm; *P*<0.016) compared with controls. • After pericardiectomy, there was a significant decrease in longitudinal early diastolic LV basal myocardial velocities (7.4 cm/s vs 6.8 cm/s; *P*=0.023), but circumferential ε and torsion remained unchanged.
Kusunose *et al.*[9], 2013	52 patients with CP (75% idiopathic, 19% previous cardiac surgery, 4% radiotherapy and 2% tubercular pericarditis), + 35 patients with RCM + 26 controls	Myocardial mechanics were evaluated by 2D-STE and all patients underwent cardiac magnetic resonance examination.	• In a comparison of RCM and controls, CP patients had significantly lower regional longitudinal systolic ε ratios (CP versus RCM and normal; LVLWS/LVSWS: 0.8±0.2 vs 1.1±0.2 and 1.0±0.2; *P*<0.01; RVFWS/LVSWS: 0.8±0.4 vs 1.4±0.5 and 1.2±0.2; *P*<0.001). • LVLWS/LVSWS was more robust than the LV lateral wall to LV septal wall ratio of early diastolic velocities at the LV base in differentiating CP from RCM (area under the curve=0.91 versus 0.76; *P*=0.011). • Pericardiectomy resulted in the improvement of the depressed LVLWS/LVSWS (0.83±0.18 vs 0.95±0.12; *P*<0.01). • Regional myocardial mechanics showed a modest inverse correlation with adjacent pericardial segment thickness (Spearman r=0.28; *P*<0.001).

Study and Year	Population	Methodology	Main findings
Motoki *et al.*[39], 2013	52 patients with CP (67% idiopathic, 21% previous cardiac surgery, 6% radiotherapy and 6% post-pericarditis) + 19 controls	Global LA longitudinal ε was calculated, which included peak negative ε, peak positive ε and the sum of those values, total LA ε, using 2D-STE with velocity vector imaging before and after pericardiectomy.	• Patients with CP showed depressed global LA εnegative, LA εtotal, and LA εpositive compared with controls. • LA contractile and reservoir ε showed significant increases after pericardiectomy. Regional analysis revealed that the improvement in LA function after surgery was more apparent in lateral segments, while the regional function of septal walls was depressed after surgery.
Liu *et al.*[40], 2013	30 patients with CP (80% viral pericarditis, 20% idiopathic) + 30 controls	Evaluation of LA mechanics in using 2D-STE analysis.	• LA reservoir ε was significantly reduced for the CP group, when compared to controls (16.5±5.5 vs 44.9±16.2%, *P*<0.01). • LA reservoir SR (0.90±0.26 vs 2.09±0.66 s^{-1}, *P*<0.01), conduit SR (-1.30±0.44 vs -2.27±0.85 s^{-1}, *P*<0.01) and contractile SR (-1.06±0.53 vs -2.30±0.78 s^{-1}, *P*>0.01) were significantly reduced in CP patients when compared to a control group.
Amaki *et al.*[12], 2014	28 patients with CP (43% idiopathic, 25% previous cardiac surgery, 21% postpericarditis, 7% malignancy and 4% radiotherapy), + 30 patients with RCM + 34 controls	GLS from long-axis views and circumferential ε from short-axis views were measured on 2D-STE and CMR cine images using the same offline software.	• GLS was higher in patients with CP than in those with RCM [-18.5% (-20.1 to -15.2) vs -11.6% (-14.6 to -9.3); *P*<0.001] and both techniques were found to have similar diagnostic value (area under the curve, 0.84 versus 0.88 for CMR and echocardiography, respectively). • The ratio between lateral and septal longitudinal ε was not significantly different among the 3 groups. • Patients with RCM had marginally lower circumferential ε when compared with CP [-23.9 (-28.3 to -20.2) vs -19.3 (-23.3 to -16.0)%, *P*=0.07].

Negishi *et al.*[37], 2015	83 patients with CP + 20 controls	Investigate if pericardiectomy improves myocardial mechanics using 2D-STE analysis. Besides LV ε, the authors studied LV longitudinal and rotational displacement	• Longitudinal displacement of LV opposing walls were similar, but both were decreased in CP compared to controls. After pericardiectomy septal displacement decreased but lateral displacement increased. • Septal longitudinal ε was similar between two groups, but lateral longitudinal ε was lower in the CP group. Septal longitudinal ε decreased significantly (-20.3±5.0% vs -17.7±4.6 %, *P*=0.032) after surgery, but lateral longitudinal ε did not (-14.7±5.8% vs -15.2±3.4%, *P*=0.51). • Patients with CP had lower absolute values of GLS (-20.1±1.9 vs -16.2±3.3%, *P*< 0.01) and GCS (-20.7±5.1 vs -14.7±5.0%, *P*< 0.01), with no significant difference in GRS (50.4±16.2 vs 40.8±18.8%, *P*=0.07) compared with controls. • No significant difference in SLRD between controls and CP (-2.3±3.3 vs -0.6±3.0º, *P*=0.07). After pericardiectomy SLRD increased significantly (-0.8±3.3% vs 2.1±3.0, *P*<0.01). • No changes in GLS (-15.6±3.9% vs -15.8±3.2, *P*=0.88) and GRS (37.4±18.9% vs 39.1±16.5%, *P*=0.73) after pericardiectomy. GCS increased (-13.5±5.7 vs -17.6±5.5, *P*<0.01) after pericardiectomy.
Liu *et al.*[41], 2015	35 patients with CP + 30 patients with RCM + 30 healthy controls	Evaluation of LA mechanics in using 2D-STE analysis.	• The LA global and regional reservoir ε were significantly reduced in patients with CP and RCM compared with the normal controls (16.8±7.4 vs 11.5±5.5% vs 40.0±11.2, *P*<0.01). • Patients with RCM had a significantly lower LA septal reservoir ε compared with CP patients and controls (30.7±13.4 vs 13.9±9.7 vs 43.7±10.7%, *P*<0.01), although the lateral wall reservoir ε of patients with CP and patients with RCM were not significantly different (14.7±9.3 vs 14.7±7.4%, *P*=ns).

ε: strain; 2D-STE: two-dimensional speckle-tracking echocardiography; CP: constrictive pericarditis; CRM: cardiac magnetic resonance; GCS: global circumferential strain; GLS: global longitudinal strain; GRS: global radial strain; LA: left atrial; LV: left ventricle; LVLWS: left ventricle lateral wall strain; LVSWS: left ventricle septal wall strain; RCM: restrictive cardiomyopathy; RVFWS: right ventricle free wall strain; SLRD: septal-to-lateral rotational displacement.

Table 4: Echocardiographic differences between constriction and restriction.

	Constrictive pericarditis	Restrictive cardiomyopathy
1. Two-dimensional echocardiography		
Left ventricle ejection fraction	Normal	Normal or slightly decreased
Pericardium appearance	Thickened / Bright	Normal
Interventricular septum movement	Abnormal	Normal
Interventricular septum position	Varies with respiration	Normal
2.Doppler echocardiography		
E/a ratio	Increased (≥ 2)	Increased (≥ 2)
E/a ratio response to Valsalva maneuver	Variation > 25%	Minimal variation
E wave decelerating time	Decreased (≤ 160ms)	Decreased (≤ 160ms)
E' septal (cm/s)	≥ 8	< 8
E' septal/lateral	Septal > lateral	Lateral > septal
S' (cm/s)	>5	<5
Mitral valve inflow propagation	Normal or increased (≥100cm/s)	<55cm/s
Hepatic vein flow	Diastolic flow reversion during expiration	Diastolic flow reversion during inspiration
3.Two-dimensional speckle-tracking echocardiography		

Circumferential strain	Decreased	Normal
Radial strain		
Basal	Decreased	Normal
Apical	Normal	Normal
Longitudinal strain		
Septal	Normal	Decreased
Lateral	Decreased	Decreased
Basal segments	Normal	Decreased
Apical segments	Decreased	Decreased
Global	Decreased	Decreased
Twist motion	Decreased	Normal
Apical rotation	Decreased	Normal
Left atrial reservoir strain		
Lateral	Decreased	Decreased
Septal	Increased	Decreased

Supplemental Table 1: Newcastle–Ottawa quality score

Quality Assessment Criteria	Acceptable(*)	Sengupta (2008)	Motoki (2013)	Kusunose (2013)	Liu (2013)	Amaki (2014)	Neigishi (2015)	Liu (2015)
Selection								
Representativeness of exposed cohort?	Representative of average adult in community		*	*	*	*	*	*
Selection of the non-exposed cohort?	Drawn from same community as Exposed cohort	*	*	*	*	*	*	*
Ascertainment of exposure?	Secured records, Structured interview	*	*	*	*	*	*	*
Demonstration that outcome of interest was not present at start of study?	Presence of disease	*	*	*	*	*	*	*
Comparability								
Study controls for age/sex?	Yes	*	--	*	*	*	--	--

Study controls for at least 3 additional risk factors?	Adjustment for risk-factors.	--	--	--	--	--	--	--
Outcome								
Assessment of outcome?	Independent blind assessment	*	-	*	-	*	*	-
Was follow-up long enough for outcome to occur?	Follow-up – 20-30 days	*	*	*	*	*	*	*
Adequacy of follow-up of cohorts?	Complete follow-up, or subjects lost to follow-up unlikely to introduce bias	*	*	*	*	*	*	*
Overall Quality Score (Maximum = 9)		8	6	8	7	8	7	6

Figure 1

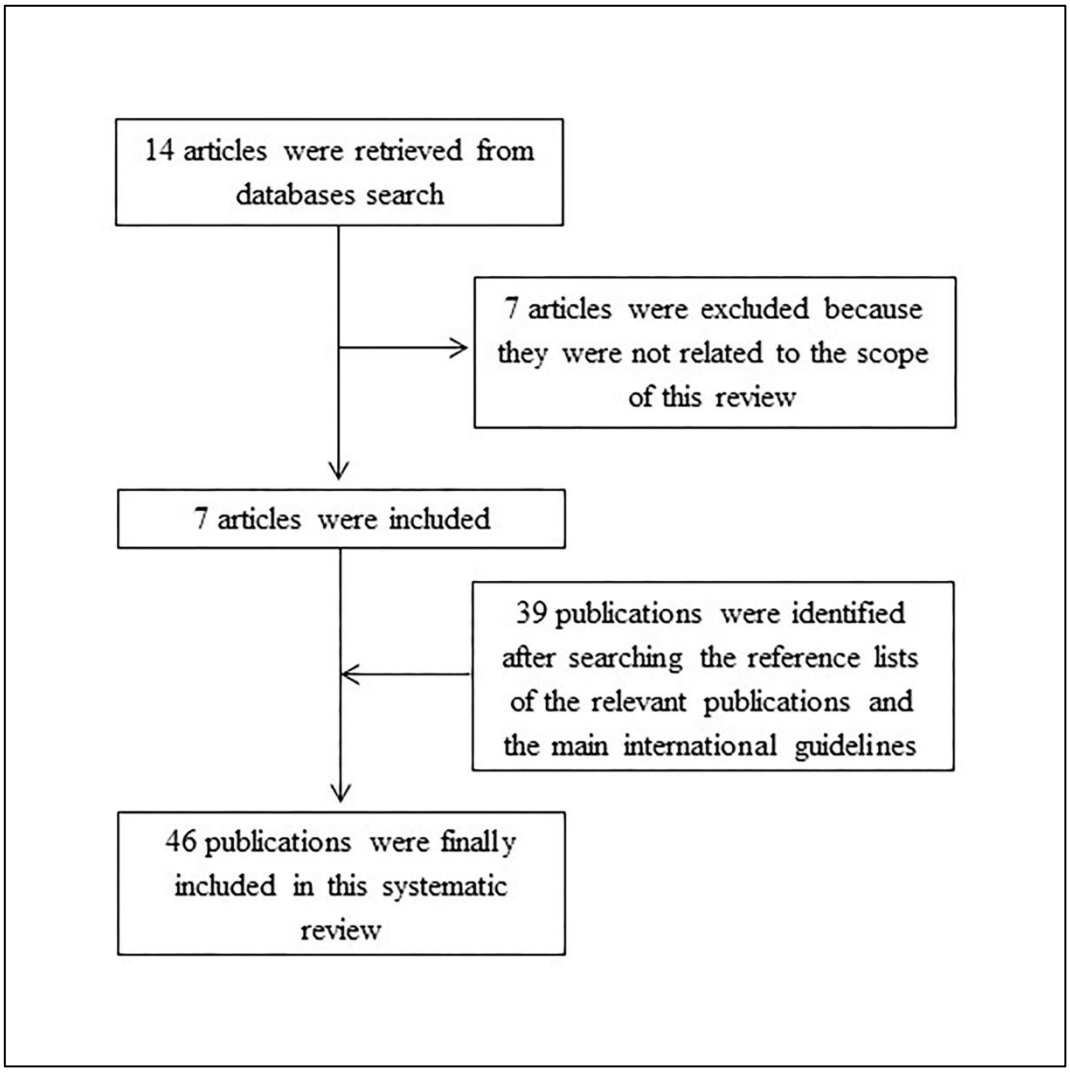
14 articles were retrieved from databases search
7 articles were excluded because they were not related to the scope of this review
7 articles were included
39 publications were identified after searching the reference lists of the relevant publications and the main international guidelines
46 publications were finally included in this systematic review

Figure 2

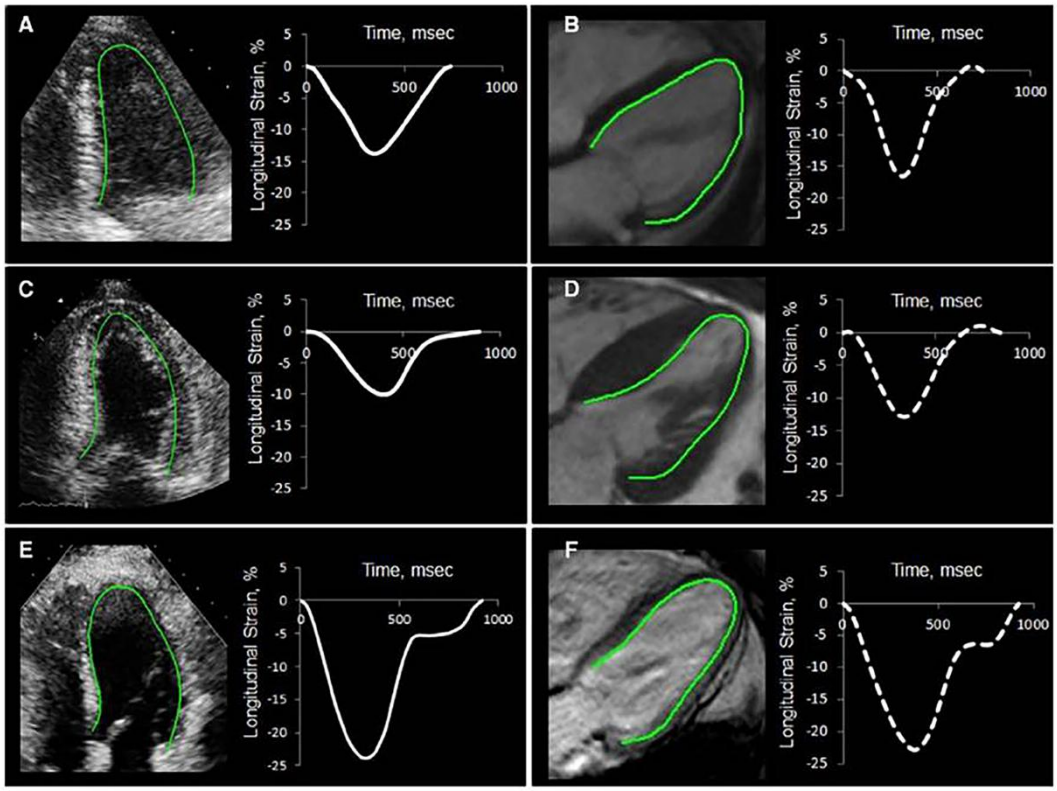
A
B
C
D
E
F
Time, msec
Longitudinal Strain, %
0
500
1000
5
0
-5
-10
-15
-20
-25

Figure 3

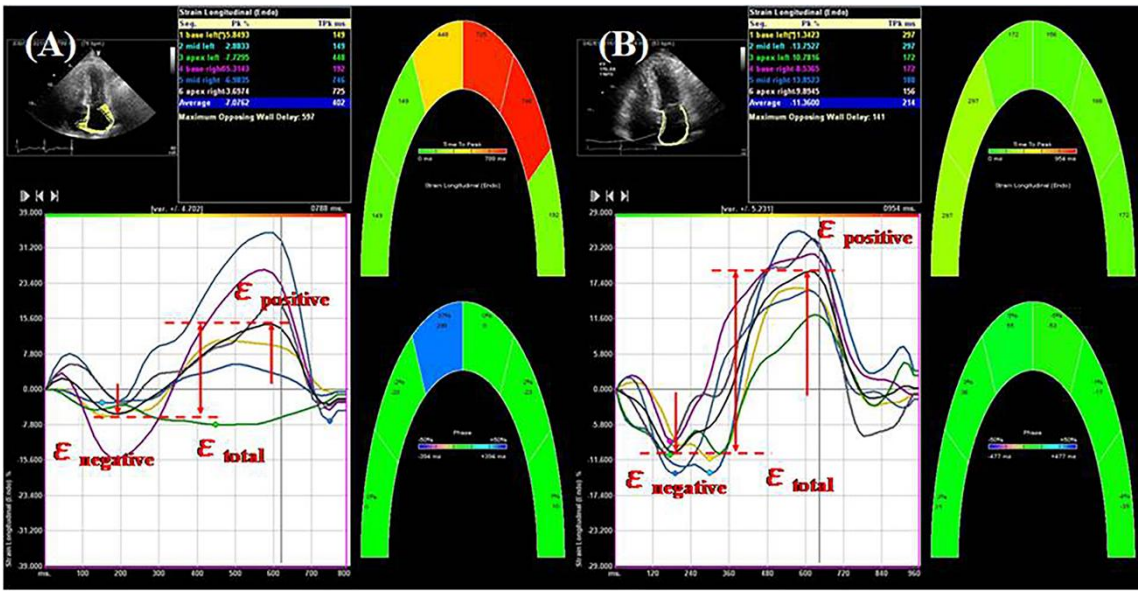
(A)
(B)
ε positive
ε negative
ε total
ε positive
ε negative
ε total

Figure 4

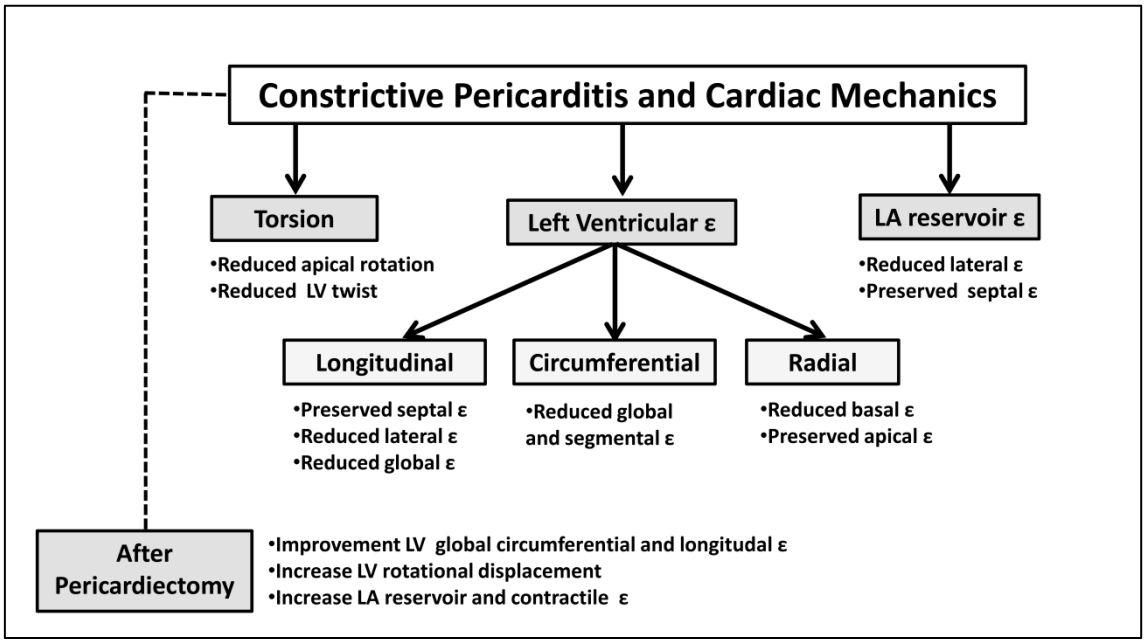
Constrictive Pericarditis and Cardiac Mechanics
Torsion
•Reduced apical rotation
•Reduced LV twist
Left Ventricular ε
LA reservoir ε
•Reduced lateral ε
•Preserved septal ε
Longitudinal
•Preserved septal ε
•Reduced lateral ε
•Reduced global ε
Circumferential
•Reduced global and segmental ε
Radial
•Reduced basal ε
•Preserved apical ε
After Pericardiectomy
•Improvement LV global circumferential and longitudal ε
•Increase LV rotational displacement
•Increase LA reservoir and contractile ε

References

1. Mor-Avi V, Lang RM, Badano LP, Belohlavek M, Cardim NM, et al. (2011) Current and evolving echocardiographic techniques for the quantitative evaluation of cardiac mechanics: ASE/EAE consensus statement on methodology and indications endorsed by the Japanese Society of Echocardiography. J Am Soc Echocardiogr 24: 277-313.

2. Miller MJ, McKay RG, Ferguson JJ, Sahagian P, Nakao S, et al. (1986) Right atrial pressure-volume relationships in tricuspid regurgitation. Circulation 73: 799-808.

3. Vieira MJ, Teixeira R, Goncalves L, Gersh BJ (2014) Left atrial mechanics: echocardiographic assessment and clinical implications. J Am Soc Echocardiogr 27: 463-478.

4. Leitman M, Lysyansky P, Sidenko S, Shir V, Peleg E, et al. (2004) Two-dimensional strain-a novel software for real-time quantitative echocardiographic assessment of myocardial function. J Am Soc Echocardiogr 17: 1021-1029.

5. Reisner SA, Lysyansky P, Agmon Y, Mutlak D, Lessick J, et al. (2004) Global longitudinal strain: a novel index of left ventricular systolic function. J Am Soc Echocardiogr 17: 630-633.

6. Sirbu C, Herbots L, D'Hooge J, Claus P, Marciniak A, et al. (2006) Feasibility of strain and strain rate imaging for the assessment of regional left atrial deformation: a study in normal subjects. Eur J Echocardiogr 7: 199-208.

7. Cameli M, Lisi M, Giacomin E, Caputo M, Navarri R, et al. (2011) Chronic mitral regurgitation: left atrial deformation analysis by two-dimensional speckle tracking echocardiography. Echocardiography 28: 327-334.

8. Tops LF, Delgado V, Bertini M, Marsan NA, Den Uijl DW, et al. (2011) Left atrial strain predicts reverse remodeling after catheter ablation for atrial fibrillation. J Am Coll Cardiol 57: 324-331.

9. Ersboll M, Andersen MJ, Valeur N, Mogensen UM, Waziri H, et al. (2013) The prognostic value of left atrial peak reservoir strain in acute myocardial infarction is dependent on left ventricular longitudinal function and left atrial size. Circ Cardiovasc Imaging 6: 26-33.

10. D'Andrea A, Scarafile R, Riegler L, Salerno G, Gravino R, et al. (2009) Right atrial size and deformation in patients with dilated cardiomyopathy undergoing cardiac resynchronization therapy. Eur J Heart Fail 11: 1169-1177.

11. Padeletti M, Cameli M, Lisi M, Malandrino A, Zaca V, et al. (2012) Reference values of right atrial longitudinal strain imaging by two-dimensional speckle tracking. Echocardiography 29: 147-152.

12. Peluso D, Badano LP, Muraru D, Dal Bianco L, Cucchini U, et al. (2013) Right atrial size and function assessed with three-dimensional and speckle-tracking echocardiography in 200 healthy volunteers. Eur Heart J Cardiovasc Imaging 14: 1106-1114.

13. Saraiva RM, Demirkol S, Buakhamsri A, Greenberg N, Popovic ZB, et al. (2010) Left Atrial Strain Measured by Two-Dimensional Speckle Tracking Represents a New Tool to Evaluate Left Atrial Function. J Am Soc Echocardiogr 23: 172-180.

14. McMurray JJ, Adamopoulos S, Anker SD, Auricchio A, Bohm M, et al. (2012) ESC Guidelines for the diagnosis and treatment of acute and chronic heart failure 2012: The Task Force for the Diagnosis and Treatment of Acute and Chronic Heart Failure 2012 of the European Society of Cardiology. Developed in collaboration with the Heart Failure Association (HFA) of the ESC. Eur Heart J 33: 1787-1847.

15. Evangelista A, Flachskampf F, Lancellotti P, Badano L, Aguilar R, et al. (2008) European Association of Echocardiography recommendations for standardization of performance, digital storage and reporting of echocardiographic studies. Eur J Echocardiogr 9: 438-448.

16. Rudski LG, Lai WW, Afilalo J, Hua L, Handschumacher MD, et al. (2010) Guidelines for the echocardiographic assessment of the right heart in adults: a report from the American Society of Echocardiography endorsed by the European Association of Echocardiography, a registered branch of the European Society of Cardiology, and the Canadian Society of Echocardiography. J Am Soc Echocardiogr 23: 685-713; quiz 786-688.

17. Natori H, Tamaki S, Kira S (1979) Ultrasonographic evaluation of ventilatory effect on inferior vena caval configuration. Am Rev Respir Dis 120: 421-427.

18. Lang RM, Bierig M, Devereux RB, Flachskampf FA, Foster E, et al. (2005) Recommendations for chamber quantification: a report from the American Society of Echocardiography's Guidelines and Standards Committee and the Chamber Quantification Writing Group, developed in conjunction with the European Association of Echocardiography, a branch of the European Society of Cardiology. J Am Soc Echocardiogr 18: 1440-1463.

19. Kaul S, Tei C, Hopkins JM, Shah PM (1984) Assessment of right ventricular function using two-dimensional echocardiography. Am Heart J 107: 526-531.

20. Lindqvist P, Waldenstrom A, Henein M, Morner S, Kazzam E (2005) Regional and global right ventricular function in healthy individuals aged 20-90 years: a pulsed Doppler tissue imaging study: Umea General Population Heart Study. Echocardiography 22: 305-314.

21. Nageh MF, Kopelen HA, Zoghbi WA, Quinones MA, Nagueh SF (1999) Estimation of mean right atrial pressure using tissue Doppler imaging. Am J Cardiol 84: 1448-1451, A1448.

22. Dubin J, Wallerson DC, Cody RJ, Devereux RB (1990) Comparative accuracy of Doppler echocardiographic methods for clinical stroke volume determination. Am Heart J 120: 116-123.

23. Ommen SR, Nishimura RA, Appleton CP, Miller FA, Oh JK, et al. (2000) Clinical utility of Doppler echocardiography and tissue Doppler imaging in the estimation of left ventricular filling pressures: A comparative simultaneous Doppler-catheterization study. Circulation 102: 1788-1794.

24. Lancellotti P, Moura L, Pierard LA, Agricola E, Popescu BA, et al. (2010) European Association of Echocardiography recommendations for the assessment of valvular regurgitation. Part 2: mitral and tricuspid regurgitation (native valve disease). Eur J Echocardiogr 11: 307-332.

25. Yock PG, Popp RL (1984) Noninvasive estimation of right ventricular systolic pressure by Doppler ultrasound in patients with tricuspid regurgitation. Circulation 70: 657-662.

26. Abbas AE, Fortuin FD, Schiller NB, Appleton CP, Moreno CA, et al. (2003) A simple method for noninvasive estimation of pulmonary vascular resistance. J Am Coll Cardiol 41: 1021-1027.

27. Kurt M, Wang J, Torre-Amione G, Nagueh SF (2009) Left atrial function in diastolic heart failure. Circ Cardiovasc Imaging 2: 10-15.

28. Bland JM, Altman DG (1986) Statistical methods for assessing agreement between two methods of clinical measurement. Lancet 1: 307-310.

29. Shrout PE, Fleiss JL (1979) Intraclass correlations: uses in assessing rater reliability. Psychol Bull 86: 420-428.

30. Anne W, Willems R, Roskams T, Sergeant P, Herijgers P, et al. (2005) Matrix metalloproteinases and atrial remodeling in patients with mitral valve disease and atrial fibrillation. Cardiovasc Res 67: 655-666.

31. Kuppahally SS, Akoum N, Burgon NS, Badger TJ, Kholmovski EG, et al. (2010) Left Atrial Strain and Strain Rate in Patients With Paroxysmal and Persistent Atrial Fibrillation / CLINICAL PERSPECTIVE. Circulation Cardiovasc Imaging 3: 231-239.

32. Her A-Y, Choi E-Y, Shim CY, Song BW, Lee S, et al. (2012) Prediction of Left Atrial Fibrosis With Speckle Tracking Echocardiography in Mitral Valve Disease: A Comparative Study With Histopathology. Korean Circ J 42: 311-318.

33. Melenovsky V, Hwang SJ, Redfield MM, Zakeri R, Lin G, et al. (2015) Left atrial remodeling and function in advanced heart failure with preserved or reduced ejection fraction. Circ Heart Fail 8: 295-303.

34. Kutty S, Padiyath A, Li L, Peng Q, Rangamani S, et al. (2013) Functional maturation of left and right atrial systolic and diastolic performance in infants, children, and adolescents. J Am Soc Echocardiogr 26: 398-409 e392.

35. Padeletti M, Cameli M, Lisi M, Zaca V, Tsioulpas C, et al. (2011) Right atrial speckle tracking analysis as a novel noninvasive method for pulmonary hemodynamics assessment in patients with chronic systolic heart failure. Echocardiography 28: 65